Investigation of Anti-Cancer Effects of a Palladium Compound (Pd(bpma)(barb).Cl • H_2O) in Colorectal Cancer Cell Lines

by

Merve Kayış

A Dissertation Submitted to the

Graduate School of Health Sciences in Partial Fulfillment of the Requirements for the Degree of

Doctor of Philosophy

in

Cellular and Molecular Medicine

KOÇ ÜNİVERSİTESİ

June 2024

Investigation of Anti-Cancer Effects of a Palladium Compound (Pd(bpma)(barb).Cl • H_2O) in Colorectal Cancer Cell Lines

Koc University

Graduate School of Health Sciences

This is to certify that I have examined this copy of a doctoral dissertation by

Merve Kayış

and have found that it is complete and satisfactory in all respects,

and that any and all revisions required by the final

examining committee have been made.

Committee Members:

Assoc. Prof. Zelal Adıgüzel (Advisor)

Prof. Dr. Engin Ulukaya [Co-Advisor]

Assist. Prof. Emel Sokullu

Assoc. Prof. Dr. Suat Erus

Prof. Dr. Pınar Obakan Yerlikaya

Prof. Dr. Zeliha Gökmen

Date: 04.06.2024

ÖZETÇE

Paladyum Pd(II) (Pd(bpma)(barb).Cl • H_2O) Bileşiğinin Kolorektal Kanser Hücre Hattında Anti-kanser Etkisinin Araştırılması

Merve Kayış

Hücresel ve Moleküler Tıp, Doktora, Hazitan 2024

Arka Plan ve Amaç:

Kolon kanseri, dünya çapında en yaygın görülen üçüncü kanser türüdür. Tedavi sürecinde ve sonrasında karşılaşılan en önemli sorun ise kanser hücrelerinin ilaçlara karşı direnç kazanarak tedaviye yanıt vermemeleridir. Bu nedenle kolon kanseri tedavisine yönelik olarak kanserin altında yatan moleküler tüm yolaklar incelenerek yeni terapötik hedeflerin belirlenmesinin oldukça önemli olduğu düşünülmektedir. Son yıllarda yapılan çalışmalar, bazı metal bileşiklerin umut verici etkilerinden dolayı tedavide ilaç adayı olarak kullanılabileceğini göstermektedir. Kolon kanseri üzerinde yapılan araştırmalar apoptozun genellikle bir hayatta kalma mekanizması olarak rol aldığını göstermektedir.

Yöntemler:

Bu nedenle bu tez çalışmasında, Palladyum (II) bileşiğinin [[Pd(bpma)(barb)]Cl.H_2O] insan kolon kanseri hücre hatları (HCT-15, HCT-116 ve HT-29) üzerine anti kanser ve sitotoksik etkileri araştırılmıştır. Pd (II) bileşiğinin hücre canlılığı üzerine olan etkileri MTT canlılık testi ile belirlenmiştir. Bileşiğin sebep olduğu hücre ölümü mekanizmasının belirlenmesi amacıyla akım sitometri yöntemi kullanılarak oksidatif stres, DNA hasarı, otofaji, annexin V yolakları incelenmiştir. Hücrelerde apoptozun gerçekleştiği Hoechst 33342/Propidyum İyodür boyama yöntemi ile floresan mikroskopta gösterilmiştir. Son olarak tüm bu yolaklarla ilişkilendirilen toplamda 82 adet genin gen ekspresyon seviyeleri RT-qPCR metodu ile incelenmiştir.

Sonuçlar ve Yorum:

Sonuç olarak Pd (II) bileşiğinin HCT-15 hücre soyunda anti apoptotik aktivitenin artışına neden olduğu bulunmuştur. Pd (II) bileşiğinin yeni ve daha etkin bir tedavi seçeneği olarak anti kanser ilaç adayı olarak kullanılabileceği tahmini ile daha güncel çalışmaların yapılmasının hem klinik hem de ileride yapılacak yeni kanser çalışmalarında yol gösterici olacağı düşünülmektedir.

Anahtar Kelimeler: Kolon kanseri, Apoptoz, Palladyum (II) bileşiği

ABSTRACT

Investigation of Anti-Cancer Effects of a Palladium Compound (Pd(bpma)(barb).Cl • H_2O) in Colorectal Cancer Cell Lines

Merve Kayış

Cellular and Molecular Medicine, PhD, June 2024

Background and Objective:

Colon cancer ranks as the third most prevalent form of cancer globally. An eminent issue that arises during and after the treatment procedure is the development of drug resistance in cancer cells, rendering them unresponsive to therapy. Therefore, it is crucial to develop novel therapeutic targets for colon cancer therapy by thoroughly investigating all molecular pathways associated with the disease. Recent studies have shown that some metal compounds have intriguing therapeutic benefits, making them potential candidates for medication development. Studies on colon cancer indicate that apoptosis often functions as a pathway for survival.

Methods:

This thesis research aimed to explore the anti-cancer and cytotoxic effects of the Palladium (II) compound [[Pd(bpma)(barb)]Cl.H_2O] on human colon cancer cell lines (HCT-15, HCT-116, and HT-29). The impact of the Pd (II) compound on cell viability was assessed using the MTT viability assay. To ascertain the cellular process by which the substance induces cell death, we investigated the impact of oxidative stress on DNA, autophagy, and the annexin V pathways using the flow cytometry technique. The process of programmed cell death, known as apoptosis, was seen in cells using the Hoechst 33342/Propidium Iodide staining technique, with the use of a fluorescence microscope. Ultimately, the RT-qPCR technique was used to analyze the gene expression levels of a total of 82 genes that are linked to these pathways.

Results and Conclusion:

The study revealed that the Pd (II) compound led to enhanced anti apoptotic activity and apoptosis in the HCT-15 cell line. Given the prediction that the Pd (II) molecule has potential as a candidate for an anti-cancer therapy, it is believed that doing more in vivo trials will provide valuable guidance for both clinical applications and future cancer research investigations.

Keywords: Colorectal carcinoma, Programmed cell death, Palladium (II) complex

ACKNOWLEDGMENTS

İstanbul gibi bir şehirde bir kadın olarak tek başıma ayaklarımın üzerinde durup, moleküler biyoloji ve genetik gibi zor bir alanda akademik kariyere devam edip doktora eğitimini tamamlamak, oldukça zor ve bir o kadar da gurur verici bir başarı benim için. Pandemi döneminde başladığım ve ilk 2 yılını pandemi döneminde tamamladığım bu zorlu doktora sürecini tamamlarken teşekkür etmek istediğim bazı kişiler var.

Hayatımda danışman değişikliği yapmak zorunda kaldığım, yeterlilik sınavı öncesi bir kriz döneminde karşıma çıkıp, geriye kalan tüm süreci çok daha huzurlu ve mutlu tamamlamamı sağlayan, çalışmaktan oldukça keyif aldığım bu tez konusunu bana önerip desteği ile tezimi tamamlamamda yardımcı olan, sadece danışman hoca değil aynı anda bana arkadaş olan, hayatımın her alanında iyilikleri ile yanımda olan, sevgili danışman hocam Doç. Dr. Zelal Adıgüzel'e

Tanıştığımız ilk günden itibaren çalışma hevesime inanıp bana birçok projede destek olan, tüm deney sonuçlarım için en az benim kadar heyecanlanan ve bir sonraki deneysel adımı benimle planlayan ve bu tezin tamamlanmasında büyük katkısı olan eş danışmanım saygıdeğer hocam Prof. Dr. Engin Ulukaya'ya

Hayatımın en kritik anlarında her zaman arkamda duran, benim olmadığım durumlarda bile benim iyiliğim için beni düşünen, bana her konuda inanıp güvenen ve destek olan, tanıştığım ve beraber çalışma fırsatı yakaladığım için büyük mutluluk ve gurur duyduğum çok sevgili hocam Dr. Öğr. Üyesi Emel Sokullu'ya

Tez savunma jürimde yer alarak zamanlarını bana ayıran ve soruları ile tezime önemli katkılar sunan sevgili hocalarım Prof. Dr. Pınar Obakan Yerlikaya, Doç. Dr. Suat Erus ve Prof. Dr. Zeliha Gökmen'e

Zengin altyapılarıyla tez çalışmam için gerekli koşulları sağlayan Koç Üniversitesi Hastanesi KUTTAM laboratuvarları ve Istinye Üniversitesi Tıp Fakültesi Kanser Araştırma Merkezi İSUMKAM laboratuvarlarına

Doktora serüvenim boyunca Istanbul'da ve hatta başka ülkelerde çok güzel anılar biriktirdiğim, beraber gülüp ağladığım, seyahat edip gezdiğim, çalıştığım, tüm stresimi zor zamanları destekleri ile atlattığım bu süreçte hayatıma girmiş olan tüm arkadaşlarıma

Bugüne kadar binbir zorluk ve emekle beni yetiştirip büyüten, çok zor ve yıllar süren tüm eğitim hayatım boyunca maddi manevi her zaman yanımda olan her konuda beni destekleyen hep arkamda duran, haklarını asla ödeyemeyeceğim canım anne ve babama, ablalarıma, aileme

Ama en çok sabahlara kadar çok çalışmaya devam ettiğim, türlü türlü zorluklarla tek başıma mücadele ettiğim, zaman zaman ağlayıp pes etmeyi düşündüğüm yine de vazgeçmeyip gözyaşlarımı silip pes etmeden devam ettiğim ve her daim kendimi geliştirme odaklı olduğum için, en çok KENDİME

SONSUZ TEŞEKKÜRLER…

Haziran 2024, İstanbul

Merve Kayış

Funding

This project was funded by TUSEB B GROUP Research Project (project no:33524) research funds. Merve Kayış was funded by Koç University during her PhD education. This study was conducted using the service and infrastructure of Koç University Hospital Research Center for Translational Medicine (KUTTAM).

TABLE OF CONTENTS

ABSTRACT v

ÖZETÇE iv

ACKNOWLEDGMENT vii

LIST OF TABLES xii

LIST OF FIGURES xiv

ABBREVIATIONS xxiii

CHAPTER 1 1

1. INTRODUCTION 1

1.1. Cancer 1

1.1.2. Biology of Cancer 1

1.1.3. Hallmarks of Cancer 2

1.2. Colorectal Cancer (CRC) 5

1.2.1. Anatomy of Colorectal Cancer 5

1.2.2. Colorectal Cancer (CRC) Epidemiology 7

1.2.3. Stages of Colon Cancer 8

1.2.4. Colon Cancer Risk Factors 10

1.2.5. Colon Cancer Diagnostic Criteria 11

1.2.6. Genetic Features of Colorectal Cancer 11

1.2.7. Histological Features of Colorectal Cancer 12

1.2.8. Subtypes of Colorectal Cancer 13

1.2.9. Intrinsic Subtypes of Colorectal Cancer 13

1.3. Cancer Therapy 14

1.3.1. Chemotherapy 15

1.4. Drug Resistance 16

1.4.1. Cis-Platin Resistance 17

1.5. As an anti cancer agents: Chemical Compounds 18

1.5.1. Palladium Compounds in Cancer Therapy 19

1.5.2. Structure of the Palladium Compound 20

1.6. Cell Death Pathways 21

1.6.1. Apoptosis 22

1.6.1.1. Intrinsic Apoptosis Pathway 24

1.6.1.2. The Extrinsic Pathway 28
CHAPTER 2 30
2. MATERIAL AND METHODS 30
2.1. Chemicals 30
2.2. Consumables 31
2.3. Devices 32
2.4. Method 33
2.4.1. Preparation of Palladium Compound 33
2.4.2. Cell Culture 33
2.4.2.1. Preparation of the Cell Medium 33
2.4.2.2. Removal of Cell Strains from Stock 33
2.4.2.3. Passaging of Cell Lines 33
2.4.2.4. Stocking of Cell Lines 34
2.4.2.5. Counting Cells 34
2.4.3. MTT (Metil-tiazo-tetrazolium) Cell Viability Method 35
2.4.3.1. NAC (N-Acetyl Cysteine) Treatment 37
2.4.3.2 % Viability Measurement 37
2.4.4. Cell Migration Experiment 37
2.4.5. Determining the Death Method of Cells by Fluorescent Staining 38
2.4.5.1. Double Staining Method 38
2.5. Flow Cytometry Analysis 39
2.5.1. Annexin-V-FITC Test 40
2.5.2. Determination of DNA Damage by Gamma H2A.X Activation 41
2.5.3. Determination of Oxidative Stress 43
2.5.4. Autophagy Analysis 44
2.6. Gene Expression Analyzes by Real Time-PCR (qPCR-quantitative) 45
2.6.1. RNA Isolation 45
2.6.2. Spectrophotometric analysis of RNA samples and quantification of RNA template amounts for cDNA synthesis 47
2.6.3. Primer Design for Gene Expression Analysis with Real-Time PCR 47
2.6.4. Gene Expression Analysis by Real-Time PCR 47
2.6.5. cDNA synthesis 47
2.6.6. Detection of qPCR Products 49

2.6.7. Data Analysis for Gene Expression Study 50
2.7. Statistical Analysis 51
2.7.1. Editing and Statistical Analysis of Expression Data 51
CHAPTER 3 52
3. RESULTS 52
3.1 Results of MTT Cell Viability 52
3.2. Results of Double Staining 53
3.3. Flow Cytometry Results 55
3.3.1. Evaluation of Annexin-V (FITC) 55
3.3.2. Determining DNA Damage 57
3.3.3. Assesment of Oxidative Stress (ROS) 59
3.3.4. Results of N-acetyl-L-cysteine (NAC) Treatment 60
3.3.5. Results of Autopaghy Analysis 61
3.4. Effect of Pd(II) Compound on Migration Abilities in HCT-15 Cell Line 63
3.5. Analysis the Expression levels of 82 genes that Related to Apoptosis 64
CHAPTER 4 139
4. DISCUSSION 139
BIBLIOGRAPHY 158

LIST OF TABLES

Table 2.1. Quantities of prepared mixture for cDNA synthesis 48

Table 2.2. Mixture Amounts Prepared for Gene Expression Analysis 49

Table 3.1. IC50 and IC90 values during the 48-hour treatment period according to the MTT viability test results in cell lines applied with Pd (II) compound 67

Table 3.2. Genes whose expression increases at 24h 68

Table 3.3. Genes whose expression decreases at 6h 69

Table 3.4. Genes whose expression decreases at 24h 69

Table 3.5. M, SD, median, min-max, Q1, Q3 and p values of the relevant Genes at the 6th hour according to Control and Drug IC90 Groups 70

Table 3.6. M, SD, median, min-max, Q1, Q3 and p values of the relevant Genes at the 24th hour according to Control and Drug IC90 Groups 73

Table 3.7. Hypothesis Test Summary for AKT1 Gene 76

Table 3.8. Hypothesis Test Summary for ATG7 Gene 78

Table 3.9. Hypothesis Test Summary for BAG1 Gene 79

Table 3.10. Hypothesis Test Summary for BAG3 Gene 81

Table 3.11. Hypothesis Test Summary for BCL10 Gene 82

Table 3.12. Hypothesis Test Summary for BCLAF1 Gene 84

Table 3.13. Hypothesis Test Summary for BCLXL Gene 85

Table 3.14. Hypothesis Test Summary for BID Gene 87

Table 3.15. Hypothesis Test Summary for BIM Gene 88

Table 3.16. Hypothesis Test Summary for BIRC2 Gene 90

Table 3.17. Hypothesis Test Summary for BIRC3 Gene 91

Table 3.18. Hypothesis Test Summary for BIRC5 Gene 93

Table 3.19. Hypothesis Test Summary for BIRC6 Gene 94

Table 3.20. Hypothesis Test Summary for BMI1 Gene 96

Table 3.21. Hypothesis Test Summary for BNIP1 Gene 97

Table 3.22. Hypothesis Test Summary for BNIP3L Gene 99

Table 3.23. Hypothesis Test Summary for CASP3 Gene 100

Table 3.24. Hypothesis Test Summary for CASP4 Gene 102

Table 3.25. Hypothesis Test Summary for CASP6 Gene 103
Table 3.26. Hypothesis Test Summary for CASP7 Gene 104
Table 3.27. Hypothesis Test Summary for CDC20 Gene 106
Table 3.28. Hypothesis Test Summary for CDK4 Gene 107
Table 3.29. Hypothesis Test Summary for DCR Gene 109
Table 3.30. Hypothesis Test Summary for DR4 Gene 110
Table 3.31. Hypothesis Test Summary for DR5 Gene 112
Table 3.32. Hypothesis Test Summary for ERCC1 Gene 113
Table 3.33. Hypothesis Test Summary for ERCC3 Gene 115
Table 3.34. Hypothesis Test Summary for FAS Gene 116
Table 3.35. Hypothesis Test Summary for GAD45A Gene 118
Table 3.36. Hypothesis Test Summary for GSTP1 Gene 119
Table 3.37. Hypothesis Test Summary for LIG4 Gene 121
Table 3.38. Hypothesis Test Summary for MCL1 Gene 123
Table 3.39. Hypothesis Test Summary for MDM2 Gene 124
Table 3.40. Hypothesis Test Summary for MGMT Gene 126
Table 3.41. Hypothesis Test Summary for NEK2 Gene 127
Table 3.42. Hypothesis Test Summary for NOXA Gene 129
Table 3.43. Hypothesis Test Summary for PRDX1 Gene 130
Table 3.44. Hypothesis Test Summary for PUMA Gene 132
Table 3.45. Hypothesis Test Summary for RAD52 Gene 133
Table 3.46. Hypothesis Test Summary for SOD1 Gene 135
Table 3.47. Hypothesis Test Summary for XPA Gene 136
Table 3.48. Hypothesis Test Summary for XRCC5 Gene 138

LIST OF FIGURES

Figure 1.1. Tumor Types According to Their Origin 2
Figure 1.2. Hallmarks of Cancer 3
Figure 1.3. Anatomy of Colorectal Cancer 6
Figure 1.4. Different Type of Colon Tissue 6
Figure 1.5. Colon Cancer Epidemiology 8
Figure 1.6. Primary stages of Colon Cancer 9
Figure 1.7. Colorectal Cancer TNM staging 10
Figure 1.8. Healthy Colon Immunohistochemistry staining 12
Figure 1.9. Intrinsic Colon Cancer subtypes 14
Figure 1.10.Structure of Pd(II) Complound 21
Figure 1.11.Cell Death Pathways 22
Figure 1.12.Apoptosis 23
Figure 1.13. Intrinsic and Extrinsic Pathway 27
Figure 2.1. The Mitochondrial Reductase Converts Yellow MTT into Purple Formazan 35
Figure 2.2. MTT Assay Principle 36
Figure 2.3. Diagram Illustrating the Annexin V Apoptosis Assay 39
Figure 2.4. Annexin V Analysis 41
Figure 2.5. DNA Damage (γ-H2AX) Activation 42
Figure 2.6. Oxidative Stress (ROS) Analysis 44
Figure 2.7. Microscopic image when HCT-15 colon cancer cells begin to aggregate for RNA isolation at the 6th hour 46
Figure 2.8. Microscopic image when HCT-15 colon cancer cells begin to aggregate for RNA isolation at the 24th hour 46
Figure 2.9. Genes analyzed in Template 1 50
Figure 2.10. Genes analyzed in Template 2 50
Figure 3.1. % Cell Viability Graph of HCT-116, HCT-15 and HT-29 cell lines 52
Figure 3.2. Fluorescence Microscope Images of HCT-15 cell line after 24-h Pd(II) compound treatment 54
Figure 3.3. Fluorescence Microscope Images of HCT-15 cell line after 48-h Pd(II) compound treatment 55

Figure 3.4. 12-hour histograms of % apoptotic values obtained by Annexin-V (FITC) evaluation of Pd (II) compound (77,6 μM) in HCT-15 colon cancer cell line 56
Figure 3.5. 24-hour histograms of apoptotic percentage values obtained by Annexin-V (FITC) assessment of Pd(II) compound (77,6 μM) in HCT-15 colon cancer cell 56
Figure 3.6. 12-hour histogram of p-γH2AX percentage values of Pd(II) compound (77,6 μM) in HCT-15 colon cancer control cells 57
Figure 3.7. 12-hour histogram of p-γH2AX percentage values of Pd(II) compound (77,6 μM) in HCT-15 colon cancer treatment cells 57
Figure 3.8. 24-hour histogram of p-γH2AX percentage values of Pd(II) compound (77,6 μM) in HCT-15 colon cancer control cells 58
Figure 3.9. 24-hour histogram of p-γH2AX percentage values of Pd(II) compound (77,6 μM) in HCT-15 colon cancer cells 58
Figure 3.10. 12-hour histogram of ROS percentage values of Pd(II) compound (77,6 μM) in HCT-15 colon cancer control cells 59
Figure 3.11. 12-hour histogram of ROS percentage values of Pd(II) compound (77,6 μM) in HCT-15 colon cancer treatment cells 59
Figure 3.12. 24-hour histogram of ROS percentage values of Pd(II) compound (77,6 μM) in HCT-15 colon cancer control cells 60
Figure 3.13. 24-hour histogram of ROS percentage values of Pd(II) compound (77,6 μM) in HCT-15 colon cancer treatment cells 60
Figure 3.14. % Cell Viability Graph of HCT-15 colon cancer lines after pre-treatment with N-acetyl-L-cysteine (NAC) 61
Figure 3.15. Results of Autophagy Analysis 62
Figure 3.16. Migration images of Pd(II) compound application in HCT-15 colon cancer cell line 63
Figure 3.17. Graphical representation of the expression levels of prosurvival genes after 6 h treatment with Pd(II) compound (77,6 μM) in HCT-15 colon cancer cell line 64
Figure 3.18. Graphical representation of the expression levels of pro-apoptotic genes after 6 h treatment with Pd(II) compound (77,6 μM) in HCT-15 colon cancer cell line 65
Figure 3.19. Graphical representation of the expression levels of DNA damage or stress genes after treatment with Pd(II) compound (77,6 μM) for 6 hours in the HCT-15 colon cancer cell line 65

Figure 3.20. Graphical representation of expression levels of prosurvival genes after 24 h treatment with Pd(II) compound (77,6 μM) in HCT-15 colon cancer cell line 66
Figure 3.21. Graphical representation of expression levels of pro-apoptotic genes after 24 h treatment with Pd(II) compound (77,6 μM) in HCT-15 colon cancer cell line 66
Figure 3.22. Graphical representation of the expression levels of DNA damage or stress genes after 24 h treatment with Pd(II) compound (77,6 μM) in HCT-15 colon cancer cell line 67
Figure 3.23. AKT1 6h Gene Result 77
Figure 3.24. AKT1 24h Gene Result 77
Figure 3.25. ATG7 6h Gene Result 78
Figure 3.26. ATG7 24h Gene Result 79
Figure 3.27. BAG1 Gene Results 6h 80
Figure 3.28. BAG1 Gene Results 24h 80
Figure 3.29. BAG3 Gene Results 6h 81
Figure 3.30. BAG3 Gene Results 24h 82
Figure 3.31. BCL10 Gene Results 6h 83
Figure 3.32. BCL10 Gene Results 24h 83
Figure 3.33. BCLAF1 Gene Results 6h 84
Figure 3.34. BCLAF1 Gene Results 24h 85
Figure 3.35. BCLXL Gene Results 6h 86
Figure 3.36. BCLXL Gene Results 24h 86
Figure 3.37. BID Gene Results 6h 87
Figure 3.38. BID Gene Results 24h 88
Figure 3.39. BIM Gene Results 6h 89
Figure 3.40. BIM Gene Results 24h 89
Figure 3.41. BIRC2 Gene Results 6h 90
Figure 3.42. BIRC2 Gene Results 24h 91
Figure 3.43. BIRC3 Gene Results 6h 92
Figure 3.44. BIRC3 Gene Results 24h 92
Figure 3.45. BIRC5 Gene Results 6h 93
Figure 3.46. BIRC5 Gene Results 24h 94

Figure 3.47. BIRC6 Gene Results 6h 95

Figure 3.48. BIRC6 Gene Results 24h 95

Figure 3.49. BMI1 Gene Results 6h 96

Figure 3.50. BMI1 Gene Results 24h 97

Figure 3.51. BNIP1 Gene Results 6h 98

Figure 3.52. BNIP1 Gene Results 24h 98

Figure 3.53. BNIP3L Gene Results 6h 99

Figure 3.54. BNIP3L Gene Results 24h 100

Figure 3.55. CASP3 Gene Results 6h 101

Figure 3.56. CASP3 Gene Results 24h 101

Figure 3.57. CASP4 Gene Results 6h 102

Figure 3.58. CASP4 Gene Results 24h 103

Figure 3.59. CASP6 Gene Results 6h 103

Figure 3.60. CASP6 Gene Results 24h 104

Figure 3.61. CASP7 Gene Results 6h 105

Figure 3.62. CASP7 Gene Results 24h 105

Figure 3.63. CDC20 Gene Results 6h 106

Figure 3.64. CDC20 Gene Results 24h 107

Figure 3.65. CDK4 Gene Results 6h 108

Figure 3.66. CDK4 Gene Results 24h 108

Figure 3.67. DCR Gene Results 6h 109

Figure 3.68. DCR Gene Results 24h 110

Figure 3.69. DR4 Gene Results 6h 111

Figure 3.70. DR4 Gene Results 24h 111

Figure 3.71. DR5 Gene Results 6h 112

Figure 3.72. DR5 Gene Results 24h 113

Figure 3.73. ERCC1 Gene Results 6h 114

Figure 3.74. ERCC1 Gene Results 24h 114

Figure 3.75. ERCC3 Gene Results 6h 115

Figure 3.76. ERCC3 Gene Results 24h 116

Figure 3.77. FAS Gene Results 6h 117

Figure 3.78. FAS Gene Results 24h 117

Figure 3.79. GAD45A Gene Results 6h 118

Figure 3.80. GAD45A Gene Results 24h 119

Figure 3.81. GSTP1 Gene Results 6h 120

Figure 3.82. GSTP1 Gene Results 24h 120

Figure 3.83. LIG4 Gene Results 6h 121

Figure 3.84. LIG4 Gene Results 24h 122

Figure 3.85. MCL1 Gene Results 6h 123

Figure 3.86. MCL1 Gene Results 24h 123

Figure 3.87. MDM2 Gene Results 6h 124

Figure 3.88. MDM2 Gene Results 24h 125

Figure 3.89. MGMT Gene Results 6h 126

Figure 3.90. MGMT Gene Results 24h 126

Figure 3.91. NEK2 Gene Results 6h 127

Figure 3.92. NEK2 Gene Results 24h 128

Figure 3.93. NOXA Gene Results 6h 129

Figure 3.94. NOXA Gene Results 24h 129

Figure 3.95. PRDX1 Gene Results 6h 130

Figure 3.96. PRDX1 Gene Results 24h 131

Figure 3.97. PUMA Gene Results 6h 132

Figure 3.98. PUMA Gene Results 24h 132

Figure 3.99. RAD52 Gene Results 6h 133
Figure 3.100. RAD52 Gene Results 24h 134
Figure 3.101. SOD1 Gene Results 6h 135
Figure 3.102. SOD1 Gene Results 24h 135
Figure 3.103. XPA Gene Results 6h 136
Figure 3.104. XPA Gene Results 24h 137
Figure 3.105. XRCC5 Gene Results 6h 138
Figure 3.106. XRCC5 Gene Results 24h 138

ABBREVIATIONS

AKT2	AKT Serine/Threonine Kinase 2
APAF-1	Apoptotic Protease Activating Factor
ATG-7	Autophagy Related 7
ATM	ATM Serine/Threonine Kinase
ATR	ATR Serine/Threonine Kinase
AURKA	Aurora kinase A
BAD	BCL2 Associated Agonist Of Cell Death
BAG1	BAG Cochaperone 1
BAG3	BAG Cochaperone 3
BAG4	BAG Cochaperone 4
BAK1	BCL2 Antagonist/Killer 1
BAX	Bcl-2 Associated X-protein
BCL2	BCL2 Apoptosis Regulator
BCL2A1	BCL2 Related Protein A1
BCL10	BCL10 Immune Signaling Adaptor
BCL2L2	BCL2 Like 2
BECN1	Beclin 1
BFAR	Bifunctional Apoptosis Regulator
BIRC2	Baculoviral IAP Repeat Containing 2
BID	BH3 Interacting Domain Death Agonist
BIK	BCL2 Interacting Killer
BIM	Bcl-2 Interacting Mediator of cell death
BMI1	BMI1 Proto-Oncogene
CASP-6	Caspase 6
CAT	Catalase
BMF	Bcl2 Modifying Factor
CDC25C	Cell Division Cycle 25C
CDK4	Cyclin Dependent Kinase 4
DCR	Down Syndrome Chromosome Region
TNFRSF10A	TNF Receptor Superfamily Member 10A
ERCC1	Excision Repair Cross-Complementation 1
FADD	Fas Associated Death Domain

FAS	Fas Cell Surface Death Receptor
GADD45A	Growth Arrest And DNA Damage Inducible Alpha
GPX1	Glutathione Peroxidase 1
GRB	Growth Factor Receptor Bound Protein
GST1	Glutathione S-Transferase Pi 1
MDM2	MDM2 Proto-Oncogene
NOXA	NADPH Oxidase Activator 1
PUMA	P53-Upregulated Modulator Of Apoptosis
RAD52	RAD52 Homolog, DNA Repair Protein
XRCC5	X-Ray Repair Cross Complementing 5
LIG4	DNA Ligase 4
GAPDH	Glyceraldehyde-3-Phosphate Dehydrogenase
HPRT1	Hypoxanthine Phosphoribosyltransferase 1
YWHAZ	Tyrosine 3-Monooxygenase/Tryptophan 5-Monooxygenase Activation Protein Zeta
SOD1	Superoxide Dismutase 1
3-MA	3-Methyladenine
5-FU	5-Flurouracil
7-AAD	7-Aminoactinomycin D
AIF	Apoptosis inducing factor (Apoptosis inducing factor)
ATP	Adenosine Tri-phosphate
BCA	Bi- choninic Acid
BHR	Bcl-2 Homology Regions
BSA	Bovine serum albümin
CAD	Caspase Activating DNase
CK18	Cytokeratin 18
DAPK	Death Associated Protein Kinase
DD	Death Domain
DHEA	Dehydroepiandrosterone
DHT	Dihydrotestosterone
DISC	Death Inducing Signalling Complex
DMSO	Dimethyl Sulfoxide
DNA	Deoxy ribonucleic acid (Deoxyribonucleic acid)
DNA PK	DNA Dependent Protein Kinase (DNA-Dependent Protein Kinase)

EDTA	Ethylene Diamine Tetraacetic Acid
EGFR	Epidermal Growth Factor Receptor
ER	Endoplasmic Reticulum
FBS	Fetal Bovine Serum
FITC	Fluorescein Isothiocyanate
GST	Glutathione S-transferase
GTP	Guanosine Triphosphate
IGF	Insulin-Like Growth Factor
Kbp	Kilobase Pair
kDa	Kilo Dalton
MOMP	Mitochondria Outer Membrane Permeabilization
mTOR	Mammalian Target of Rapamycin
MTT	(3-(4,5-Dimethylthiazol-2-yl)-2,5-Diphenyl tetrazolium Bromide
NAC	N-asetil-L-sistein
PARP	Poly ADP-Ribose Polymerase
PBS	Phosphate buffered saline
PCR	Polymerase Chain Reaction
RT PCR (qPCR)	Real-time Polymerase Chain Reaction (quantitative PCR)
cDNA	Complementary DNA
Pd	Palladium
PI	Propdium Iodide
PS	Phosphatidylserine
Pt	Platin
PTEN	Phosphatase and Tensin Homologous Protein
Rb	Retinoblastoma
RNA	Ribonucleic Acid
ROCK1	Rho-Associated Helix-Forming Kinase 1
ROS	Reactive Oxygen Species
RPMI	Roswell Park Memorial Institute Medium
SDS	Sodium Dodecyl sulfate
SDS-PAGE	Polyacrylamide Gel Electrophoresis
SRB	Sulforhodamine B
TCA	Trichloroacetic Acid

TdT	Terminal Deoxynucleotidyl Transferase
TNF	Tumor Necrosis Factor
TRAIL	TNF Related Apoptosis Inducing Ligand
VEGF	Vascular Endothelial Growth Factor
z-VAD-FMK	General Caspase Inhibitor

CHAPTER 1

INTRODUCTION

1.1. Cancer

Cancer is a significant global issue, characterized by intricate molecular genetic and pathological processes that impact the development, advancement, and management of many types of malignancies. Using advanced technology in cancer research, particularly by fully understanding the biological mechanisms of cancer and employing novel informatics-based molecular genetic techniques, scientists have successfully unraveled intricate molecular pathways responsible for tumor development, invasion, and metastasis. Therefore, our understanding of cancer has expanded in comparison to past years (1,2). Researchers have comprehensively analyzed the molecular pathways involved in many types of cancer such as brain, blood, lung cancer. They have identified the specific molecular cell pathways that trigger to the development and spread of cancer by angiogenesis, tumorigenesis, and EMT (epithelial to mesenchymal transition) (3, 4). The rise in popularity of genomics, proteomics, bionformatics, and other related techniques and technologies has significantly transformed our understanding of cancer. This has highlight to the emergence of individualized diagnostic and treatment strategies as prominent approaches in the field (5). The many research and acquired information have provided a fresh perspective on the interactions among cancer cells and their tumor micro environment. Additionally, these studies have contributed to the creation of novel drugs and the design of drug development studies targeting specific genes within the pathways (6,7). Comprehensive research has been performed on the molecular biology of cancer, focusing on the genes including cancer development and cancer signal pathways. Despite the ongoing studies, there is still a strong interest in discovering new biomarkers and alternative treatment methods. The goal is to utilize this knowledge in clinical trials to improve treatment outcomes and increase patient survival rates. Consequently, the domain of molecular cancer biology remains a promising and ever-evolving area in the treatment of cancer.

1.1.2. Biology of Cancer

Cancer is a pathological condition characterized by the uncontrolled proliferation and metastasis of certain cells inside the body. Cancer can originate in almost every region of the human body, which is composed of many cells. Cancer cells may be categorized and designated based on their site of origin (Fig 1.1). A primary tumor is a kind of abnormal growth that begins and progresses at a single location in the body, ultimately becoming a solid mass. The vast majority of solid tumors arise at their initial location but may later undergo metastasis or spread to distant anatomical regions. These

extra cancers are reported to be invasive. An invasive tumor is a kind of cancer that originates from a specific tissue or cells, infiltrates them, and then spreads to surrounding healthy tissues (8,9).

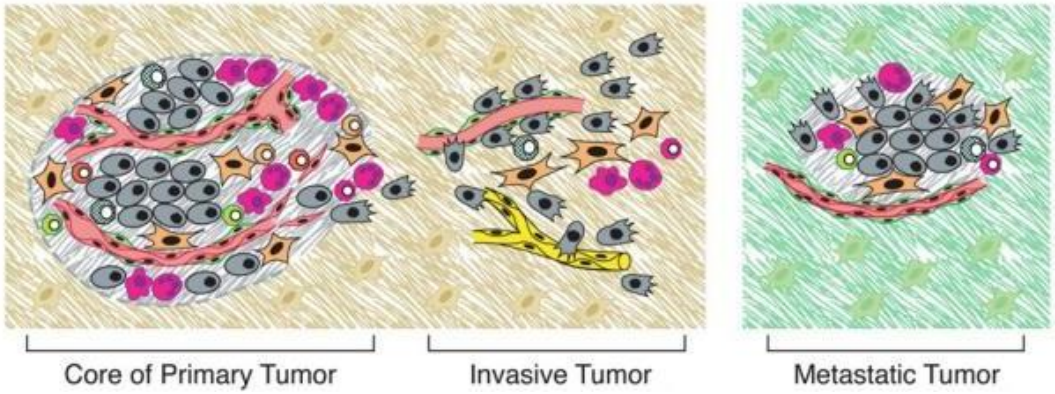

Figure 1.1. Tumor Types According to Their Origin

Cancer cells have distinct characteristics in compare to normal healthy cells. For instance, the mechanisms governing the cell cycle arrest significantly in cancer cells. Tumor cells exploit the cell cycle by manipulating mechanisms such as cell proliferation, replication, and growth to benefit themselves. Cancer cells have distinct characteristics that differentiate them from normal, healthy cells. These are sometimes referred to as cancer hallmarks. Approximately 11 years later, the first 6 characteristics were expanded to a total of 11 hallmark (10,13) (Figure 1.2).

1.1.3. Hallmarks of Cancer

The cancer hallmarks are a collection of biological characteristics that tumor cells acquire throughout their intricate evolution. The characteristics of this phenomenon are continuous cell division, evasion of growth inhibitors, spread to other tissues, indefinite replication, formation of new blood vessels, resistance to cell death, altered cellular glicose metabolism and invasion of the body immune system. Two distinct factors, namely the "tumor-promoting microenvironment and macroenvironment" and "cancer epigenetics, genome instability, and mutation," are crucial in facilitating the acquisition of cancer hallmarks by cells (11,12). The eight fundamental characteristics of cancer include continuous stimulation of cell division, the ability to replicate indefinitely, resistance to programmed cell death, stimulation of blood vessel formation, invasion and spread to distant sites, and disruption of cellular energy balance. Furthermore, the hallmarks of cancer, as described by experts, include many characteristics such as resistance to programmed cell death, promotion of tumor-related inflammation, and disrupted regulation of metabolism. Furthermore, the defining features of advanced cancer indicate two developing traits: alteration of sugar metabolism and avoidance of immune annihilation (12, 13). The hallmarks of cancer notion functions as a precious framework for

translational research focused on strengthening early detection, screening, therapy, and quality of life for individuals with cancer (14,15). Multiple types of cancer have 10 shared characteristics, known as "hallmarks," which dictate the process of normal cells transitioning into cancerous cells (8, 16). The hallmarks of cancer serve as a valuable conceptual tool for comprehending the underlying mechanisms and connections among various forms of human cancer, with possible implications for cancer treatment (17, 18).

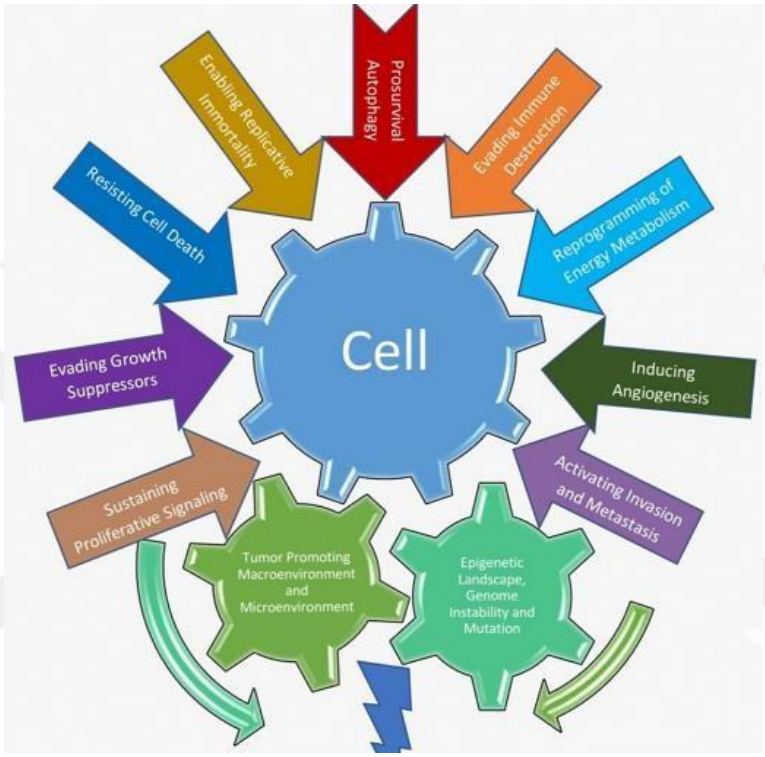

Figure 1.2. Hallmarks of Cancer

Typically, healthy cells possess all the necessary checkpoints in the cell cycle to regulate cell division and cell proliferation and growth. By responding to signals from these checkpoints, cells either continue dividing or halt division and enter a dormant state. Nevertheless, the circumstances vary with cancer cells. Signals that trigger to continiue cell cycle in normal cells, such as DNA damage or cell death, result in the activation of mechanisms that cell growth. Tumor cells exhibit the complete opposite pathway (19). Because of the disruption of certain proteins and signaling pathways, the cell cycle of cancer cells deviates from that of normal cells. Survivin, a protein linked to cell cycle initiation, is present during all phases of the cell cycle in cytokine-stimulated CD34+ cells. In contrast, it is only produced during the G2/M phase in cancer cells (20). Moreover, several chemicals play crucial functions in cancer cells by exerting their own unique influence on the cell cycle. For instance, studies have shown that it may trigger programmed cell death and halt the cell cycle in the G2 phase

via a route that relies on the p53 protein in ovary cancer cells that are resistant to cisplatin (21). For instance, research has shown that miRNA-372 inhibits cell development and triggers cell cycle arrest in the S/G2 phase in human cervical cancer cell lines (22). GAS5 has been discovered to cause growth arrest of gastric cancer cells by inhibiting the transition from the G1 phase to the S phase (23). Another instance is that, in contrast to healthy cells, cancer cells use a distinct glycolysis pathway exclusive to them. Healthy cells get the ATP they need existence of oxygen by the oxidative phosphorylation. During periods of insufficient oxygen or intense physical activity, the body temporarily relies on the glycolysis system. The scenario with cancer cells is precisely the inverse. Cancer cells persist in using glycolysis despite the existence of oxygen. The occurrence being cited to is known as the Warburg effect (24,29). Due to their incessant proliferation, cancer cells need a greater amount of energy compared to normal cells. They get their energy via this process. Another benefit for cancer cells is their ability to uptake increased amounts of glucose and generate larger levels of lactate (25,26). Furthermore, several molecules that guarantee the uninterrupted progression of this route have elevated expression levels (28). Oncogenic signaling pathways, including mTOR, BRAF, and c-Myc, have been shown to enhance glycolysis in cancer cells, resulting in the buildup of lactate in the tumor microenvironment (29,30). In addition, cancer cells possess metabolic adaptability that enables them to transition between sugar metabolism and oxidative phosphorylation during the development of tumors and the spread of cancer to different cell and tissue of the body. Put simply, cancer cells use cellular and metabolic pathways that align with their specific requirements. Cancer cells have successfully altered their whole metabolic process to ensure their survival, proliferation, and even metastasis. Thus, this aberrant and unregulated cell requires a much greater amount of energy for its rapid growth compared to typical, healthy cells. The occurrence of aberrant cell divisions and metabolic alterations is one of the ten fundamental characteristics of cancer (8, 31). Research has shown that blocking glycolic pathways might trigger programmed cell death, known as apoptosis, in cancer cells, particularly those that have an excessive amount of certain proteins like ErbB2. An example of this is the combination of glycolysis inhibitors with rapamycin, which has shown synergistic benefits in combating many forms of cancer. The PI3K/AKT/mTOR pathway is a crucial controller of glycolysis in cancer cells, impacting their metabolic activity and proliferation. Moreover, it has been shown that the glycolytic inhibitor 2-deoxyglucose stimulates several pathways that promote cell survival in cancer cells, such as the IGF1R signaling pathway. Approximately 50% of certain cancer types possess mutations that impede the production of genes responsible for suppressing tumor growth. Furthermore, the anomalous characteristics of cancer, such as the excessive uptake of glucose by the cell and the heightened synthesis of DNA, organelles, proteins, and fats, serve as evidence that it promotes the development and dissemination of tumors (32, 33).

One distinguishing characteristic of cancer is the development of a defensive mechanism that enables its survival, setting it apart from other diseases. Cancer cells experience several registered and metabolic challenges. However, they have developed specific temperature-based defensive mechanisms via metabolic reprogramming to counteract these pressures. When identifying the therapeutic target, it is crucial to understand the metabolic reprogramming that enables cancer patients to survive under diverse stressful settings (34,35). Due to variations in their response throughout the process of cancer healing. The primary cause for this is the enhancement of several therapies for cancer survival. It is advisable to use novel strategic approaches for cancer treatment plans in cases when the existing procedures may not be enough (36,37).

1.2. Colorectal Cancer (CRC)

Colon cancer is a complex illness with several molecular subtypes that have a substantial effect on prognosis, responsiveness to therapy, and clinical consequences. Colorectal cancer, overall known as colon cancer, is an important health issue that dramatically contributes to the morbidity and death associated with cancer. The molecular biology of colon cancer is an intricate and diverse route that involves genetic, epigenetic, and molecular alterations that cause the beginning, advancement, and spread of this illness. Gaining comprehension of these molecular pathways is crucial for the development of precise therapeutic interventions and novel pharmaceutical and therapy approaches. Colorectal cancer originates when normal cells in the colon or rectum lining undergo alterations and proliferate uncontrollably, resulting in the formation of an abnormal growth known as a tumor. The one of the different types of colon cancer is determined adenocarcinoma (38,39).

1.2.1. Anatomy of Colorectal Cancer

Several research have been undertaken to examine the molecular and histological characteristics of colon cancer tissue to receive unsurpassed learning of its architecture. Studies have identified certain proteins and genetic alterations in colon cancer tissues that have a role in the advancement and spread of the illness. The large intestine is a component of the gastrointestinal (GI) tract, which is also known as the digestive system. The colon and rectum comprise the large intestine, which is crucial for the body's waste processing function. The colon comprises the first 5 to 6 feet of the large intestine, while the rectum constitutes the last 6 inches, terminating at the anus. The colon and rectum consist of five distinct regions (Figure 1.3). The ascending colon is the segment that stretches from the cecum, a pouch-like structure, to the region of the colon in proximity to the liver. The cecum is the first segment of the large intestine where the small intestine discharges its contents. It is located on the right side of the abdomen. The transverse colon traverses the superior region of the abdomen. The descending

colon transports waste down the left side. Ultimately, the waste is transported via the lower sigmoid colon to the rectum, advancing a few millimeters. Excrement is expelled from the body via the anüs (40,41).

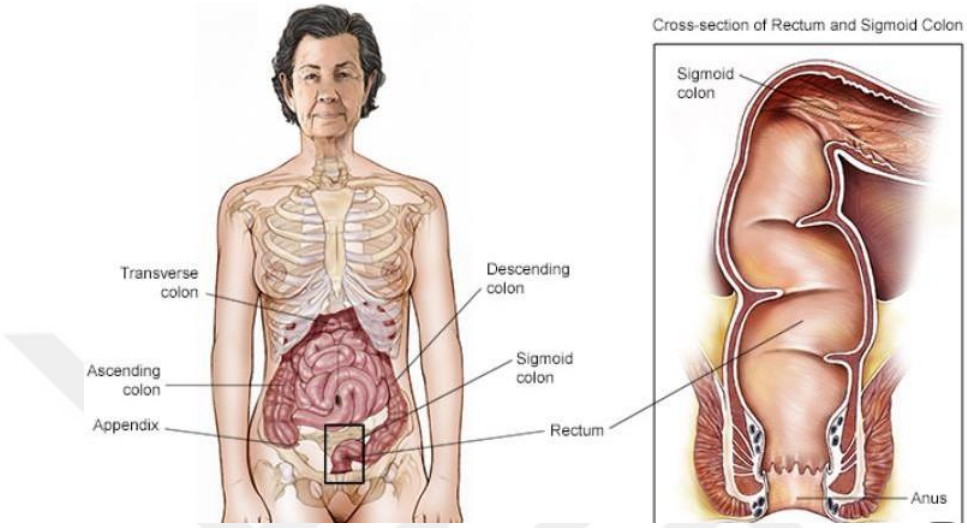

Figure 1.3. Anatomy of Colorectal Cancer

Staining tissues for histological imaging enables the visualization of cancer's morphological characteristics, facilitating the categorization procedure. It displays several structural characteristics of intestinal glands in colorectal cancer, such as cellular arrangement, gland development, and stromal components (Fig 1.4). Colon tissue typically exhibits a consistent and uniform structure, but malignant tumor tissues display a broader and more varied disruption of normal histological characteristics (42,43).

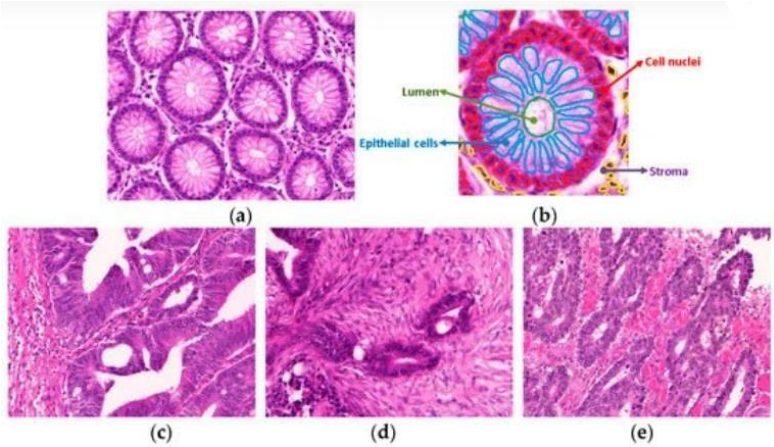

Figure 1.4. Different Type of Colon Tissue

Researchs have been shown that some proteins are increased in human colon cancer tissues, indicating the significance of mitochondrial proteins in the survival and ability of cancer cells to respond to oxidative stress (44). Furthermore, several cellular enzymes have been shown to facilitate epigenetic alterations, which have been linked to heightened proliferation and metastasis in colon cancer. This underscores the significance of histone demethylases in determining the aggressiveness of the illness (45). Moreover, scientific studies have shown the presence of viral DNA in the tissue membrane of the human colon and in cases of colorectal cancers. This indicates a possible connection between viral infections and colorectal neoplasms (46). Also research has used cutting-edge imaging methods to analyze recently removed human colonic tissues and distinguish between distinct tissue types by examining their absorption and refractive index spectra. These imaging approaches provide insights into the anatomical makeup of colon cancer tissues, serving diagnostic and research objectives (47). Moreover, the detection of distinct biomarkers and molecular changes in colon cancer tissues has unveiled the advancement of the illness and possible targets for treatment. These indicators provide valuable information on the molecular composition of colon cancer and its effect upon patient outcomes. Consequently, the structure of colon cancer tissue is composed of a complex network of molecular, genetic, and histological characteristics that impact the behavior of the illness and how it responds to therapy (48,49).

1.2.2. Colorectal Cancer (CRC) Epidemiology

Epidemiology is a scientific discipline that investigates the patterns of occurrence and spread of various illnesses, including cancer, across diverse populations. It is regularly updated on an annual basis. As of 2024, it will be essential to compile all research on the epidemiology, risk factors, treatment results, and molecular processes of colon cancer in order to develop comprehensive strategies for early detection and tailored treatment methods. By consolidating the latest study results, we may enhance our comprehension of colon cancer epidemiology and lay the groundwork for improved patient outcomes in the future (50,51). Recently, colorectal cancer (CRC) has consistently ranked as one of the most prevalent cancer in males and women in terms of global occurrence (Figure 1.5). Additionally, it ranks as one of the most worst type of cancer. Experts predict that the mortality rate will rise by a factor of ten by the year 2035 (52,53).

Figure 1.5. Colon Cancer Epidemiology

1.2.3. Stages of Colon Cancer

Categorizing colon cancer into distinct subtypes based on their molecular and genetic features has enhanced our understanding of the illness and facilitated the development of novel therapeutic approaches. Recent research has discovered several molecular subtypes of colon cancer, each exhibiting distinct features. Studies that have classified colon cancer into molecular subtypes based on gene expression patterns have shown distinct variations in gene expression and signaling pathways (54,55). These subcategories provide current information on the many underlying causes of colon cancer. Therefore, innovative and individualized therapy approaches are unveiled. Therefore, this molecular genetic information also has advantages for the clinic (56). Furthermore, research on certain microRNAs in relation to epigenetics suggests that each specific kind of colon cancer elicits a distinct immune response (57). These subgroups provide crucial insights into the tumor microenvironment, immunological responses, and possible biomarkers for prognosis and therapy choice. Researchers integrated proteomic, genomic, and informatics data allowing its use in clinical settings. Therefore, many molecular subtypes of colon cancer were categorized (58). The stage of colon cancer is subject to change both when diagnosis and over the course of therapy. Colon cancer is classified using both primary and the Tumor, Node, Metastasis (TNM) staging system, as well as Stage Grouping, which categorizes the disease as Stage 0, I, II, III, or IV. Primary stages may be further categorized into more precise subtypes (Figure 1.6-7). For instance, Stage II might be separated into stage IIa, IIb, or IIc. The subtype of the stage can have an impact on the available treatment choices. The efficacy of the therapy may be contingent upon the stage of diagnosis. Colon cancer advances through many phases, beginning with the main tumor, each exhibiting distinct features. Right colon cancers are characterized by their bigger size and more invasiveness compared

to left colon tumors. Furthermore, the outlook for colon cancer differs according on the phase of the disease. Patients diagnosed with stage III left-sided colon cancer have more favorable outcomes in comparison to patients diagnosed with other stages, as shown by studies (59,60).

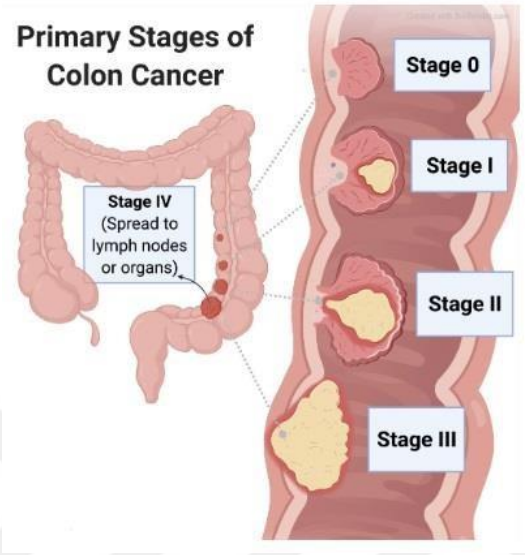

Figure 1.6. Primary stages of Colon Cancer

For the colon cancer staging is a complex process that involves several factors, such as T stage, lymph node status, and the need of adjuvant treatment. The TNM staging approach is based on evaluating the dimensions of the tumor, the extent of lymph node infiltration, and the existence of metastases on other organs or tissues. Lymph nodes have a dramatically affect not only the diagnosis of colon cancer but also for categorizing all types of cancer into specific subgroups (Fig 1.7). Furthermore, scientists have also categorized stage I/II/III colon cancer rely on the status of lymph nodes (mN0, mN1, and mN2) (61,62). Consequently, a novel categorization system was created by merging T stage and lymph node status. The categorizations are crucial in enhancing the efficacy of illness therapies. For instance, it is well recognized that adjuvant chemotherapy is helpful for individuals with stage III colon cancer (63). Nevertheless, investigations are currently under progress for stage II illnesses. The staging of colon cancer is crucial for determining survival rates and the efficiency of therapy. The relative survival rates for 1, 3, and 5 years decline significantly when colorectal cancer advances from stage 0 to stage 4. Multiple research have concentrated on creating classification methods to more effectively classify patients according to illness features and outcomes (64,65). For instance, the T stage, which assesses the degree of initial tumor infiltration, has significant importance in categorizing cancer subtypes, particularly in stage II colon cancer. Recent iterations of classification

methods have enhanced the detection of high-risk stage II colon tumors, enabling doctors to more accurately evaluate prognosis (66).

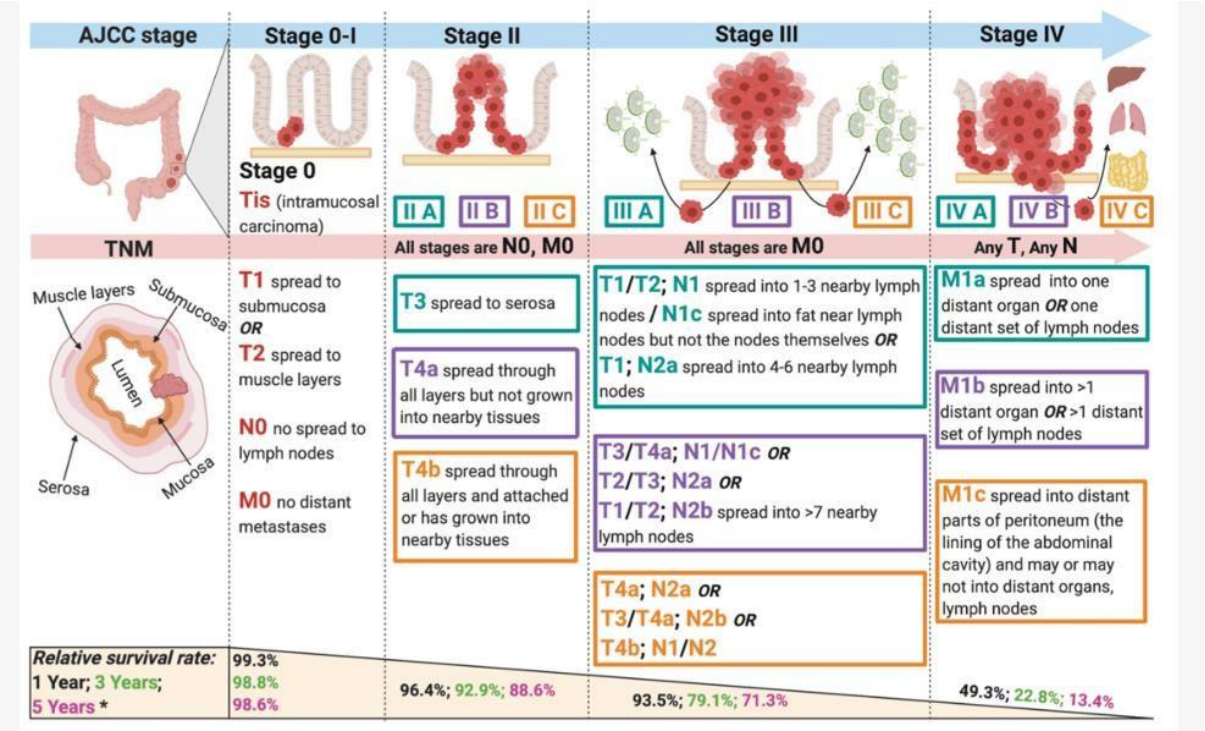

Figure 1.7. Colorectal Cancer TNM staging

1.2.4. Colon Cancer Risk Factors

Colorectal cancer is a important global overall health issue, influenced by many diverse risk factors. Gaining knowledge about these risk factors is crucial not only for colon cancer, but for all forms of cancer. Colon cancer risk factors include several behavioral, genetic, and environmental variables that influence an individual's vulnerability to the illness. Studies have shown that lifestyle variables, such absence of physical exercise, obesity, and unwholesome dietary, elevate the likelihood of acquiring colon cancer. Physical inactivity and obesity have been linked to a higher likelihood of developing colon adenomas. In addition, nutritional variables and alterations in the gut flora may impact the impact of physical exercise on levels of metabolic pathways (66,67). Furthermore, some hereditary factors may also conduce to the susceptibility of developing colon cancer, in addition to the aforementioned environmental causes. Various variables, including a genetic predisposition, genetic alterations and metabolic disorders such as insulin resistance syndrome, significantly elevate the likelihood of getting colon cancer. Furthermore, there is a correlation between the socioeconomic class of a neighborhood and the different chances of developing colon and rectal cancer. This

correlation is also influenced by behavioral factors. Researchers have been analyze the combined impact of these variables in order to identify groups at a greater risk of developing colon cancer and implement tailored treatment approaches to alleviate the burden of the disease. Researchers may create targeted prevention, early diagnosis, and tailored treatment options for colon cancer by studying the impact of lifestyle choices, genetic predispositions, and environmental exposures (68,69).

1.2.5. Colon Cancer Diagnostic Criteria

Microarray gene expression profiling is an effective method for identifying gene signatures that might predict prognosis. Gene expression analysis under supervision has been used to uncover gene signatures for the identification of colon cancer patients at risk of recurrence. Also endoscopy is the primary diagnostic technique, which may be performed using either sigmoidoscopy (since more than 35% of tumors are found in the rectosigmoid region) or, preferable, a whole colonoscopy. Endoscopy has many benefits, such as accurately determining the location of a tumor and doing a biopsy, detecting more tumor lesions and removing polyps. The comprehensive assessment should encompass the morphological identification of the specimen. Details of the surgical procedure performed, precise determination of the tumor's location and size, identification of any visible tumor perforation, classification of the histological type. To evaluation level of the tumor's extent within the bowel wall and neighboring organs (T stage), measurement of the distance between the cancer and margins that have been surgically removed (including those on the proximal, distal, and radial sides). identification of any tumor deposits. Assessment of invasion, observation of tumor budding, documentation of the site and number of regional lymph nodes removed. Then any potential penetration by cancer cells (N stage), and lastly, examination for possible involvement of other organs if they were removed or biopsied (M stage) (70,71).

1.2.6. Genetic Features of Colorectal Cancer

Colon cancer is characterized by a wide range of genetic and epigenetic factors that cause the conversion of healthy colon epithelial cells into cancerous tumors. The genetic foundation of colon cancer include mutations in tumor suppressors and oncogenes, changes in DNA methylation, and variations in signaling pathways. Epigenetic alterations, including DNA methylation, histone modifications, and dysregulation of non-coding RNAs, are intricate processes that impact the molecular etiology, gene expression levels, and all cellular activities associated with colon cancer. Genetic predispositions, including a family history of cancer, environmental variables, and bad lifestyle choices, all contribute to the development of colon cancer and make it more complicated.

miRNAs play a crucial role in controlling gene expression in colon cancer. They exhibit specific expression patterns that are linked to the advancement of tumors, the spread of cancer cells to other parts of the body, and the effectiveness of therapy. The molecular subclassification of colon cancer, using miRNA expression patterns, has yielded significant insights into the diversity and clinical significance of the illness. Genomic profiling studies provide data on the genetic changes in colon cancer that are linked to various clinical outcomes and therapeutic responses. The identification of novel genetic markers, particularly those implicated in the immune response and lymphangiogenesis, has enhanced our comprehension of the development and treatment approaches for colon cancer (72,73).

1.2.7. Histological Features of Colorectal Cancer

The histological characteristics of colon cancer include several structural alterations that expedite the development of tumors. Comprehending these histological characteristics is essential for precise identification, categorization of risk, and tailoring therapy for individuals with colon cancer. An examination of colon cancer at the cellular level reveals details on the tumor's cellular structure, the condition of the tissue, and the arrangement of the tissue as shown below on healthy colon tissue (Fig 1.8). Different histological subtypes of colon cancer, including adenocarcinoma types, have been exhibit distinct morphological characteristics that impact clinical outcomes and therapeutic approaches (74). Histological characteristics, including not clearly differentiated or not differentiated cells, mucinous differentiation may serve as prognostic indicators in colon cancer. These characteristics are linked to a more advanced stage of the illness, a more aggressive activity of the tumor, and worse prognosis for the patient. Put simply, the histological type of a tumor plays a crucial role in determining the appropriate therapy for patients in a clinical setting. Furthermore, the examination of colon cancer cells by histological assessment may provide crucial insights into tumor grade, lymphovascular invasion, perineural invasion, and other high-risk characteristics that impact therapy recommendations and patient prognosis. Identifying unfavorable histological characteristics in colon cancer might affect decide on whether to use adjuvant chemotherapy (75).

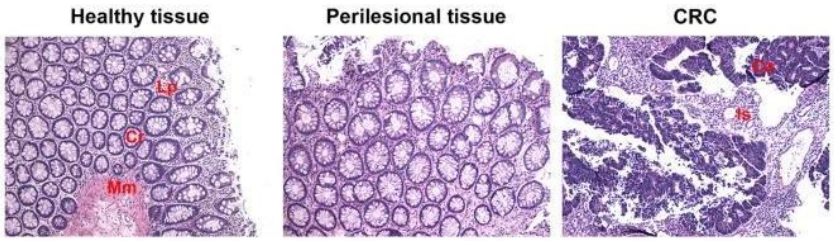

Figure 1.8. Healthy Colon Immunohistochemistry staining

1.2.8. Subtypes of Colorectal Cancer

In order to find new subtypes, an alternative technique might be used including the use of certain analyses. Clustering algorithms are used to bring together samples that have similar expression characteristics. This method has the potential to give rise to new subtypes of colon malignancies or reinterpret the absence categorization, leading to the formation of more homogeneous groupings of tumors. Molecular tumor homogeneity is necessary to delineate distinct molecular pathways that are impacted, to identify specific pharmacological targets within each subgroup for therapeutic interventions, or to develop personalized survival classifiers. Prior efforts to categorize colon cancers into distinct subgroups. Attempts to establish sub-classes or establish a relationship between gene expression and Dukes phases using unsupervised analysis have not shown definitive results. While several writers successfully classified normal colon, others could not identify any new subgroups. Several publications have shown disparities in gene expression between normal and malignant tissue, as well as variances in gene expression between metastatic and nonmetastatic samples. Additionally, these findings have been able to distinguish normal tissue from initial carcinomas, as well as from liver metastases and carcinomatoses. Other scientists have using class comparison to identify a gene signature that may be utilized to classify patients as either low-risk or high-risk. Another intriguing method included identifying a gene expression profile derived from an experimental model of colon cancer metastasis. This profile was capable of accurately predicting cancer recurrence in individuals diagnosed with colon cancer. According to reports, the EGF receptor pathway was shown to be increased in colon metastasis, whereas angiogenesis was found to be increased in liver metastasis. Regrettably, despite the existence of a wide range of gene signatures documented in scientific literature, hardly any of them have been used in clinical practice. Prognostic and predictive criteria are necessary to provide reliable information for medical choices in regular clinical practice. Furthermore, comprehending the molecular mechanisms that underlie each tumor subtype might possibly aid in the identification of the most suitable treatment regimen in the future (76,77).

1.2.9. Intrinsic Subtypes of Colorectal Cancer

Recent studies have shown the use of genome-wide gene expression profiling to subtype colon cancer. Several tumor subtypes have been found, which provide prognostic information. However, only a limited number of unique subgroups have also been identified, which are associated with therapy response. Figure 1.9 illustrates the association between pathological parameters, such as tumor location, and molecular markers, such as MSI status, across several tumor types. Intrinsic CRC subtypes are identified by analyzing clinical, pathological, and molecular commonalities. There are five distinct subtypes that may be identified: consensus molecular subtype like CMS 1, CMS2, CMS3,

CMS4, and an unidentified subtype (Fig 1.9). Each unique intrinsic subtype is shown in one of the CMS, as seen in this diagram. (MSI refers to microsatellite instability in tumors, whereas MSS refers to microsatellite stability in tumors. CIN, on the other hand, stands for chromosomal instability. Mut refers to mutations, wt stands for wild-type, and TA refers to transit amplifying) (78,79).

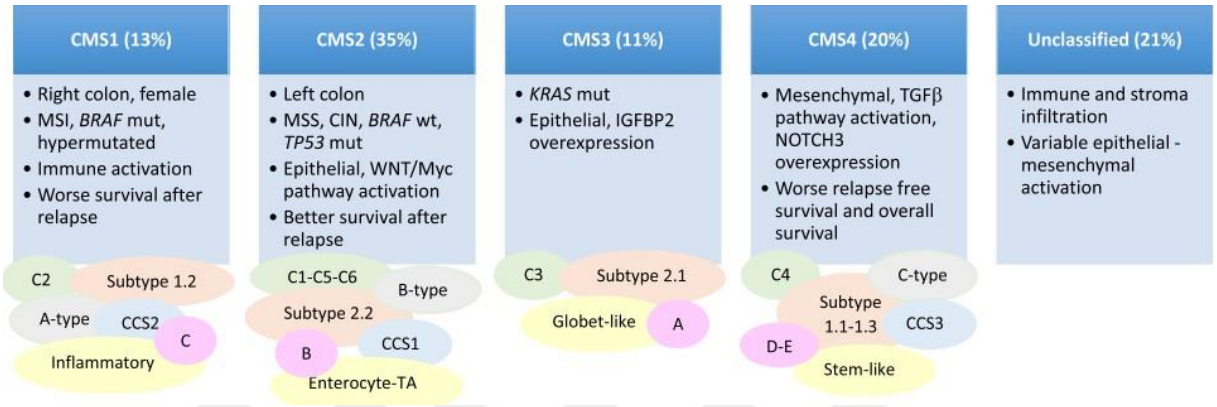

Figure 1.9. Intrinsic Colon Cancer subtypes

1.3. Cancer Therapy

Cells exhibiting genetic damage undergo uncontrolled division and proliferation, in contrast to normal, healthy cells. Cancer leads to the degradation of the structure and functionality of the tissue or organ. The immune system of the body plays a significant role in combating cancer cells. Nevertheless, this protection is not always adequate. Cancer has the ability to metastasize and move to other regions of the body. The process you are referring about is known as metastasis. The prevailing cancer kinds in our nation and globally include lung, breast, and colon cancers. Furthermore, other subcategories of cancer manifest in various tissues and organs. The main goal of cancer treatment is to eliminate the malignant tissue via surgical procedures or other therapeutic approaches, with the goal of preventing its recurrence inside the body. The field of cancer therapy is seeing fast development in both treatment approaches and medications, thanks to the progress made in scientific research and technology. The primary therapeutic modalities used for cancer patients may be enumerated as follows: Medical procedures include as surgery, chemotherapy, radiotherapy, immunotherapy, hormone treatment, and light therapy. For some patient, a single therapy strategy may be enough. Multiple therapy modalities are used in conjunction for some forms of cancer. This treatment approach is referred to as combination therapy. The therapeutic approach for cancer is entirely tailored to each individual patient. The objective of cancer therapy is to achieve total

eradication of cancer cells from the body and prevent the reoccurrence of malignant cells. The adverse effects of the illness may be relieved in some instances of advanced-stage metastatic cancer, rely on the specific kind and stage of the cancer. The objective is to extend the patient's lifespan, since the body will not get rid of malignant cells. Multiple strategies have been devised to battle diverse forms of cancer, ranging from conventional chemotherapy to cutting-edge personalized targeted medicines and immunotherapies (80). The development of novel drugs, such as PARP inhibitors like niraparib, for the therapy of ovary tumor has revolutionized cancer therapy by providing innovative approaches for customized and highly successful treatment regimens (81). A separate research focused on the development of screening techniques, such as the ABC approach, for the detection of stomach cancer. With an emphasis on customized medicine, focused therapies, and interdisciplinary methods, the ongoing development of cancer therapy is expected to lead to a progressive improvement in success rates. The area of cancer therapy is progressing towards a future where enhanced clinical results and higher level of life for cancer patients are prioritized via the use of breakthrough medicines, precise diagnostics, and complete patient care techniques.

1.3.1. Chemotherapy

Chemotherapy is a medical treatment including of medicines to kill or inhibit the growth of cancer cells. It is the administration of chemotherapy medications to the patient via various means with the aim of eradicating cancer cells. Chemotherapy is used to supress the proliferation, replication, and metastasis of tumors. This mechanism impacts both fast dividing cancer and normal cells. So chemotherapy has a detrimental impact on healthy cells, leading to the development of side effects in patients. Potential adverse effects resulting from chemotherapy-induced damage to healthy cells in patients include diminished appetite, nausea, vomiting, and weakness. It is a medical process that takes into account factors such as the kind and location of the tumor, the extent of its dissemination, the general health state, and the age of the patient. Chemotherapy can be classified in 2 categories:

1. Neoadjuvant chemotherapy: is administered to reduce the size of the metastasized tumor. The patient is prepared for the surgery. Furthermore, it is feasible to differentiate malignant tissue from normal tissue. It is mostly used for treating localized but advanced forms of cancer, such as breast, colon, and rectal cancer.

2. Adjuvant Chemotherapy: Following surgical removal of the tumor, this treatment is administered to eradicate any residual cancer cells in the body. The objective is to decrease the likelihood of cancer relapse. It is often referred to as prophylactic therapy. Chemotherapy medicines include a diverse range of more than 100 distinct kinds of medications. These drugs are delivered at separate intervals

to reduce adverse effects and potential interactions. The administration technique is customized to the every person and is designed to enhance the drug's efficacy.

Chemotherapy medications may be delivered to patients using many methods:

1. Intravenous chemotherapy is often delivered via the brachial vein in the arm. Occasionally, the medication may be delivered via a catheter into the body's bigger veins.

2. Intramuscular or subcutaneous chemotherapy involves the administration of the medication by injection. The substance is administered intramuscularly, specifically targeting the abdomen, arm, and leg muscles.

3. Oral chemotherapy refers to the management of chemotherapy medications in the form of pills or capsules. It is ingested via the mouth.

The frequency of chemotherapy delivery varies based on the specific chemotherapy regimen. Chemotherapy is administered in scheduled regimens, commencing with the first session. The patient is aware of the frequency and duration of his chemotherapy treatments. Each session of chemotherapy might vary in duration, ranging from a few minutes to many days. During the course of therapy, certain time periods are allocated for the patient to engage in rest and recuperation. The number of cycles, length, or kind of medicine is subject to variation according on the patient's reaction to therapy (82,83).

1.4. Drug Resistance

Patients face a major obstacle in the form of medication resistance, which is produced by complex genetic pathways that hinder the efficiency of cancer treatment. Several studies have been conducted to understand the molecular pathways that contribute to the development of treatment resistance in cancer cells. Research has shown many molecular mechanisms associated with treatment resistance in some types of cancer, including ovary cancer. The mechanism via which cancer cells acquire resistance has been well elucidated (85,86). Gaining insight into the molecular basis of medication resistance is crucial for addressing therapeutic obstacles and devising improved, precise treatment approaches. The connection between ATP-binding cassette carriers and signaling pathways that d to treatment resist in ovary cancer has been elucidated in research (87). Furthermore, studies have shown that tumor stem cells including drug resistance and have identified some cell types within this group that may be used as a therapeutic approach in clinic (88). Research on the BRCA1 signaling system in breast cancer has provided insight into the connection between resistance mechanisms and BRCA1 (89). The identification of novel therapeutic targets, such as some miRNA species involved in the

development of tumors and invasion, has also offered a fresh viewpoint (90). The presence of multi drug resistance (MDR) in tumor cells is a significant obstacle in chemotherapy as it diminishes the efficacy of several anticancer medications. MDR is primarily caused by ATP-dependent transporters (ABC transporter protein), which are a group of membrane proteins that actively remove medications from cells. This process reduces the amount of pharmaceuticals within the cells, leading to lower drug concentrations and ultimately treatment failure. Specifically, P-glycoprotein (P-gp/ABCB1), multidrug resistance-associated protein 1 (MRP1/ABCC1), and breast cancer resistance protein BCRP/ABCG2) facilitate multidrug resistance (MDR) by promoting the removal of drugs from cells (91,92). ABC transport proteins use the ATP to actively expel a diverse scope of chemotherapy drugs from inside the cell. Consequently, it diminishes the buildup of medications in cancerous cells, leading to the development of drug resistance, preventing the entry of drugs into the cell (93,94). Elevated levels of ABC transporters such as MRP1 and BCRP, have been linked to unfavorable treatment results and low rates of survival (95). Furthermore, to address multidrug resistance (MDR) and enhance the efficacy of chemotherapy, a separate research devised many approaches to regulate the activity of ABC transporters. These approaches included manipulating the PI3K/Akt signaling pathway and using plant phenols (96,97). As our learning of the intercellular communication and molecular pathways between cancer cells and the tumor microenvironment improves, it is anticipated that novel remedies and treatment strategies for drug resistance will be devised.

1.4.1. Cis-Platin Resistance

Various types chemotherapy medicines origine of platinum family, including cisplatin, carboplatin, and oxaliplatin, are often used in the treatment of different types of malignancies. Nevertheless, the inherent resistance of cancer cells to these medications diminishes the efficacy of cancer therapy. Gaining a comprehensive understanding of the molecular and genetic factors that contribute to platinum resistance is crucial in order to effectively eliminate this resistance. Studies have examined the intricate molecular pathways linked to platinum resistance in diverse cancer types and uncovered many methods used by cancer cells in order to evoid the harmful effects of platinum medicines (98). For instance, it is known that DNA repair mechanisms, mutations, and genomic alterations in certain genes, such as BRCA1 and BRCA2, which have become biomarkers in lung cancer, contribute to the development of resistance to platinum-based treatments (99). Furthermore, researchers have examined the synergistic effects of platinum medicines and other inhibitors to get insights into how pharmacological interactions at the cellular level might impact the absorption of platinum and, therefore, the efficacy of therapy (100). In addition, the advancement of novel therapeutic options, such as platinum-loaded nanoparticles and medicines that specifically target mitochondrial DNA,

elucidates the continuous endeavors to enhance treatment efficacy by surmounting platinum resistance (101,102). Another ongoing study is examining the multiple effects of certain reductase molecules on cisplatin resistance. Additionally, researchers are investigating the involvement of certain miRNA molecules in platinum resistance (103,104). The ongoing endeavors to combat platinum resistance and create novel cancer therapies persist via the integration of several disciplines, including nanotechnology, genetics, and target-specific drug design. The outcomes of scientific research aimed at addressing medication resistance will provide promising prospects for novel therapies in clinical settings.

1.5. As an anti cancer agents: Chemical Compounds

A wide range of heterogeneous metal complexes, characterized by distinct chemical structures, may serve as potential anti-cancer therapeutic candidates, offering an alternative to traditional chemotherapy medications. Significant achievements have been made, particularly in the use of combination therapies including biomolecules like inhibitors or nanoparticles. In addition to this, copper, ruthenium, zinc, nickel, silver, and gold may also serve as active constituents in newly formulated medications. Certain platinum-based medications, including cisplatin, are extensively used in the treatment of cancer. Nevertheless, the primary concern about the medications mentioned in the literature and used in chemotherapy is the adverse effects they induce in patients. High dosages of some chemotherapeutic medications may result in significant toxicity, leading to adverse side effects. Drug resistance mechanisms may arise in some individuals in response to these medications (105). To address these issues, several investigations are conducted to synthesize and characterize chemical substances as an alternative. Currently, several medications are used not just for colon cancer but also for cancer therapy in general. Unfortunately, these medications diminish the quality of life for patients due to their adverse effects. Hence, it is basic to discovery novel medications that have minimal adverse effects on patients. In recent years, chemicals produced from palladium have been widely used in medications that exhibit reduced toxicity. In the last twenty years, the Palladium complex has become more popular as a novel chemotherapeutic medication due to its chemical composition resembling Platinum and its exceptional effectiveness. Palladium-containing metallic compounds have undergone extensive testing as anti-cancer drugs in recent years, with promising findings (106,107).

Palladium-containing compounds may be classified into 2 distinct groups:

1. Individuals with a single palladium atom

The first set of compounds has a solitary palladium atom positioned at the core. Typically, these compounds consist of pyridine-like substances that exhibit significant biological efficacy.

2. Individuals with two palladium atoms

The second group consists of two palladium atoms positioned near the center (108).

This research have been determined the anti-cancer effects of a palladium (II) compound on the HCT-15 colon cancer cell line.

1.5.1. Palladium Compounds in Cancer Therapy

Carcinogenesis is an intricate process that requires the synchronized interaction of several genes, proteins, signaling pathways, and cell types. Consequently, the question of how to enhance the efficacy of cancer therapy is a subject of ongoing investigation. Currently, chemotherapy, being the primary therapeutic choice, is inadequate in the context of available medications, and it fails to offer effective treatment for several cancer types. Hence, the emergence of novel cancer prophylactic medications in recent times is seen as a captivating and auspicious domain. The use of metal compounds as medications has been prevalent, particularly in cancer therapy, owing to their promising efficacy against a diverse range of tumor cell lines (109,110). Studies have shown that anticancer drugs containing metal compounds like Pt and Pd alter the cytotoxic and apoptotic effects by inducing the creation of interstrand cross-links and DNA adducts inside the DNA molecule (111).

Palladium (Pd) is a metal compound that has antifungal, antiviral, anticancer, and antibacterial properties. Chemicals with this structure are favored because to their high solubility in water, ability to readily traverse membranes and interact with DNA inside cells, and reduced incidence of adverse effects. Furthermore, research has shown that Pd (II) compounds induce apoptosis by enhancing cell death in cancer cells (112,113). Furthermore, it has been shown that Pd (II) compounds induce this cytotoxic impact by inflicting significant DNA damage (114). Cisplatin, carboplatin, and oxaliplatin are platinum-based anti-cancer drugs that have been in use for 30 years. They are often used in clinical settings to treat many forms of cancer, such as ovarian, testicular, uterine, head, neck, small cell lung, colorectal, cervix, and lymphoma (115,116). Currently, there is a growing number of tumor-inhibiting metal compounds being synthesized, alongside the already effective metal-based therapies. These compounds have various modes of action. Palladium derivatives; It has cytotoxic effectiveness comparable to typical platinum-based medications like cisplatin, carboplatin, and oxaliplatin, while also having less adverse effects than other heavy metal anti-tumor chemicals. Cisplatin, although widely recognized as the most potent anti-tumor medication globally, is hindered by its significant toxicities such as nephrotoxicity, neurotoxicity, vomiting, and nausea. Consequently, the dosage administered to patients is restricted. Apoptosis, sometimes known as programmed cell death, is a biological process. Cancer cells of many kinds may acquire resistance to cisplatin, a commonly used drug in cancer treatment, by mechanisms such as inactivation (117,118). Pd (II) compounds are

believed to possess anti-tumor capabilities due to their chemical and structural resemblance to Pt (II) compounds. Recent studies have shown that some Pd (II) compounds have notable cytotoxic effects in laboratory settings, surpassing the effectiveness of commonly used platinum-based medicines such as cisplatin, carboplatin, and oxaliplatin (119,120). Furthermore, many Pd compounds have been shown to have greater antitumor efficacy and less renal damage compared to cisplatin, a commonly used medication in cancer therapy (110,121).

Ulukaya and colleagues have been describe that the chemical Pd (II) compounds exhibit growth suppressing and cytotoxic properties. The effects of it on human breast cancer cell lines (MDA-MB-231 and MCF-7) were examined, taking into account the dosage and duration of exposure. The in vitro experiment has proven the powerful inhibitory impact of the Pd(II) compound on growth. Furthermore, this phenomenon was validated in live Balb/c mice. It was noted that the Pd compound successfully hindered the development of tubules on the matrigel, suggesting its anti-invasive activity in MDA-MB-231 cells. In this work, it was shown that the Pd (II) molecule triggers apoptosis by activating the apoptotic cell death genes DR4 and DR5 (109,110). Ulukaya and colleagues have been also examined the suppressive effects on growth of novel Pt (II) and Pd (II) compounds in three distinct lung cancer cell lines (A549, H1299, and PC3). Overall, the study demonstrates that the Pd (II) compound effectively hinders cell growth in all cell lines by impeding mitosis and promoting necrotic cell death. Furthermore, this anti-growth impact surpasses that of cisplatin, the conventional chemotherapy drug for lung cancer (110). Upon comparing the impact of the examined Pd (II) compounds on various types of human cancer cells with doxorubicin, it was determined that the Pd (II) compounds exhibited noteworthy cytotoxic action. Consequently, these research have dramatic affect in advancing cancer therapy and expanding the scope of novel targets and techniques.

1.5.2. Structure of the Palladium Compound

The Pd(II) compound used in this thesis was synthesized by Prof. Dr. Veysel Turan Yılmaz from Uludağ University, Faculty of Science, Department of Chemistry. The compound was produced, analyzed and then reported and developed by Prof. Dr. Veysel Turan Yılmaz and his research team. Palladium (II) ions are used in the production of a palladium (II) compound (Fig 1.10). The coordination of chloride ions (Cl-) and water leads to the formation of barbituric acid. Below is the molecular structure of the Pd(II) complex, which has an open configuration.

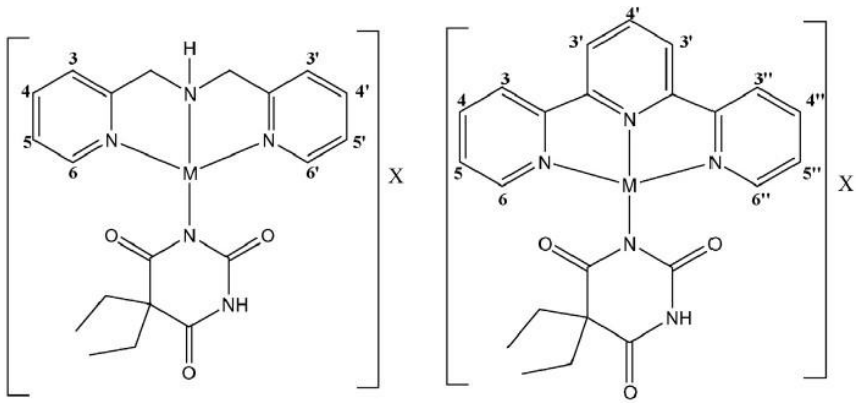

Figure 1.10. Structure of Pd(II) Complound

Barbiturates are kinds of barbituric acid, namely pyrimidine-2,4,6 (1H, 3H, 5H)-trione. Several barbiturates possess strong sedative and soporific properties, making them suitable for inducing sleep and providing anesthesia. Additionally, they are used in the management of anxiety, epilepsy, and several other mental conditions (122). 5,5-Diethylbarbituric acide is a long-standing barbiturate that has been used in medicine. It is also recognized by other names such as barbital, veronal, and diemal. Barbiturates have a broad distribution throughout the body. They may readily enter the fetal circulation and milk. Barbiturates exhibit varying coordination capacities with various metal ions. They create coordination polymers by forming metal complexes using mononuclear polymers, which include either the protonated nitrogen or carbonyl oxygen atoms, or both. Several recent investigations in the literature have examined the supermolecular and coordination characteristics of barbiturates (123).

1.6. Cell Death Pathways

The categorization of cell death into several kinds, including apoptosis, autophagy, and necrosis, offers a structure for comprehending the molecular and cellular processes that occur during various forms of cell death (Fig 1.11) (124). Discovering the genes and signaling pathways responsible for cell death processes provides a better learning of the control process of cell destiny choices (125). Gaining insight into the molecular and cellular mechanisms of cell death is essential for deciphering the causes of diseases, creating innovative treatment approaches, and enhancing our understanding of basic biological processes. Hence, the wide range of ways in which cells die is a reflection of the intricate nature of cellular reactions to different stimuli and pressures. Studying the interplay of various cell death processes is essential for understanding disease pathophysiology, exploring potential therapeutic targets, and improving scientific research.

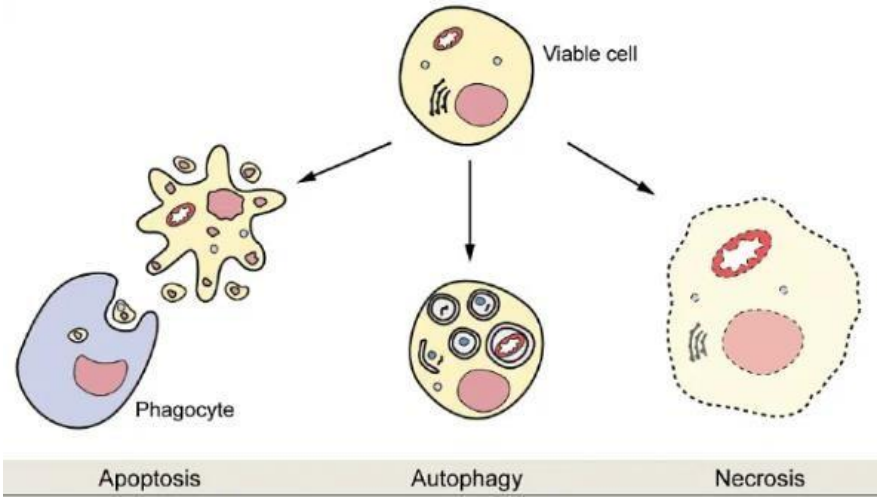

Figure 1.11. Cell Death Pathways

1.6.1. Apoptosis

Apoptosis is a essential death pathway which is responsible for maintaining the balance of tissues, removing cells that are damaged or not needed, and controlling cell growth. The dysregulation of apoptosis is a characteristic feature of cancer, particularly colon cancer. In this kind of cancer, the aberrant survival of cells and their resistance to cell death play a key role in the creation and advancement of tumors. Eukaryotic cells undergo a process of birth, lifespan, and eventual death (126). The duration of this life cycle varies based on the specific kind of cell. For instance, the lifespan of intestinal cells is 3-5 days, but skin cells have a lifespan of 20-25 days. Unlike other types of cells, such as neurons, cardiac muscle cells persist throughout an individual's whole lifespan. Neurons perish exclusively prior to the complete establishment of synapses. These cellular deaths occur via the process of apoptosis. The word apoptosis was first used in 1972 to describe a distinct kind of cell death that is separate from necrosis and is characterized as a physiological process. It cited to the process in which cells die in a predetermined manner when the appropriate moment arrives. Apoptosis, derived from the ancient Greek language, refers to the process of natural shedding of leaves from trees and petals from flowers (127,128). Apoptosis eliminates around one million cells from the body each second. Replacement structures are now under construction. There exists a regulated equilibrium between the process of cell division (mitosis) and cell death (apoptosis). Imbalance in either promoting or inhibiting apoptosis has a role in the development of several significant illnesses. Examples of diseases in which apoptosis occurs or accelerates unnecessarily include AIDS, neurodegenerative diseases, insulin-dependent type diabetes, hepatitis C infection,

myocardial infarction, and atherosclerosis. On the other hand, autoimmune diseases and cancer are examples of diseases in which apoptosis slows down (129,130). The schematic view of the apoptosis mechanism is given below (Fig 1.12).

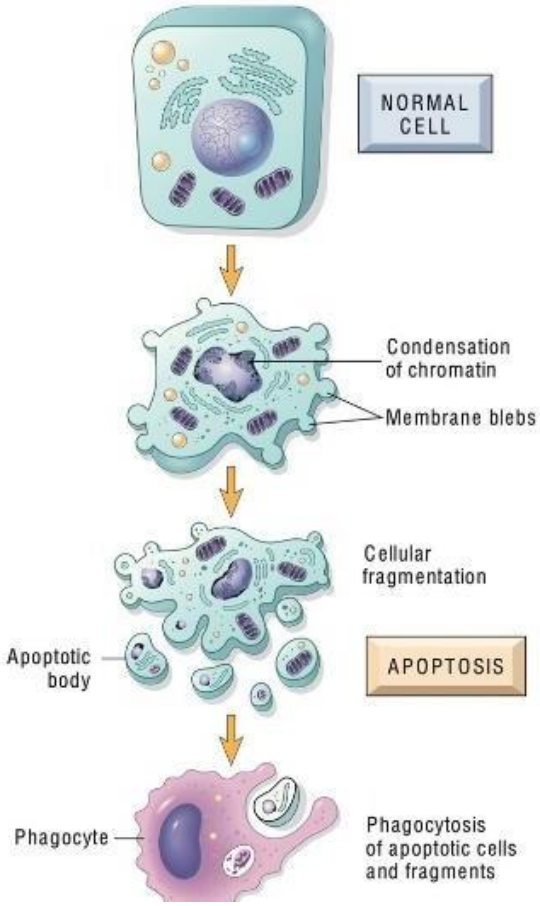

Figure 1.12. Apoptosis

Gaining knowledge about the molecular processes that cause programmed cell death in colon cancer is crucial for understanding how the illness develops and finding possible targets for treatment. Colon cancer is a diverse illness with numerous molecular subgroups that display distinct apoptotic profiles. The different subtypes of colorectal cancer have been linked to distinct apoptotic signal pathways and variations in how cells respond to stimuli that induce cell death (131). The molecular subtypes of colon cancer provide crucial insights into the apoptotic processes that influence tumor activity and clinical consequences. Alterations in crucial genes such as p53, KRAS, and BRAF may impact the apoptotic pathways in colon cancer cells, hence influencing their responsiveness to apoptotic signals and chemotherapy drugs (132). Epigenetic alterations can also regulate apoptotic pathways in colon cancer, impacting cell viability and the advancement of tumors (133). Recent studies have

emphasized the significance of apoptosis in the disseminate of colon cancer to other parts of the body and its response to therapy. Cytocapsular tubes (CTs) and CT networks are physical pathways that enable the spread of colon cancer cells to distant tissues and organs, highlighting the significance of controlling cell death (apoptosis) in the process of metastasis (134). Moreover, studies have shown that immune infiltration characteristics and interactions between immune cells in the TME have a precise affect on apoptotic pathways and patient outcomes in colon cancer (135). Colon cancer may be classified into several metabolic subtypes, such as glycolytic and ketolytic subtypes, which have unique patterns of cell death and may affect how the cancer responds to metabolic therapies, including ketogenic interventions (136). Gaining insight into the relationship between metabolism, apoptosis, and tumor growth is essential for the development of precise therapeutic approaches that use apoptotic pathways to treat colon cancer (137).

This thesis aims to explore the intricate connection between apoptosis and colon cancer by examining the molecular processes, signaling pathways, and therapeutic implications of apoptotic dysregulation in the setting of this prevalent malignancy. Our objective is to enhance our comprehension of tumor biology and discover novel approaches to enhance patient consequences in the curing of colon cancer by clarifying the function of apoptosis in its etiology.

Apoptosis Mechanisms

2 main mechanisms are implicated in the initiation of apoptosis:

1. Intrinsic pathway: The mitochondria/cytochrome-C mediated apoptosis or intrinsic pathway.

2. The extrinsic pathway: Involves the activation of death activators that bind to receptors on the cell surface.

1.6.1.1. Intrinsic Apoptosis Pathway

The intrinsic or mitochondrial route is regulated by the Bcl-2/Bax gene family, which includes both pro-apoptotic and anti-apoptotic members. When stimulated, it triggers the release of cytochrome-c from the mitochondria, which initiates the process of cell death. Both the extrinsic and intrinsic pathways converge into a common mechanism that involves the activation of a protease cascade called caspase. This cascade dismantles regulatory and structural elements, resulting in the cell's destruction. Bcl-2 and Bcl-XL, members of the anti-apoptotic category, promote cell viability by preventing the activation of caspases or the release of apoptogenic chemicals from the mitochondria. Conversely, pro-apoptotic proteins such as Bax, Bad, Bim, and Bid promote the process of apoptosis inside the cell.

In typical conditions, the function of Bax and Bak proteins is inhibited by Bcl-2. When an apoptotic signal is received, Bcl-2 ceases to function, while activated Bax and Bak cause the formation of pores in the outer membrane of mitochondria and a change in membrane potential. The crucial step in the mitochondrial process is the permeabilization of the mitochondrial outer membrane. As a result, mitochondrial membrane proteins, such as cytochrome c and endonuclease D, are released into the cytosol. After being released from the inner membrane surface of mitochondria and entering the cytosol, cytochrome c binds with the cytoplasmic protein Apoptotic Protease Activating Factor-1 (Apaf-1), therefore activating it. The Apaf-1/cytochrome c complex undergoes oligomerization to form a heptameric structure in the presence of dATP/ATP. The formation of this configuration enables procaspase 9 to interact with Apaf-1, leading to the formation of the apoptosome complex. The main function of the apoptosome is to initiate the activation of caspase 9, which is the initiator caspase. Upon activation, caspase 9 subsequently triggers the caspase cascade by activating caspase-3 or other caspases that promote cellular apoptosis. The proteins listed include active caspase 3, caspase-activated DNase inhibitor poly (ADP-ribose) polymerase (PARP, a DNA repair enzyme), Rho-associated coil forming kinase I (ROCKI), actin, fodrin, and lamin. It triggers the formation of cell death characteristics by altering cellular components. In typical cells, CAD exists in an inert state, in which it is linked to ICAD. When CAD is activated, it causes chromatin to condense and DNA to be cleaved into nucleosomal fragments. Moreover, there are several inhibitors of apoptosis (IAPs) that obstruct the activation of caspases and are counteracted by functional equivalents such as Smac or Omi/HtrA2. Upon the release of Smac and Omi/HtrA2, proteins located in the mitochondria that facilitate cell death, from dying cells, they inhibit the activity of IAPs. This hinders the suppression of promoter caspases, resulting in apoptosis in the cells. The mechanisms of the intrinsic and extrinsic pathways are characteristic of caspase-dependent apoptosis. Furthermore, there exists a mechanism in which caspase activation is lacking, and it is hypothesized to trigger apoptosis without the participation of caspases. During this process, apoptosis-inducing factor (AIF) is released from the mitochondria and moves to the nucleus, where it activates nucleases and causes DNA damage. Apoptosis may be induced by AIF, steroids, granzyme B, and endonuclease G, without the involvement of caspases. The intrinsic apoptosis, also known as the mitochondrial apoptosis pathway, is a vital biological process that plays a critical role in regulating programmed cell death (138,139).

Various cellular stresses, including DNA damage, oxidative stress, and exposure to cytotoxic substances, activate this pathway. The intrinsic route is tightly regulated by a sophisticated network of pro- and anti-apoptotic proteins, namely those that are part of the B-cell lymphoma 2 (BCL-2) family. These proteins are essential for preserving the structural integrity of the mitochondria's outer membrane. An essential stage in the intrinsic apoptosis pathway involves the disturbance of the outer membrane of the mitochondria, resulting in the liberation of apoptogenic chemicals such cytochrome c from the space between the membranes into the cytoplasm. Cytochrome c subsequently interacts with apoptotic protease activating factor 1 (Apaf-1) to form the apoptosome complex, initiating the activation of procaspase-9 and initiating the caspase cascade. Caspase-9 activation leads to the fragmentation and activation of downstream effector caspases, including caspase-3, which ultimately initiates apoptosis. The control of the intrinsic apoptosis pathway relies on the balance between pro-apoptotic and anti-apoptotic BCL-2 family members. Pro-apoptotic proteins, such as BCL-2-associated -XL), obstruct this process and limit the release of cytochrome c. Interference with the intrinsic apoptotic pathway may have profound effects on the survival of cells and contribute to many diseases, including cancer. Researchers have discovered a promising method to induce programmed cell death in cancer cells and increase their sensitivity to chemotherapy and other treatments by targeting key regulators of the intrinsic pathway, such as BCL-2 family members (140).

The intrinsic apoptosis pathway is a vital mechanism for maintaining cellular equilibrium and eliminating cells that are either impaired or surplus. Understanding the complex signaling pathways and regulatory mechanisms involved in this pathway is essential for the development of new therapeutic approaches for diseases characterized by aberrant cell death, such as cancer. Various cellular stresses, including DNA damage, oxidative stress, and exposure to cytotoxic substances, activate this pathway. The intrinsic route is tightly regulated by a sophisticated network of pro- and anti-apoptotic proteins, namely those that are part of the B-cell lymphoma 2 (BCL-2) family. These proteins are essential for preserving the structural integrity of the mitochondria's outer membrane. An essential stage in the intrinsic apoptosis pathway involves the disturbance of the outer membrane of the mitochondria, resulting in the liberation of apoptogenic chemicals such cytochrome c from the space between the membranes into the cytoplasm. Cytochrome c subsequently interacts with apoptotic protease activating factor 1 (Apaf-1) to form the apoptosome complex, initiating the activation of procaspase-9 and initiating the caspase cascade. Caspase-9 activation leads to the fragmentation and activation of downstream effector caspases, including caspase-3, which ultimately initiates apoptosis. The control of the intrinsic apoptosis pathway relies on the balance between pro-

apoptotic and anti-apoptotic BCL-2 family members. Pro-apoptotic proteins, such as BCL-2-associated -XL), obstruct this process and limit the release of cytochrome c. Interference with the intrinsic apoptotic pathway may have profound effects on the survival of cells and contribute to many diseases, including cancer. Researchers have discovered a promising method to induce programmed cell death in cancer cells and increase their sensitivity to chemotherapy and other treatments by targeting key regulators of the intrinsic pathway, such as BCL-2 family members (140).

The intrinsic apoptosis pathway is a vital mechanism for maintaining cellular equilibrium and eliminating cells that are either impaired or surplus. Understanding the complex signaling pathways and regulatory mechanisms involved in this pathway is essential for the development of new therapeutic approaches for diseases characterized by aberrant cell death, such as cancer.

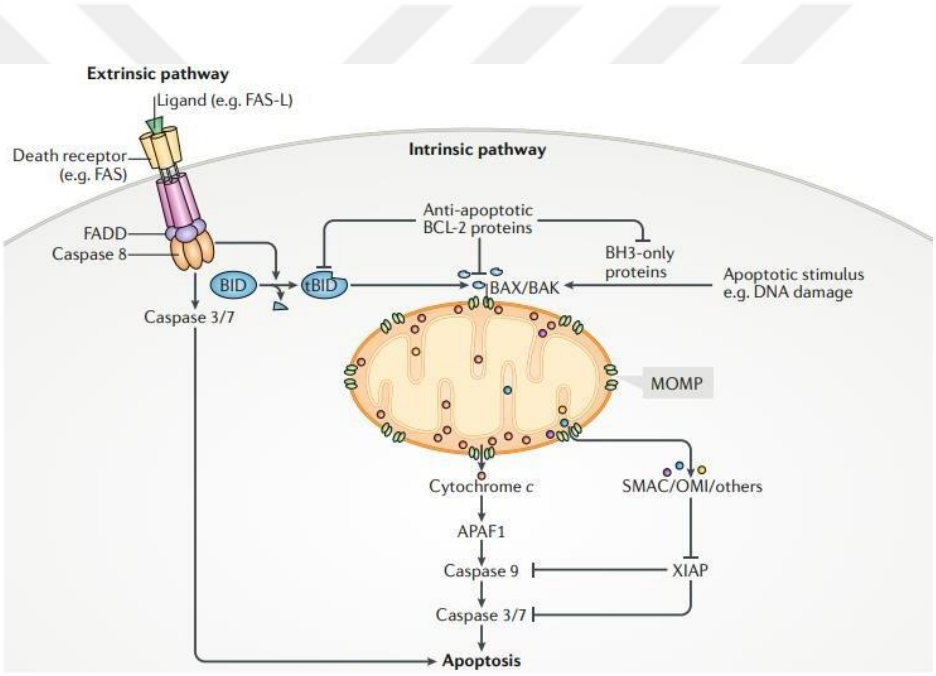

Figure 1.13. Intrinsic and Extrinsic Pathway

1.6.1.2. The Extrinsic Pathway

The receptors in question are often known as death receptors (DR) and are part of the Tumor Necrosis Factor Receptor (TNFR) gene family. Some examples of these receptors are TNFR-1 and Fas/CD95/APO-1. Apoptosis is initiated by the interaction between TNF-Related Apoptosis Inducing Ligand (TRAIL) receptors DR-3 (TRAMP), DR-4 (TRAIL-R1), and DR-5 (TRAIL-R2) and their corresponding ligands. TNFR superfamily members are type I transmembrane proteins, each possessing extracellular domains (subdomains) that have a high concentration of cysteine. This attribute enables the clear identification of TNFR superfamily members based on their specific ligands. Death receptors have an 80 amino acid long intracellular Death Domain (DD). This domain plays a vital role in conveying the apoptotic signal. The ligands binding to death receptors, including FasL, TNFα, and TRAIL, are proteins that possess a comparable structure to the receptors and belong to the TNF superfamily. The death ligands are expressed as type II transmembrane proteins. At times, these proteins may experience proteolytic cleavage and then be released. Ligands, particularly activators, stimulate the assembly of death receptor oligomers, resulting in their activation. Activation of the receptor results in the formation of a protein complex called the Death Inducing Signal Complex (DISC). The DISC complex comprises the adapter proteins Fas-associated death domain (FADD) and TNFR-1-associated death domain protein (TRADD). These locations associated with mortality initiate the activation of procaspase-8. When procaspase 8, located in the DISC structure, is activated, it initiates a series of caspase activations, resulting in the sequential activation of caspase 3, 6, and 7. Caspase 8 activation triggers Bid activation. tBid infiltrates the mitochondria and initiates the liberation of cytochrome c, SMAC (Second mitochondria-derived caspase activator), and calcium. The extrinsic apoptosis pathway, also known as the death receptor pathway, is a crucial mechanism by which cells undergo programmed cell death in response to external signals. The initiation of this pathway takes place when death-inducing molecules, such as tumor necrosis factor (TNF) or Fas ligand (FasL), attach to death receptors located on the outer surface of the cell, such as TNF receptor 1 (TNFR1) or Fas receptor (Fas). The activation of these death receptors leads to the recruitment and activation of caspase enzymes, which have a vital function in apoptosis. When a ligand attaches to death receptors, adaptor proteins such as Fas-associated death domain (FADD) are recruited to the receptor complex and facilitate the activation of initiator caspases, namely caspase-8. Upon activation, Caspase-8 cleaves and activates effector caspases, such as caspase-3 (141).

This mechanism induces apoptosis by cleaving many cellular substrates and inducing cell demise. The extrinsic apoptosis pathway plays a crucial role in immune surveillance by allowing the immune system to eliminate cells that are either damaged or polluted. Furthermore, interference with the

extrinsic pathway might possibly contribute to the onset of several diseases, including as cancer, autoimmune disorders, and neurodegenerative diseases. Several studies have shown the importance of the extrinsic apoptotic pathway in the management of cancer. An approach that has been investigated to trigger programmed cell death (apoptosis) in cancer cells and improve the effectiveness of anticancer therapies is to selectively focus on death receptors or the elements involved in their signaling cascades. Furthermore, both naturally occurring compounds and artificially produced medications that control the extrinsic pathway show promise as therapeutic agents for cancer therapy (142).

CHAPTER 2

MATERIAL AND METHODS

2.1. Chemicals

Palladium (II) compound, Uludağ University Chemistry Department, Turkey

MTT (3-(4,5-Dimethylthiazol-2-yl)-2,5 Diphenyltetrazolium Bromide), Invitrogen™, USA

Muse® Annexin V & Dead Cell Assay Kit, Merck Millipore, Germany

Muse® Mitopotential Assay Kit, Merck Millipore, Germany

Muse® Oxidative Stress Kit, Merck Millipore, Germany

Muse® H2A.X Activation Dual Detection Kit, Merck Millipore, Germany

Muse Autophagy LC3 Antibody Based Detection Kit, Cytek Biosciences, USA

Muse® Autopaghy Activation Dual Detection Kit, Merck Millipore, Germany

Nucleospin RNA Kit, Macherey-Nagel MN, Germany

iScript cDNA Synthesis Kits, Bio-rad, California, USA

SYBR® Green master mix, Bio-rad, California, USA

SYBR® Green, Qiagen, Germany

L-glutamine, Gibco, USA

Phosphate-Buffered Saline (PBS), Sigma-Aldrich, Germany

RPMI-1640 Medium Mix with L-glutamine, Gibco™, USA

Trypsin-EDTA (0.25%), phenol red, Gibco™, USA

Trypsin-EDTA (0.05%), phenol red, Gibco™, USA

0,05% Tripsin-Etilen Diamin Tetraasetik Asit (Tripsin-EDTA), Gibco, USA

Dimetil sülfoksit (DMSO), Sigma-Aldrich, Germany

Triton X-100, Sigma-Aldrich, Germany

Tripan Blue (% 0,5), Sigma-Aldrich, Germany

SDS Molecular Biology grade, BioChemica Applicham, Germany

DMEM (Dulbecco's Modification of Eagle's Medium) High Glucose, Gibco™, USA

Fetal Bovine Serum (FBS), Gibco, New York, ABD

Penisilin-Streptomisin Solution(100X), Gibco, New York, ABD

Tripan blue (%0,5), Biological Industries, İsrail

Annexin V, Apoptosis Kit Plus BioVision, ABD

N-acetyl-l-cystine (NAC), Sigma-Aldrich, Germany

ß-merkaptoetanol, Merck Millipore, Germany

2.2. Consumables

Filter tip with filter, 100 µl Biosphere, BioTipp, Denmark

Filter tip with filte, 200 µl Biosphere, BioTipp, Denmark

Filter tip with filte, 10 µl Biosphere, BioTipp, Denmark

Filter tip with filte, 1000 µl Biosphere, BioTipp, Denmark

Eppendorf™ Research™ plus EU-IVD Single Channel Variable Volume Pipette Set, Eppendorf™, Germany

25 cm^2 Greiner Bio-One CELLSTAR Cell Culture Flasks, Thermo Fisher Scientific, USA

75 cm^2 Greiner Bio-One CELLSTAR Cell Culture Flasks, Thermo Fisher Scientific, USA

6 well Cell Culture Plates, Thermo Fisher Scientific, USA

12 well Cell Culture Plates, Thermo Fisher Scientific, USA

96 well Cell Culture Plates, Thermo Fisher Scientific, USA

5 ml Nunc™ Serological Pipettes, Thermo Fisher Scientific, USA

10 ml Nunc™ Serological Pipettes, Thermo Fisher Scientific, USA

25 ml Nunc™ Serological Pipettes, Thermo Fisher Scientific, USA

50 ml Nunc™ Serological Pipettes, Thermo Fisher Scientific, USA

Eppendorf® Tube Rack for 0.5 mL Tubes, Sigma-Aldrich, USA

1,5 ml Snap Cap Low Retention Microcentrifuge Tubes, Thermo Fisher Scientific, USA

2 ml Snap Cap Low Retention Microcentrifuge Tubes, Thermo Fisher Scientific, USA

PCR Tubes, 0.2 mL, flat cap, Thermo Fisher Scientific, USA

TrueNorth® Cardboard Cryovial Box Cell Divider, Sigma-Aldrich, USA

Corning® Cryogenic Vial, Sigma-Aldrich, USA

Hemocytometer, Thermo Fisher Scientific, USA

Falcon™ 50 mL High Clarity Conical Centrifuge Tubes, Thermo Fisher Scientific, USA

Falcon™ 15 mL High Clarity Conical Centrifuge Tubes, Thermo Fisher Scientific, USA

10 – 100µL Eppendorf Research® plus Multi-channel Micropipettes, Sigma-Aldrich, USA

30 – 300µL Eppendorf Research® plus Multi-channel Micropipettes, Sigma-Aldrich, USA

2.3. Devices

Muse Cell Analyzer, Merck Millipore, Germany

Synergy H1 Microplate Reader, BioTek, Agilent, USA

Applied Biosystem Real-Time qPCR, Life Technologies, Thermo Fisher Scientific, USA

Precision Balances and Scale, METTLER TOLEDO

-80 °C Deep Freeze, Nüve DF 590, Turkey

-20 °C Deep Freeze, Beko, Turkey

+4 °C Freezer, Beko, Turkey

Microfuge 20R Centrifuge, Beckman Coulter, USA

Olympus Light Microscope CK40, Japan

Leica Light Microscope, Germany

Cell Imaging System Fluorescent Microscope, Thermo Fisher Scientific, USA

Lab Homogenizer and Vortexer, Heidolph-Instruments, Germany

VWB 12 Water Baths, VWR, UK

SL 8 Small Benchtop Centrifuge Series, Thermo Scientific, USA

CO_2 Incubators, Thermo Scientific, USA

Laminar Flow Hood, Thermo Scientific, USA

Biological Safety Cabinets Clean Benches, Thermo Scientific, USA

Autoclaves Steam Sterilizers, Nüve OT4060, Turkey

96-well T100 PCR Thermal Cycler, Bio-Rad, USA

2.4. Method

2.4.1. Preparation of Palladium Compound

Chemical formula of Pd (II) is [[Pd(bpma)(barb)]Cl.H_2O]. And moleculer weight is stated as 542.307 g/mol. Because the compound dissolves with DMSO, attention should be paid to the DMSO ratio when preparing the main stock. The highest concentration was 100 µM when designing dose response experiments. Therefore the main stock was prepared with the highest dose of DMSO concentration, % 0,2 in 50 mM DMSO. For this, 27 mg of the compound was weighed and dissolved in 1 ml DMSO on 37 °C. Dissolved Pd(II) main stock was stored in 0.25 ml tubes at -20 ^{0}C and then aliquot with 25 µl.

2.4.2. Cell Culture

The human colon cancer cells HCT-15 and HCT-116 and HT-29 used in the experiments were obtained from Prof. Dr. Engin Ulukaya's laboratory at the Molecular Cancer Research Centre at the University of İstinye. These cells were stored in refrigerators in tubes called cryovial tubes at -80 ^{0}C.

2.4.2.1. Preparation of the Cell Medium

To prepare the medium used for cell lines:

A mixture of 10% FBS, 1% Penicillin-Streptomycin (10,000 U/ml peniciline, 10 mg/ml streptomycine) and 1% L-glutamine was added to the RPMI 1640 medium. The prepared mixture was passed through the filter and injected into milliliters of falcon tubes. Then it was kept at +4 ^{0}C. It was raised to +4 ^{0}C before use and kept at room temperature for 1 hour or in a water bath for 15 minutes to reach an optimal temperature.

2.4.2.2. Removal of Cell Strains from Stock

In order to reproduce the cells, cryovials were taken from -80^{o}C and quickly dissolved in a hot water bath. The cell suspension was taken into a 5ml RPMI (Roswell Park Memorial Institute medium) containing 10% FBS, 1% penicillin-streptomycin and 1% L-glutamine. After centrifuging the supernatant part at 300 g of the Falcon tube, 1 ml of nutrient was added to the cell pellets to allow the cells to become a suspension. It was taken in 25 cm^2 cell plate containing 5 ml of nutrients in cell suspension and incubated in an environment containing 5% CO_2 at 37 °C.

2.4.2.3. Passaging of Cell Lines

When the cell lines used in the experiments completely covered the surface of the flask (became confluent), the medium in the flask was aspirated. To purify the cells from the old medium, approximately 1-2ml 1X PBS (Sigma-Aldrich, USA) was added into the 25cm2 flask and the cells in the flask were gently washed. After the PBS was removed from the environment by aspirating, 0.5ml

of 0.05% Trypsin-EDTA solution was used to separate the cells adhering to the flask surface from the surface, and the cells were incubated for 5 minutes at 37ºC in a 5% CO_2 environment. At least twice as much medium was added to the cells that appeared to be floating away from the flask surface when viewed under the microscope, to inhibit trypsin. Thus, trypsin was prevented from starting to damage cell membranes after detaching the cells from the surface. The cell suspension in the flask was taken into a 15 ml falcon tube containing medium (the total volume in the falcon should be 10 times that of trypsin). After centrifugation at 300 g for 5 minutes, the supernatant was aspirated. And after the resulting cell pellet was dissolved in 1 ml of cell medium, approximately 10 ml of medium was added and 10 ml of cell suspension was placed in 75 cm^2 flasks and incubated at 37ºC in an environment containing 5% CO_2 was left. In this way, the cells were allowed to multiply until they reached the desired number.

2.4.2.4. Stocking of Cell Lines

When the cells completely covered the surface of the flask, the medium in the flask was removed from the cell flask by aspirating. After the cells were washed gently with 1X PBS (Sigma-Aldrich, USA), the PBS was removed by aspirating. Then 0.05 % Trypsin-EDTA solution was added to allow the cells to lift off the flask surface. The cells were incubated for 5 minutes at 37 ºC in a 5% CO_2 environment. At least twice as much medium was added to the cells, which were considered to have separated from the flask surface when viewed under the microscope, to inhibit trypsin. The cell suspension in the flask was placed into a 15 ml falcon tube containing the medium. After centrifugation at 800 rpm for 5 minutes, the supernatant was aspirated and 1 ml of freezing medium mixture (9 ml DMEM + 1 ml DMSO) was added to the pellet in the dark for each cryovial. The cell suspension was distributed into cryovials as 1 ml each and stored at -80 ºC.

2.4.2.5. Counting Cells

The cells, separated from the surface of the flask with the help of Trypsin-EDTA solution, are centrifuged in a 15 ml falcon tube at 1000 rpm for 5 minutes, and then the supernatant is discarded. Depending on the density of the cell pellet, medium is added to dissolve the pellet. Take 10 µl of this cell suspension and add it to an empty well of a 96-well cell culture dish. 10 µl of trypan blue dye (Biological Industries, Israel) was added and mixed by pipetting. Then, 10 µl of this mixture was taken and transferred to the hemacytometer slide on both sides, and the cells in a total of four large square areas on this slide or the cells in the middle gingham area were counted under the microscope. The number found was multiplied by the dilution coefficient to calculate how many cells were in 1 ml of medium.

2.4.3. MTT (Metil-tiazo-tetrazolium) Cell Viability Method

The MTT technique was initially used by Mosmann et al. in 1983. This approach primarily relies on the colorimetric measurement of the activity of an enzyme have a role a mitocondrial activity in live cells. The MTT test is a quantitative method that evaluates the viability of cells by measuring their ability to convert a yellow tetrazolium salt (MTT) into a purple formazan product. The process based on the ability of live cells to transform MTT (yellow) into a formazan cyristal (purple), which can be quantified using a spectrophotometer. The cellular oxidoreductase enzyme, which relies on NAD(P)H as a cofactor, is located in the mitochondria and catalyzes the process seen in Figure 2.1.

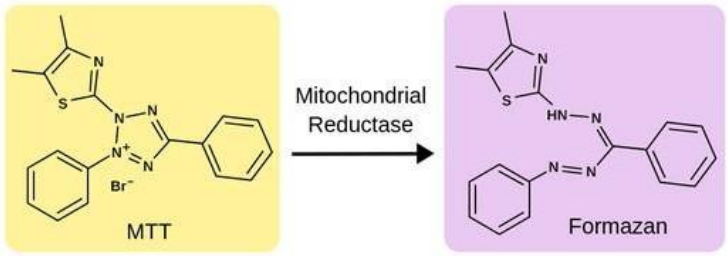

Figure 2.1. The mitochondrial reductase converts yellow MTT into purple formazan

The MTT substance is a yellow tetrazolium salt that can be dissolved in water. It is received by living cells and converted into water-insoluble formazan crystals with a dark purple color by the enzymes found in the mitochondria called succinate dehydrogenase (Figure 2.2).

When cells are exposed to a cytotoxic agent, their viability decreases, resulting in a reduction of MTT tetrazolium salt to formazan. To summarize, living cells with functioning mitochondria are stained blue-violet, whereas dead cells with impaired mitochondria do not undergo any color change. The extraction of formazan crystals, which were generated by the mitochondrial activity succinate dehydrogenase, was performed using a solution consisting of 10% sodium dodecyl sulfate, sterile distilled water, and 0.01 N HCl. The compounds are rendered soluble in water and their color intensity is detected by using a spectrophotometer at a wavelength of 570 nm. After the measurement is completed, the viability rate (%) of the cells is calculated by comparing the color intensity in the control cells does not treated to the compound or drug.

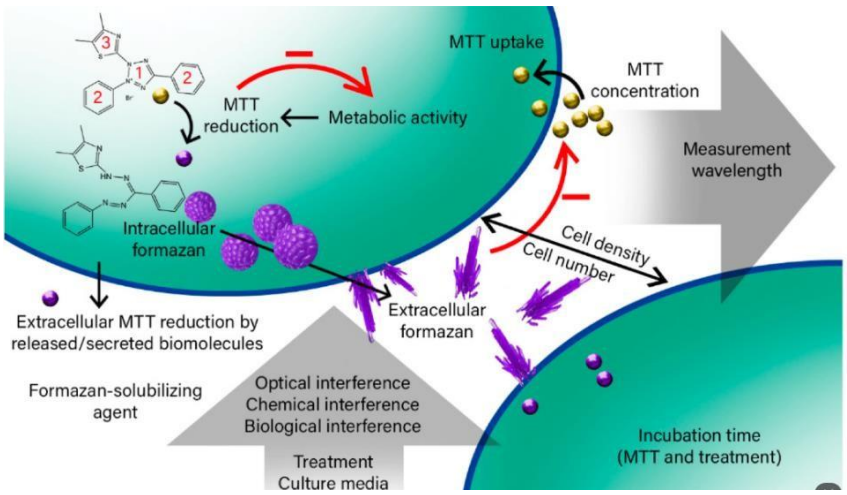

Figure 2.2. MTT Assay Principle

No change in color is seen in cells exhibiting impaired mitochondrial activity. The extraction of formazan crystals, which were generated by the activity of mitochondrial succinate dehydrogenase, was performed using SDS (10% sodium dodecyl sulfate) solution together with sterile distilled water and 0.01N HCl. The compounds are rendered soluble in water and their color intensity is measured using a spectrophotometer at a wavelength of 570 nm. The viability rate (%) of the cells is determined at the conclusion of the measurement by comparing the color intensity in the control cells that were not exposed to the medication. Variables that impact the ultimate optical density (OD) measurements in the MTT experiment. These factors encompass the MTT reagent concentration, the fraction of the reagent that enters the cell. The cellular metabolic activity, the number of cells, the timing of formazan crystal extrusion and chemical interference such as non-biological reduction of MTT.

For the MTT method, they were first planted at 5×103 cells/well in 96-well cell culture dishes and then allowed to adhere overnight. After the cells adhered and gained their healthy morphology, they were treated with Pd (II) compound. In order to select the appropriate dose of the compound used, the cells were analyzed with Pd (II) compound by making serial dilutions at different concentrations (3-100 µM) for 24, 48 and 72 hours. According to the MTT viability method, as a result of the experiment with the Pd (II) compound, the IC50 dose of HCT-116 cells in 48 hours was 22.5 µl, 20.4 µl for HCT-15 and 51.9 µl for HT-29 dose has been selected. MTT chemical was prepared as stock in 5 mg/ml PBS buffer at pH=7.2. The prepared MTT solution was filtered and thus made sterile. After adding 20 µl of MTT dye to each well, the cells were incubated at 37^0C for approximately 4 hours. To solubilize the formed formazan crystals, 100 µl of 10% SDS solution was added to all wells and incubated overnight at 37^0C in an oven with 5% CO_2. At the end of the incubation period, the absorbance values of the cells were measured on a spectrophotometer at a wavelength of 570 nm. Viability rates of the cells were calculated and graphs were drawn with the Graphad Prism program.

Since the best graph and the lowest IC50 value were obtained in the HCT-15 cell, further experiments were performed only with the HCT-15 cell and IC90 value.

2.4.3.1. NAC (N-Acetyl Cysteine) Treatment

The oxidative stress inhibitor antioxidant NAC to be used was treated with cells for 48 hours in the dose range of 25, 50 and 70 µM. For cells, only cells seeded in broth medium were used as a negative control of death (maximum viability). 200 µl of medium was added into the wells reserved for the blank. Then, the cells were incubated in a 37^0C, 5% CO_2 incubator environment for the desired treatment periods.

2.4.3.2 % Viability Measurement

The viability of the cell used as the control without palladium chemical application was accepted as 100%, and the viability rates of the drug-treated cells were calculated using the formula below. During the experiment, each concentration was repeated in three different wells, independent of each other.

% Viability was calculated as =[100×(Mean of cell absorbance treated with compound-blind mean)/(Mean of control cell absorbance-blind mean)].

2.4.4. Cell Migration Experiment

As a good anti cancer drug candidate Pd (II) compound is expected to prevent cancer cell migration. Because the compounds used prevent the migration of cancer cells while also preventing them from spreading to surrounding tissues and growing. Therefore in this study, we conducted a cell migration assay, sometimes referred to as a wound healing test, to assess any alterations in the migratory capacity of HCT-15 colon cancer cells after treatment with a Pd (II) molecule. In order to facilitate wound healing, HCT-15 colon cancer cells were introduced into 2 ml of media at a density of $25x10^6$ cells per well. The cells were cultured for a period of 24 hours, including overnight, to facilitate their attachment to the plate and develop their characteristic structure. The control group did not receive any Pd (II), whilst the other experimental groups were given varying amounts of 10 µM and 20 µM Pd (II). Following a 24-hour incubation period, a wound was created in each well by drawing straight lines using a 10 µl pipette tip. The liquid was removed by suction and replaced with fresh liquid. Three distinct regions from each well were identified and photos were captured at the start of the experiment. After 0-24-48-72 hours, photos were taken of the designated regions under a microscope for each group. The observed difference in migration was dependent on both time and dosage.

2.4.5. Determining the Death Method of Cells by Fluorescent Staining

2.4.5.1. Double Staining Method

Phosphatidyl serine (PS), a kind of membrane lipid, is often found on the cytoplasmic side of the cell membrane in normal cells. When a cell undergoes apoptosis, phosphatidylserine (PS) molecules, which are typically found on the inner surface of the cell membrane, migrate to the outer surface (Figure 2.3). Apoptotic cells undergo this movement at the first phases of cell death, before the integrity of the cell membrane is compromised (Ulukaya 2013). Annexin-V (FITC) is a protein that can attach to PS, which moves to the outer surface of cells during apoptosis. By marking apoptotic cells with a fluorescent material like FITC, they become visible and may be studied using fluorescence microscopy. Propidium iodide (PI) is used as a supplementary dye in the analysis of Annexin-V (FITC) binding since it may also be seen on the surfaces of necrotic cells. PI is a fluorescent dye for nucleic acids that selectively enters cells with broken membranes, resulting in the labeling of dead cells (either primary necrotic or late apoptotic/secondary necrotic). Living cells discharge this dye. Primary necrosis, characterized by an increase in cell volume without fragmented or pyknotic nuclei, is the typical kind of cell death that occurs in response to toxic circumstances such as hypoxia, ischemia, and hyperthermia. Secondary necrosis is defined by the presence of a pyknotic or fragmented nucleus and represents the advanced phase of apoptosis. While the cell membranes of cells undergoing apoptosis in the cell culture environment remain intact throughout the early stages of apoptosis, the integrity of these membranes is destroyed when the cells progress toward late apoptosis or secondary necrosis in later time periods. If cells are stained with non-vital dyes (such as PI) during the time leading up to the secondary necrosis stage, they will not be able to be stained with these dyes due to the unbroken membrane, despite the presence of apoptosis. During the latter phases after the development of secondary necrosis, cells undergo a decline in membrane integrity and become stained with non-vital dyes. Consequently, they exhibit positive staining for PI and Hoechst. The cells are stained with both Hoechst (blue fluorescence) and the non-vital dye propidium iodide (red fluorescence) at the same time. Living cells identified as Hoechst positive whereas dead cells identified as PI positive. This staining method allows for the distinction between these different cell types (110).

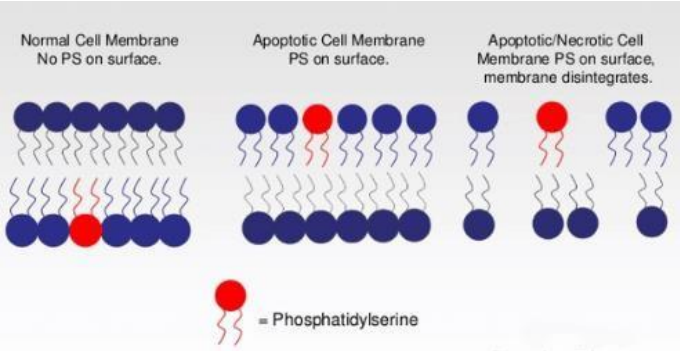

Figure 2.3. Diagram Illustrating the Annexin V Apoptosis Assay

HCT-15 colon cancer cells were enumerated and seeded in 96-well cell culture plates at a density of 5×10^3 cells in 100 µl (with 3 duplicates). The sample was placed in an incubator and kept at a temperature of 37°C for a duration of 24 hours. The incubator was also maintained at a carbon dioxide concentration of 5%. Next, the cells were exposed to a 77,6 µM IC90 concentration of Pd (II) compound and kept in an incubator at 37°C with 5% CO_2 for 24 and 48 hours. After the incubation time, almost all of the media (about 180 µl) was carefully extracted from the cells without causing any harm, and the process of dou Staining staining was carried out. To perform this procedure, 2.25 µl of a solution containing Annexin-V-Fluorescein with a concentration of 20 mM and 0.5 µg of PI dye in a volume of 3 microliters were combined with 3 ml of PBS. Furthermore, to analyze the cellular nuclear structure, Hoechst 33342 dye was introduced into the mixture at a concentration of 200 µg/ml, resulting in a final concentration of 5 µg/ml after a 40-fold dilution. A volume of 30 µl of the dye mixture was transferred into each well using a pipette. The mixture was then left to incubate at room temperature for a duration of 30 minutes. Following the incubation period, the effects of the treatments on cell death were assessed by examining the cells using a fluorescence microscope.

2.5. Flow Cytometry Analysis

In order to do analysis using flow cytometry, it is necessary to have cells suspended in a liquid medium. During the process of measurement, it is necessary to individually suspend the cells in a liquid and ensure that the suspension, which contains the cells, flows continuously past the laser beam. Within the flow cytometry apparatus, a large number of cells per second traverse the flow cell region, where they come into contact with a laser beam, causing the cells to be stimulated by the laser light. Every cell deflects a portion of the laser light and simultaneously produces fluorescent light due to excitation from the laser light, resulting in an excess of energy. The cells are cultured with antibodies that are specifically targeted towards the proteins located on their surface or inside the cell, facilitating the binding of the antibodies to the antigens. Each individual antibody is tagged with

fluorescent dyes, such as FITC. Therefore, by analyzing the fluorescent signals emitted by cells containing a particular antigen upon exposure to a laser beam, it is possible to identify the specific antigen present in that cell.

2.5.1. Annexin-V-FITC Test

Annexin V is a Ca^{+2} depending protein has a strong interaction to phosphatidylserine (PS) and using detect apoptotic cells by labeling them with a fluorescent label like FITC. The proportion of cell death inducing by apoptose is controlled by the correlation among phosphatidylserine (PS) molecules and the Annexin-V-FITC complex in the presence of calcium ions (Ca^{+2}). This approach also utilizes the 7-Aminoactinomycin D (7-AAD) dye. This dye is a fluorescent chemical molecule that has a high attraction to DNA. Due to its inability to readily traverse the undamaged cell membrane, it selectively attaches to the GC-rich segments of double-stranded DNA inside cells that have compromised membrane integrity name as late apoptose tumoric cell and necrotic cells. The summary below outlines the response of dyes to cells at different stages. Cells do not developing apoptosis may be identified by the absence of Annexin V staining and 7-AAD staining. Early apoptotic cells may be identified by their positive expression of Annexin V and negative expression of 7-AAD.

Cells at the late stage of apoptosis and cells that are dead may be identified by their positive staining for Annexin V and 7-AAD. Excessive nuclear debris is present, shown by the absence of Annexin V and the presence of 7-AAD. In order to conduct this research utilizing the Muse TM Annexin V & Dead Cell Kit, HCT-15 cells were enumerated and seeded in 6-well cell culture plates at a density of 25×10^4 cells per mililiter. After incubated for 24 hours at a temperature of 37 °C and CO_2 concentration of 5%, 1 ml of the medium was extracted from the negative control wells and replaced with 1 ml of new media. After applying inhibitors for 24 hours, the cells were exposed to a dosage of 77,6 µM of Pd (II) compound and incubated for 12 and 24 hours at a temperature of 37 ºC with a 5% CO_2 concentration. After the treatment times concluded, the kit components were allowed to reach room temperature. After the incubation period, the liquid from the wells treated with the medication was collected in 15 ml tubes, whereas the liquid from the wells used as negative controls was discarded. The cells were detached using trypsin and then gathered into appropriate containers. Subsequently, they were rotated at a velocity of 800 revolutions per minute for a period of 5 minutes. After centrifugation the supernatant above the pellet in the falcon tubes was discarded. Then, 100 µl of a solution containing 1% FBS was introduced and 100 µl of the cell mixture was transferred into Eppendorf tubes that were properly labeled. These eppendorfs were supplemented with 100 µl of Annexin-V kit sample. The process of vortexing was performed for roughly 5 seconds at a moderate

pace. Following 20 minute period of incubation in a lightless environment at ambient temperature, the Muse™ Cell Analyzer instrument (Fig 2.4) was used to take measurements.

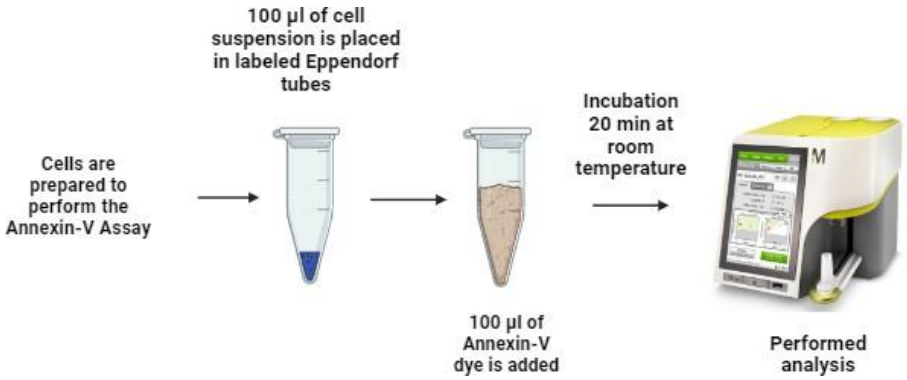

Figure 2.4. Annexin V Analysis

2.5.2. Determination of DNA Damage by Gamma H2A.X Activation

The nucleic acide molecule is continuously subjected to many stimuli that induce harmful stress on the cell. Various intrinsic and extrinsic physical, chemical and biological stimuli induce disruptions in the sugar-phosphate backbone, resulting in DNA damage and subsequent chain breakage. Specifically, DNA ds breaks are the most hazardous kinds of DNA damage can occur persistently throughout the lifespan of a cell, and their efficient repair is of utmost significance for the cell to sustain its healthy functioning. Genomic instability, which is unable to be fixed, may result in mutations trigger to the progress of tumor transformation. Nucleosomes serve as the fundamental components of chromatin, play a key role in the structural organization and functional processes involved in DNA repair. A nucleosome is composed of a 147 base pair DNA strand that is wrapped around two copies of each of the four core histones. The nucleosome structure consists of four main histone families: H2A, H2B, H3, and H4. The H2A histone protein family has many variations, including H2A1 and H2AX. The H2AX protein which is a significant variant of H2A, makes up 2-25 % of the H2A histone pool in mammals, with the exact percentage varying based on the specific cell and tissue type. The H2AX protein is a conserved kind of H2A histone found in eukaryotes. It has a highly conserved region in its carboxyl tail. H2AX, similar to other members of the H2A histone family, controls several physiological processes via phosphorylation, acetylation, and ubiquitination. Because of its participation in the process of repairing DNA damage, this specific histone variant, found in damaged regions, has a significant impact on many different metabolic and genetic process like cell division, growth, and regulation of immuno receptors. Consequently, it is closely associated with genomic instability and syndromes related to DNA damage repair. H2AX is an immediately

members in the process respond to DNA damage. Gamma H2AX (γH2AX) is the term used to refer to phosphorylated H2AX. It is responsible for the formation of visible nuclear foci in the event of DNA double-strand breaks. Therefore, the measurement of γH2AX expression has become a commonly used method in recent years to accurately identify DNA double-strand breaks. Following DNA repair, protein phosphatase 2A dephosphorylates γ-H2AX, hence controlling the quantity of γ-H2AX in the cell. Phosphorylation of γ-H2AX is an ideal measure for studying DNA repair due to this reason. The Muse™ H2A.X Activate Kit is used to ascertain the phosphorylation of γ-H2AX.

To achieve this objective, the HCT-15 cells were seeded in 6 well cell culture plates (25.10^4 cells per ml and each well). After incubated for 24 hours at 37 °C and in an environment with 5% CO_2, the cells were treated to 77,6 μM of Pd (II) compound. The cells were then incubated for an additional 24 hours under the same conditions. After the treatment times ended, the kit components were first allowed to reach room temperature. The liquid in the 6-well cell culture dishes was removed by suction. To eliminate the cells from the serum, the cell surface was rinsed by introducing 1 ml of 1X PBS into the wells. Following the removal of PBS from the environment by aspiration, a 0.5 ml solution of 0.05% Trypsin was used to detach the cells adhering to the surface. Then HCT-15 cells were incubated for 5 minutes at a temperature of 37°C in an atmosphere containing 5% CO_2. After incubation, cells were centrifuged. After the centrifugation process was completed, the samples were rinsed with a solution of 1X PBS. During the fixation stage, the samples were immobilized on ice for a duration of 5 minutes using the fixative included in the kit. Then cells centrifugated again at 500 g at 4 min. After supernatants were discarded and the cells were then incubated on ice for 5 min. Then performed permeabilization step according to kit. Following that, the samples underwent centrifugation at 300 g for 5 minutes. Subsequently, the supernatant was discarded and incubated with the prepared working solution containing the antibodies from the kit. This incubation took place for 30 minutes at room temperature in the absence of light. After the incubation period the cells centrifugated at 300g at 5 min. Finally the cells diluted by using the working solution and assessed for DNA damage using the Muse™ Cell Analyzer equipment. The workflows of all process are shown in Figure 2.5 below.

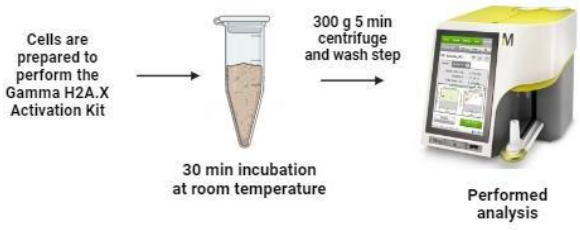

Figure 2.5. DNA Damage (γ-H2AX) Activation

2.5.3. Determination of Oxidative Stress

ROS, also known as Reactive Oxygen Species, are chemical compounds including $O2\cdot-$, H_2O_2 and OH•. These compounds are produced in tiny quantities as a result of regular oxygen metabolism. ROS may trigger free radical chain reactions, resulting in the formation of different free radicals that lead to the production of carbon based free radicals inside the cell. They can continuously arise as intermediate products at the active sites of enzymes during enzymatic reactions in the cell's regular metabolic processes. When exposed to certain factors such inflammation, radiation, age, elevated levels of oxygen (pO2), ozone (O3), nitrogen dioxide (NO_2 •), chemicals, and medications, the formation of ROS in cells enhanced. This increase in ROS creation has an impact on the lipids, proteins, DNA, carbohydrates, and enzymes inside the cells. They have an impact on all crucial chemicals. It has a significant impact on a range of pathophysiological conditions including cancer, and cardiovascular illnesses. The Muse® Oxidative Stress kit detects intracellular superoxide radicals and quantifies the level of oxidative stress seen in cells. The kit also includes a solution for detecting the quantity of reactive oxygen species (ROS) in the cells, which is a measure of oxidative stress.

In the oxidative stress test, the number of cells was determined and then placed in 6 well cell culture plates at a concentration of 25.10^4 cells per milliliter. Following a 24 hour incubation period at 37°C, with 5% CO_2, 1 ml of media was extracted from the negative control wells and substituted with 1 ml of new medium. Following a 24-hour incubation period, cells were exposed to a IC 90 dosage of 77,6 µM Pd(II) compound and incubated at a temperature of 37°C with a 5% CO_2 concentration for an additional 24 hours. After the treatment times concluded, the kit components were first allowed to reach the ambient temperature. The liquid in the 6 well cell culture dishes was removed by suction. To extract the serum from the cells, 1 ml of 1X PBS was introduced into the wells and the cell surface was rinsed. Following the removal of PBS from the environment by aspiration, a 0.5 ml solution of 0.05% Trypsin was used to detach the cells adhering to the surface. The cells were then incubated at a temperature of 37°C with a 5% concentration of CO_2 for a duration of 5 minutes. After the incubation period, the liquid above the sediment in the wells treated with the medication was collected in 15 ml containers and spun at a speed of 800 g at 5 min. Following centrifugation, the cell pellet was treated with the oxidative stress working solution included in the kit at a concentration of $1x10^6$ cells per ml. The mixture was then incubated for 30 minutes following a brief pipetting step. After the incubation period, the samples have been meausered by using the Muse™ Cell Analyzer instrument (Figure 2.6).

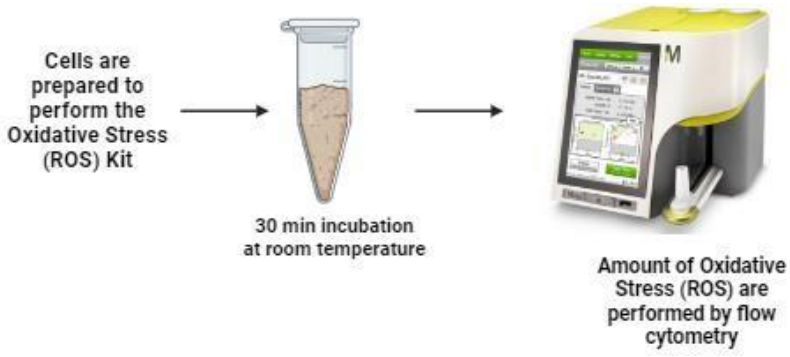

Figure 2.6. Oxidative Stress (ROS) Analysis

2.5.4. Autophagy Analysis

LC3 plays a crucial role in the selection of autophagy substrates and the formation of autophagosomes. It serves as the most often used indicator of autophagosomes. LC3 was first characterized as a microtubule-associated protein in rats upon its discovery. Subsequently, LC3 was shown to have a role in autophagy and the elongation of autophagic vesicle membranes, which includes the breakdown of organelles inside the cytoplasm. During the process of autophagy, the LC3 protein forms a covalent bond with phosphatidylethanolamine, which is a kind of lipid molecule. Lipid molecules adhere to autophagic membranes, resulting in membrane elongation. The non-bound form of LC3 is referred to as LC3-I. LC3 is attached to the fatty acid molecule. Then attached to autophagic vesicles it is referred to as LC3-II. In recent years, the conversion of LC3-I to LC3-II upon autophagy stimulation has been widely recognized and used as a reliable marker for autophagy. The Muse® LC3 kit gives data on the proportion of LC3-II that is associated with autophagic vesicles inside cells.

For the LC3-II autophagy test, the HCT-15 cells were seeded on 6-well cell culture plates (4.10^6 ls in each well). On the next day, a 77,6 µM concentration of Pd (II) compound was applied to cells, and it was then incubated for overnight at a temperature of 37°C and a CO_2 concentration of 5%. 1ml of medium was extracted from the negative control wells and replaced with 1ml of new medium. After the cell treatment times concluded, the kit components were first allowed to reach room temperature. The liquid in the 6-well cell culture dishes was removed by suction. To eliminate the cells from the serum, the cell surface was rinsed by introducing 2 ml of 1X HBSS into the wells. Following the removal of HBSS from well by aspiration, 0.5 ml of a 0.05% Trypsin-EDTA solution was used to detach the cells adhering to the surface. The cells were then incubated for 5 minutes at a temperature of 37ºC in an atmosphere containing 5% CO_2. After the incubation period, the liquid above the

sediment in the wells treated with the medication was gathered into 15ml tubes and spun at a speed of 800 revolutions per minute for 5 minutes. Following centrifugation, the cell groups that were subjected to treatment and those that were not were then incubated with the autophagy solution A from the kit for a duration of 2-6 hours. Following the incubation period, the cells were subjected to centrifugated 500 g at 5 minutes. Next, the liquid portion above the sediment was removed by suction. Each cell group was treated with 100 µl of autophagy solution B and incubated for 5 minutes. After the incubation time, the cells were spun at a speed of 2500 rpm at 5 min and then rinsed with a solution that was diluted to a concentration of 1X. Following the pipetting of the working solution, the samples were assessed using the Muse Autophagy LC3-Antibody Based Kit equipment**.**

2.6. Gene Expression Analyzes by Real Time-PCR (qPCR-quantitative)

To conduct gene expression study using a Real Time device, it is necessary to first isolate RNA and then synthesize a cDNA library. Initially, HCT-15 colon cancer cells were seeded in 6-well cell culture plates at a density of 25×10^6 cells. Following a 24 hour incubation at 37ºC with 5% CO_2, a Pd(II) compound was administered to the wells, excluding the control group, at a concentration of 77,6 µM in a volume of 100 µl for another 24 hours. After applying the chemical, the cells were subjected to Trypsin-Edta treatment at the 6th and 24th hours, resulting in the collection of cell pellets. During the 6 hour, the cells exhibited a phase characterized by neither total cell death nor a fully healthy appearance. Pellets were collected during the 6th hour due to our anticipation of early apoptosis in the cells at this time. Subsequently, pellets were acquired upon microscopic examination, which revealed that the bulk of the cells had undergone apoptosis and perished within 24 hours. The MN Macherel Negel RNA isolation procedure was used to extract RNA from the cell pellets.

2.6.1. RNA Isolation

In order to perform expression analyzes of genes related to apoptosis, autophagy and DNA damage, total RNAs were first isolated from HCT-15 colon cancer cells. For this purpose, 5 and 24 hour treatment was applied by giving 77,6 µM palladium to the cells in 6-well plates in the compound treated groups (Figure 2.7). At the end of the treatment period, RNAs of appropriate purity and concentration were obtained by applying the NucleoSpin RNA, Mini kit for RNA purification (MN Macherey-Nagel, 740955.50) protocol, each step of which is explained in detail below.

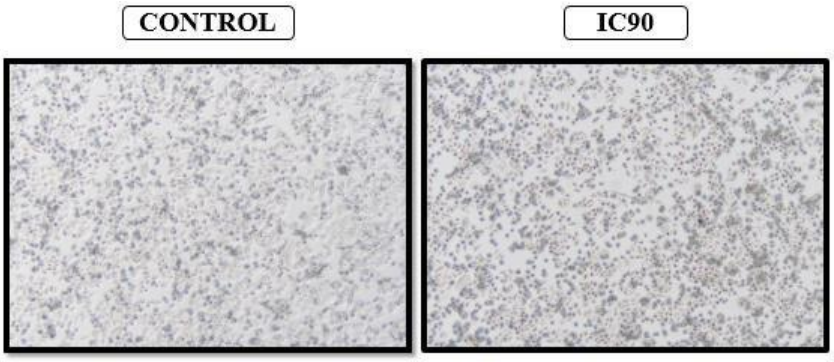

Figure 2.7. Microscopic image when HCT-15 colon cancer cells begin to aggregate for RNA isolation at the 6th hour

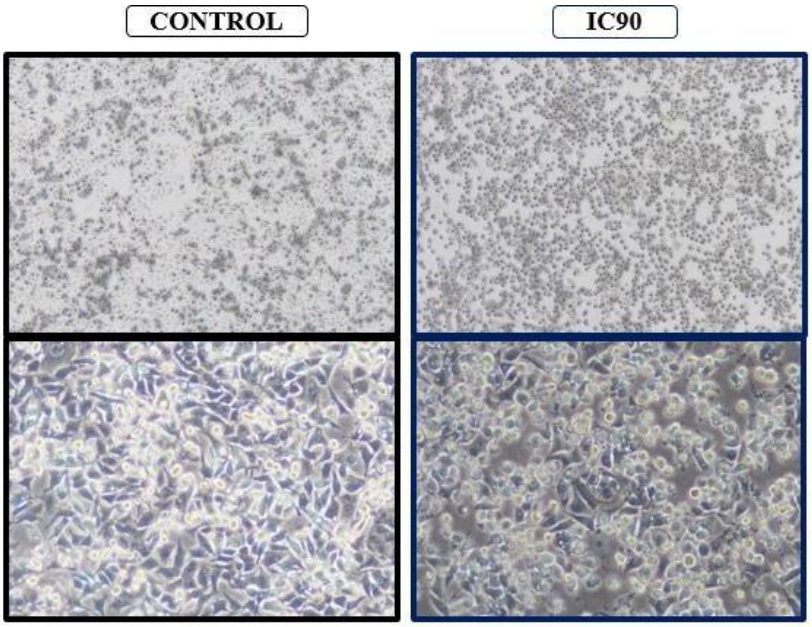

Figure 2.8. Microscopic image when HCT-15 colon cancer cells begin to aggregate for RNA isolation at the 24th hour

RNA Isolation Procedure:

Cells are lifted with trypsin and centrifugation is performed. Discard the supernatant and onto the cell pellet add 350 microliters of Buffer RA1 and 3.5 microliters of ß mercapto-ethanol (ß-ME). After vortex, it is placed in a filtered ependort tube. Perform centrifuge at 11000 g for 1 minute. The filter is removed and 350 µL 70% ethanol is added to the sample and placed in a new tube. 350 µL of 70% ethanol is added to it. It is vortexed. Performed centrifuge at 11000 g for 30 seconds. The filter is placed in a new tube. 350 microliters of MDB buffer is added. Centrifuge for 1 minute at 11000 g. Add 10 µL rDNase and 90 µL Reaction Buffer. Incubate for 15 minutes at room temperature. 200

microliters of RAW2 Buffer is placed on it. Centrifuge at 11000 g for 30 seconds. The filter is placed in a new tube. 600 microliters of RA3 buffer is added. Performed centrifuge at 11,000 g for 30 seconds. The supernatant is discarded. 250 microliters of RA3 Buffer is added to the filter. Centrifuge at 11,000 g for 2 minutes. The filter is placed in the new tube. The isolated RNA is now attached to the filter. To obtain RNA from the filter, 60 µL of distilled water is added. Centrifuge at 11,000g for 1 minute. The RNA concentration is measured by using nanodrop. And it is stored at -80°C.

2.6.2. Spectrophotometric analysis of RNA samples and quantification of RNA template amounts for cDNA synthesis

The Nanodrop spectrophotometer is use to measure the concentration of RNA samples. The samples A260/A280 ratios were carefully monitored to ensure that they were between 1.7 and 2. To synthesize with cDNA BioRad iScript Cdna Synthesis Kit (1708890), 1 µg/µl of RNA from each sample was added to a 30 µl reaction volume. Thus, by using equal amounts of RNA in all samples, cDNA synthesis was ensured, and gene expression variances across samples were not driven by variations in template RNA amounts.

2.6.3. Primer Design for Gene Expression Analysis with Real-Time PCR

Primer designs for a total of 82 genes related to apoptosis, autophagy, DNA damage and oxidative stress pathways were designed by Assoc. Prof. Dr. Zelal Adıgüzel byusing the Primer Express 3.0 (Applied Biosystems) program. GAPDH, YWHAZ and HCRT genes were used as an endogenous controls. Primer sequences of the genes were determined from the National Institute for Biotechnology Information (NCBI) database.

2.6.4. Gene Expression Analysis by Real-Time PCR

Real-time PCR is a method used in gene expression measurement to amplify and determine the amount of the targeted cDNA or DNA sequence. The real-time PCR method is a preferred method due to its efficiency and accuracy, as well as measuring mRNA expression. Gene expression study with real-time PCR; It consists of three stages: cDNA synthesis, detection of PCR products and data analysis.

2.6.5. cDNA synthesis

The mixture amounts and conditions required for cDNA synthesis from RNA samples obtained from the control and palladium (II) compound-treated treatment groups are as follows:

A cDNA mixture (mix) was prepared in the appropriate reaction tube based on the amounts in Table 2.1. The amount of RNA in the mixture was calculated to be 1 mg. Thus, equal amounts of RNA were

used for all samples. Thus, it was ensured that gene expression differences in the samples were not due to variability in template RNA amounts. After the total volume in all tubes was prepared to be 20 ml, the tubes were placed in the PCR device and this protocol was applied using the BioRad iScript Cdna Synthesis Kit (1708890) cDNA kit. Total RNAs were specifically converted into cDNA under PCR conditions of 5 min at 25°C, 20 min at 46°C, and 1 min at 95°C. The obtained cDNA samples were stored at -20°C for expression analysis. For expression analysis, cDNAs were created from GAPDH and the other two, which were selected as endogenous controls, three genes whose expression levels would be determined, and the reference control obtained from the pool created from the RNAs of healthy individuals (control RNA pool called 0).

Table 2.1. Quantities of prepared mixture for cDNA synthesis

Reaction Component	**Amount (for 1×)**
5× Reaxion Mix	4 µl
RNA	1 µg*
Reverse Transkriptase	1 µl
dH_2O	12 µl
Total	20 µl

* 1 µg of each RNA sample was taken and used in cDNA synthesis. (RNA amounts vary in each sample; the table above is representative).

[6h Control RNA] = 433,6 ng/ul 1 µg RNA in **2,3 µl**

[6h IC50 RNA] = 434,1 ng/ul 1 µg RNA in **2,3 µl**

[6h IC50 RNA] = 363,5 ng/ul 1 µg RNA in **2,75 µl**

[24h Control RNA] = 497,5 ng/ul 1 µg RNA in **2,01 µl**

[24h IC50 RNA] = 754 ng/ul 1 µg RNA in **1,32 µl**

[24h IC90 RNA] = 353,4 ng/ul 1 µg RNA in **2,83 µl**

2.6.6. Detection of qPCR Products

At this stage, real-time measurement of the PCR products created was performed. A total of 25 µl of the expression mixture, including cDNA, prepared based on the amounts specified in Table 2.2, was placed in each well of the 96-well Real Time plate. All genes whose expression will be analyzed were placed on the 96 qPCR well plate, respectively, as shown in Figure 2.9 and Figure 2.10. In the plate, no cDNA was added to 4 wells for GAPDH, YWHAZ, HPRT1 and the 0 control pool. Then, the plate was covered with film so that no air bubbles remained and was placed in the heat block of the Real-time device (Applied Biosystem QuantStudio). 5 min at 94°C in the start up phase, 40 s at 94°C, 30 s at 60°C, 40 s at 68°C, and 40 cycles of 1 min at 94°C, 55°C in the cycling phase. Real-time PCR analysis was performed for 1 min at 94°C and 15 s at 94°C.

Table 2.2. Mixture Amounts Prepared for Gene Expression Analysis

Reaction Component	**Amount (for 1×)**
2x QuantiNova SYBR Green RT-PCR Master Mix (MN 208252)	12,5 µl
dH_2O	* µl
For each gene F+R primer	2 µl
GAPDH YVHAZ HPRT1	2 µl
cDNA	10 ng each well
Total	25 µl

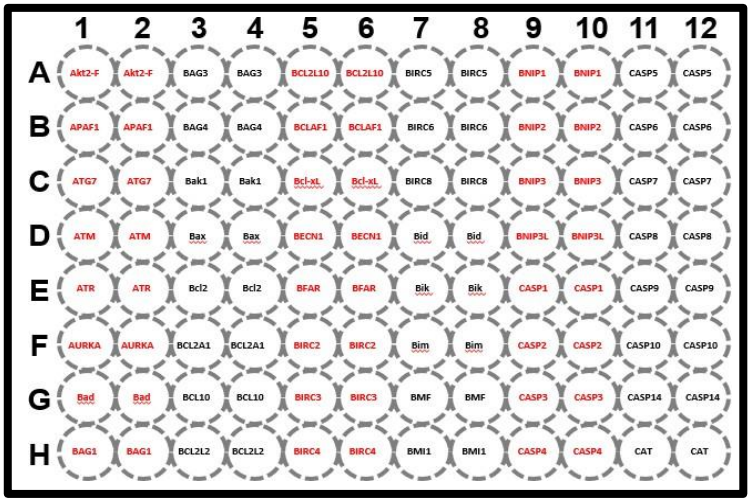

Figure 2.9. Genes analyzed in Template 1

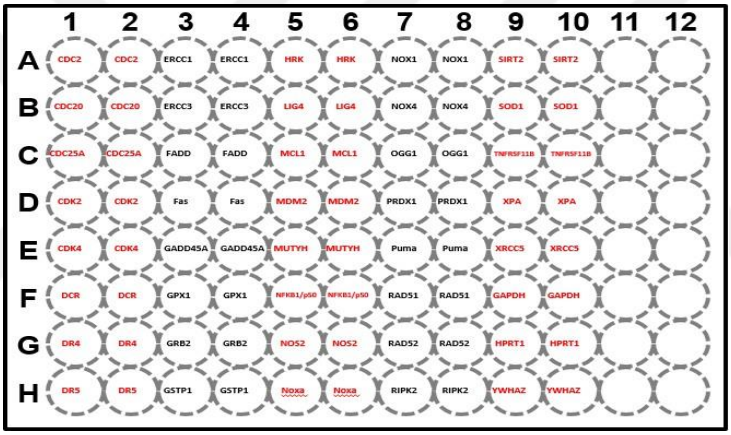

Figure 2.10. Genes analyzed in Template 2

2.6.7. Data Analysis for Gene Expression Study

At the final stage, the gene amounts in the control group and the Pd(II) applied drug group (endogenous control and target gene) are comparing the positive control samples and the difference in the gene amount were detected. To demonstrate these changes in gene expression levels, $2^{-\Delta\Delta CT}$ values were found and analyzed using Excel, Graphed Prism 9.4.1 and IBM SPSS Statistics 28.0 programs.

2.7. Statistical analysis

2.7.1. Editing and Statistical Analysis of Expression Data

Statistical analyzes related to this study were carried out by Koç University Department of Biostatistics Faculty Member Dr. Made by Mert Veznikli. Due to the low sample size of the gene data, the Whitney U test, a un parametric method, was used. Analysis of expression values was performed after calculating the 2-ΔΔCT method. The descriptive statistics table of the expressions includes mean, standard deviation, median, mode, minimum, maximum, 25% (Q_1) and 75% (Q_3) values, respectively. Descriptive statistics are expressed as frequency and percentage. In the analysis, the p value is take as 0.05 for the istatistical significance level. A value of $p<0.05$ was considered significant. IBM SPSS Statistics 28.0 program was used to analyze the data.

CHAPTER 3

3. RESULTS

3.1 Results of MTT Cell Viability

A Pd (II) compound was treatment to HCT-116, HCT-15, and HT-29 colon cancer cells (Figure 3.1) by serial dilution at various doses (ranging from 3 to 100 μM) for durations of 24, 48, and 72 hours. Statistically significant reductions in % cell viability were found in the cell lines treated with the Pd (II) compound, as the concentration rose with time and IC50 an IC90 dosage ($p<0.05$). Figure 3.1 displays the findings. Significant reductions in cell viability were found in HCT-15, HCT-116, and HT-29 colon cancer cells compared to the control when treated with Pd (II) compound at concentrations of 100, 50, and 25 μM. These reductions were dependent on time and were statistically significant ($p<0.001$). To further experiments the according to the our protocol the IC90 values have been used.

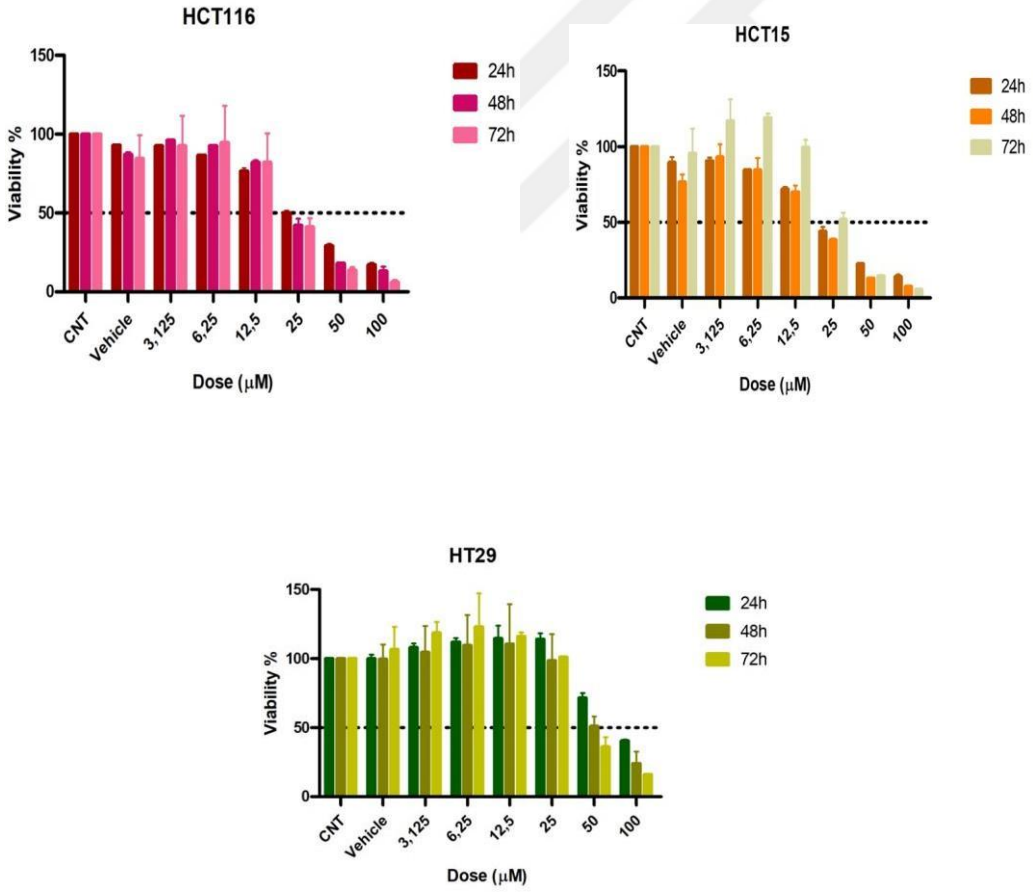

Figure 3.1. % Cell Viability Graph of HCT-116, HCT-15 and HT-29 cell lines

According to MTT results; important in demonstrating the cytotoxic activity of the Pd(II) compound on HCT-116, HCT-15 and HT-29 cell lines are IC50 (the concentration that die 50% of the cells after treatment with the Pd(II) compound compared to control cells. And IC90 (the values that concentration that kills 90% of the cells after treatment with the Pd (II) compound compared to control cells) are given in Table 3.1.

Table 3.1. IC50 and IC90 values during the 48-hour treatment period according to the MTT viability test results in cell lines applied with Pd (II) compound

	HCT116			HCT15			HT29		
uM	24H	48H	72H	24H	48H	72H	24H	48H	72H
IC50	25	22,5	22,2	22,3	20,4	26,4	84,9	51,9	44,7
IC90	**>100**	**>100**	72,9	**>100**	77,6	75,9	**>100**	**>100**	**>100**

3.2. Results of Double Staining

Annexin-V (FITC) binds to phosphatidyl sherine (PS) on the outer surface of the cell which undergoing apoptosis and indicates whether the cell has undergone apoptosis or not. Because in a normal healthy cell, this molecule is located on inside the cell. When a fluorescent material is added to Annexin-V (FITC), apoptotic cells become visible and can be examined using a fluorescence microscope. Moreover, since Annexin-V binding is observed on the outer surfaces of necrotic cells, the incorporation of propidium iodide (PI) as an additional dye is carried out during the investigation of this technique. When cells are stained with both Annexin-V (FITC) Fluorescein and the non-vital dye propidium iodide (red fluorescein). Normal living cells can be seen under the microscope with Hoechst 33342. PI dye is also added to the medium to demonstrate apoptotic or necrotic cells. Red cells stained with PI are seen at the bottom. We can say that these cells died by late apoptosis or necrosis. However, those seen in blue are normal living cells stained with Hoechst 33342. A double staining method (use together both Hoechst 33342 and PI staining) is used and evaluated under fluorescence microscopy at 24 and 48 hours after Pd(II) treatment. After a 24 hour treatment with the Pd(II) compound alone, a decrease in cell density was detected in the HCT-15 cell line compared to the control (Figure 3.2). Also some cells are called pignotic. These pignotic structures show that the nuclei of the cells are smaller compared to the control. This results imply that the cell will undergo

apoptosis. It can be concluded that the cells undergo late apoptosis or necrosis, as seen in the image below. In the 48-hour images, we see red PI stained apoptotic cells more intensely (Figure 3.3).

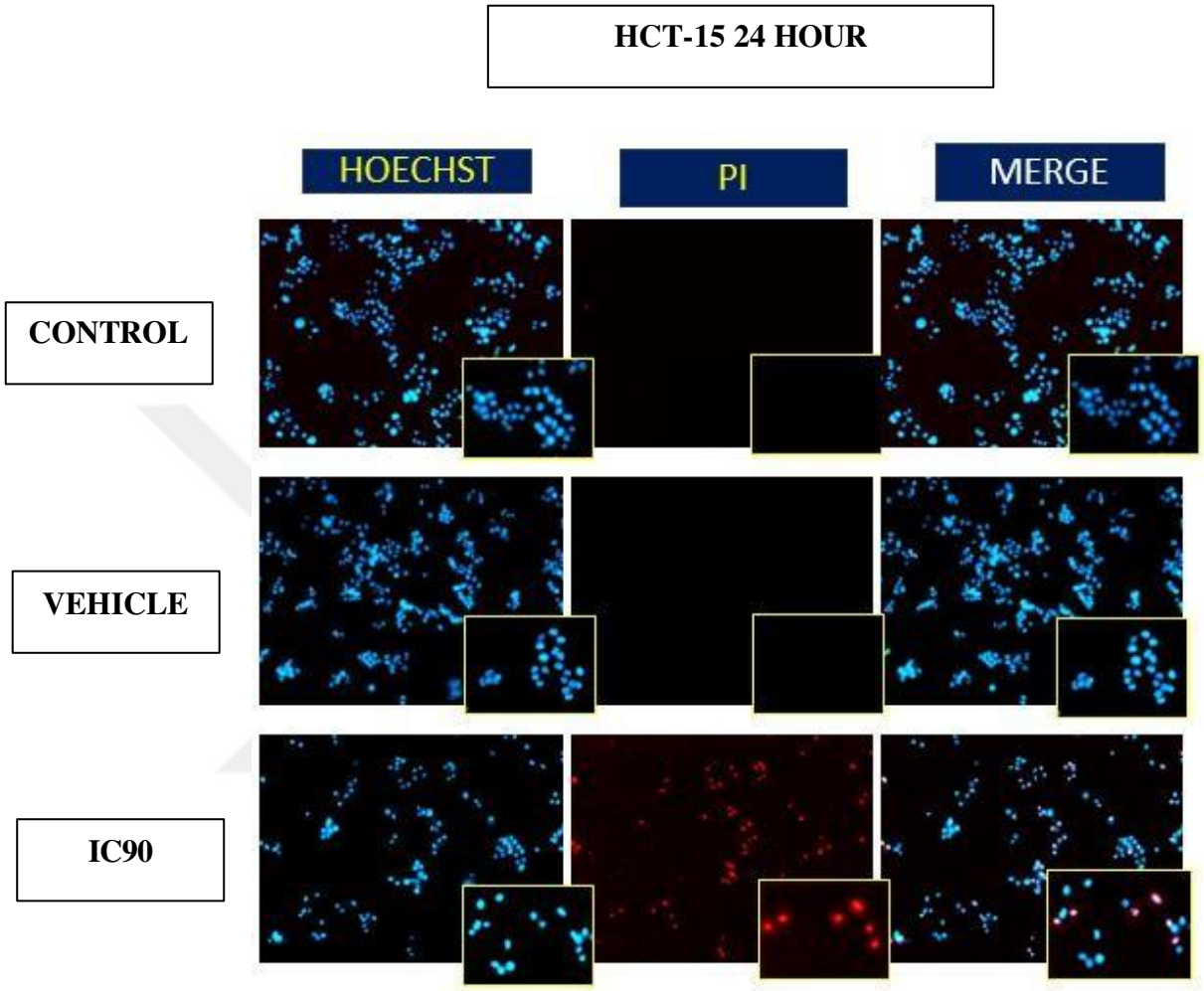

Figure 3.2. Fluorescence Microscope Images of HCT-15 cell line after 24-h Pd(II) compound treatment

Hoechst 33342 (Blue), PI (propidium iodide) (Red)

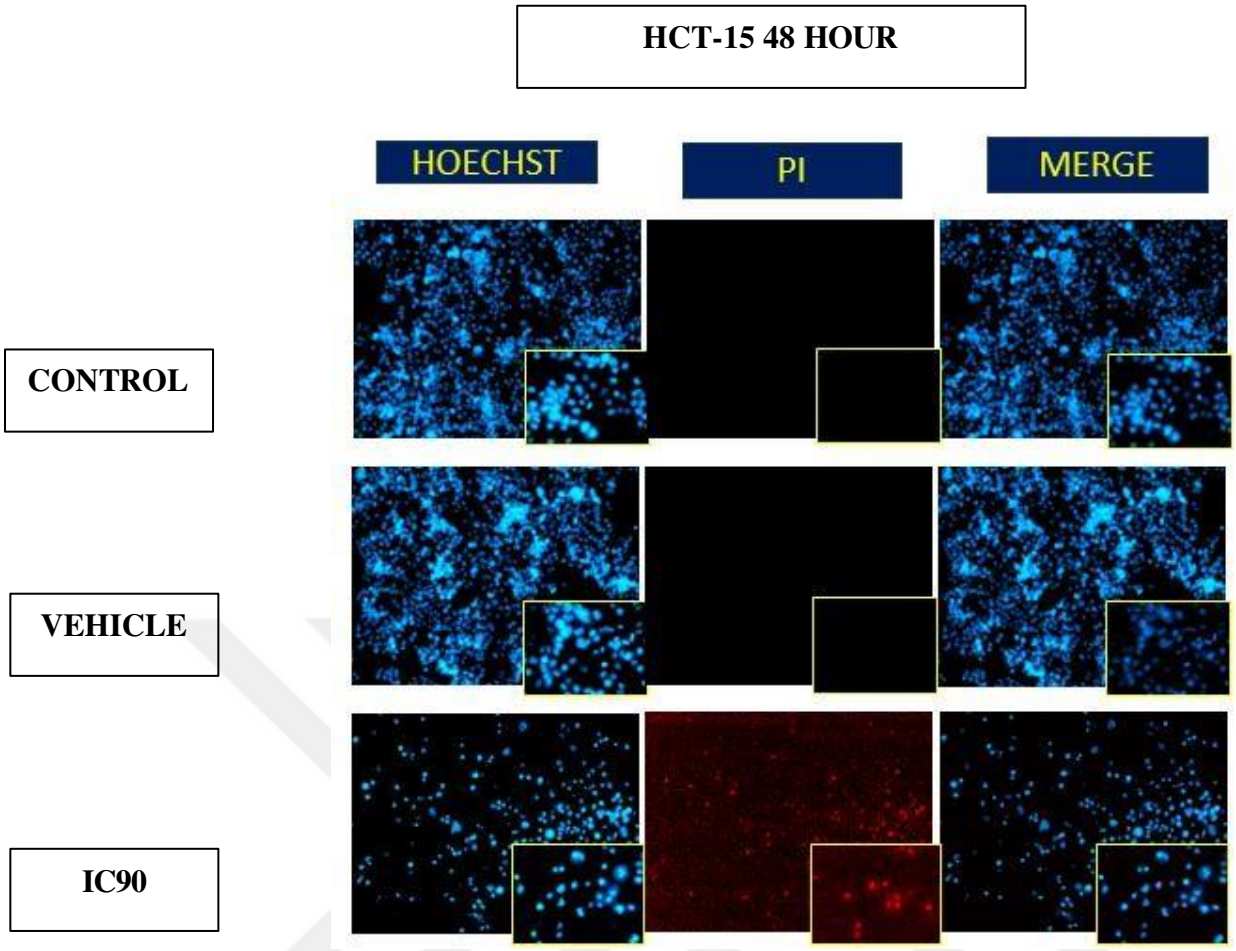

Figure 3.3. Fluorescence Microscope Images of HCT-15 cell line after 48-h Pd(II) compound treatment

Hoechst 33342 (Blue), PI (propidium iodide) (Red)

3.3. Flow Cytometry Results

3.3.1. Evaluation of Annexin-V (FITC)

As a result of Annexin-V (FITC) of the apoptotic cell death mechanism in flow cytometry; After 12 hours of treatment in the HCT-15 cell line, the early apoptotic rate of Pd (II) compound was determined to be %4,14; late apoptosis rate was found to be % 16,05. After 24 hours of treatment, the ratio of early apoptotic cells was found to be %4,41 and late apoptotic ratio was found to be %25,74 as a result of treatment with Pd (II) complex (Figure 3.4 and 3.5). According to these results, it was observed that the our Pd(II) compound induced cell death by apoptosis after 12 and 24 hours of treatment.

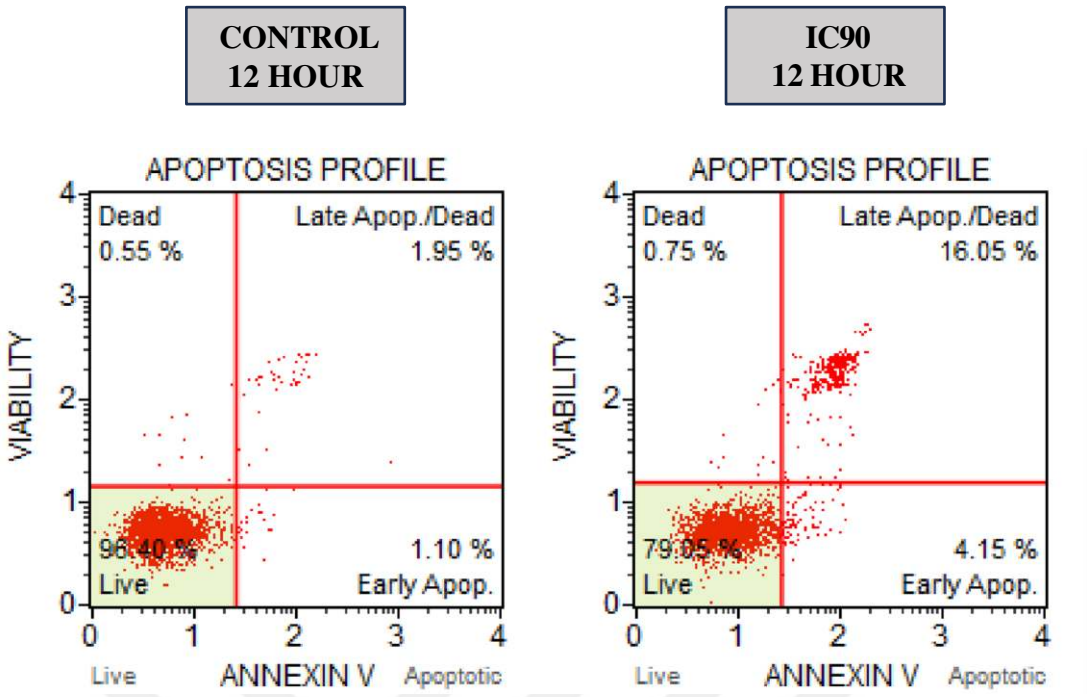

Figure 3.4. 12-hour histograms of % apoptotic values obtained by Annexin-V evaluation of Pd (II) compound (77,6 µM) in HCT-15 colon cancer cell line

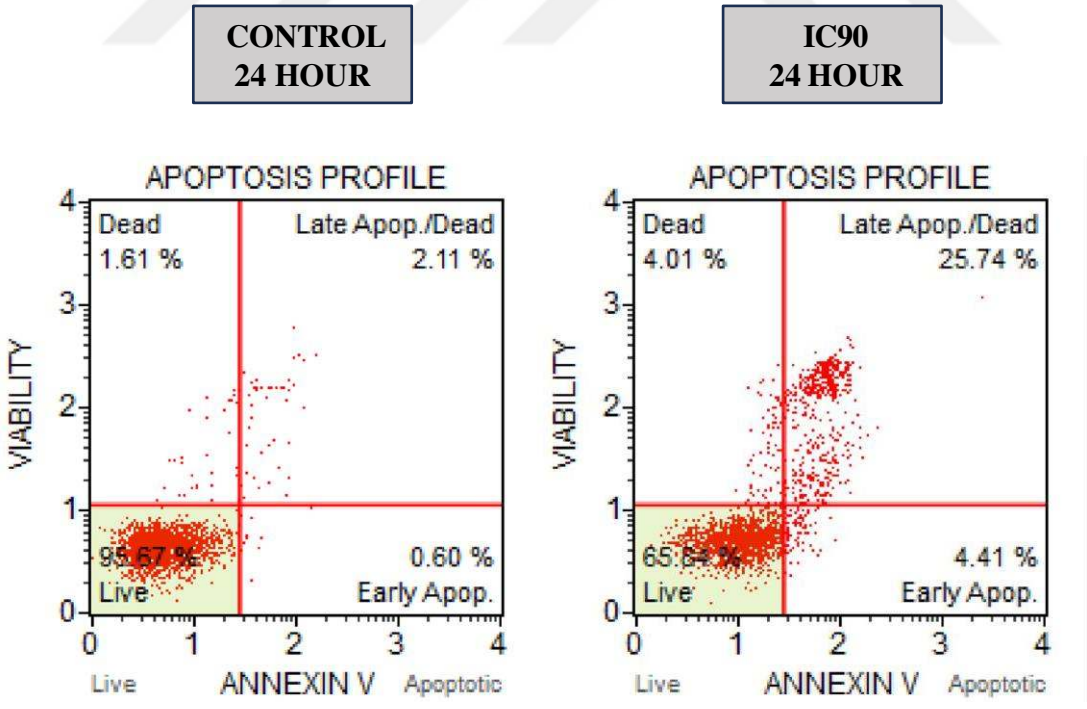

Figure 3.5. 24-hour histograms of apoptotic percentage values obtained by Annexin-V (FITC) assessment of Pd(II) compound (77,6 µM) in HCT-15 colon cancer cell

3.3.2. Determining DNA Damage

Expression of H2AX is a specific marker to detect DNA double strand breaks. As a result of the evaluation of H2AX in flow cytometry, it was found that after 12 hours, the Pd (II) compound caused % 99,1 DNA damage in the HCT-15 cell compared to the control (Figure 3.6). After 24 hours of treatment, Pd(II) compound was found to cause 67.2% DNA damage in HCT-15 cells compared to the control. (Figure 3.9).

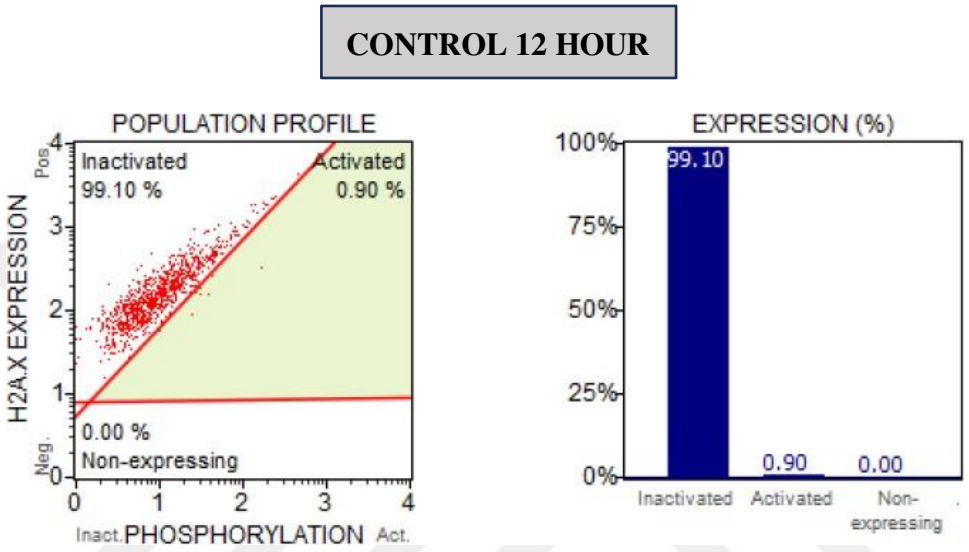

Figure 3.6. 12-hour histogram of p-γH2AX percentage values of Pd(II) compound (77,6 µM) in HCT-15 colon cancer control cells

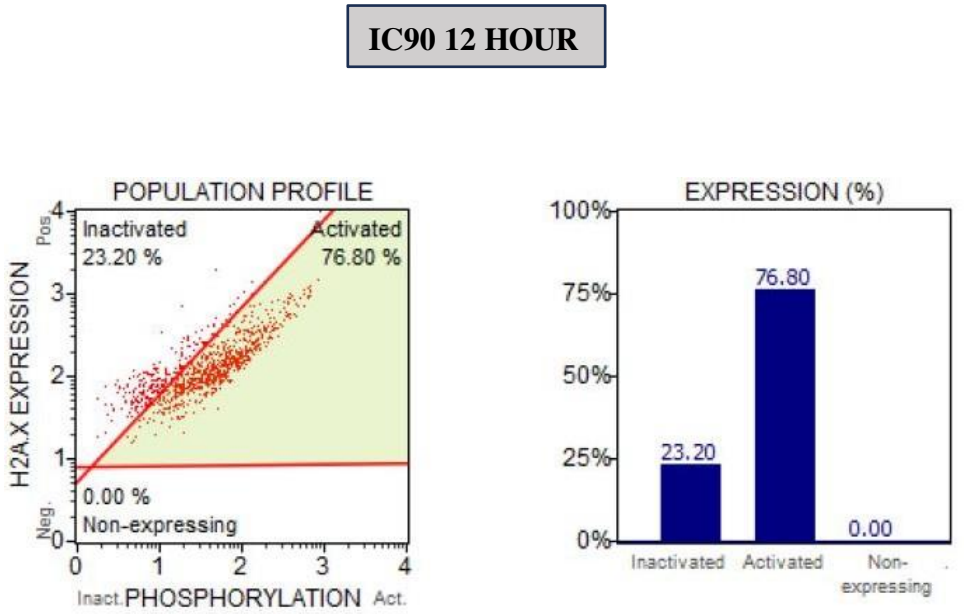

Figure 3.7. 12-hour histogram of p-γH2AX percentage values of Pd(II) compound (77,6 µM) in HCT-15 colon cancer treatment cells

CONTROL 24 HOUR

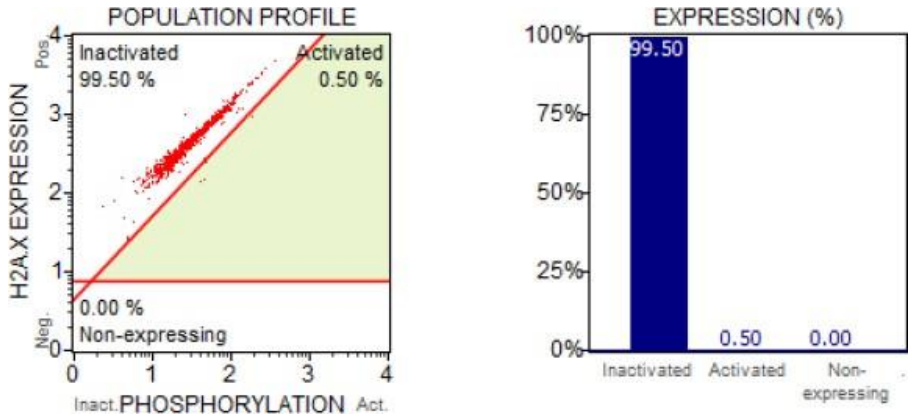

Figure 3.8. 24-hour histogram of p-γH2AX percentage values of Pd(II) compound (77,6 µM) in HCT-15 colon cancer control cells

IC90 24 HOUR

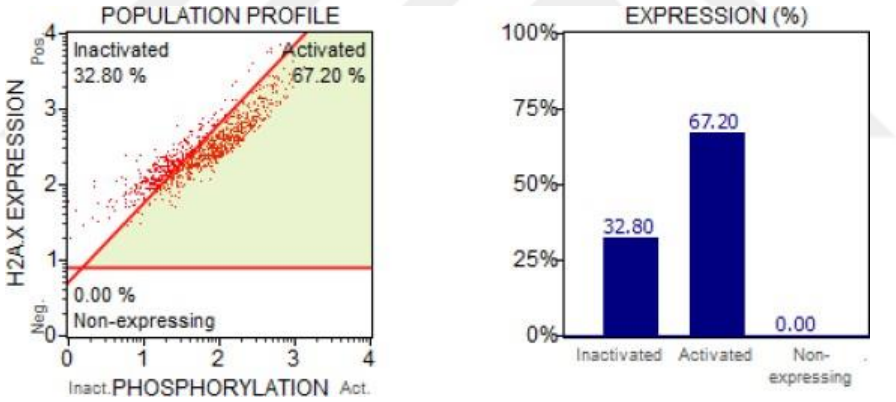

Figure 3.9. 24-hour histogram of p-γH2AX percentage values of Pd(II) compound (77,6 µM) in HCT-15 colon cancer cells

3.3.3. Assesment of Oxidative Stress (ROS)

In response to the question of whether DNA damage was caused by ROS, the amount of ROS was examined in flow cytometry (Figure 3.10). It was observed that the application of Pd (II) compound treatment in HCT-15 cells did not cause a change in the amount of ROS compared to the control (Control ROS amount: 0.13%; Pd (II) compound ROS amount: 0.50% (Figure 3.11).

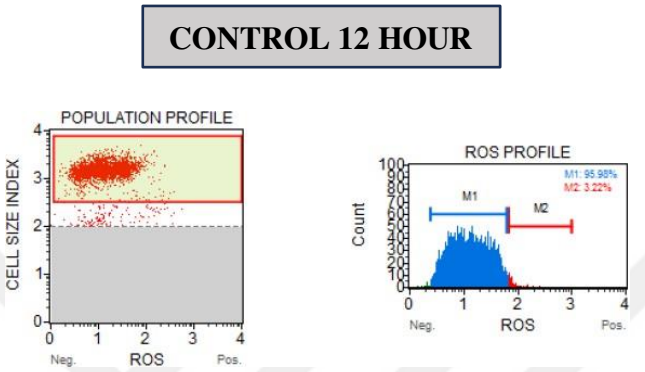

Figure 3.10. 12-hour histogram of ROS percentage values of Pd(II) compound (77,6 µM) in HCT-15 colon cancer control cells

M1: ROS negative cells(–); M2: ROS positive cells ROS(+)

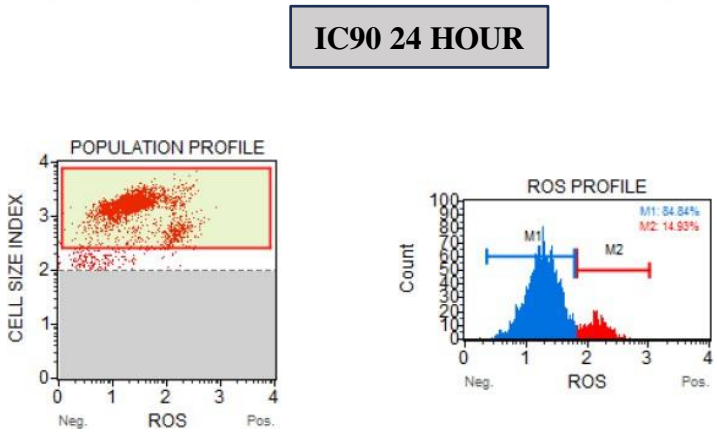

Figure 3.11. 12-hour histogram of ROS percentage values of Pd(II) compound (77,6 µM) in HCT-15 colon cancer treatment cells

M1: ROS negative cells(–); M2: ROS positive cells ROS(+)

CONTROL 24 HOUR

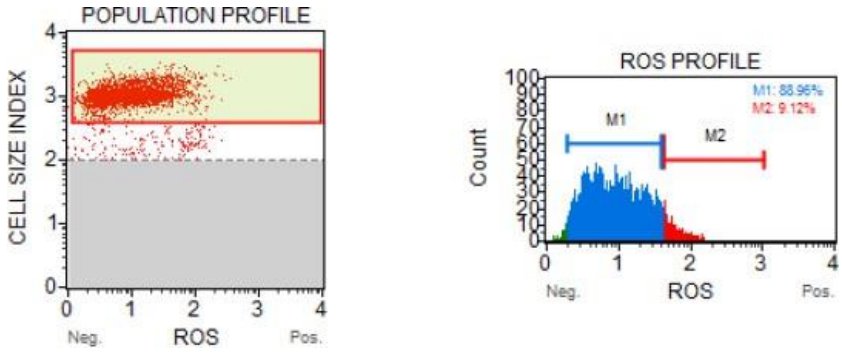

Figure 3.12. 24-hour histogram of ROS percentage values of Pd(II) compound (77,6 µM) in HCT-15 colon cancer control cells

M1: ROS negative cells(–); M2: ROS positive cells ROS(+)

IC90 24 HOUR

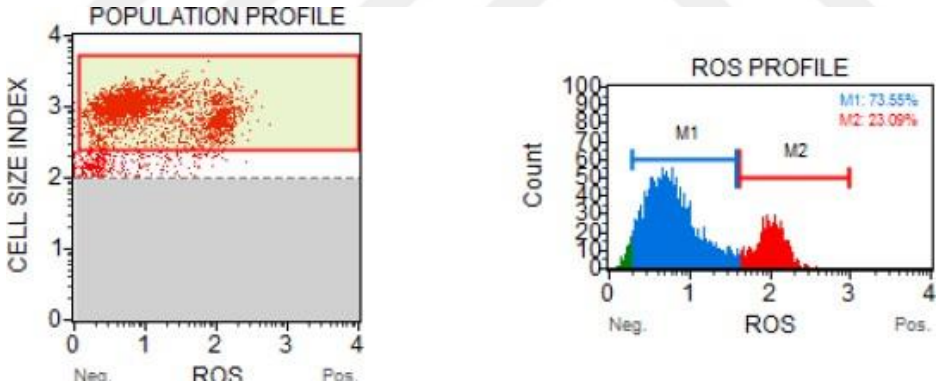

Figure 3.13. 24-hour histogram of ROS percentage values of Pd(II) compound (77,6 µM) in HCT-15 colon cancer treatment cells

M1: ROS negative cells(–); M2: ROS positive cells ROS(+)

3.3.4. Results of N-acetyl-L-cysteine (NAC) Treatment

In order to confirm the findings in the HCT-15 cell line, the ROS experiment was verified by using N-acetyl-L-cysteine (NAC), a well-known substance that eliminates ROS. Prior to experimentation, HCT-15 cells were exposed to a 5 mM concentration of NAC for a duration of 3 hours. Subsequently, the medications were delivered sequentially. The impact of NAC and the chemical was assessed using

the MTT cell viability assay. The findings indicate that the cytotoxic effects of the medicines ceased with the application of NAC, which is recognized as a reactive oxygen species (ROS) scavenger. An augmentation in the quantity of viable cells was found in HCT-15 cells when exposed to both the pre-application of a Pd (II) compound and a NAC inhibitor, as well as in cells treated with the Pd (II) compound and NAC. It was noted that NAC, which is recognized as a scavenger of reactive oxygen species (ROS), counteracted the negative impact on cell viability caused by treatment with Pd (II) compounds alone in HCT-15 cells (Figure 3.14). The reduction in levels of reactive oxygen species (ROS) and the removal of the inhibitory impact on vitality via the use of NAC suggest that oxidative stress is a significant factor in the regulation of the transition between apoptosis and autophagy.

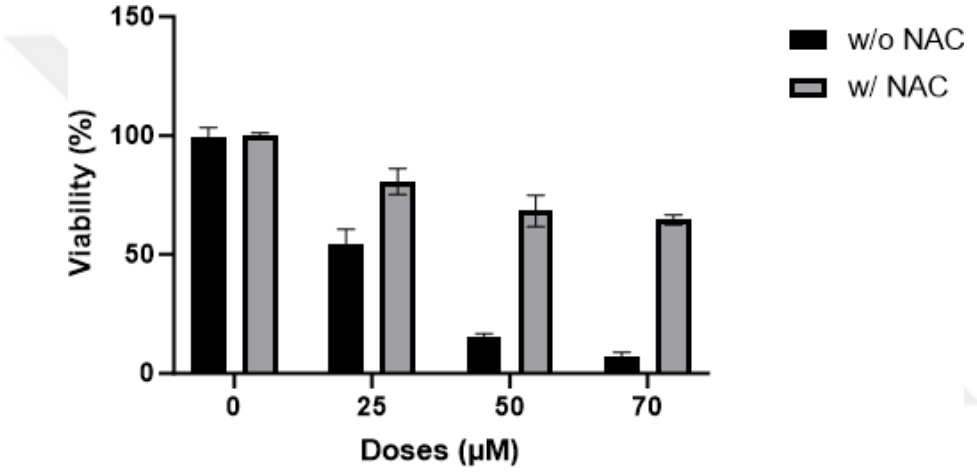

Figure 3.14. % Cell Viability Graph of HCT-15 colon cancer lines after pre-treatment with N-acetyl-L-cysteine (NAC)

3.3.5. Results of Autopaghy Analysis

Expression of LC3-II, an important autophagy protein, was measured in flow cytometry with the Muse Analyzer device. According to the results, a significant increase was detected in HCT-15 cells treated with Pd (II) compound, especially at the 12th hour, compared to the control. It was determined that autophagy intensity decreased at the 24th and 48th hours. The result here was interpreted as the cells using autophagy as a survival method, not a death method, and therefore it caused a huge increase at the 12th hour (Figure 3.15).

Control

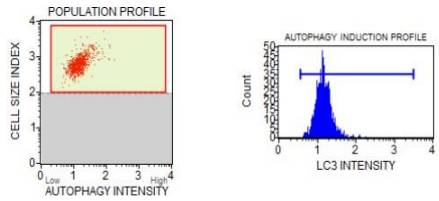

	Mean Autophagy Intensity	Autophagy Induction Ratio	Total # of Cells	Sample Type
Autophagy (LC3 detection)	17.1	1.0	1000	control

Positive Control

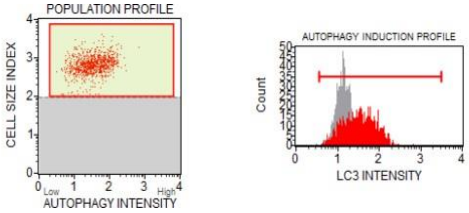

	Mean Autophagy Intensity	Autophagy Induction Ratio	Total # of Cells	Sample Type
Autophagy (LC3 detection)	46.9	2.8	999	target

6h

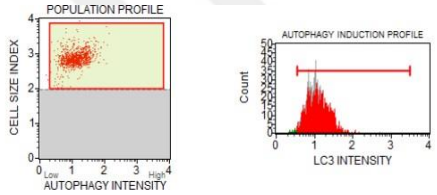

	Mean Autophagy Intensity	Autophagy Induction Ratio	Total # of Cells	Sample Type
Autophagy (LC3 detection)	16.2	1.3	982	target

12h

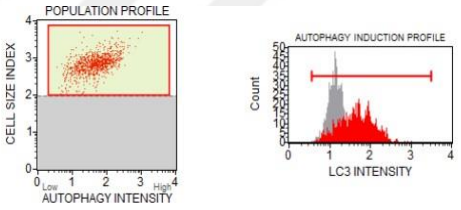

	Mean Autophagy Intensity	Autophagy Induction Ratio	Total # of Cells	Sample Type
Autophagy (LC3 detection)	69.2	4.1	999	target

24h

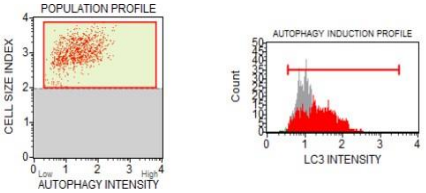

	Mean Autophagy Intensity	Autophagy Induction Ratio	Total # of Cells	Sample Type
Autophagy (LC3 detection)	38.5	3.1	988	target

48h

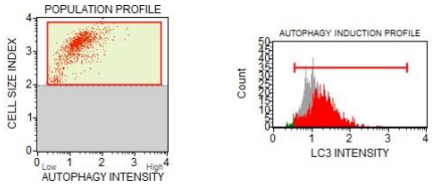

	Mean Autophagy Intensity	Autophagy Induction Ratio	Total # of Cells	Sample Type
Autophagy (LC3 detection)	30.0	2.4	970	target

Figure 3.15. Results of Autophagy Analysis

3.4. Effect of Pd(II) Compound on Migration Abilities in HCT-15 Cell Line

Measurements were made for 24, 48 and 72 hours after the application of Pd(II) compound in the HCT-15 colon cancer cell line. This experiment was repeated 2 times. As a result, it was observed that it did not cause any increase in migration compared to the control Figure 3.16).

1.try

2.try

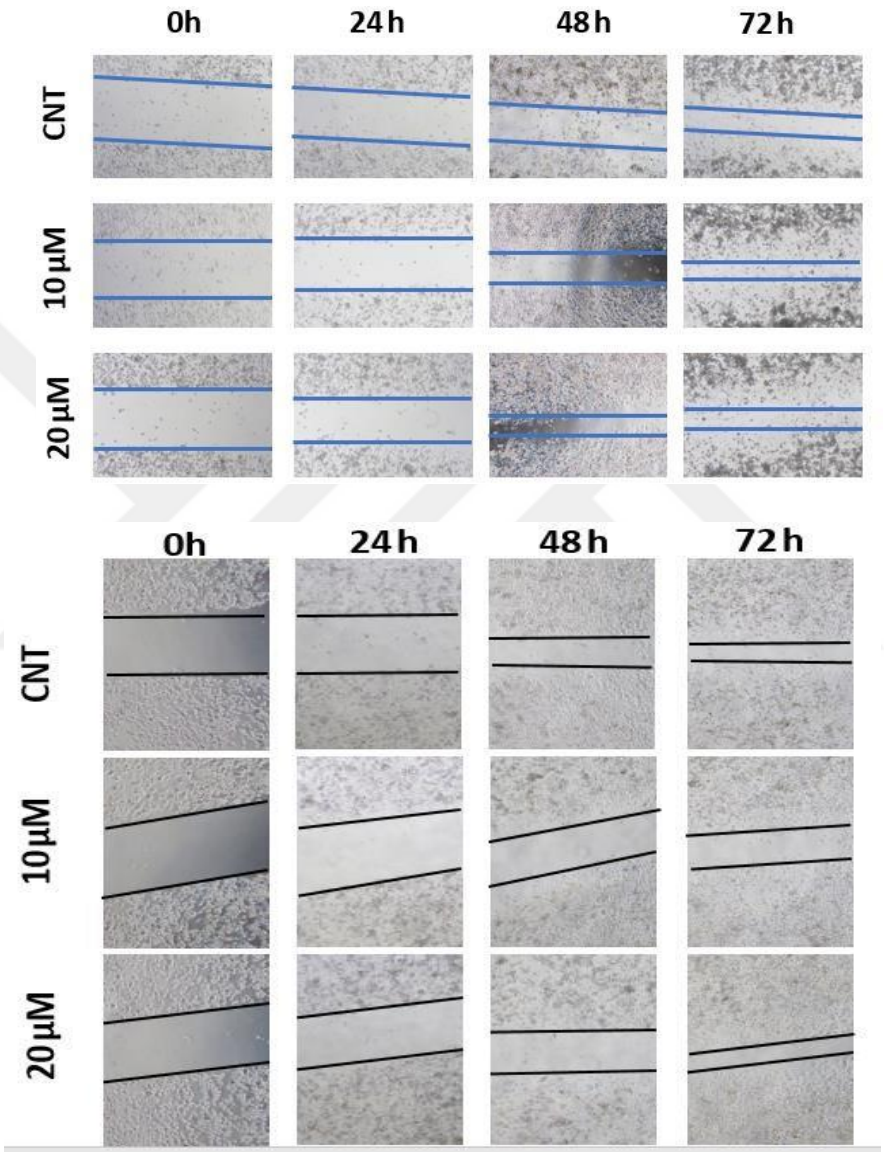

Figure 3.16. Migration images of Pd(II) compound treatment in HCT-15 colon cancer cell line

3.5. Analysis the Expression levels of 82 genes that Related to Apoptosis

The expression levels of a total of 82 genes, which are known to play an important role in important cellular pathways such as apoptosis, autophagy and DNA damage, were evaluated according to the control and treatment groups and p values were calculated. As a result, genes whose expression levels were significant were shown in both the table and the graph. P value tables for each significant gene are given below (Table 3.5 and Table 3.6). Genes were divided into 3 classes: pro-survival, pro-apoptotic, and DNA damage. All gene expression graphs are shown below (Fig 3.17-Figure 3.22)

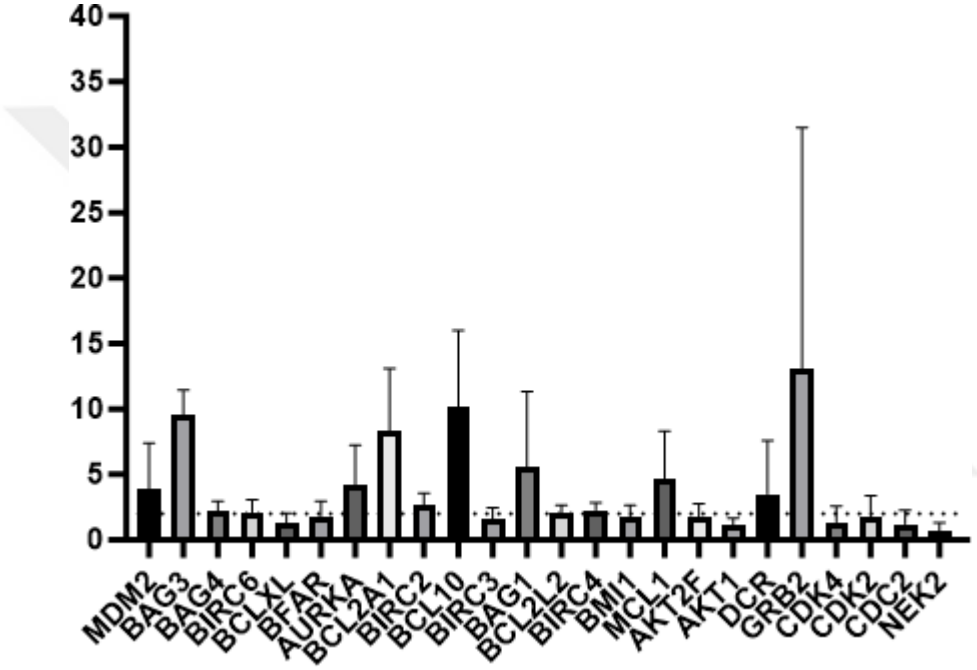

Figure 3.17. Graphical representation of the expression levels of prosurvival genes after 6 h treatment with Pd(II) compound (77,6 µM) in HCT-15 colon cancer cell line

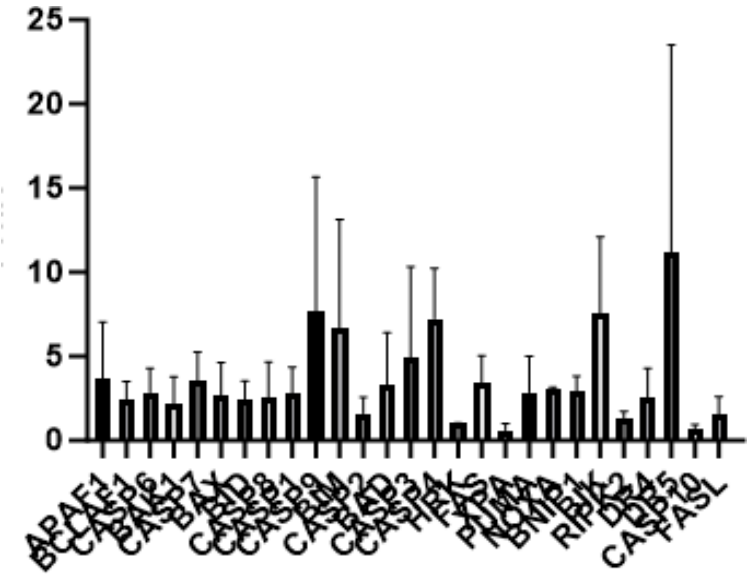

Figure 3.18. Graphical representation of the expression levels of pro-apoptotic genes after 6 h treatment with Pd(II) compound (77,6 µM) in HCT-15 colon cancer cell line

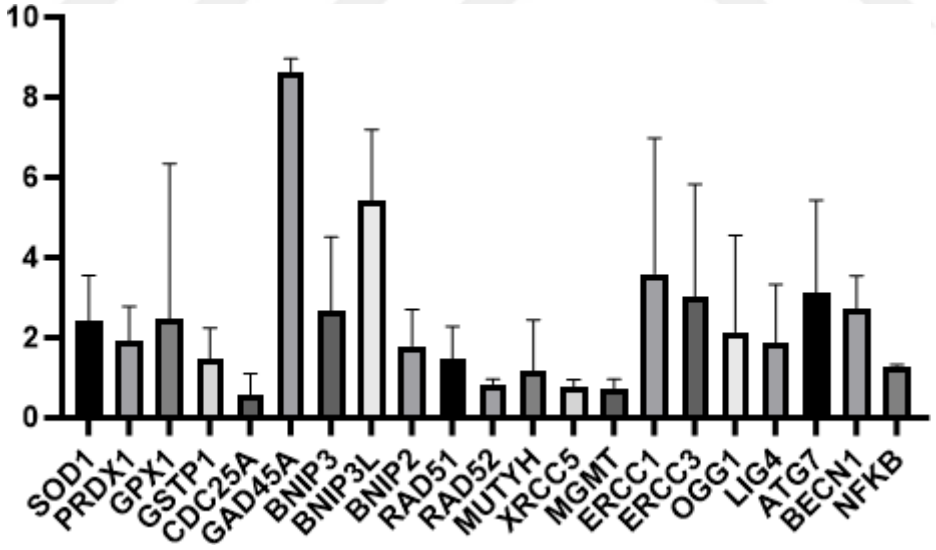

Figure 3.19. Graphical representation of the expression levels of DNA damage or stress genes after treatment with Pd(II) compound (77,6 µM) for 6 hours in the HCT-15 colon cancer cell line

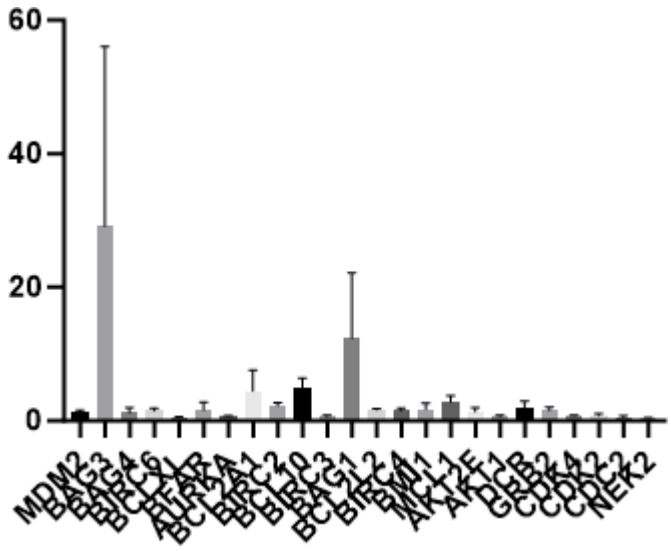

Figure 3.20. Graphical representation of expression levels of prosurvival genes after 24 h treatment with Pd(II) compound (77,6 µM) in HCT-15 colon cancer cell line

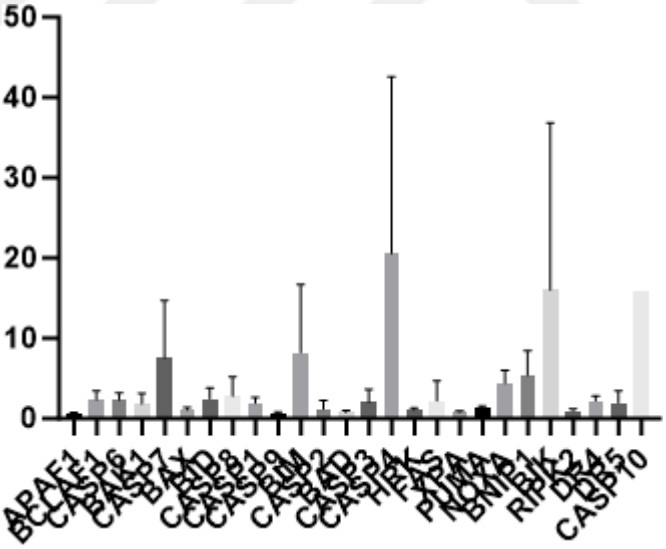

Figure 3.21. Graphical representation of expression levels of pro-apoptotic genes after 24 h treatment with Pd(II) compound (77,6 µM) in HCT-15 colon cancer cell line

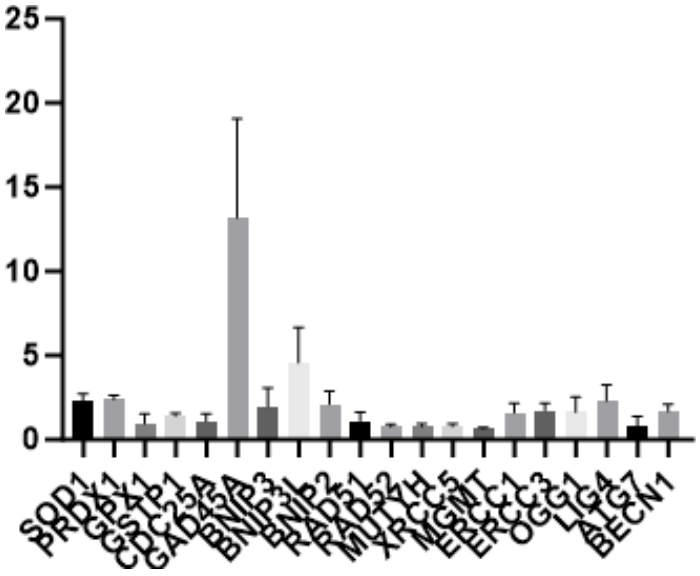

Figure 3.22. Graphical representation of the expression levels of DNA damage or stress genes after 24 h treatment with Pd(II) compound (77,6 µM) in HCT-15 colon cancer cell line

As mentioned above, the following tables were created based on the 2 delta CT values calculated for the 6th and 24th hours after the gene expression analysis. The tables were categorized as genes whose expression increased and decreased at the 6th and 24th hours. All tables are given below (Table 3.1-Table 3.4).

Table 3.1. Genes whose expression increases at 6h

	6 h			
Gene	**exp 1**		**exp 2**	
BAG3	26,53	42,86	21,17	36,42
BNIP1	4,99	4,57	-	-
CASP6	3,14	3,59	1,24	-
CASP7	26,08	25,12	2,90	2,69
BID	-	-	2,11	1,41
BNIP3L	10,71	18,23	1,49	1,06
BIRC2	3,53	3,81	1,64	1,03
BIM	9,22	9,18	2,88	1,28
BCL10	4,91	6,49	6,96	7,56
CASP3	142,79	85,38	1,23	0,82
BAG1	17,15	6,16	1,17	1,38

CASP4	267,22	299,18	4,32	2,83
LIG4	3,89	3,91	0,91	1,29
SOD1	-	-	1,92	1,71
PUMA	20,06	22,09	2,15	1,55
DR4	3,32	3,07	1,35	1,03
RAD52	5,48	5,52	-	-
NOXA	0,25	0,27	9,03	7,36
BIRC6	1,53	2,00	-	-
BMI1	2,65	2,80	0,44	0,63
ATG7	8,40	8,83	1,65	1,61
FAS	11,21	16,36	3,98	5,55
MDM2	1,23	1,22	2,15	1,97
XPA	1,96	2,03	1,73	-
GAD45A	34,34	40,44	14,56	14,47
DCR	22,70	25,48	1,77	0,94
DR5	5,04	3,60	6,20	3,61

Table 3.2. Genes whose expression increases at 24h

	24 h			
Gene	**exp 1**		**exp 2**	
BAG3	8,31	10,89	66,60	30,70
BNIP1	2,21	4,15	9,30	5,97
CASP6	1,61	1,62	3,33	2,74
CASP7	1,51	2,58	17,06	9,08
BID	1,50	1,31	3,96	3,21
BNIP3L	3,74	7,15	2,26	5,18
BIRC2	2,38	1,58	2,32	2,72
BIM	1,02	1,32	17,94	12,66
BCL10	4,08	6,82	5,31	3,29
CASP3	-	-	3,80	3,01
BAG1	14,17	1,74	8,75	24,92
CASP4	4,44	-	45,67	11,60

LIG4	3,22	3,05	1,41	1,55
SOD1	2,87	2,33	2,13	1,89
PUMA	8,86	8,36	20,98	14,48
DR4	1,25	1,32	3,39	1,95
RAD52	1,70	2,00	2,99	2,30
NOXA	3,08	3,14	4,91	6,46
XRCC5	1,47	1,30	1,65	1,43
BCL2L2	1,77	1,54	1,78	-
ERCC1	1,53	1,43	1,05	2,40
ERCC3	2,09	1,91	1,10	1,84
MCL1	3,64	3,56	1,76	2,39
PRDX1	2,23	2,37	2,17	2,75
GSTP1	1,61	1,42	1,41	1,22

Table 3.3. Genes whose expression decreases at 6h

	6 h			
Gene	**exp 1**		**exp 2**	
APAF1	-	-	0,73	0,64
BCLXL	0,35	0,43	0,84	0,30
CDC2	0,14	0,14	0,39	0,44
BCLAF1	0,94	1,18	0,66	0,74
AKT1	0,48	0,58	0,60	0,46
XRCC5	0,10	0,10	0,90	0,77

Table 3.4. Genes whose expression decreases at 24h

	24 h			
Gene	**exp 1**		**exp 2**	
APAF1	0,80	0,70	0,43	0,43
BCLXL	0,65	0,56	0,33	0,44
CDC2	0,75	0,72	0,30	0,33
GAD45A	0,82	0,76	0,44	0,42

DR5	0,80	0,91	0,75	0,56
BIRC3	0,68	0,77	0,31	0,75
NEK2	0,40	0,38	0,45	0,44
CDK4	0,89	0,78	0,65	0,50
MGMT	0,58	0,56	0,71	0,70
BIRC5	0,32	0,47	0,51	0,50

Table 3.5. M, SD, median, min-max, Q1, Q3 and p values of the relevant Genes at the 6th hour according to Control and Pd(II) IC90 Groups

M: Mean; SD: standard deviation; Q (Querter) Q1=25%, Q3=75%, h: hour

Target Gene	Group	6h							
		M	**SD**	**Median**	**Mode**	**Min**	**Max**	**Q25**	**Q75**
AKT1	**Control**	,0588	,0268	,0547	,0361[a]	,0361	,0895	,0363	,0812
	Pd(II) IC90	,0500	,0170	,0473	,0334[a]	,0334	,0723	,0371	,0630
APAF1	**Control**	,0033	,0029	,0033	,0007[a]	,0007	,0061	,0008	,0058
	Pd(II) IC90	,0048	,0011	,0045	,0039[a]	,0039	,0063	,0040	,0056
ATG7	**Control**	,0040	,0021	,0038	,0022[a]	,0022	,0063	,0022	,0058
	Pd(II) IC90	,0105	,0013	,0105	,0088[a]	,0088	,0119	,0095	,0114
BAG1	**Control**	,0109	,0102	,0109	,0011[a]	,0011	,0206	,0021	,0197
	Pd(II) IC90	,0160	,0109	,0177	,0029[a]	,0029	,0258	,0071	,0250
BAG3	**Control**	,0010	,0005	,0010	,0004[a]	,0004	,0014	,0006	,0013
	Pd(II) IC90	,0379	,0115	,0379	,0261[a]	,0261	,0497	,0282	,0476
BCL10	**Control**	,0018	,0020	,0015	,0000[a]	,0000	,0039	,0001	,0034
	Pd(II) IC90	,0248	,0286	,0239	,0000[a]	,0000	,0514	,0001	,0495
BCLAF1	**Control**	,0513	,0382	,0502	,0163[a]	,0163	,0886	,0184	,0842
	Pd(II) IC90	,0605	,0119	,0590	,0491[a]	,0491	,0750	,0509	,0701
BCLXL	**Control**	,0700	,0258	,0658	,0450[a]	,0450	,1035	,0502	,0899
	Pd(II) IC90	,0719	,0316	,0759	,0314[a]	,0314	,1044	,0479	,0959
BID	**Control**	,0661	,0244	,0655	,0438[a]	,0438	,0896	,0451	,0871

	Pd(II) IC90	,1519	,0212	,1516	,1264[a]	,1264	,1781	,1379	,1659
BIM	**Control**	,0020	,0005	,0021	,0014[a]	,0014	,0025	,0017	,0023
	Pd(II) IC90	,0146	,0127	,0145	,0033[a]	,0033	,0263	,0036	,0257
BIRC2	**Control**	,0126	,0091	,0107	,0050[a]	,0050	,0241	,0052	,0200
	Pd(II) IC90	,0213	,0058	,0230	,0132[a]	,0132	,0261	,0172	,0255
BIRC3	**Control**	,0015	,0012	,0010	,0008[a]	,0008	,0033	,0008	,0022
	Pd(II) IC90	,0015	,0005	,0015	,0011[a]	,0011	,0020	,0011	,0020
BIRC5	**Control**	,0354	,0092	,0359	,0241[a]	,0241	,0455	,0283	,0424
	Pd(II) IC90	,0498	,0359	,0498	,0175[a]	,0175	,0820	,0186	,0809
BIRC6	**Control**	,0152	,0049	,0157	,0096[a]	,0096	,0197	,0111	,0193
	Pd(II) IC90	,0213	,0128	,0208	,0090[a]	,0090	,0343	,0103	,0322
BMI1	**Control**	,0128	,0071	,0112	,0069[a]	,0069	,0218	,0071	,0184
	Pd(II) IC90	,0137	,0049	,0133	,0094[a]	,0094	,0187	,0095	,0178
BNIP1	**Control**	,0046	,0010	,0043	,0039[a]	,0039	,0060	,0040	,0052
	Pd(II) IC90	,0075	,0043	,0067	,0040[a]	,0040	,0128	,0040	,0111
BNIP3L	**Control**	,0072	,0067	,0072	,0011[a]	,0011	,0133	,0014	,0130
	Pd(II) IC50	,0118	,0057	,0107	,0071[a]	,0071	,0189	,0072	,0165
CASP3	**Control**	,0010	,0010	,0008	,0001[a]	,0001	,0022	,0002	,0018
	Pd(II) IC90	,0016	,0001	,0016	,0015[a]	,0015	,0018	,0015	,0017
CASP4	**Control**	,0003	,0003	,0002	,0001[a]	,0001	,0007	,0001	,0005
	Pd(II) IC90	,0012	,0007	,0011	,0005[a]	,0005	,0019	,0006	,0018
CASP6	**Control**	,0095	,0043	,0096	,0054[a]	,0054	,0134	,0057	,0132
	Pd(II) IC90	,0191	,0053	,0196	,0131[a]	,0131	,0239	,0146	,0235
CASP7	**Control**	,0010	,0003	,0010	,0007[a]	,0007	,0014	,0008	,0013
	Pd(II) IC90	,0037	,0001	,0037	,0036[a]	,0036	,0038	,0037	,0037
CDC20	**Control**	1,0645	,3881	1,1828	,5083[a]	,5083	1,3841	,8061	1,3229
	Pd(II) IC90	,8211	,7062	,8150	,0806[a]	,0806	1,5741	,2297	1,4126
CDK4	**Control**	,0405	,0063	,0423	,0317[a]	,0317	,0457	,0361	,0449
	Pd(II) IC90	,0444	,0469	,0343	,0000[a]	,0000	,1089	,0112	,0775
DCR	**Control**	,0008	,0001	,0008	,0006[a]	,0006	,0009	,0007	,0009
	Pd(II) IC90	,0028	,0034	,0013	,0008[a]	,0008	,0080	,0010	,0047
DR4	**Control**	,0075	,0019	,0075	,0053[a]	,0053	,0097	,0061	,0089

	Pd(II) IC90	,0152	,0096	,0116	,0084[a]	,0084	,0292	,0091	,0212
DR5	**Control**	,0072	,0033	,0071	,0035[a]	,0035	,0112	,0047	,0098
	Pd(II) IC90	,0741	,0422	,0606	,0405[a]	,0405	,1349	,0463	,1020
ERCC1	**Control**	,0368	,0165	,0352	,0215[a]	,0215	,0552	,0229	,0507
	Pd(II) IC90	,0892	,0735	,0567	,0448[a]	,0448	,1987	,0469	,1315
ERCC3	**Control**	,0319	,0106	,0298	,0225[a]	,0225	,0455	,0235	,0403
	Pd(II) IC90	,0617	,0745	,0263	,0207[a]	,0207	,1733	,0226	,1007
FAS	**Control**	,0012	,0006	,0014	,0003[a]	,0003	,0016	,0008	,0015
	Pd(II) IC90	,0032	,0017	,0027	,0019[a]	,0019	,0058	,0023	,0042
GAD45A	**Control**	,0005	,0001	,0005	,0004[a]	,0004	,0005	,0004	,0005
	Pd(II) IC90	,0135	,0167	,0059	,0038[a]	,0038	,0385	,0047	,0223
GSTP1	**Control**	,4771	,0572	,4601	,4326[a]	,4326	,5554	,4345	,5196
	Pd(II) IC90	,7994	,3960	,8420	,2766[a]	,2766	1,2369	,5429	1,0559
LIG4	**Control**	,0138	,0105	,0126	,0045[a]	,0045	,0254	,0050	,0226
	Pd(II) IC90	,0137	,0124	,0133	,0026[a]	,0026	,0257	,0031	,0244
MCL1	**Control**	,2056	,1029	,2009	,1152[a]	,1152	,3056	,1169	,2944
	Pd(II) IC90	,9824	,6465	1,0307	,1829[a]	,1829	1,6853	,4865	1,4783
MDM2	**Control**	,0174	,0040	,0162	,0143[a]	,0143	,0232	,0146	,0203
	Pd(II) IC90	,0578	,0550	,0389	,0154[a]	,0154	,1382	,0238	,0919
MGMT	**Control**	,0096	,0018	,0097	,0079[a]	,0079	,0112	,0081	,0111
	Pd(II) IC90	,0086	,0020	,0082	,0065[a]	,0065	,0113	,0073	,0098
NEK2	**Control**	,0450	,0347	,0439	,0149[a]	,0149	,0775	,0151	,0750
	Pd(II) IC90	,0311	,0236	,0339	,0016[a]	,0016	,0549	,0125	,0497
NOXA	**Control**	,1386	,0740	,1399	,0705[a]	,0705	,2043	,0746	,2027
	Pd(II) IC90	1,3807	,7934	1,6632	,2314[a]	,2314	1,9650	,8561	1,9053
PRDX1	**Control**	1,4170	,6964	1,3829	,7842[a]	,7842	2,1183	,8189	2,0152
	Pd(II) IC90	2,5266	1,5968	2,7314	,5033[a]	,5033	4,1404	1,2881	3,7652
PUMA	**Control**	,0019	,0012	,0019	,0009[a]	,0009	,0031	,0009	,0029
	Pd(II) IC90	,0047	,0016	,0052	,0025[a]	,0025	,0061	,0036	,0058
RAD52	**Control**	,0041	,0007	,0042	,0032[a]	,0032	,0046	,0035	,0046
	Pd(II) IC90	,0028	,0004	,0026	,0025[a]	,0025	,0034	,0026	,0030
SOD1	**Control**	,9228	,4762	,9674	,4193[a]	,4193	1,3373	,5163	1,3294

	Pd(II) IC90	1,7427	,9088	1,9420	,5158[a]	,5158	2,5710	1,0680	2,4174
XPA	**Control**	,0184	,0146	,0124	,0089[a]	,0089	,0400	,0097	,0272
	Pd(II) IC90	,0132	,0123	,0132	,0015[a]	,0015	,0249	,0027	,0238
XRCC5	**Control**	,3114	,1427	,3125	,1750[a]	,1750	,4456	,1884	,4343
	Pd(II) IC90	,2367	,1451	,2298	,1065[a]	,1065	,3809	,1118	,3616

Table 3.6. M, SD, median, min-max, Q1, Q3 and p values of the relevant Genes at the 24th hour according to Control and Drug IC90 Groups

M: Mean; SD: standard deviation; Q (Querter) Q1=25%, Q3=75%, h: hour

Target Gene	**Group**	**24h**							
		M	**SD**	**Median**	**Mode**	**Min**	**Max**	**Q25**	**Q75**
AKT1	**Control**	,0759	,0420	,0734	,0397[a]	,0397	,1171	,0398	,1121
	Pd(II) IC90	,0398	,0098	,0399	,0302[a]	,0302	,0493	,0314	,0482
APAF1	**Control**	,0049	,0034	,0049	,0019[a]	,0019	,0081	,0020	,0079
	Pd(II) IC90	,0024	,0011	,0024	,0015[a]	,0015	,0035	,0015	,0034
ATG7	**Control**	,0169	,0173	,0165	,0018[a]	,0018	,0327	,0019	,0318
	Pd(II) IC90	,0028	,0007	,0028	,0020[a]	,0020	,0036	,0022	,0034
BAG1	**Control**	,0023	,0007	,0024	,0015[a]	,0015	,0029	,0017	,0029
	Pd(II) IC90	,0236	,0134	,0263	,0049[a]	,0049	,0367	,0153	,0318
BAG3	**Control**	,0007	,0003	,0007	,0004[a]	,0004	,0010	,0005	,0009
	Pd(II) IC90	,0155	,0084	,0138	,0083[a]	,0083	,0261	,0087	,0223
BCL10	**Control**	,0086	,0077	,0068	,0018[a]	,0018	,0190	,0027	,0144
	Pd(II) IC90	,0356	,0257	,0340	,0120[a]	,0120	,0623	,0136	,0576
BCLAF1	**Control**	,0178	,0050	,0170	,0130[a]	,0130	,0243	,0140	,0216
	Pd(II) IC90	,0450	,0287	,0438	,0201[a]	,0201	,0724	,0203	,0698
BCLXL	**Control**	,0512	,0238	,0468	,0309[a]	,0309	,0805	,0318	,0707
	Pd(II) IC90	,0231	,0048	,0240	,0172[a]	,0172	,0271	,0192	,0269
BID	**Control**	,0632	,0043	,0633	,0581[a]	,0581	,0683	,0600	,0665
	Pd(II) IC90	,1593	,0851	,1580	,0761[a]	,0761	,2451	,0866	,2320

BIM	**Control**	,0011	,0007	,0011	,0005[a]	,0005	,0019	,0006	,0017
	Pd(II) IC90	,0055	,0040	,0052	,0019[a]	,0019	,0095	,0020	,0089
BIRC2	**Control**	,0107	,0028	,0103	,0081[a]	,0081	,0141	,0085	,0129
	Pd(II) IC90	,0245	,0094	,0257	,0140[a]	,0140	,0326	,0166	,0324
BIRC3	**Control**	,0058	,0055	,0036	,0023[a]	,0023	,0140	,0023	,0094
	Pd(II) IC90	,0028	,0014	,0027	,0016[a]	,0016	,0044	,0017	,0040
BIRC5	**Control**	,0190	,0076	,0169	,0121[a]	,0121	,0299	,0142	,0237
	Pd(II) IC90	,0167	,0091	,0170	,0082[a]	,0082	,0247	,0089	,0246
BIRC6	**Control**	,0105	,0019	,0102	,0086[a]	,0086	,0128	,0089	,0120
	Pd(II) IC90	,0159	,0042	,0161	,0106[a]	,0106	,0209	,0131	,0187
BMI1	**Control**	,0095	,0026	,0094	,0066[a]	,0066	,0126	,0075	,0116
	Pd(II) IC90	,0147	,0038	,0149	,0104[a]	,0104	,0186	,0115	,0179
BNIP1	**Control**	,0019	,0006	,0017	,0014[a]	,0014	,0027	,0016	,0022
	Pd(II) IC90	,0091	,0031	,0088	,0060[a]	,0060	,0127	,0066	,0116
BNIP3L	**Control**	,0076	,0071	,0051	,0025[a]	,0025	,0178	,0028	,0124
	Pd(II) IC90	,0270	,0143	,0294	,0092[a]	,0092	,0402	,0156	,0385
CASP3	**Control**	,0005	,0002	,0005	,0003[a]	,0003	,0008	,0004	,0007
	Pd(II) IC90	,0011	,0010	,0008	,0003[a]	,0003	,0024	,0003	,0018
CASP4	**Control**	,0001	,0001	,0000	,0000	,0000	,0003	,0000	,0002
	Pd(II) IC90	,0016	,0018	,0016	,0000	,0000	,0032	,0000	,0032
CASP6	**Control**	,0083	,0012	,0082	,0071[a]	,0071	,0096	,0073	,0093
	Pd(II) IC90	,0185	,0043	,0178	,0145[a]	,0145	,0237	,0149	,0220
CASP7	**Control**	,0006	,0003	,0005	,0003[a]	,0003	,0011	,0004	,0008
	Pd(II) IC90	,0030	,0017	,0030	,0015[a]	,0015	,0045	,0016	,0045
CDC20	**Control**	1,8996	1,2465	1,7254	,8096[a]	,8096	3,3379	,8577	2,9415
	Pd(II) IC90	2,2559	1,5466	2,1087	,9171[a]	,9171	3,8892	,9349	3,5769
CDK4	**Control**	,0276	,0063	,0279	,0207[a]	,0207	,0340	,0223	,0329
	Pd(II) IC90	,0188	,0026	,0185	,0159[a]	,0159	,0222	,0171	,0205
DCK	**Control**	,0009	,0001	,0009	,0008[a]	,0008	,0010	,0008	,0010
	Pd(II) IC90	,0017	,0009	,0015	,0010[a]	,0010	,0030	,0012	,0023
DR4	**Control**	4,0062	4,6225	3,9484	,0035[a]	,0035	8,1246	,0038	8,0086
	Pd(II) IC90	,0055	,0018	,0056	,0036[a]	,0036	,0071	,0039	,0071

DR5	**Control**	3,5366	4,0758	3,4997	,0071[a]	,0071	7,1399	,0072	7,0660
	Pd(II) IC90	,0065	,0017	,0071	,0041[a]	,0041	,0079	,0056	,0075
ERCC1	**Control**	,0390	,0066	,0391	,0321[a]	,0321	,0456	,0333	,0446
	Pd(II) IC90	,0634	,0307	,0494	,0458[a]	,0458	,1092	,0458	,0810
ERCC3	**Control**	,0195	,0046	,0198	,0147[a]	,0147	,0235	,0155	,0234
	Pd(II) IC90	,0328	,0079	,0311	,0256[a]	,0256	,0433	,0268	,0387
FAS	**Control**	,0031	,0024	,0029	,0009[a]	,0009	,0054	,0010	,0051
	Pd(II) IC90	,0024	,0023	,0021	,0004[a]	,0004	,0048	,0004	,0043
GAD45A	**Control**	,0011	,0003	,0011	,0008[a]	,0008	,0014	,0009	,0014
	Pd(II) IC90	,0137	,0033	,0123	,0114[a]	,0114	,0186	,0118	,0155
GSTP1	**Control**	,7082	,3128	,6979	,4219[a]	,4219	1,0152	,4389	,9775
	Pd(II) IC90	,5872	,1066	,5609	,4948[a]	,4948	,7321	,5080	,6663
LIG4	**Control**	,0090	,0048	,0090	,0047[a]	,0047	,0133	,0048	,0131
	Pd(II) IC90	,0173	,0026	,0173	,0144[a]	,0144	,0202	,0151	,0194
MCL1	**Control**	,2122	,1097	,2144	,1060[a]	,1060	,3141	,1177	,3068
	Pd(II) IC90	,5315	,1586	,4990	,3773[a]	,3773	,7505	,4240	,6390
MDM2	**Control**	,0203	,0094	,0191	,0109[a]	,0109	,0319	,0128	,0278
	Pd(II) IC90	,0340	,0023	,0346	,0308[a]	,0308	,0358	,0323	,0356
MGMT	**Control**	,0097	,0018	,0096	,0081[a]	,0081	,0116	,0082	,0112
	Pd(II) IC90	,0063	,0019	,0062	,0045[a]	,0045	,0083	,0047	,0079
NEK2	**Control**	,1002	,0394	,1011	,0606[a]	,0606	,1379	,0664	,1340
	Pd(II) IC90	,0427	,0196	,0431	,0230[a]	,0230	,0616	,0259	,0595
NOXA	**Control**	1,1213	1,1413	1,1120	,1296[a]	,1296	2,1314	,1330	2,1095
	Pd(II) IC90	,3226	,1051	,3210	,2282[a]	,2282	,4201	,2318	,4134
PRDX1	**Control**	1,6506	,3314	1,7002	1,2376[a]	1,2376	1,9641	1,3855	1,9156
	Pd(II) IC90	3,9552	1,0707	3,7382	2,9371[a]	2,9371	5,4070	3,1791	4,7312
PUMA	**Control**	,0043	,0002	,0043	,0040[a]	,0040	,0046	,0042	,0045
	Pd(II) IC90	,0063	,0005	,0064	,0056[a]	,0056	,0067	,0060	,0066
RAD52	**Control**	4,2294	4,8814	4,2040	,0018[a]	,0018	8,5078	,0021	8,4566
	Pd(II) IC90	,0023	,0006	,0023	,0016[a]	,0016	,0029	,0018	,0028
SOD1	**Control**	1,0960	,3458	1,1537	,6823[a]	,6823	1,3942	,8107	1,3812
	Pd(II) IC90	2,4228	,4299	2,4123	1,9589[a]	1,9589	2,9078	2,0718	2,7739

XPA	**Control**	,0171	,0088	,0170	,0095[a]	,0095	,0251	,0095	,0247
	Pd(II) IC90	,0130	,0048	,0125	,0086[a]	,0086	,0183	,0090	,0170
XRCC5	**Control**	,3592	,1205	,3589	,2483[a]	,2483	,4706	,2550	,4633
	Pd(II) IC90	,2640	,0412	,2546	,2263[a]	,2263	,3206	,2343	,2937

Table 3.7. Hypothesis Test Summary for AKT1 Gene

	Null Hypothesis	**Test**	**Sig.**[a,b]	**Decision**
1	The dispersion of 6h is the consistent among of groups	Mann Whitney U Test	,686[c]	Retain the null hypothesis.
2	The dispersion of 24h is the consistent among of groups.	Mann-Whitney U Test	,343[c]	Retain the null hypothesis.

a. The importance level is 0,50.

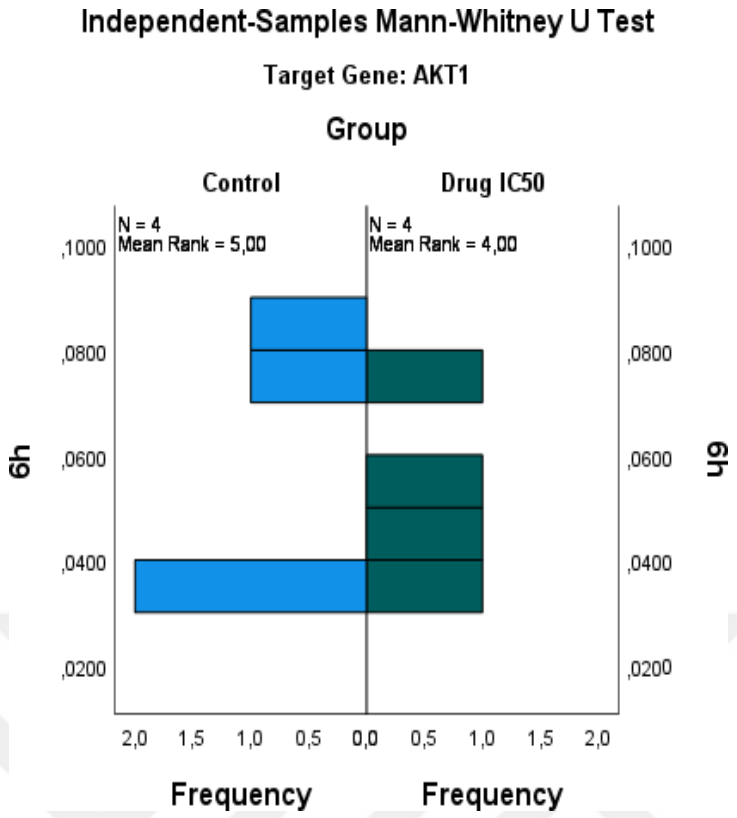

Figure 3.23. AKT1 6h Gene Result

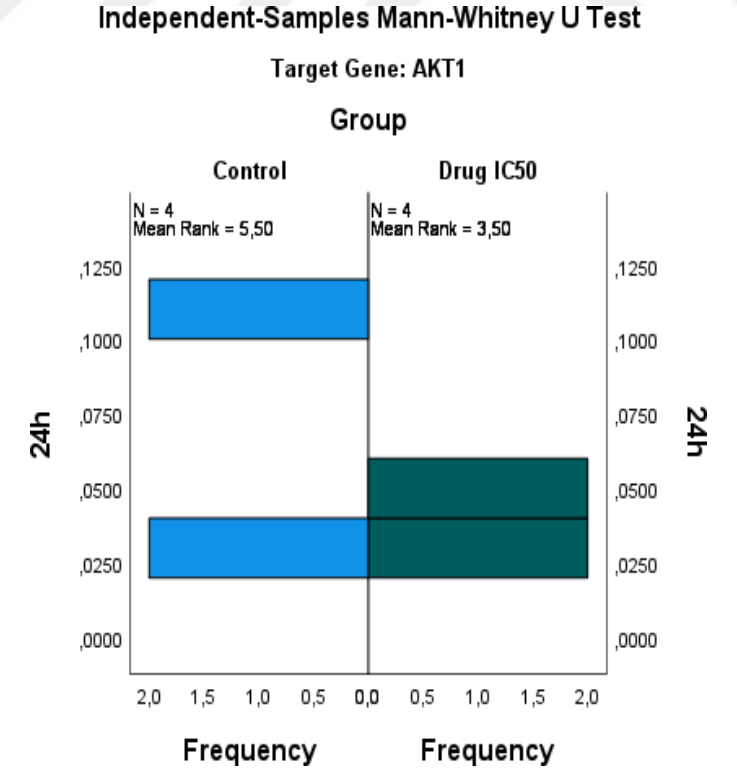

Figure 3.24. AKT1 24h Gene Result

Table 3.8. Hypothesis Test Summary for ATG7 Gene

	Null Hypothesis	Test	Sig.[a,b]	Decision
1	The dispersion of 6h is the consistent among of groups	Mann-Whitney U Test	,029[c]	Reject the null hypothesis.
2	The dispersion of 24 is the consistent among of groups	Mann-Whitney U Test	,886[c]	Retain the null hypothesis.

a. The importance level is 0,50.

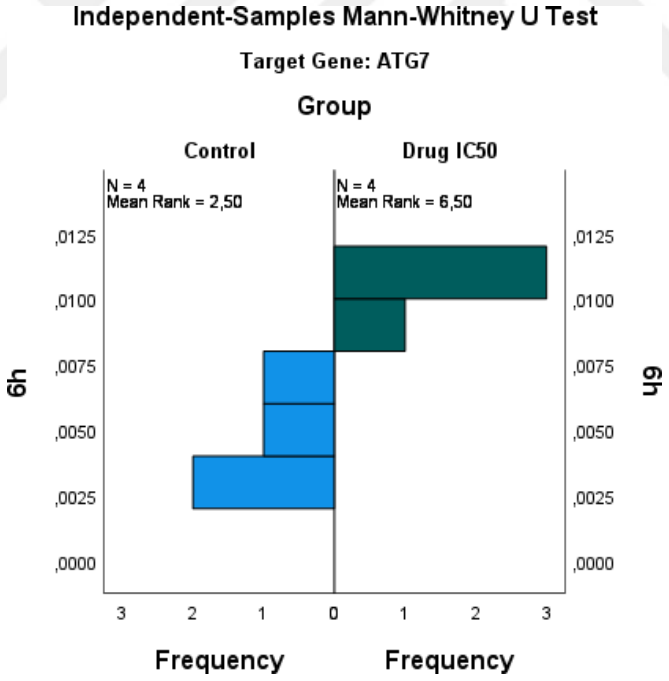

Figure 3.25. ATG7 6h Gene Result

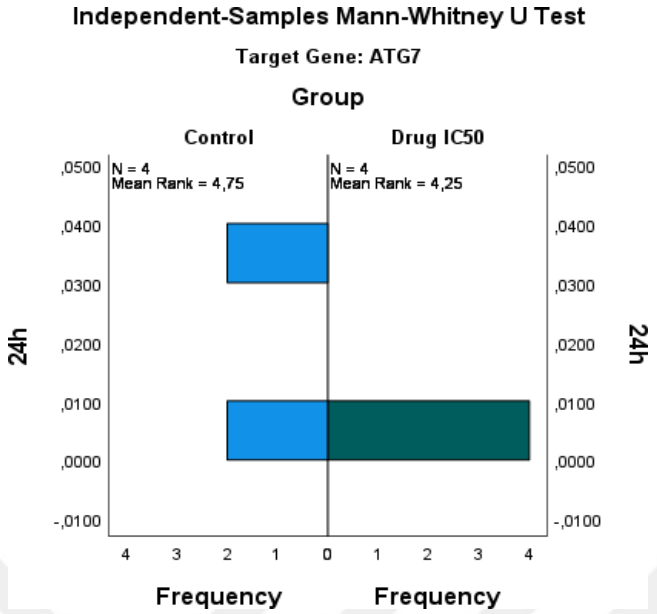

Figure 3.26. ATG7 24h Gene Result

Table 3.9. Hypothesis Test Summary for BAG1 Gene

	Null Hypothesis	Test	Sig.[a,b]	Decision
1	The dispersion of 6h is the consistent among of groups	Mann-Whitn. U Test	,486[c]	Retain the null hypothesis.
2	The dispersion of 24h is the consistent among of groups	Mann Whitn. U Test	,029[c]	Reject the null hypothesis.

a. The importance level is 0,50.

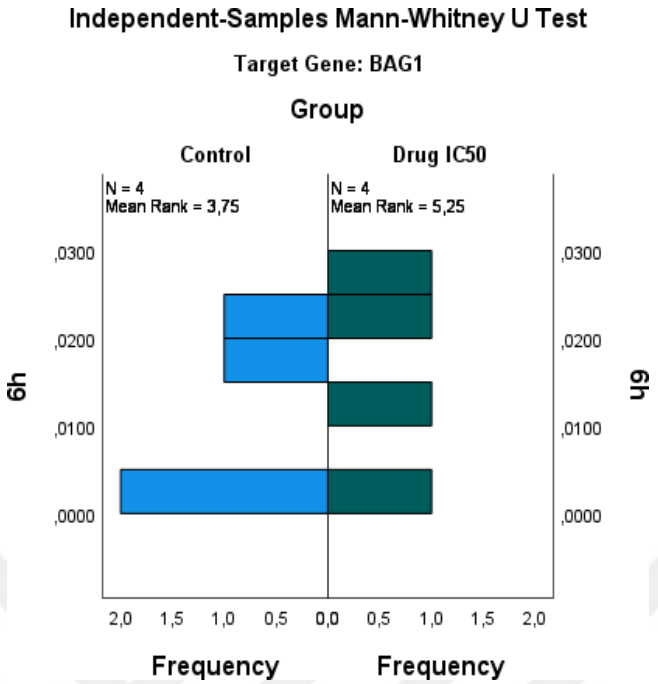

Figure 3.27. BAG1 Gene Results 6h

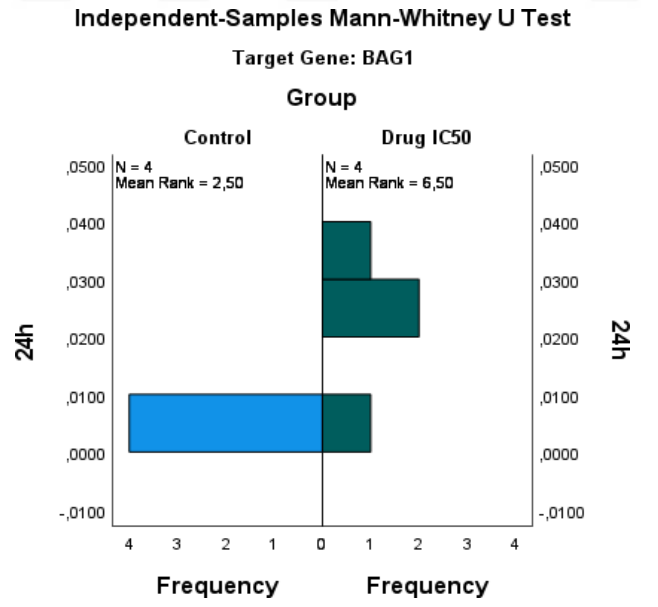

Figure 3.28. BAG1 Gene Results 24h

Table 3.10. Hypothesis Test Summary for BAG3 Gene

	Null Hypothesis	Test	Sig.[a,b]	Decision
1	The dispersion of 6h is the consistent among of groups	Mann-Whitney U Test	,029[c]	Reject the null hypothesis.
2	The dispersion of 24h is the consistent among of groups	Mann-Whitney U Test	,029[c]	Reject the null hypothesis.

a. The important level is 0,50.

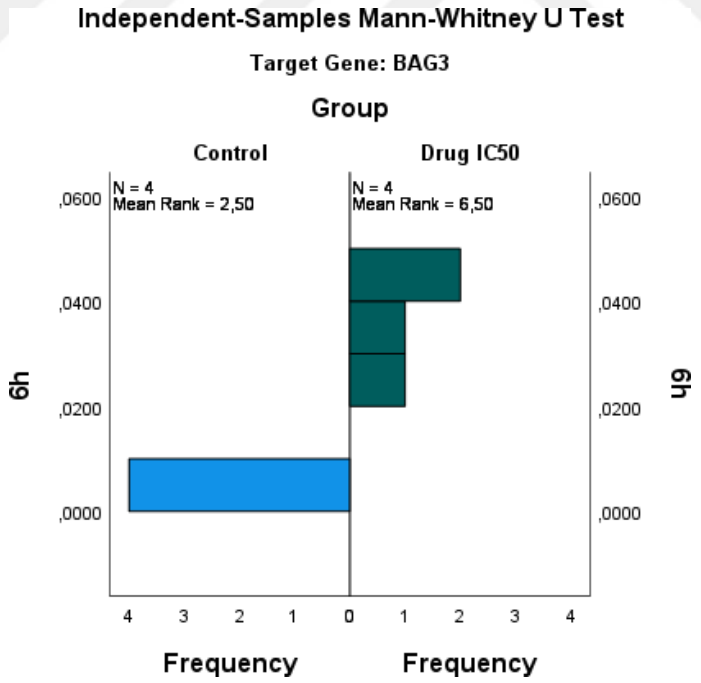

Figure 3.29. BAG3 Gene Results 6h

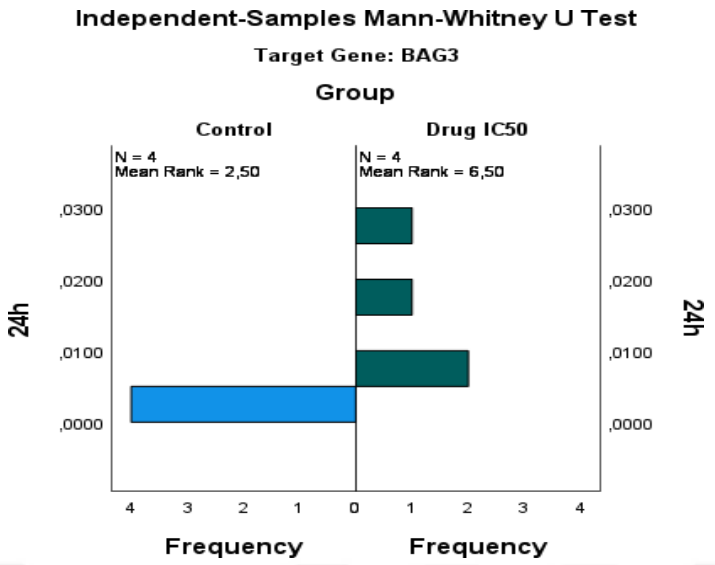

Figure 3.30. BAG3 Gene Results 24h

Table 3.11. Hypothesis Test Summary for BCL10 Gene

	Null Hypothesis	Test	Sig.[a,b]	Decision
1	The dispersion of 6h is the consistent among of groups	Mann-Whitney U Test	1,000[c]	Retain the null hypothesis.
2	The dispersion of 24h is the consistent among of groups	Mann-Whitney U Test	,114[c]	Retain the null hypothesis.

a. The important level is 0,50.

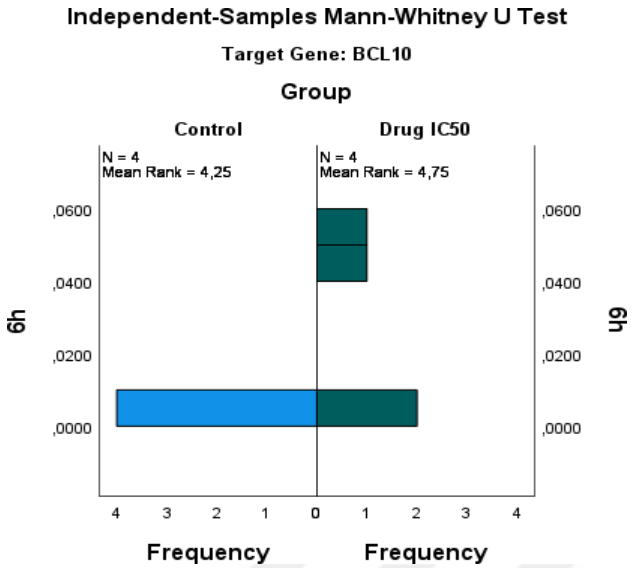

Figure 3.31. BCL10 Gene Results 6h

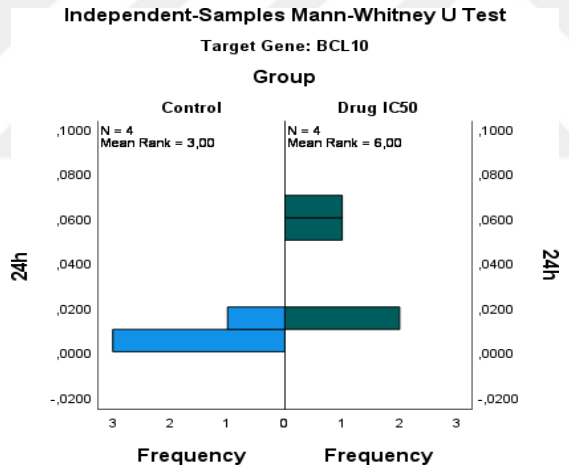

Figure 3.32. BCL10 Gene Results 24h

Table 3. 12. Hypothesis Test Summary for BCLAF1 Gene

	Null Hypothesis	Test	Sig.[a,b]	Decision
1	The dispersion of 6h is the consistent among of groups	Mann-Whitn. U Test	1,000[c]	keep the null hypothesis.
2	The dispersion of 24h is the consistent among of groups	Mann-Whitn. U Test	,114[c]	keep the null hypothesis.

a. The important level is 0,50.

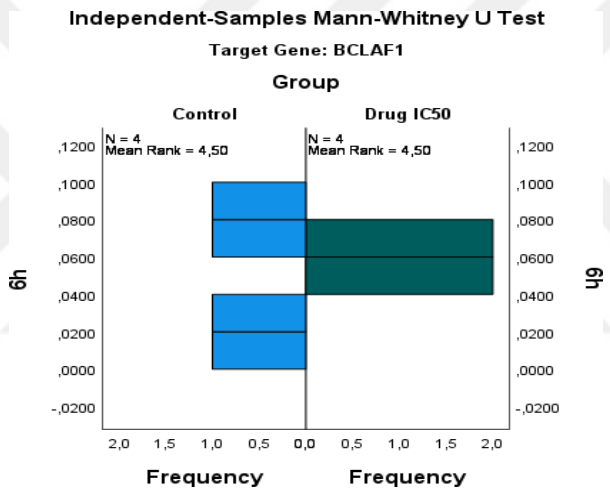

Figure 3.33. BCLAF1 Gene Results 6h

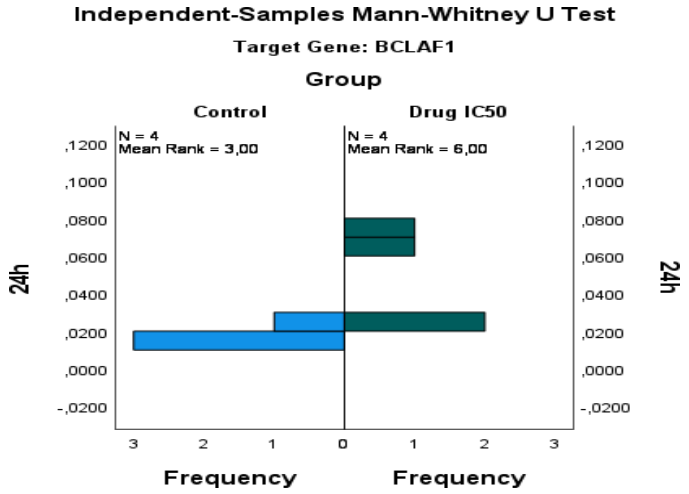

Figure 3.34. BCLAF1 Gene Results 24h

Table 3.13. Hypothesis Test Summary for BCLXL Gene

	Null Hypothesis	Test	Sig.[a,b]	Decision
1	The dispersion of 6h is the consistent among of groups	Mann-Whitn. U Test	1,000[c]	Retain the null hypothesis.
2	The dispersion of 24h is the consistent among of groups	Mann-Whitn. U Test	,029[c]	Reject the null hypothesis.

a. The important level is 0,50.

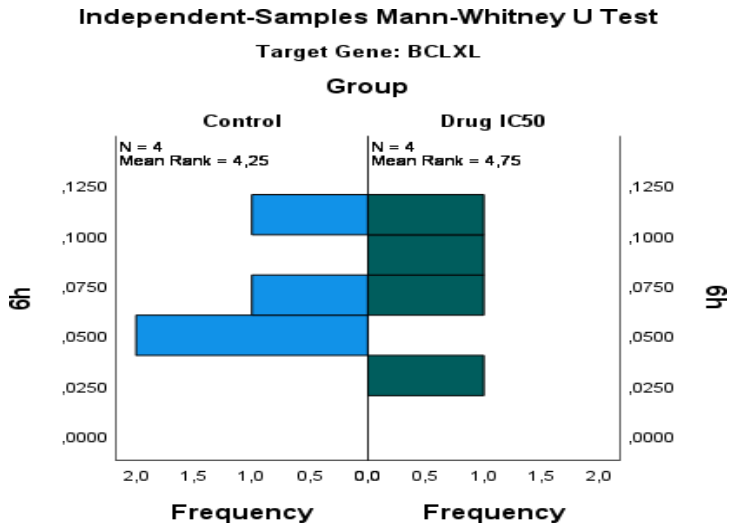

Figure 3.35. BCLXL Gene Results 6h

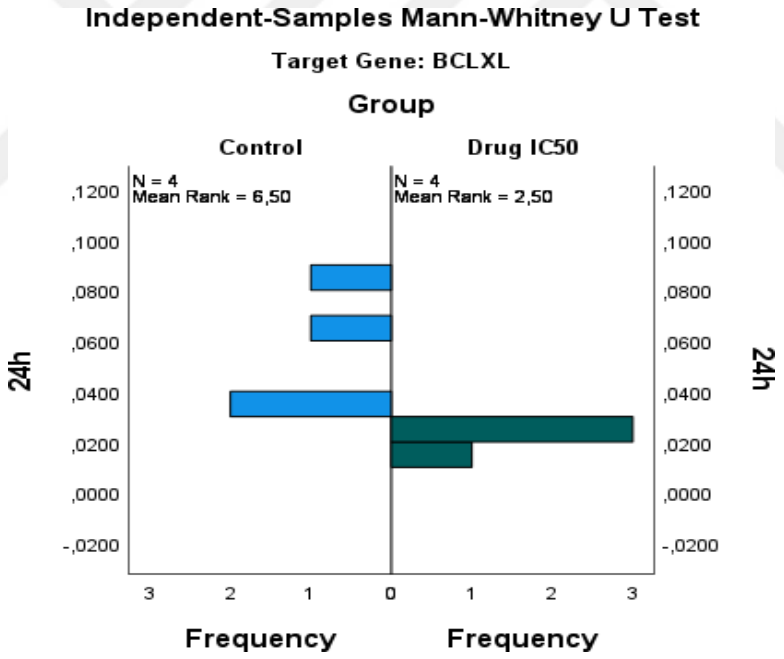

Figure 3.36. BCLXL Gene Results 24h

Table 3.14. Hypothesis Test Summary for BID Gene

Null Hypothesis	Test	Sig.[a,b]	Decision

1	The dispersion of 6h is the consistent among of groups	Mann-Whitn. U Test	,029[c]	Reject the null hypothesis.
2	The dispersion of 24h is the consistent among of groups	Mann-Whitn. U Test	,029[c]	Reject the null hypothesis.

a. The important level is 0,50.

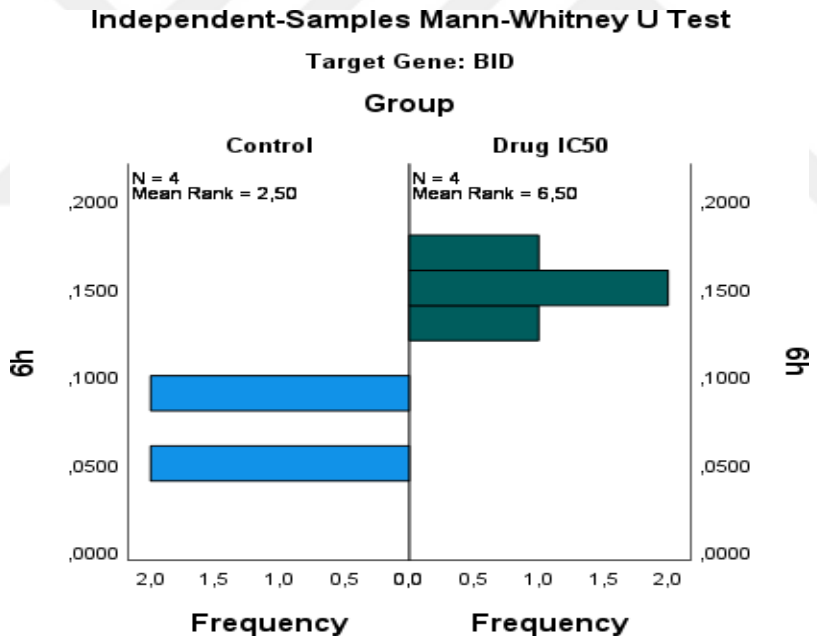

Figure 3.37. BID Gene Results 6h

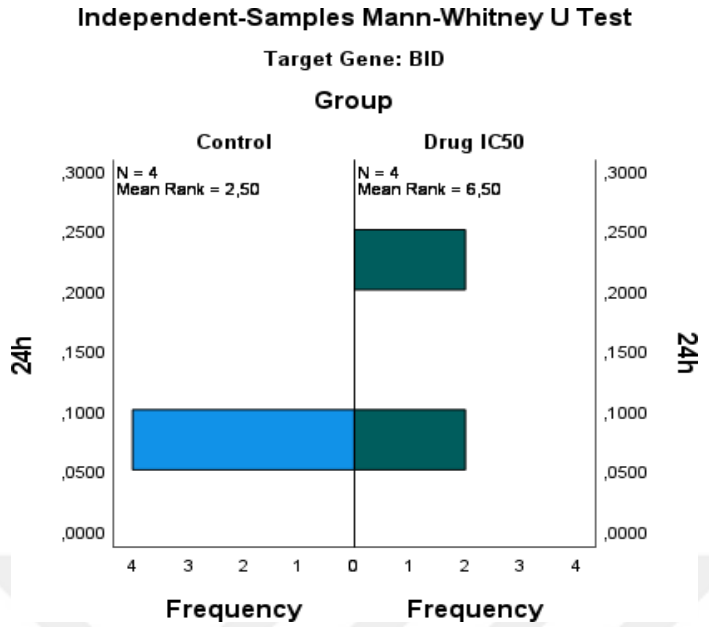

Figure 3.38. BID Gene Results 24h

Table 3.15. Hypothesis Test Summary for BIM Gene

	Null Hypothesis	Test	Sig.[a,b]	Decision
1	The dispersion of 6h is the consistent among of groups	Mann-Whitn. U Test	,029[c]	Reject the null hypothesis.
2	The dispersion of 24h is the consistent among of groups	Mann-Whitn. U Test	,029[c]	Reject the null hypothesis.

a. The important level is 0,50.

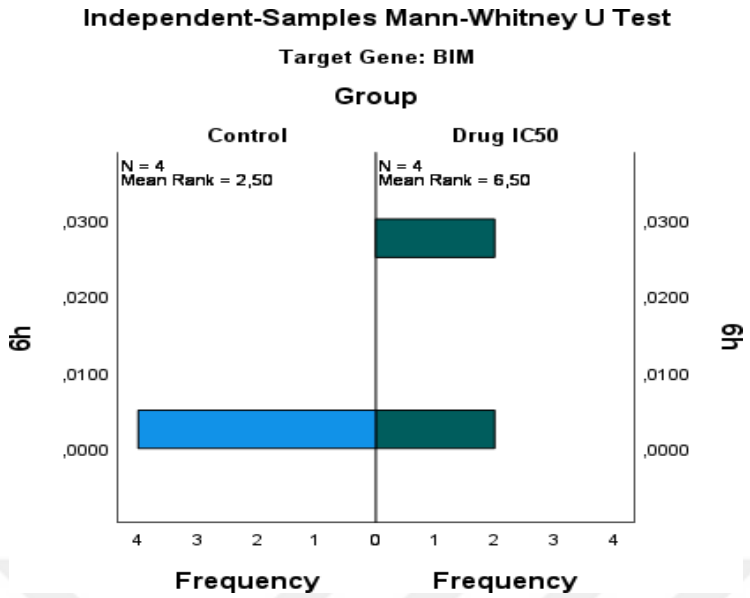

Figure 3.39. BIM Gene Results 6h

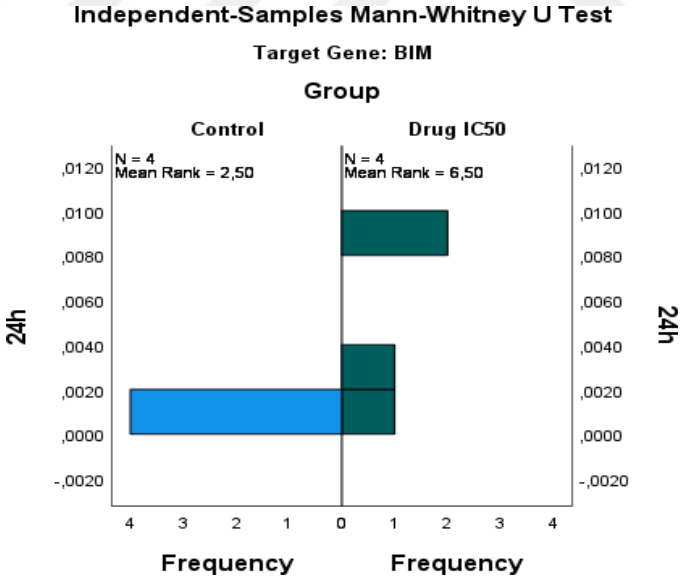

Figure 3.40. BIM Gene Results 24h

Table 3.16. Hypothesis Test Summary for BIRC2 Gene

	Null Hypothesis	Test	Sig.[a,b]	Decision
1	The dispersion of 6h is the consistent among of groups	Mann-Whitn. U Test	,200[c]	Retain the null hypothesis.
2	The dispersion of 24h is the consistent among of groups	Mann-Whitn. U Test	,057[c]	Retain the null hypothesis.

a. The important level is 0,50.

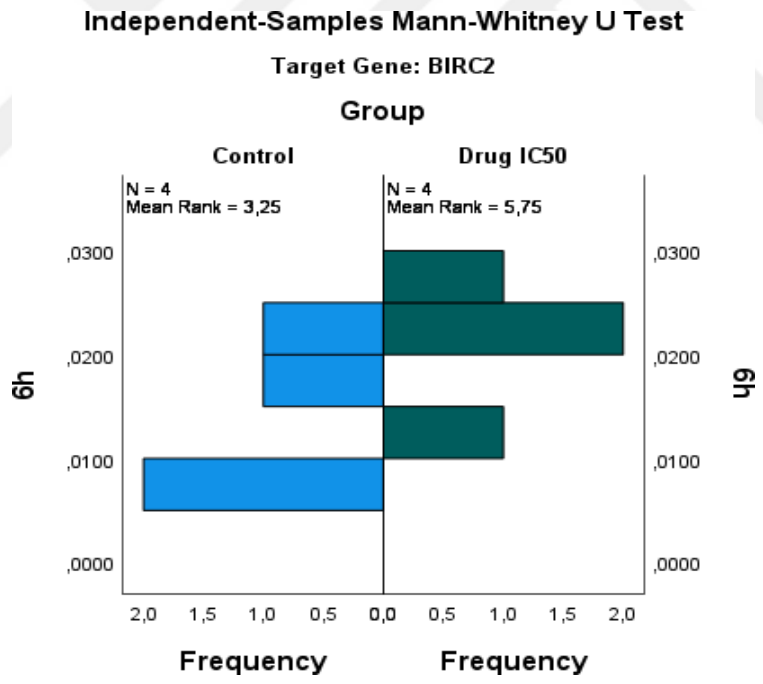

Figure 3.41. BIRC2 Gene Results 6h

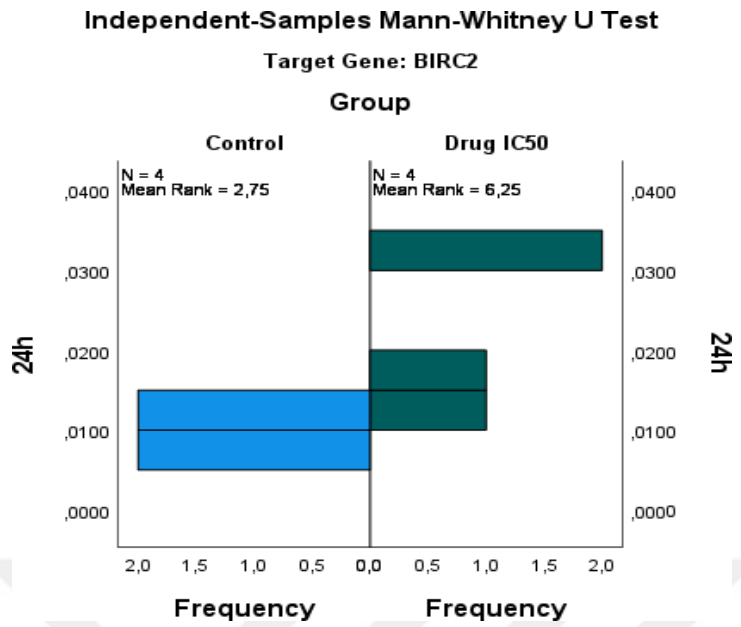

Figure 3.42. BIRC2 Gene Results 24h

Table 3.17. Hypothesis Test Summary for BIRC3 Gene

	Null Hypothesis	Test	Sig.[a,b]	Decision
1	The dispersion of 6h is the consistent among of groups	Mann-Whitn. U Test	,686[c]	Retain the null hypothesis.
2	The dispersion of 24h is the consistent among of groups	Mann-Whitn. U Test	,343[c]	Retain the null hypothesis.

a. The important level is 0,50.

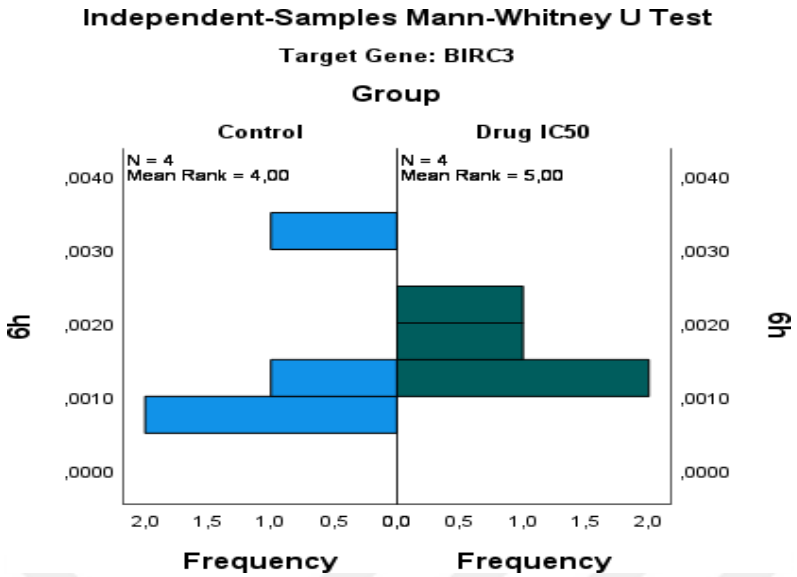

Figure 3.43. BIRC3 Gene Results 6h

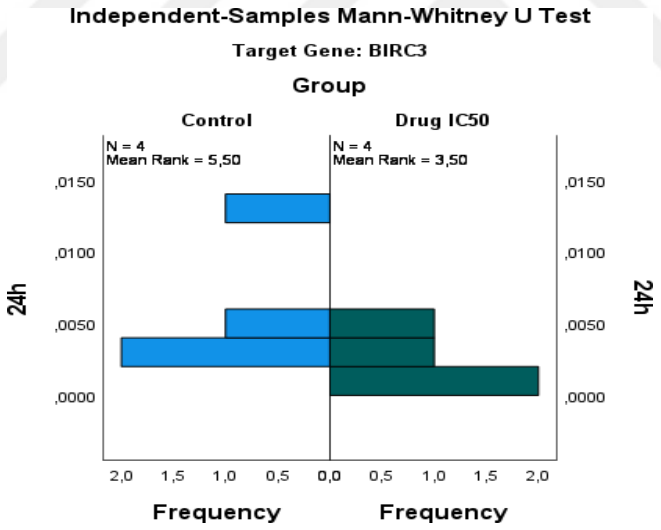

Figure 3.44. BIRC3 Gene Results 24h

Table 3.18. Hypothesis Test Summary for BIRC5 Gene

Null Hypothesis	Test	Sig.[a,b]	Decision

1	The dispersion of 6h is the consistent among of groups	Indep. Sampl. Mann-Whitn. U Test	1,000[c]	Retain the null hypothesis.
2	The dispersion of 24h is the consistent among of groups	Indep. Sampl. Mann-Whitn. U Test	,686[c]	Retain the null hypothesis.

a. The importantlevel is 0,50.

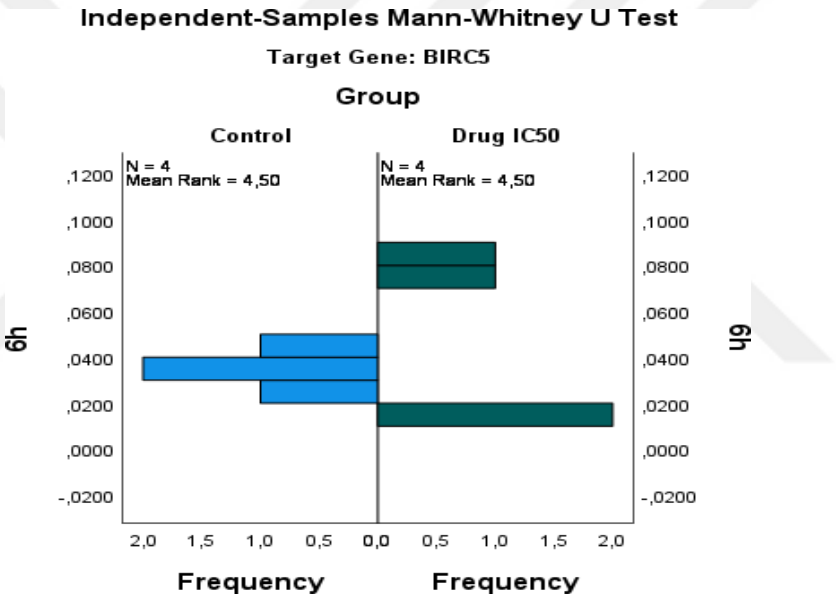

Figure 3.45. BIRC5 Gene Results 6h

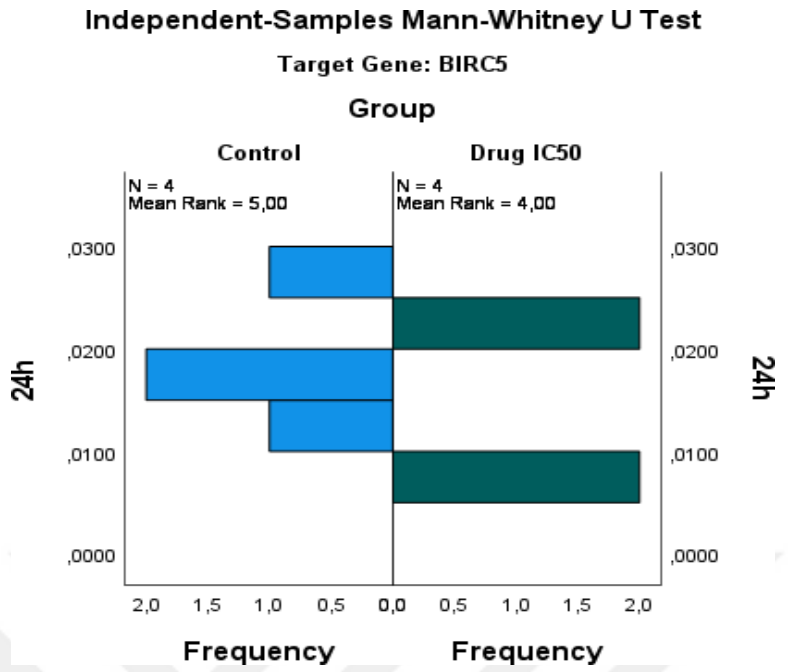

Figure 3.46. BIRC5 Gene Results 24h

Table 3.19. Hypothesis Test Summary for BIRC6 Gene

	Null Hypothesis	Test	Sig.[a,b]	Decision
1	The dispersion of 6h is the consistent among of groups	Indep. Sampl. Mann-Whitney U Test	1,000[c]	Retain the null hypothesis.
2	The dispersion of 24h is the consistent among of groups	Indep. Sampl. Mann-Whitney U Test	,114[c]	Retain the null hypothesis.

a. The important level is 0,50.

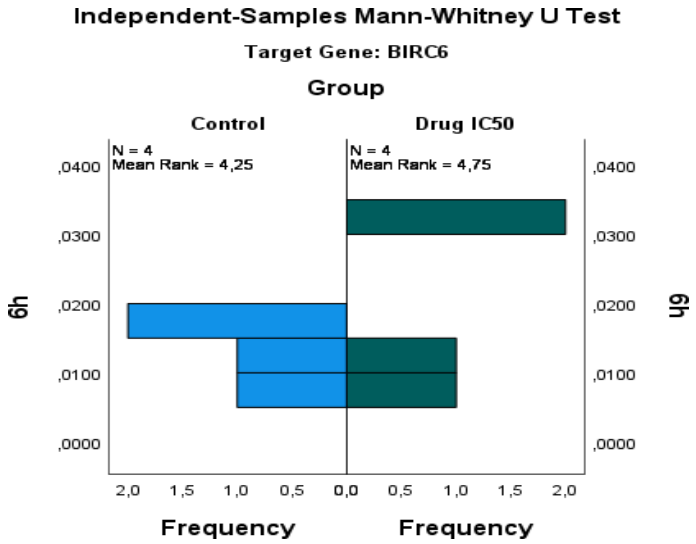

Figure 3.47. BIRC6 Gene Results 6h

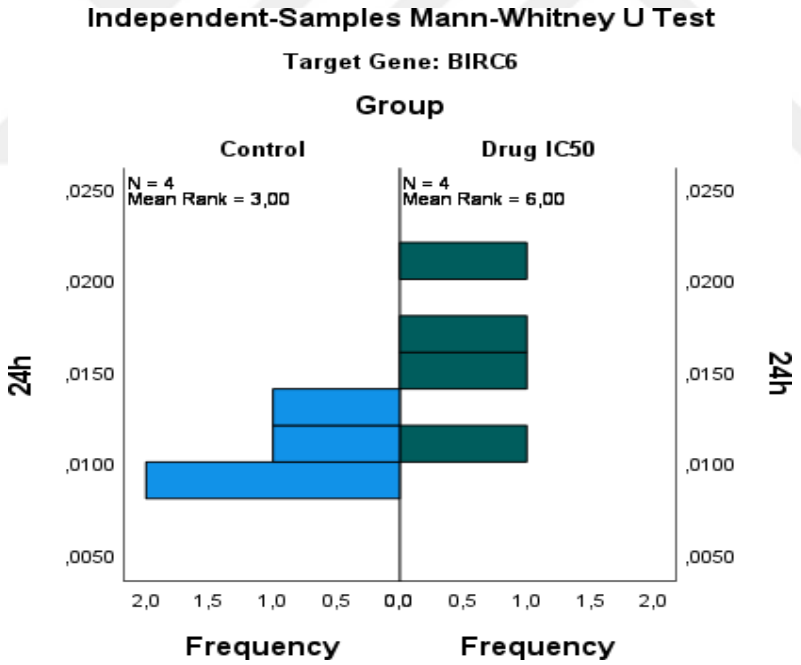

Figure 3.48. BIRC6 Gene Results 24h

Table 3.20. Hypothesis Test Summary for BMI1 Gene

	Null Hypothesis	Test	Sig.[a,b]	Decision
1	The dispersion of 6h is the consistent among of groups	Mann-Whitn. U Testi	,686[c]	Retain the null hypothesis.
2	The dispersion of 24h is the consistent among of groups	Mann-Whitn. U Testi	,114[c]	Retain the null hypothesis.

a. The important level is 0,50.

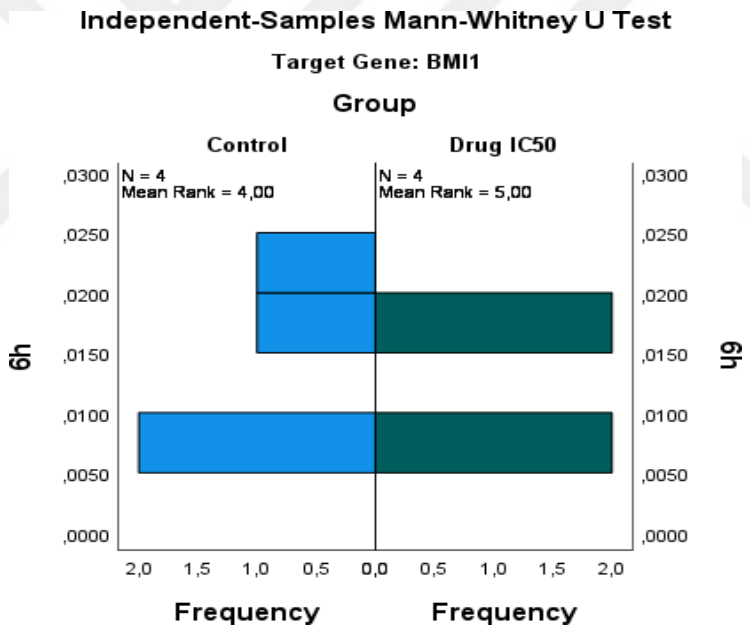

Figure 3.49. BMI1 Gene Results 6h

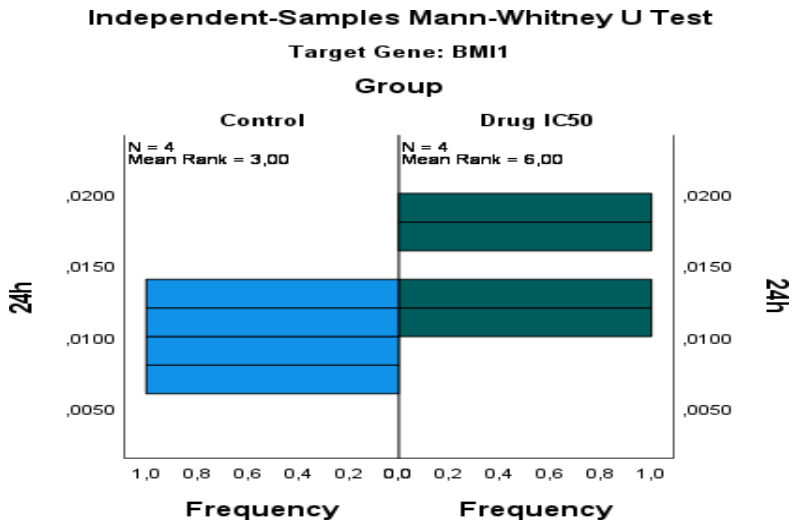

Figure 3.50. BMI1 Gene Results 24h

Table 3.21. Hypothesis Test Summary for BNIP1 Gene

	Null Hypothesis	Test	Sig.[a,b]	Decision
1	The dispersion of 6h is the consistent among of groups	Indep. Samples Mann-Whitn. U Test	,686[c]	Retain the null hypothesis.
2	The dispersion of 24 h is the consistent among of groups	Indep. Samples Mann-Whitn. U Test	,029[c]	Reject the null hypothesis.

a. The important level is 0,50.

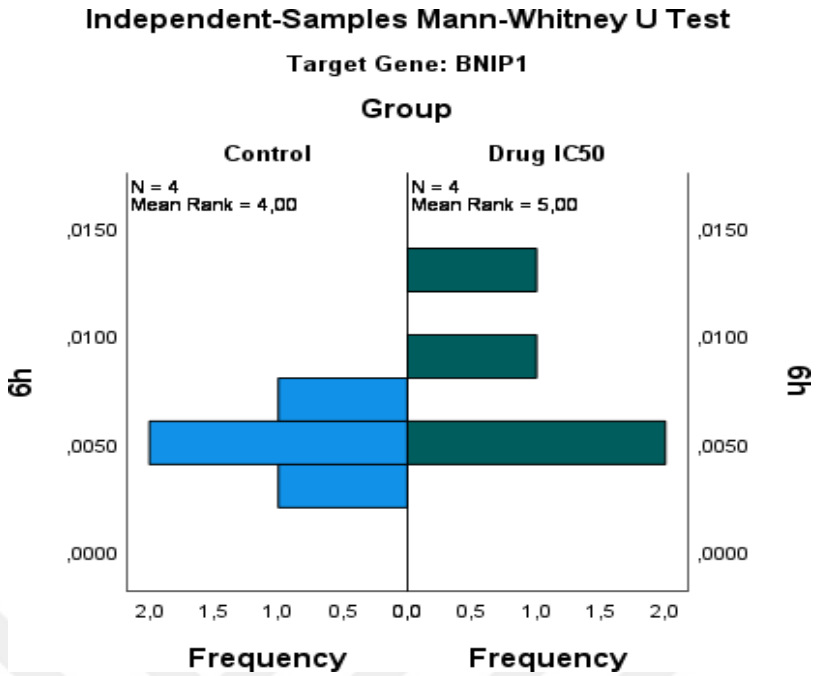

Figure 3.51. BNIP1 Gene Results 6h

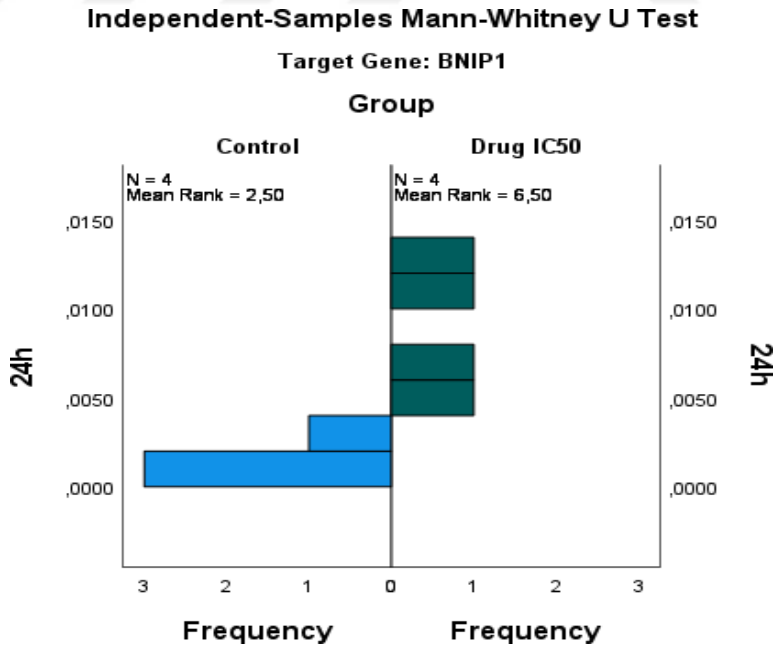

Figure 3.52. BNIP1 Gene Results 24h

Table 3.22. Hypothesis Test Summary for BNIP3L Gene

	Null Hypothesis	Test	Sig.[a,b]	Decision
1	The dispersion of 6h is the consistent among of groups	Mann-Whitn. U Test	,343[c]	Retain the null hypothesis.
2	The dispersion of 24h is the consistent among of groups	Mann-Whitn. U Test	,057[c]	Retain the null hypothesis.

a. The important level is 0,50.

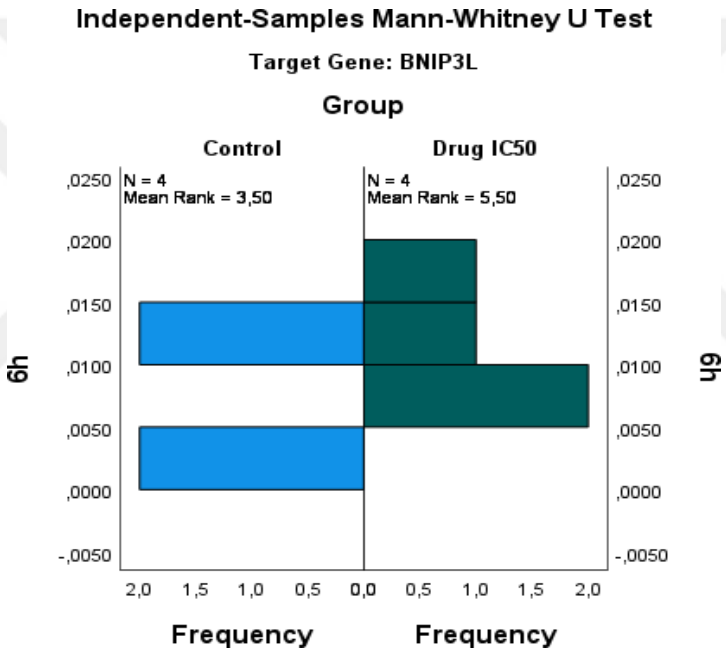

Figure 3.53. BNIP3L Gene Results 6h

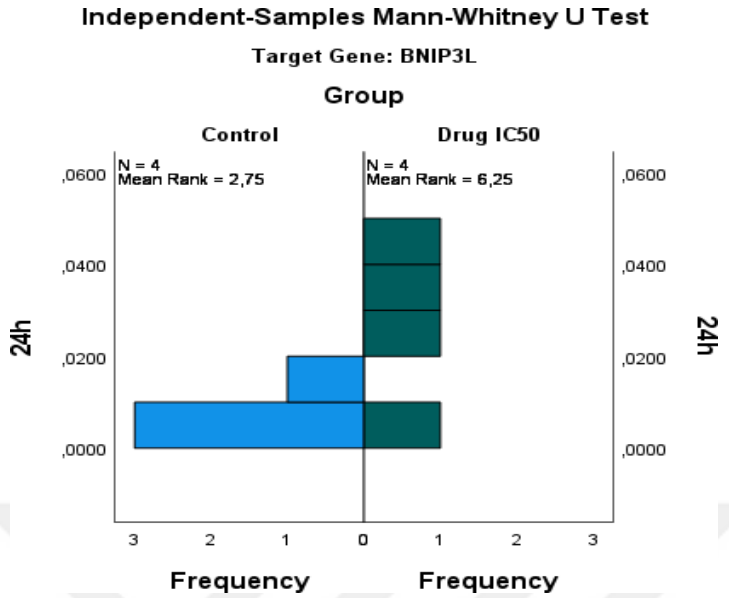

Figure 3.54. BNIP3L Gene Results 24h

Table 3.23. Hypothesis Test Summary for CASP3 Gene

	Null Hypothesis	Test	Sig.[a,b]	Decision
1	The dispersion of 6h is the consistent among of groups	Indep. Sampl. Mann and Whitney U Testi	,343[c]	Keep the null hypothesis.
2	The dispersion of 24h is the consistent among of groups	Indep. Sampl. Mann and Whitney U Testi	1,000[c]	Keep the null hypothesis.

a. The important level is 0,50.

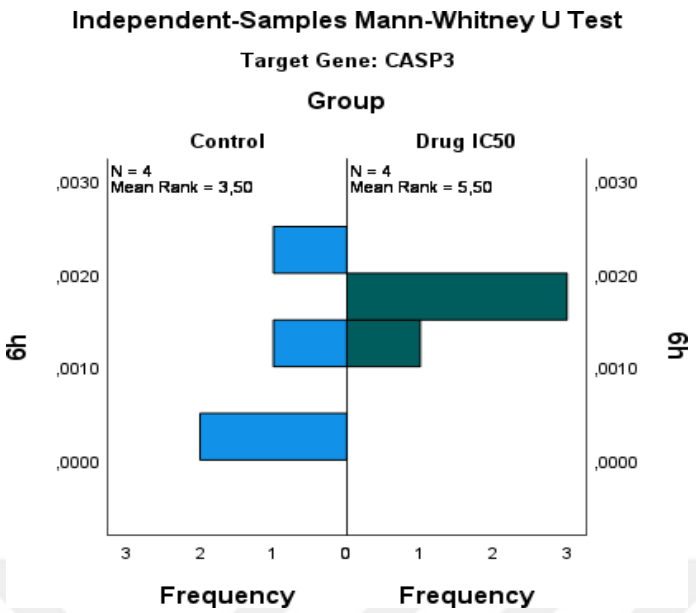

Figure 3.55. CASP3 Gene Results 6h

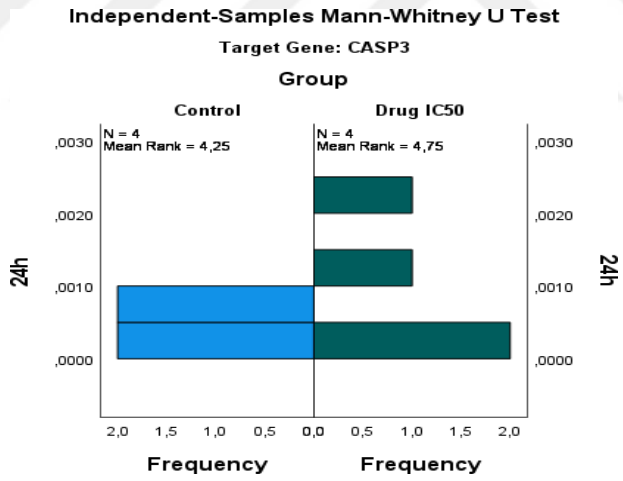

Figure 3.56. CASP3 Gene Results 24h

Table 3.24. Hypothesis Test Summary for CASP4 Gene

Null Hypothesis	Test	Sig.[a,b]	Decision

1	The dispersion of 6h is the consistent among of groups	Independent-Samples Mann and Whitney U Testi	,114[c]	Keep null hypothese.
2	The dispersion of 24h is the consistent among of groups	Independent-Samples Mann and Whitney U Testi	,686[c]	Keep the null hypothesis.

a. The importance level is 0,50.

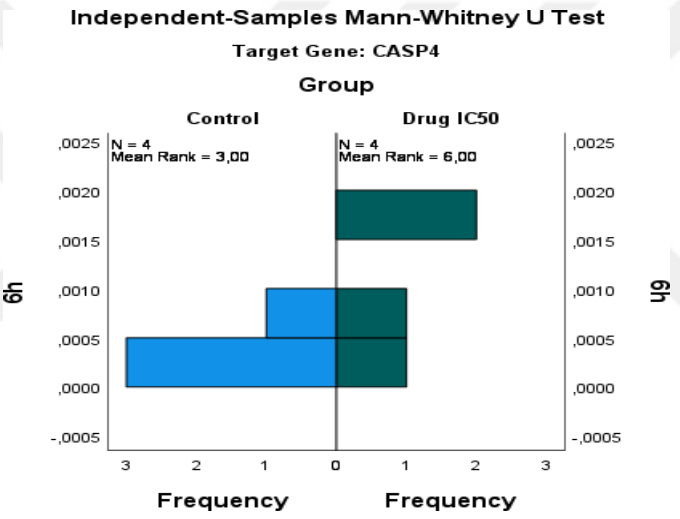

Figure 3.57. CASP4 Gene Results 6h

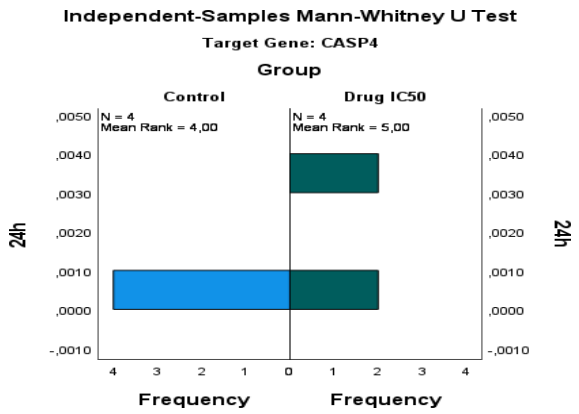

Figure 3.58. CASP4 Gene Results 24h

Table 3.25. Hypothesis Test Summary for CASP6 Gene

	Null Hypothesis	Test	Sig.[a,b]	Decision
1	The dispersion of 6h is the consistent among of groups	Independent-Samples Mann and Whitney U Testi	,057[c]	Keep the null hypothese
2	The dispersion of 24h is the consistent among of groups	Independent-Samples Mann and Whitney U Testi	,029[c]	Decline the null hypothese

a. The important level is 0,50.

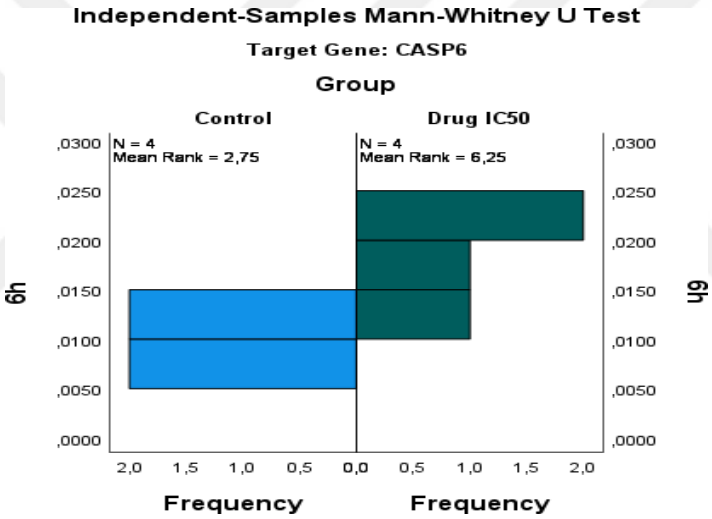

Figure 3.59. CASP6 Gene Results 6h

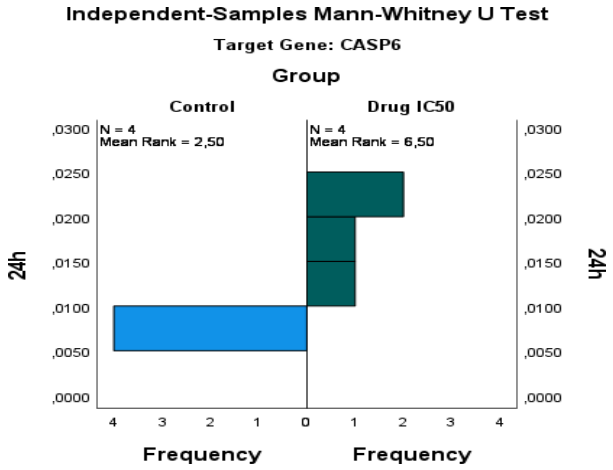

Figure 3.60. CASP6 Gene Results 24h

Table 3.26. Hypothesis Test Summary for CASP7 Gene

	Null Hypothesis	Test	Sig.[a,b]	Decision
1	The dispersion of 6h is the consistent among of groups	Independent-Samples Mann and Whitney U Testi	,029[c]	Decline the null hypothesis.
2	The dispersion of 24h is the consistent among of groups	Independent-Samples Mann and Whitney U Testi	,029[c]	Decline the null hypothesis.

a. The important level is 0,50.

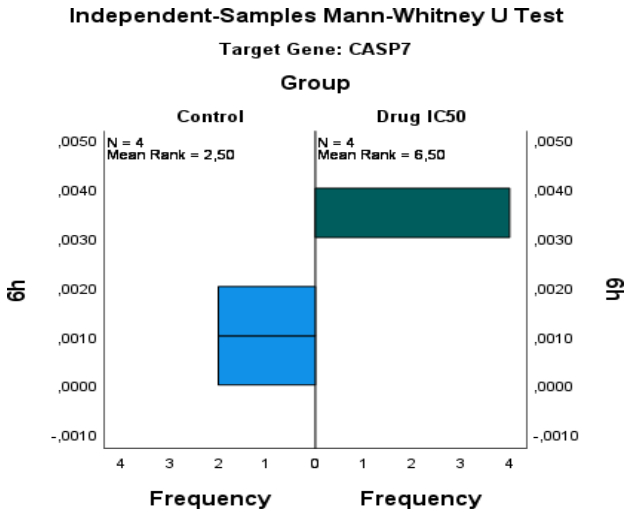

Figure 3.61. CASP7 Gene Results 6h

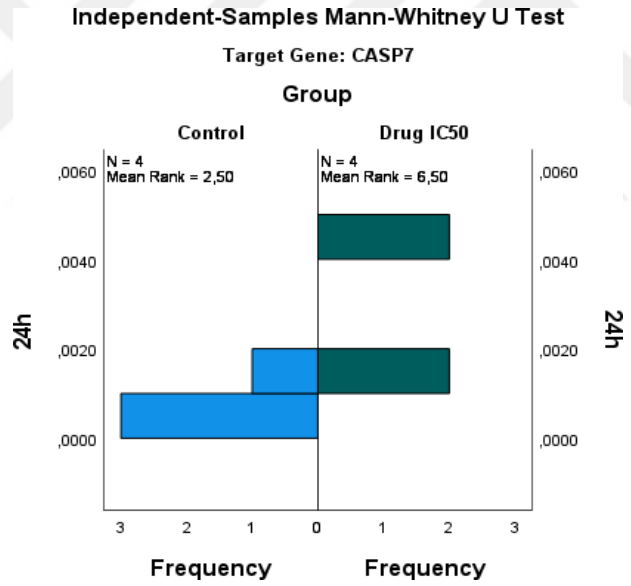

Figure 3.62. CASP7 Gene Results 24h

Table 3.27. Hypothesis Test Summary for CDC20 Gene

	Null Hypothesis	Test	Sig.[a,b]	Decision
1	The dispersion of 6h is the consistent among of groups	Independent-Samples Mann and Whitney U Testi	,686[c]	Keep the null hypothesis.
2	The dispersion of 24h is the consistent among of groups	Independent-Samples Mann and Whitney U Testi	,486[c]	Keep the null hypothesis.

a. The importance level is 0,50.

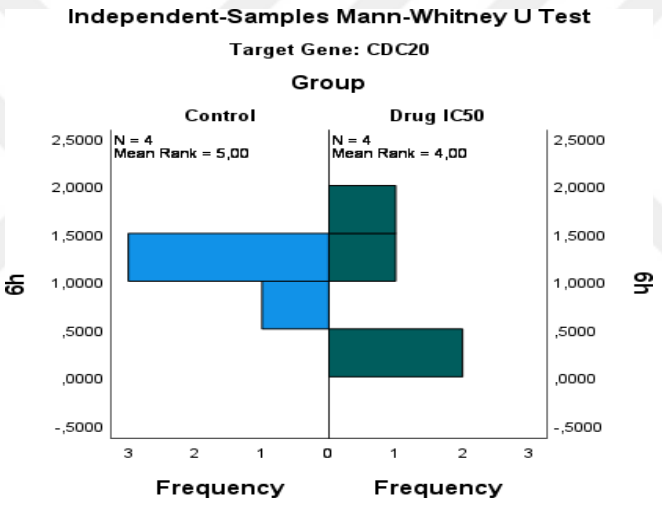

Figure 3.63. CDC20 Gene Results 6h

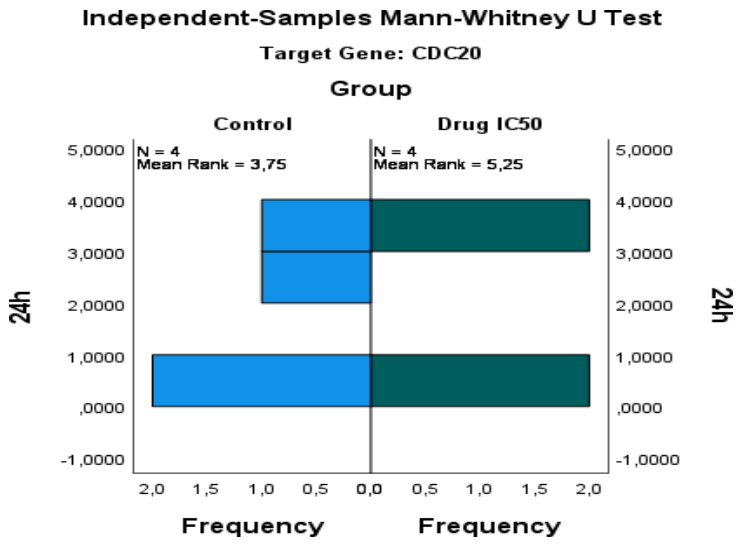

Figure 3.64. CDC20 Gene Results 24h

Table 3.28. Hypothesis Test Summary for CDK4 Gene

	Null Hypothesis	Test	Sig.[a,b]	Decision
1	The dispersion of 6h is the consistent among of groups	Independent-Samples Mann and Whitney U Testi	1,000[c]	keep the null hypothesis.
2	The dispersion of 24h is the consistent among of groups	Independent-Samples Mann and Whitney U Testi	,057[c]	keep the null hypothesis.

a. The importance level is 0,50.

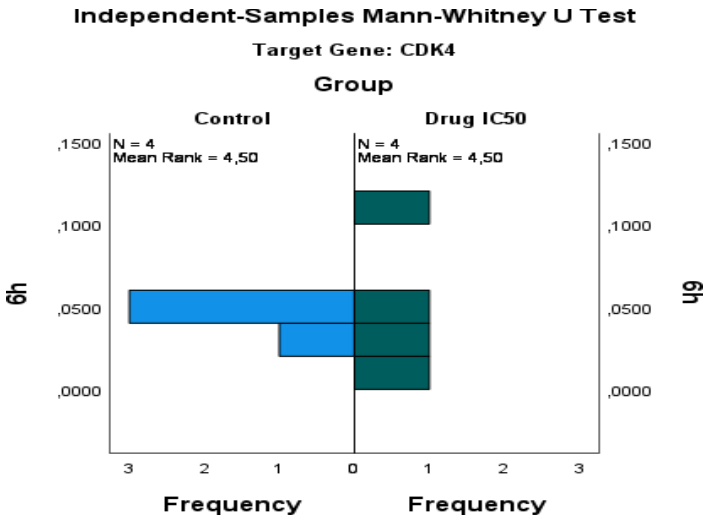

Figure 3.65. CDK4 Gene Results 6h

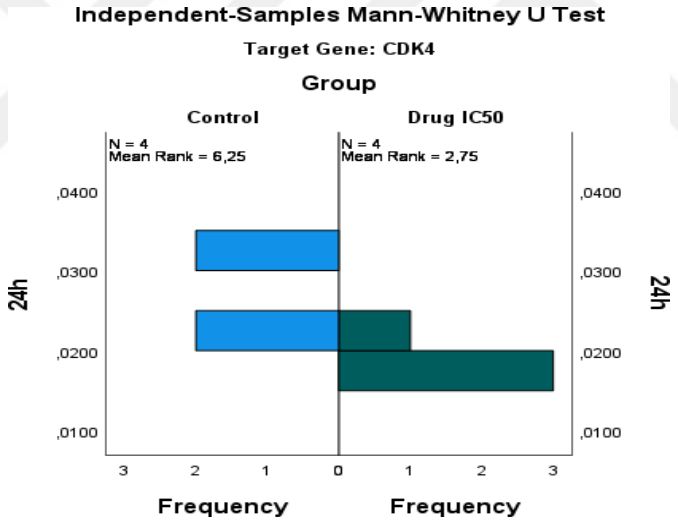

Figure 3.66. CDK4 Gene Results 24h

Table 3.29. Hypothesis Test Summary for DCR Gene

	Null Hypothesis	Test	Sig.[a,b]	Decision
1	The dispersion of 6h is the consistent among of groups	Independent-Samples Mann and Whitney U Testi	,057[c]	keep the null hypothesis.

2	The dispersion of 24h is the consistent among of groups	Independent-Samples Mann and Whitney U Testi	,029[c]	decline the null hypothesis.

a. The important level is 0,50.

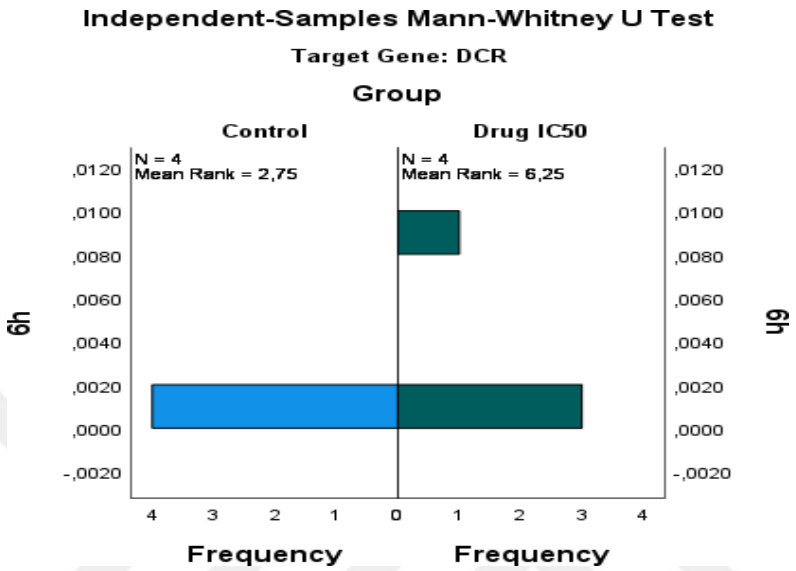

Figure 3.67. DCR Gene Results 6h

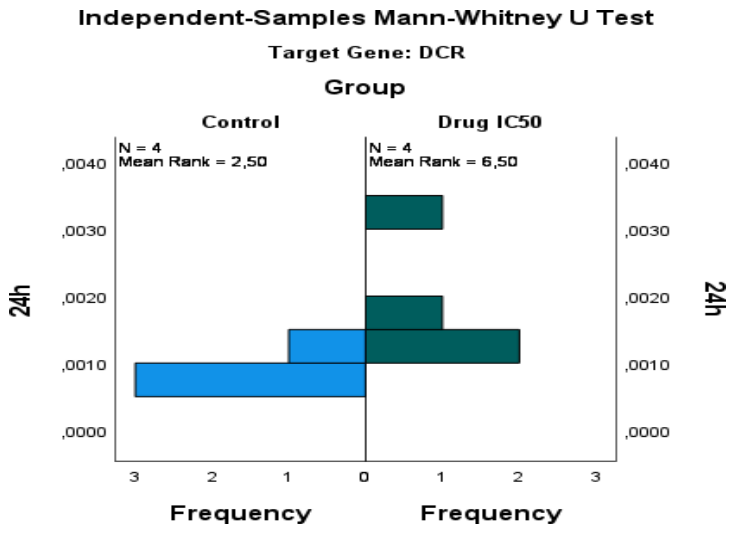

Figure 3.68. DCR Gene Results 24h

Table 3.30. Hypothesis Test Summary for DR4 Gene

	Null Hypothesis	Test	Sig.[a,b]	Decision
1	The dispersion of 6h is the consistent among of groups	Independent-Samples Mann and Whitney U Testi	,057[c]	keep the null hypothesis.
2	The dispersion of 24h is the consistent among of groups	Independent-Samples Mann and Whitney U Testi	,886[c]	keep the null hypothesis.

a. The important level is 0,50.

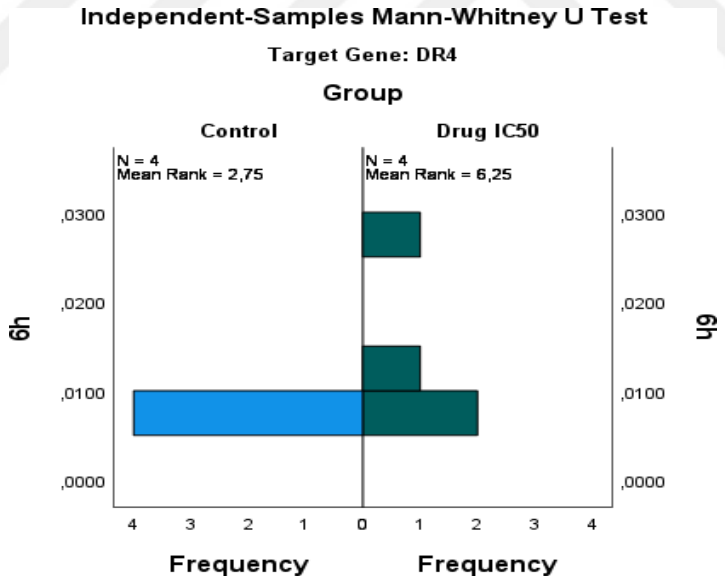

Figure 3.69. DR4 Gene Results 6h

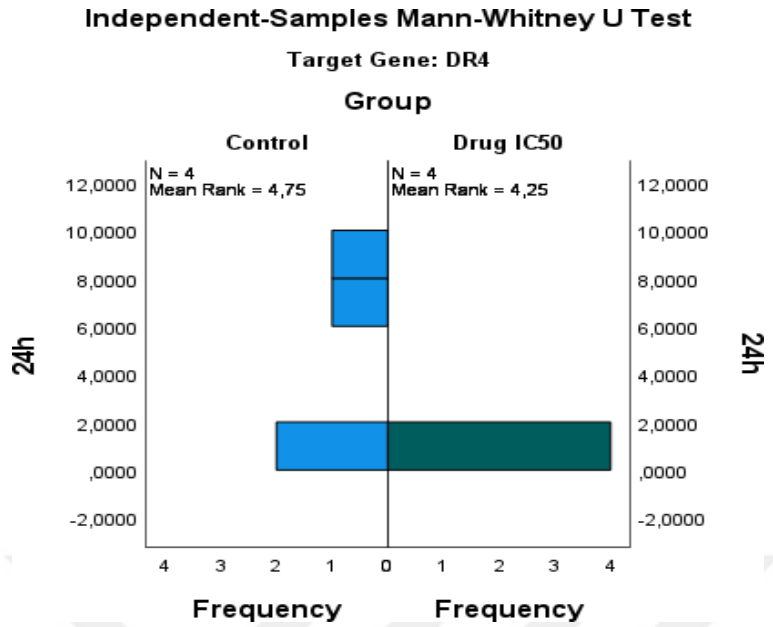

Figure 3.70. DR4 Gene Results 24h

Table 3.31. Hypothesis Test Summary for DR5 Gene

	Null Hypothesis	Test	Sig.[a,b]	Decision
1	The dispersion of 6h is the consistent among of groups	Independent-Samples Mann and Whitney U Testi	,029[c]	decline the null hypothesis.
2	The dispersion of 24h is the consistent among of groups	Independent-Samples Mann and Whitney U Testi	,343[c]	keep the null hypothesis.

a. The important level is 0,50.

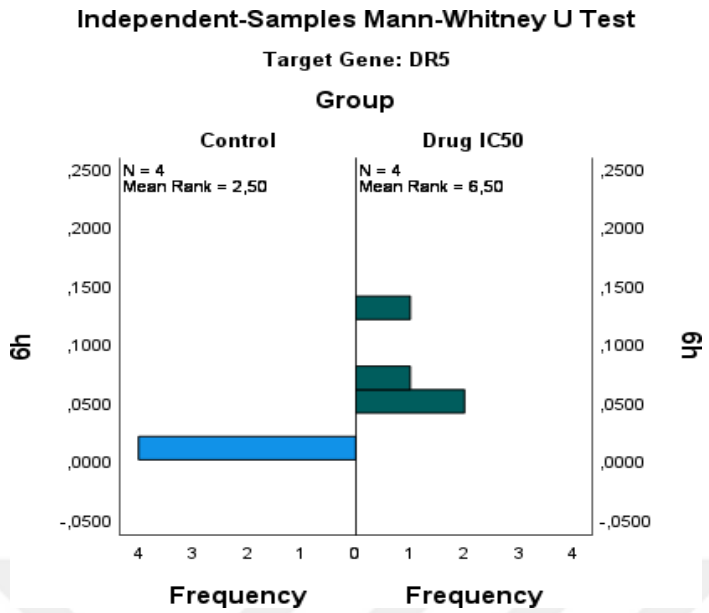

Figure 3.71. DR5 Gene Results 6h

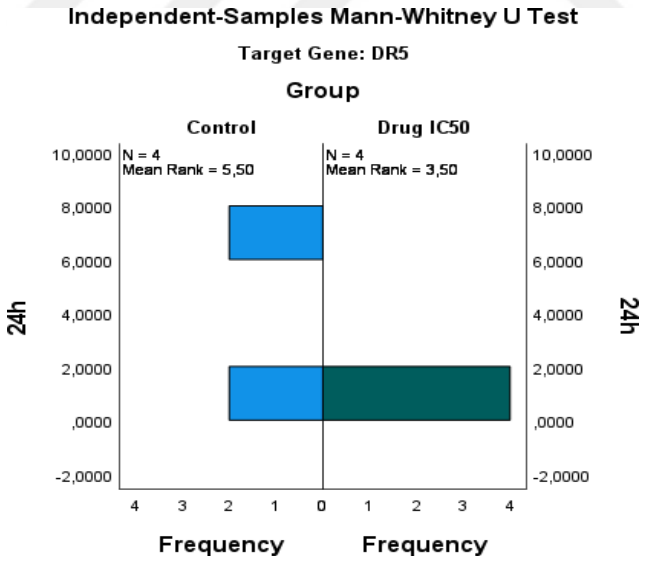

Figure 3.72. DR5 Gene Results 24h

Table 3.32. Hypothesis Test Summary for ERCC1 Gene

	Null Hypothesis	Test	Sig.[a,b]	Decision
1	The dispersion of 6h is the consistent among of groups	Independent-Samples Mann and Whitney U Testi	,200[c]	keep the null hypothesis.
2	The dispersion of 24h is the consistent among of groups	Independent-Samples Mann and Whitney U Testi	,029[c]	decline the null hypothesis.

a. The important level is 0,50.

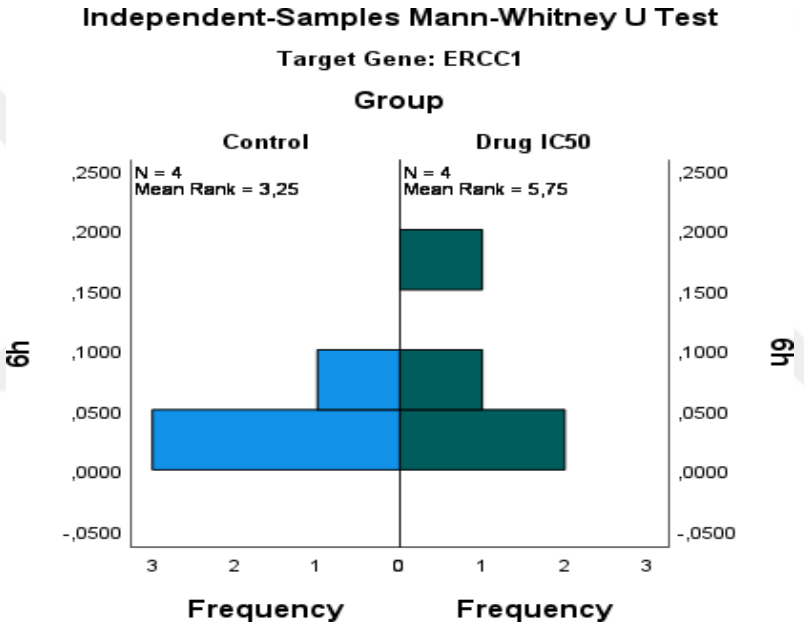

Figure 3.73. ERCC1 Gene Results 6h

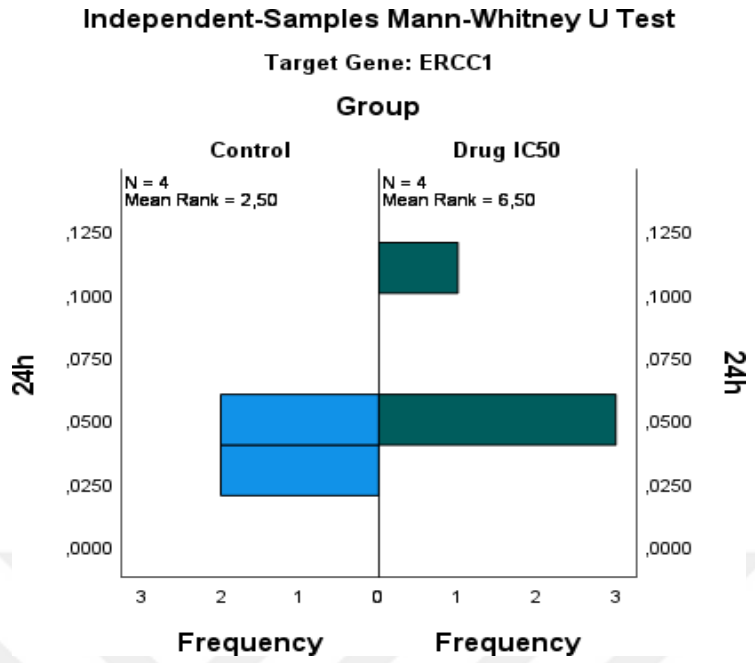

Figure 3.74. ERCC1 Gene Results 24h

Table 3.33. Hypothesis Test Summary for ERCC3 Gene

	Null Hypothesis	Test	Sig.[a,b]	Decision
1	The dispersion of 6h is the consistent among of groups	Independent-Samples Mann and Whitney U Testi	,886[c]	keep the null hypothesis.
2	The dispersion of 24h is the consistent among of groups	Independent-Samples Mann and Whitney U Testi	,029[c]	decline the null hypothesis.

a. The important level is 0,50.

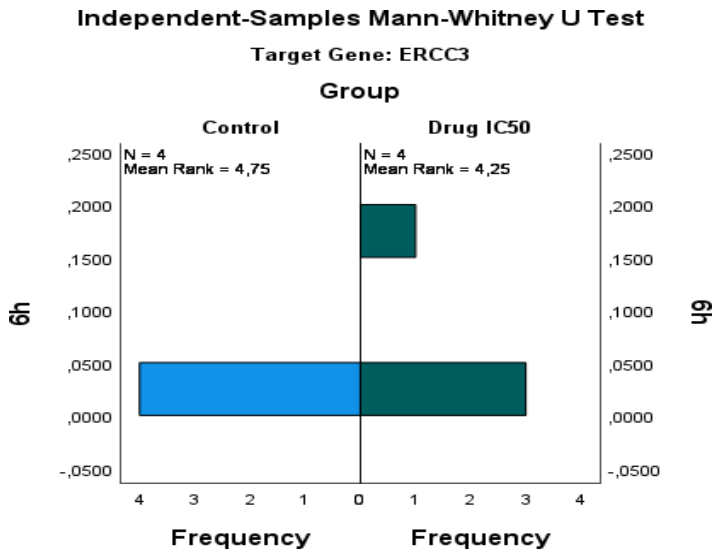

Figure 3.75. ERCC3 Gene Results 6h

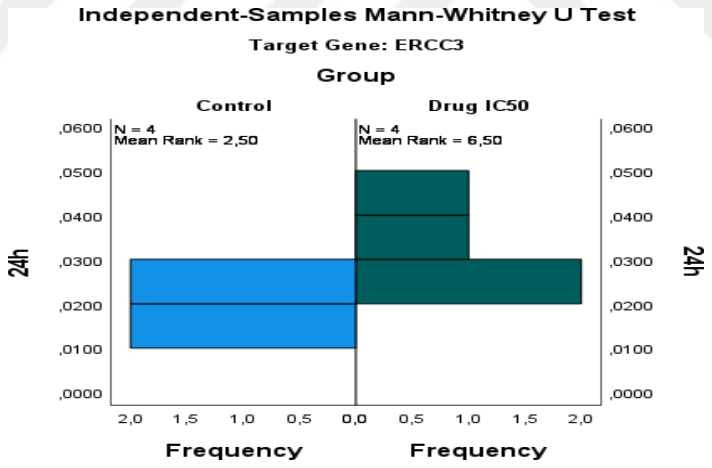

Figure 3.76. ERCC3 Gene Results 24h

Table 3.34. Hypothesis Test Summary for FAS Gene

	Null Hypothesis	Test	Sig.[a,b]	Decision
1	The dispersion of 6h is the consistent among of groups	Independent-Samples Mann and Whitney U Testi	,029[c]	decline the null hypothesis.
2	The dispersion of 24h is the consistent among of groups	Independent-Samples Mann and Whitney U Testi	,343[c]	keep the null hypothesis.

a. The important level is 0,50.

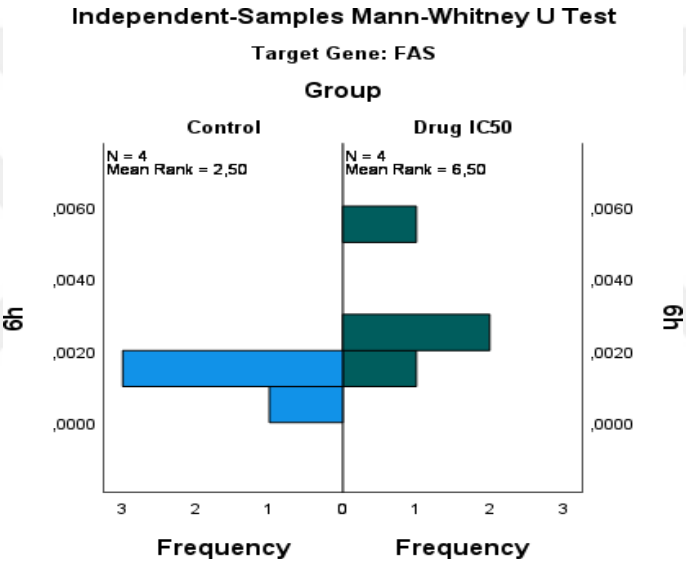

Figure 3.77. FAS Gene Results 6h

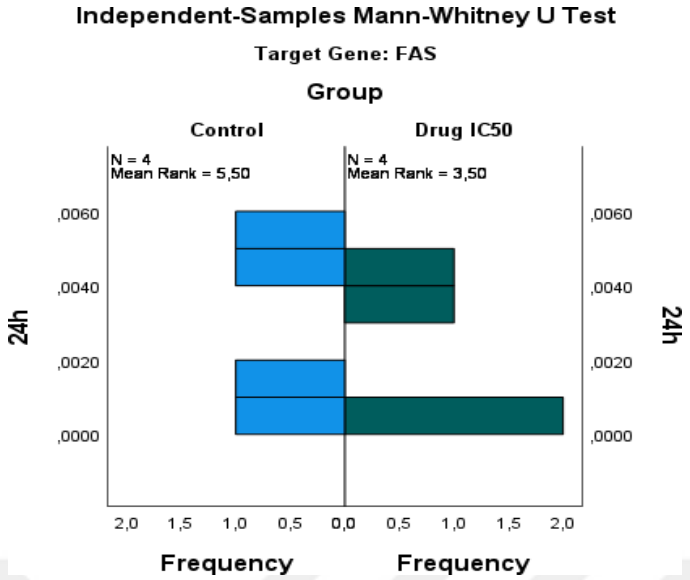

Figure 3.78. FAS Gene Results 24h

Table 3.35. Hypothesis Test Summary for GAD45A Gene

	Null Hypothesis	Test	Sig.[a,b]	Decision
1	The dispersion of 6h is the consistent among of groups	Independent-Samples Mann and Whitney U Testi	,029[c]	decline the null hypothesis.
2	The dispersion of 24h is the consistent among of groups	Independent-Samples Mann and Whitney U Testi	,029[c]	decline the null hypothesis.

a. The important level is 0,50.

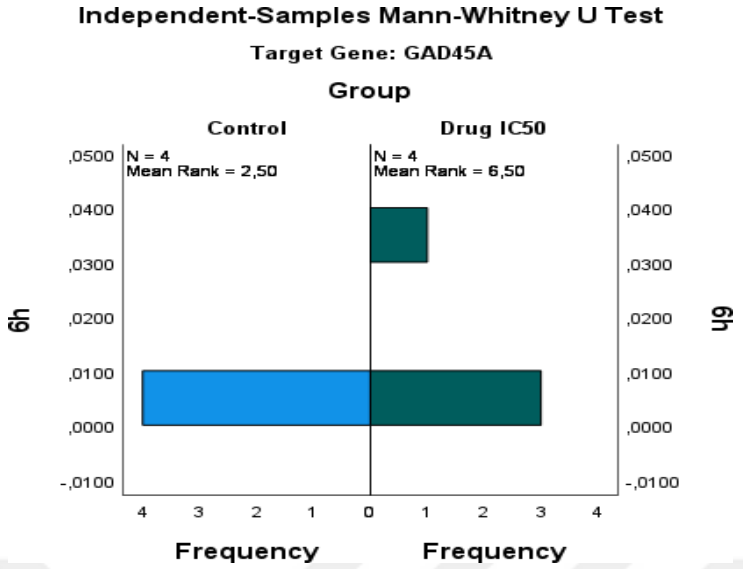

Figure 3.79. GAD45A Gene Results 6h

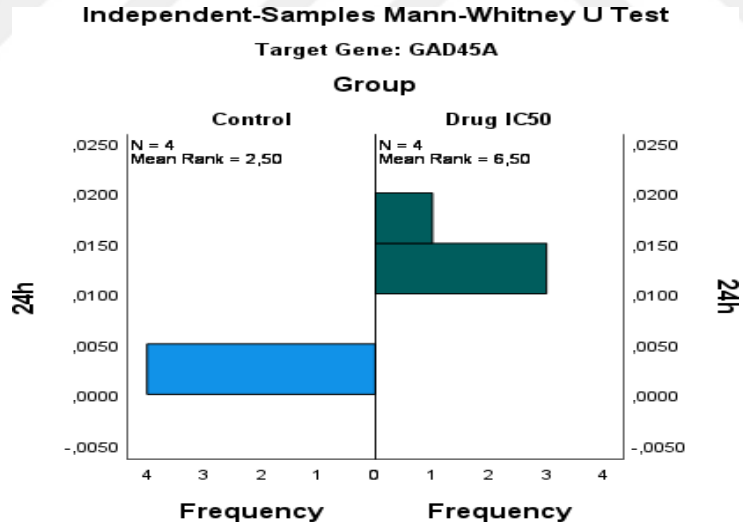

Figure 3.80. GAD45A Gene Results 24h

Table 3.36. Hypothesis Test Summary for GSTP1 Gene

	Null Hypothesis	Test	Sig.[a,b]	Decision
1	The dispersion of 6h is the consistent among of groups	Independent-Samples Mann and Whitney U Testi	,343[c]	keep the null hypothesis.
2	The dispersion of 24h is the consistent among of groups	Independent-Samples Mann and Whitney U Testi	1,000[c]	keep the null hypothesis.

a. The importance level is 0,50.

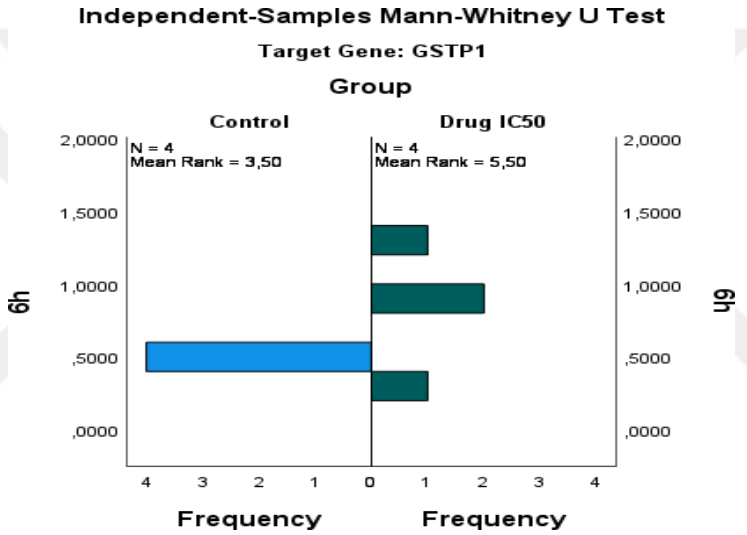

Figure 3.81. GSTP1 Gene Results 6h

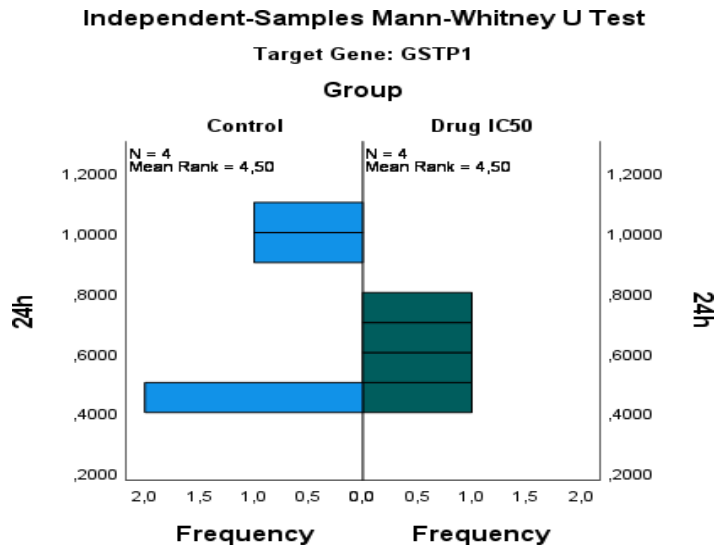

Figure 3.82. GSTP1 Gene Results 24h

Table 3.37. Hypothesis Test Summary for LIG4 Gene

	Null Hypothesis	Test	Sig.[a,b]	Decision
1	The dispersion of 6h is the consistent among of groups	Independent-Samples Mann and Whitney U Testi	,886[c]	keep the null hypothesis.
2	The dispersion of 24h is the consistent among of groups	Independent-Samples Mann and Whitney U Testi	,029[c]	decline the null hypothesis.

a. The important level is 0,50.

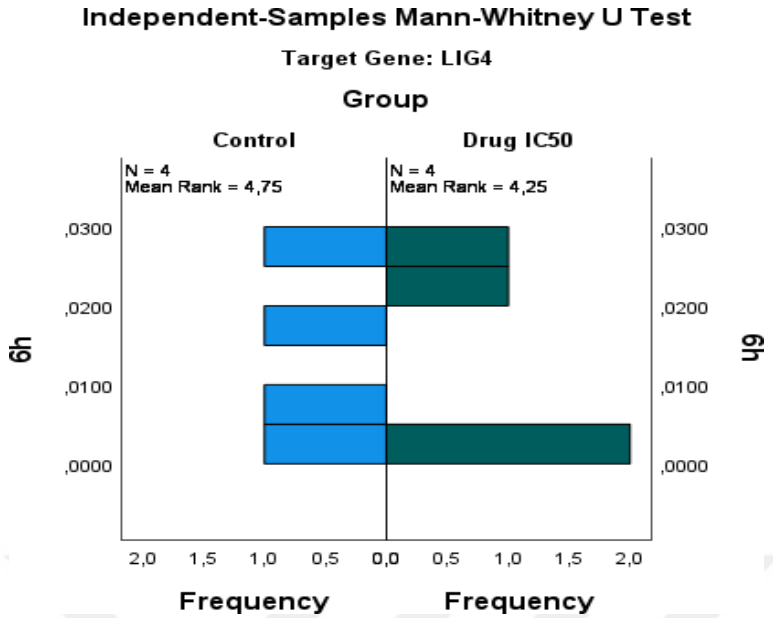

Figure 3.83. LIG4 Gene Results 6h

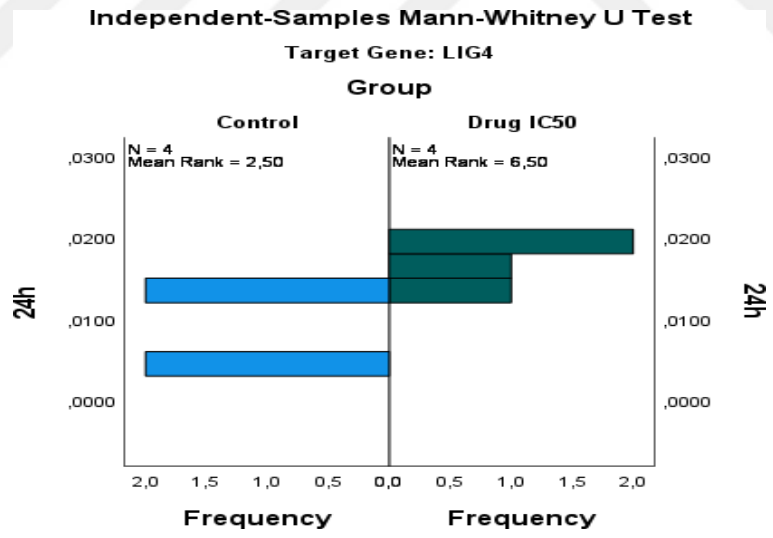

Figure 3.84. LIG4 Gene Results 24h

Table 3.38. Hypothesis Test Summary for MCL1 Gene

	Null Hypothesis	Test	Sig.[a,b]	Decision
1	The dispersion of 6h is the consistent among of groups	Independent-Samples Mann and Whitney U Testi	,114[c]	keep the null hypothesis.
2	The dispersion of 24h is the consistent among of groups	Independent-Samples Mann and Whitney U Testi	,029[c]	decline the null hypothesis.

a. The important level is 0,50.

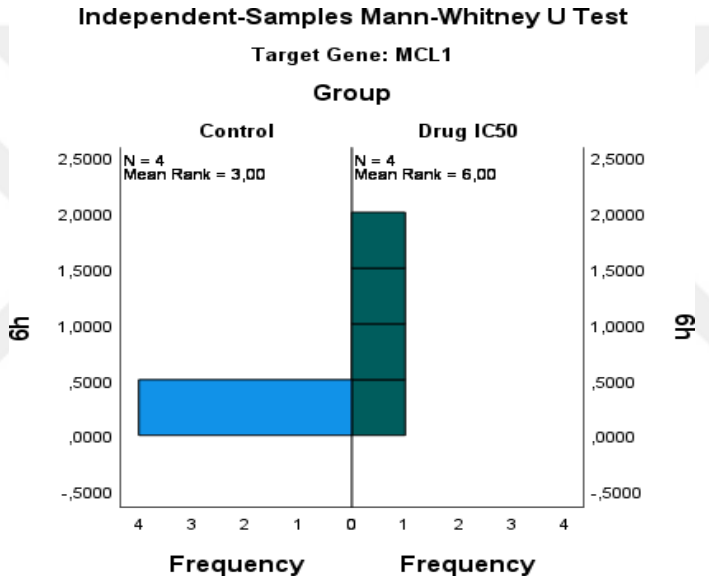

Figure 3.85. MCL1 Gene Results 6h

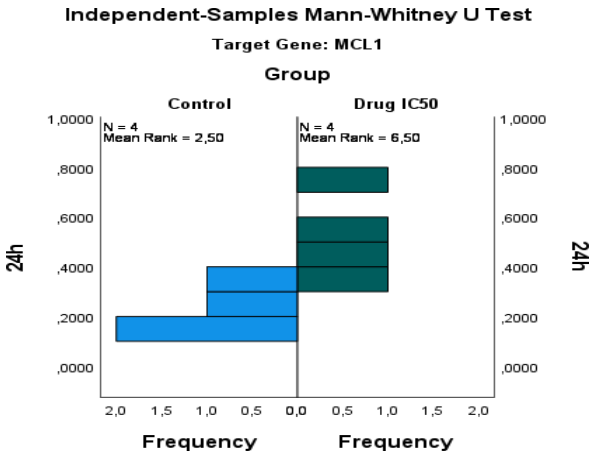

Figure 3.86. MCL1 Gene Results 24h

Table 3.39. Hypothesis Test Summary for MDM2 Gene

	Null Hypothesis	Test	Sig.[a,b]	Decision
1	The distribution of 6h is the same across categories of Group.	Independent-Samples Mann-Whitney U Test	,114[c]	keep the null hypothesis.
2	The distribution of 24h is the same across categories of Group.	Independent-Samples Mann-Whitney U Test	,057[c]	keep the null hypothesis.

a. The important level is 0,50.

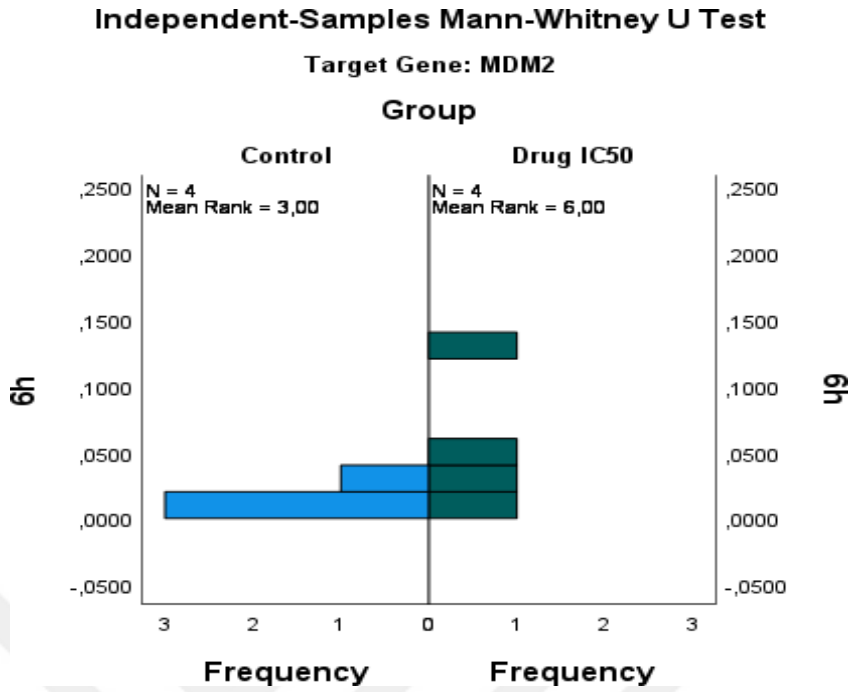

Figure 3.87. MDM2 Gene Results 6h

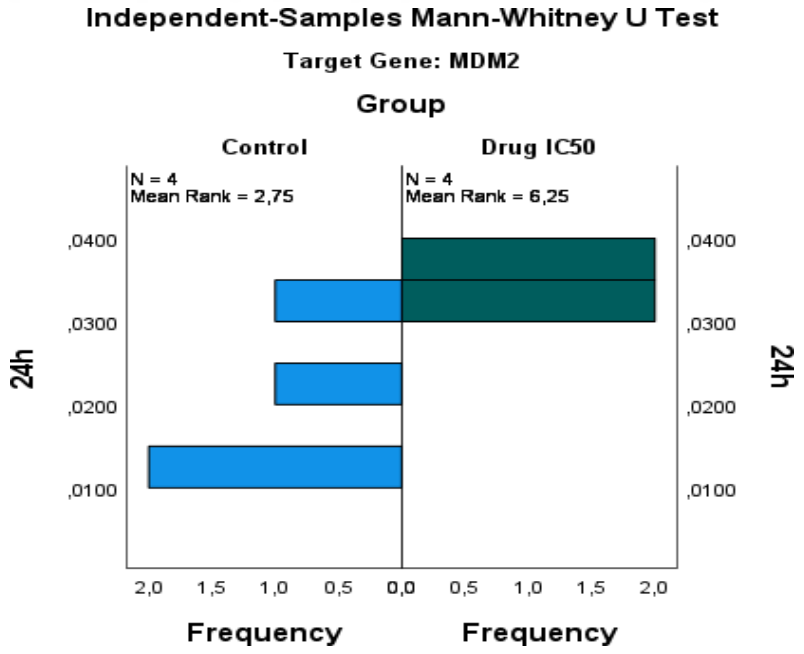

Figure 3.88. MDM2 Gene Results 24h

Table 3.40. Hypothesis Test Summary for MGMT Gene

	Null Hypothesis	Test	Sig.[a,b]	Decision
1	The dispersion of 6h is the consistent among of groups	Independent-Samples Mann and Whitney U Testi	,886[c]	keep the null hypothesis.
2	The dispersion of 24h is the consistent among of groups	Independent-Samples Mann and Whitney U Testi	,057[c]	keep the null hypothesis.

a. The important level is 0,50.

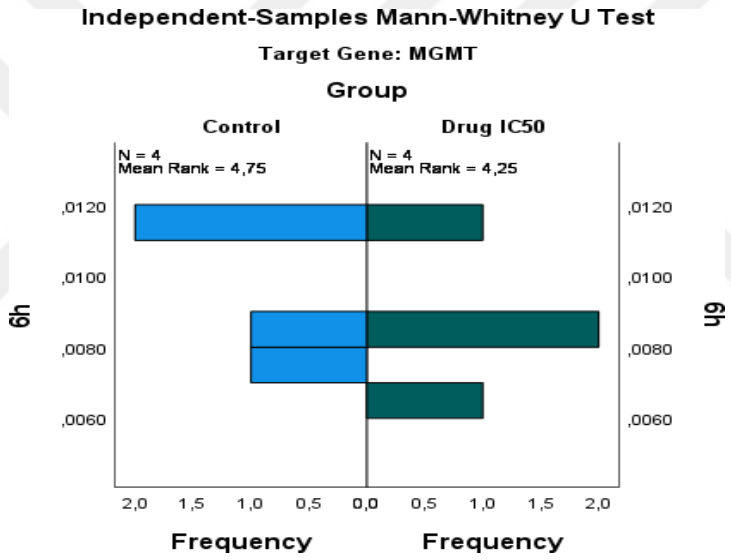

Figure 3.89. MGMT Gene Results 6h

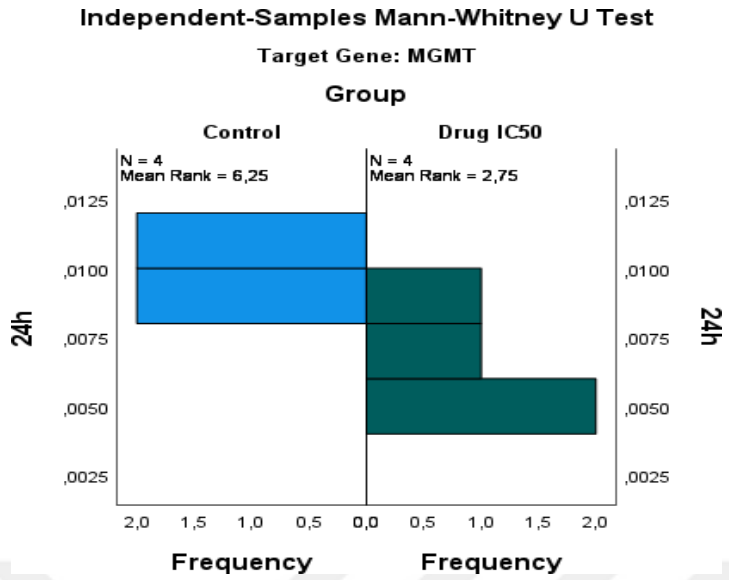

Figure 3.90. MGMT Gene Results 24h

Table 3.41. Hypothesis Test Summary for NEK2 Gene

	Null Hypothesis	Test	Sig.[a,b]	Decision
1	The dispersion of 6h is the consistent among of groups	Independent-Samples Mann and Whitney U Testi	,686[c]	keep the null hypothesis.
2	The dispersion of 24h is the consistent among of groups	Independent-Samples Mann and Whitney U Testi	,057[c]	keep the null hypothesis.

a. The important level is 0,50.

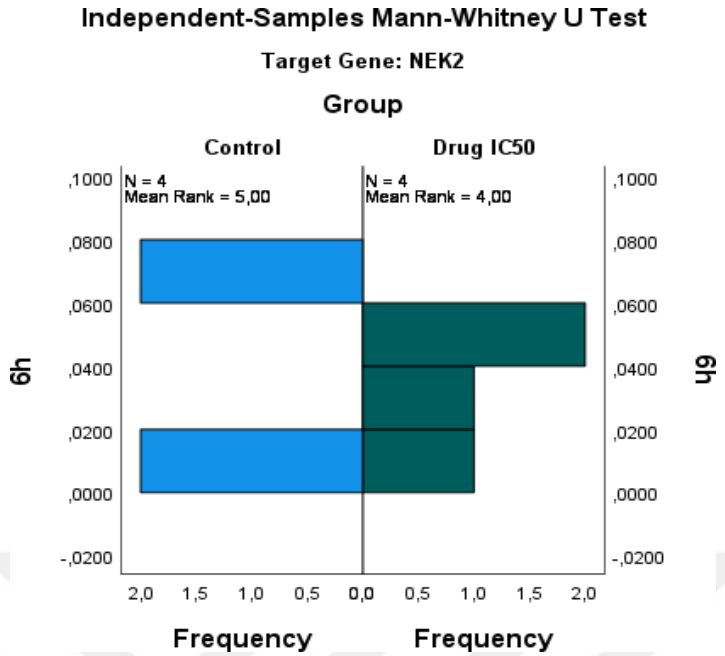

Figure 3.91. NEK2 Gene Results 6h

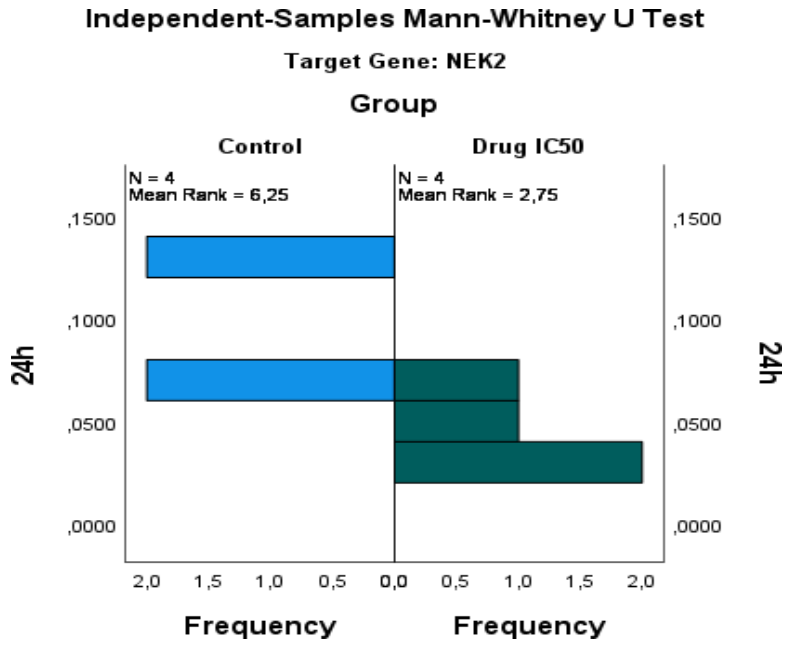

Figure 3.92. NEK2 Gene Results 24h

Table 3.42. Hypothesis Test Summary for NOXA Gene

	Null Hypothesis	Test	Sig.[a,b]	Decision
1	The dispersion of 6h is the consistent among of groups	Independent-Samples Mann and Whitney U Testi	,029[c]	decline the null hypothesis.
2	The dispersion of 24h is the consistent among of groups	Independent-Samples Mann and Whitney U Testi	1,000[c]	decline the null hypothesis.

a. The important level is 0,50.

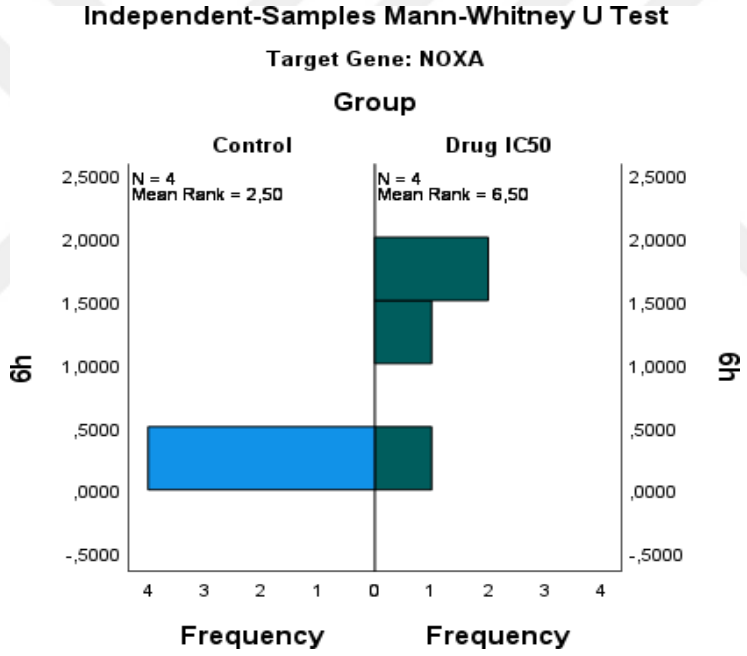

Figure 3.93. NOXA Gene Results 6h

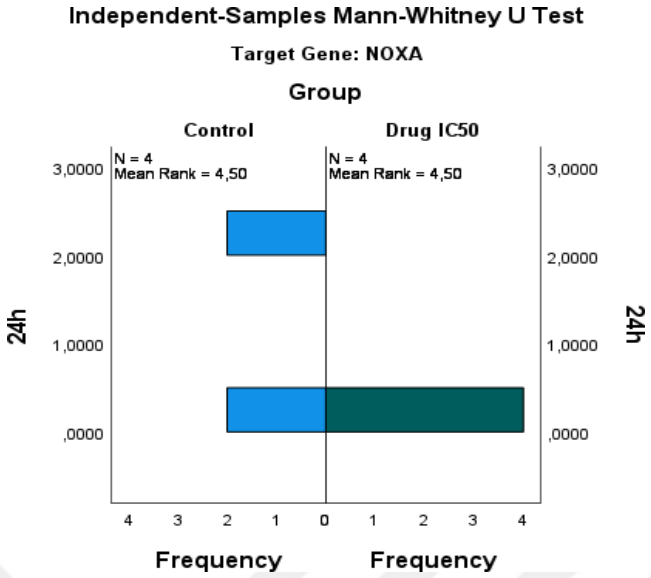

Figure 3.94. NOXA Gene Results 24h

Table 3.43. Hypothesis Test Summary for PRDX1 Gene

	Null Hypothesis	Test	Sig.[a,b]	Decision
1	The dispersion of 6h is the consistent among of groups	Independent-Samples Mann and Whitney U Testi	,486[c]	keep the null hypothesis.
2	The dispersion of 24h is the consistent among of groups	Independent-Samples Mann and Whitney U Testi	,029[c]	decline the null hypothesis.

a. The important level is 0,50.

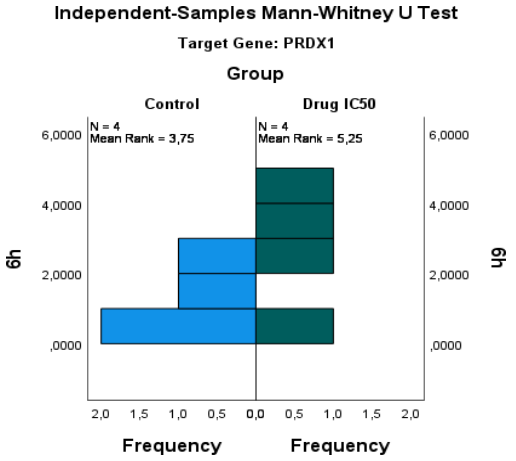

Figure 3.95. PRDX1 Gene Results 6h

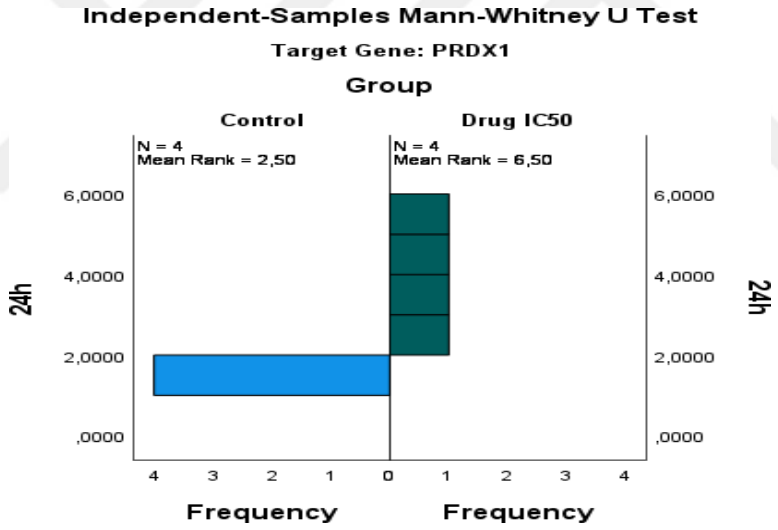

Figure 3.96. PRDX1 Gene Results 24h

Table 3.44. Hypothesis Test Summary for PUMA Gene

	Null Hypothesis	Test	Sig.[a,b]	Decision
1	The dispersion of 6h is the consistent among of groups	Independent-Samples Mann and Whitney U Testi	,114[c]	keep the null hypothesis.

2	The dispersion of 24h is the consistent among of groups	Independent-Samples Mann and Whitney U Testi	,029[c]	decline the null hypothesis.

a. The important level is 0,50.

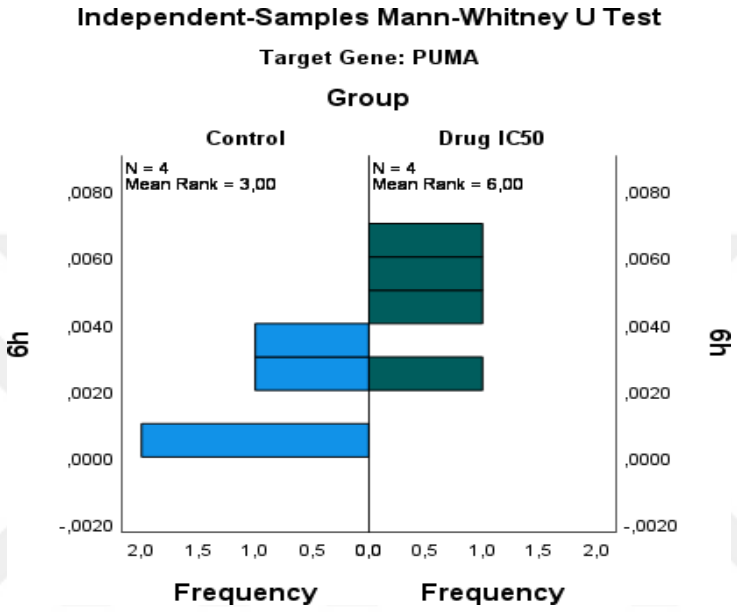

Figure 3.97. PUMA Gene Results 6h

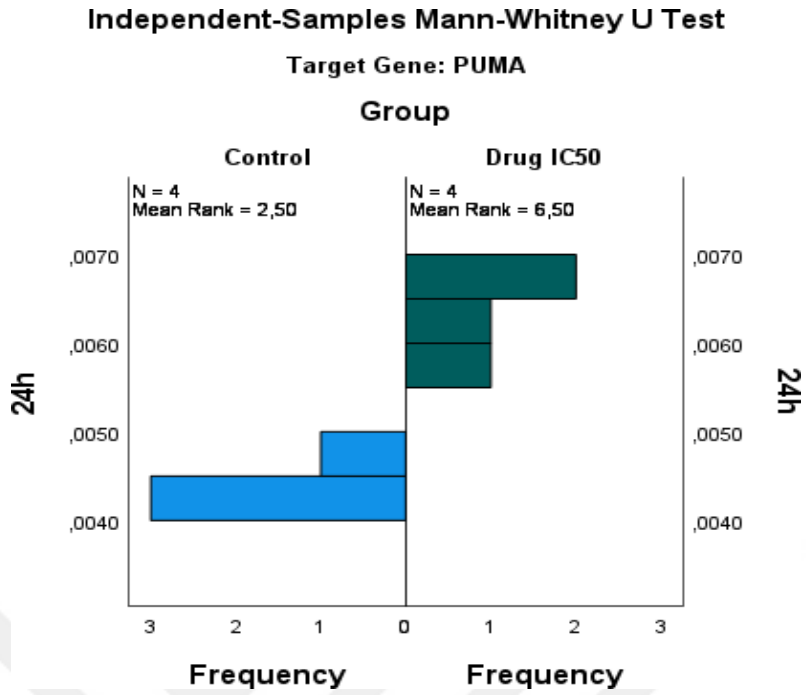

Figure 3.98. PUMA Gene Results 24h

Table 3.45. Hypothesis Test Summary for RAD52 Gene

	Null Hypothesis	Test	Sig.[a,b]	Decision
1	The dispersion of 6h is the consistent among of groups	Independent-Samples Mann and Whitney U Testi	,057[c]	keep the null hypothesis.
2	The dispersion of 24h is the consistent among of groups	Independent-Samples Mann and Whitney U Testi	,486[c]	keep the null hypothesis.

a. The important level is 0,50.

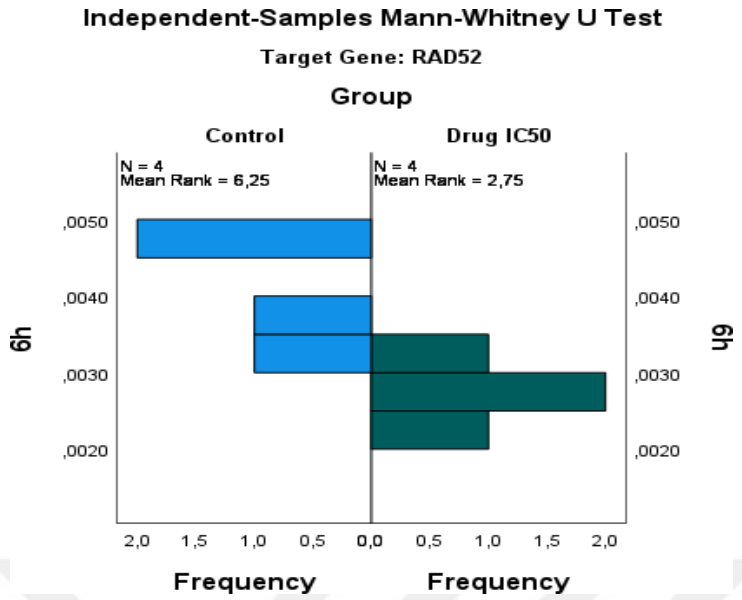

Figure 3.99. RAD52 Gene Results 6h

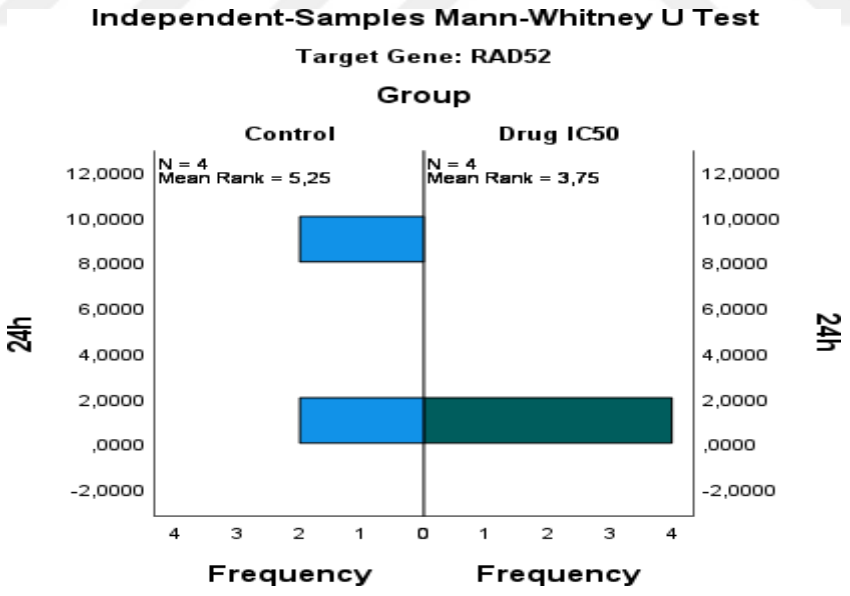

Figure 3.100. RAD52 Gene Results 24h

Table 3.46. Hypothesis Test Summary for SOD1 Gene

	Null Hypothesis	Test	Sig.[a,b]	Decision
1	The dispersion of 6h is the consistent among of groups	Independent-Samples Mann and Whitney U Testi	,200[c]	keep the null hypothesis.
2	The dispersion of 24h is the consistent among of groups	Independent-Samples Mann and Whitney U Testi	,029[c]	decline the null hypothesis.

a. The important level is 0,50.

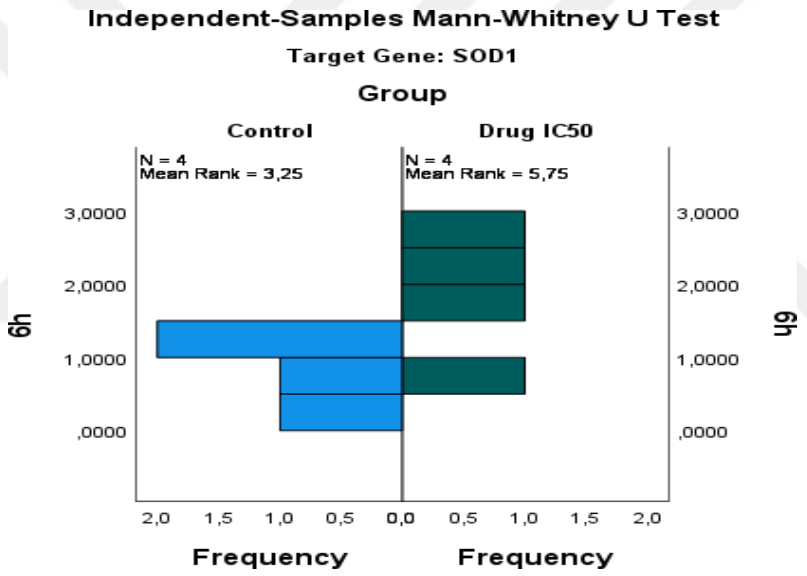

Figure 3.101. SOD1 Gene Results 6h

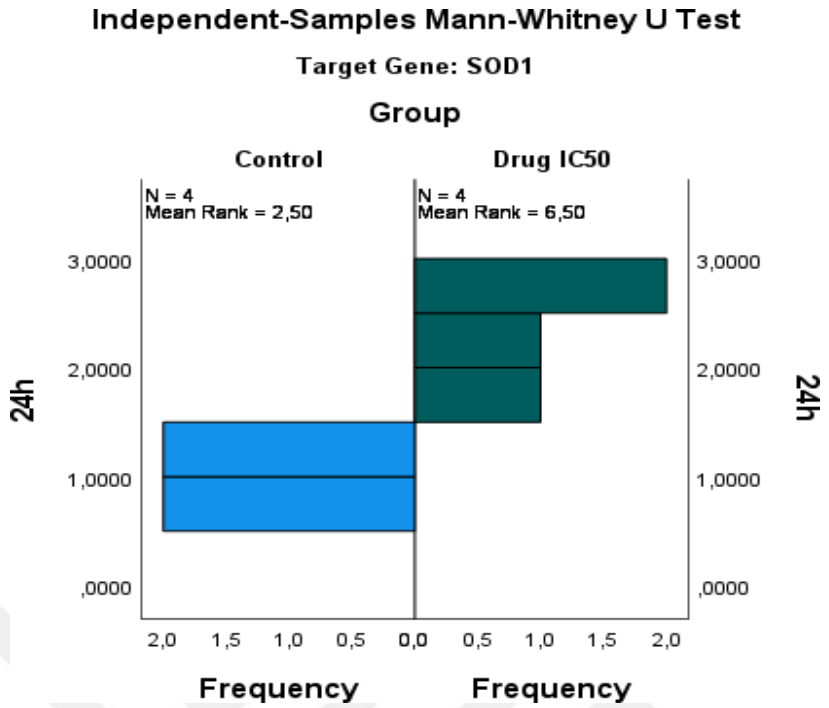

Figure 3.102. SOD1 Gene Results 24h

Table 3.47. Hypothesis Test Summary for XPA Gene

	Null Hypothesis	Test	Sig.[a,b]	Decision
1	The dispersion of 6h is the consistent among of groups	Independent-Samples Mann and Whitney U Testi	,686[c]	keep the null hypothesis.
2	The dispersion of 24h is the consistent among of groups	Independent-Samples Mann and Whitney U Testi	,343[c]	keep the null hypothesis.

a. The important level is 0,50.

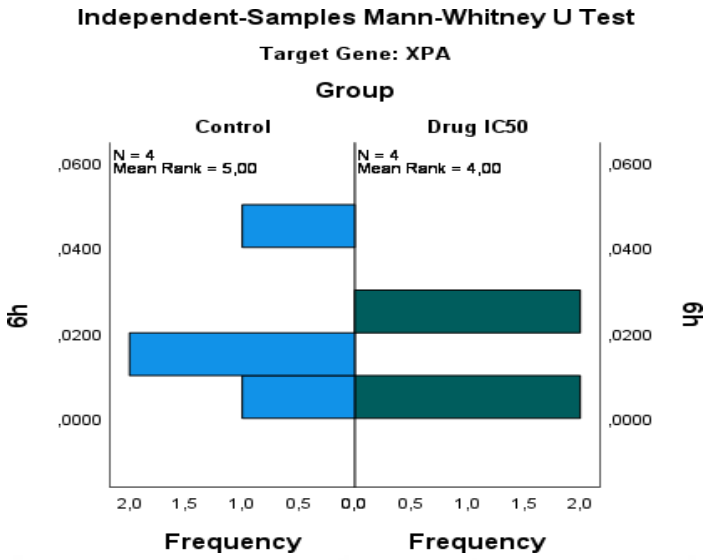

Figure 3.103. XPA Gene Results 6h

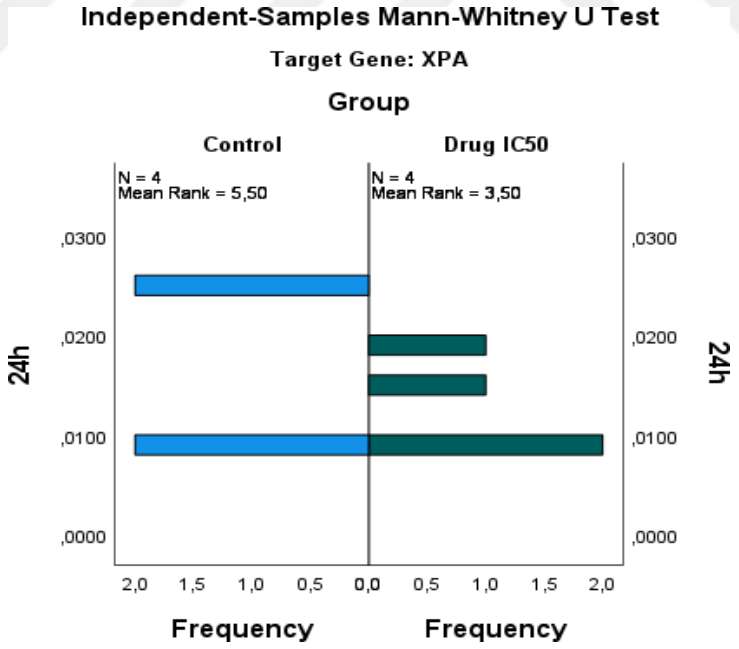

Figure 3.104. XPA Gene Results 24h

Table 3.48. Hypothesis Test Summary for XRCC5 Gene

	Null Hypothesis	Test	Sig.[a,b]	Decision
1	The dispersion of 6h is the consistent among of groups	Independent-Samples Mann and Whitney U Testi	,343[c]	keep the null hypothesis.
2	The dispersion of 24h is the consistent among of groups	Independent-Samples Mann and Whitney U Testi	,343[c]	keep the null hypothesis.

a. The important level is 0,50.

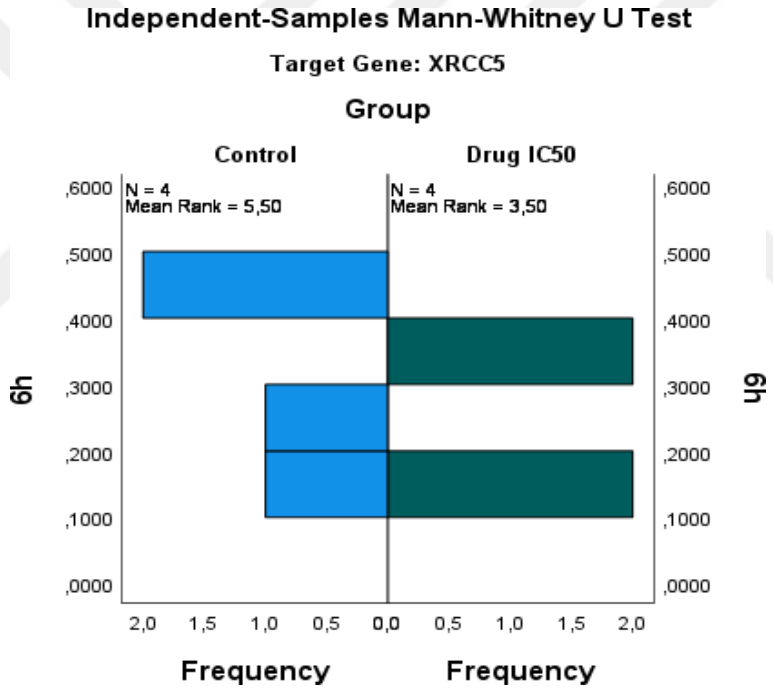

Figure 3.105. XRCC5 Gene Results 6h

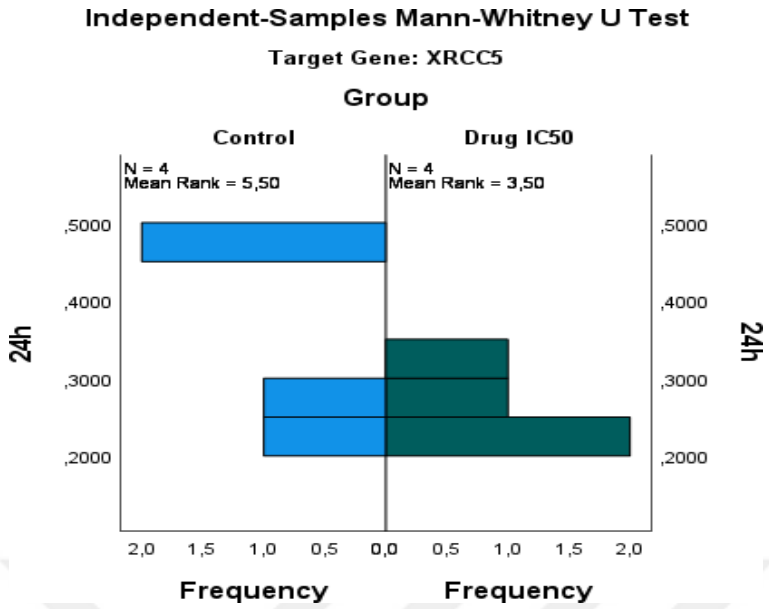

Figure 3.106. XRCC5 Gene Results 24h

CHAPTER 4
DISCUSSION

Cancer is a significant and enduring illness of our day, persisting from previous years to the present day. Annually, a substantial number of individuals get a cancer diagnosis, and a significant proportion of them succumb to the disease despite undergoing various therapies over an extended period of time. Recent study indicates that the prevalence of cancer is projected to increase twofold in the following decade. Notwithstanding these prognostications, our comprehension of the future of cancer remains incomplete. Uncertainties in risk variables make it challenging to accurately anticipate the future burden of cancer (143,144). Nevertheless, cancer research is important for a future in which cancer may be promptly recognized and efficiently treated, ultimately leading to the full eradication of cancer. Epidemiological studies and advancements in cancer genetics are crucial in influencing the future direction of cancer research and individualized cancer therapy (145,146).

Colon cancer, medically referred to as colorectal cancer, arises in the colon or rectum and is distinguished by the anomalous proliferation of cells in that area. Furthermore, colon cancer ranks as the third most prevalent form of cancer globally among both males and females. The potential cause of this condition is the presence of precancerous growths known as polyps on the inner mucosal layer of the colon. Colon cancer often progresses gradually over a span of many years and may be detected at an early stage with screening examinations like colonoscopy. Colon cancer develops by the accumulation of genetic mutations, which result in uncontrolled cell proliferation and the creation of tumors. Age, family history of colorectal cancer, and inflammatory bowel illnesses are known risk factors for developing colon cancer, as well as other forms of cancer. Common indications of colon cancer include alterations in bowel patterns, presence of blood in the stool, stomach uneasiness, inexplicable reduction in body weight, and exhaustion. The treatment for colon cancer is determined by the stage of the illness and often involves a mix of surgical procedures, chemotherapy, radiation therapy, targeted therapy, and immunotherapy. Notable progress has been achieved in the field of colon cancer medication therapy in recent years (147). Bevacizumab, a commonly used medication for the management of colon or rectal cancer, belongs to the class of monoclonal antibodies. Essentially, it is a protein that is often generated by the immune system to aid in the body's protection against infections and cancer. Colon cancer has been categorized into many subgroups based on its morphology, genetics, and histology. Furthermore, these disparities have an impact on the efficacy of therapy and the rates of patient survival. The aforementioned findings elucidate the need for advanced and more efficacious therapeutic approaches in the management of colon cancer (148, 149).

In recent years, a total of thirty-three novel cancer therapy medications, such as kinase inhibitors and monoclonal antibodies, have been included into the existing drug regimens for cancer treatment. The research undertaken suggest that this number will eventually grow (150).

An essential issue that arises during and after therapy is the development of drug resistance in cancer cells. Consequently, the latest progress in cancer medication treatment has concentrated on tackling drug resistance, formulating tailored medicines, and discovering novel therapeutic targets. The issue of drug resistance remains a significant challenge in the field of cancer treatment using chemotherapy. Hence, the study is focused on identifying prospective biomarkers that might overcome medication resistance in cancer cells. Over the last five decades, chemotherapy with 5-fluorouracil (5-FU) has been extensively used for treating colon cancer (150,151). Furthermore, there have been advancements in the development of chemotherapeutic medications, including oxaliplatin, irinotecan, and capecitabine. The conventional approach for treating metastatic and advanced colon cancer was using combinations of drugs such as 5-FU, oxaliplatin, or irinotecan. Nevertheless, the emergence of monoclonal antibodies like Bevacizumab and Cetuximab prompted the advancement of therapy approaches. Despite the advancements in therapy, such as the use of monoclonal antibodies, the survival rate for metastatic colon cancer remains very poor (152).

The primary cause for this is the development of drug resistance. Approximately 50% of individuals diagnosed with colon cancer exhibit resistance to chemotherapy medicines that are based on 5-FU (153).

As previously said, researchers are now working on developing new options in response to the detrimental impact of chemotherapy medications on both healthy cells and colon cancer cells, which has resulted in major adverse effects for patients. Therefore, ongoing research is focused on novel areas such as DNA repair, drug metabolism, and the development of new metal-based anti-cancer medicines to combat drug resistance. Another instance pertains to the advancement of medications that are based on RNA. For instance, emerging agents like antisense oligonucleotides, RNA aptamers, and ribozymes have garnered significant interest because of their remarkable effectiveness and reduced negative effects.

These instances demonstrate the difficulties that must be resolved in the management of colon cancer and the possible advantages of novel therapeutic strategies (154,155).

For instance, a research indicated that Bevacizumab was used in the treatment of colon cancer. This medication specifically attaches to a protein known as human vascular endothelial growth factor (VEGF), which is located on the outside of blood and lymphatic arteries throughout the body. The Vascular Endothelial Growth Factor (VEGF) protein stimulates angiogenesis, the formation of blood vessels inside tumors, facilitating the delivery of nutrients and oxygen to the tumor. Bevacizumab

hampers tumor growth by impeding the formation of blood vessels that transport vital nutrients and oxygen to the tumor when it attaches to VEGF. (156).

Another research reported the efficacy of some interleukins, which are part of the cytokine protein family, on cancer cells (157).

Certain people may need a mix of therapies, rather than only relying on chemotherapy. For instance, the use of auranofin and ICG-001 in combination treatment was discovered to effectively inhibit the growth and spread of colon cancer (158).

The research highlighted the significant impact of nanoparticle-based medicines, namely calcium phosphate, in the treatment of drug-resistant colon cancer (159).

Moreover, the PI3K/Akt/mTOR signaling pathway has been discovered to have a significant impact on the colon cancer stem cell hypothesis. The dual inhibitor BEZ235 has been identified as a crucial factor in addressing treatment resistance and metastases in colon cancer (160).

Novel techniques, such as the use of docetaxel-loaded aptamer-guided albumin nanoparticles, have been created to specifically transport drugs for the treatment of colon cancer (161).

Cisplatin is a chemotherapeutic agent that is extensively used for the treatment of many types of malignancies, such as colon cancer. It is renowned for its capacity to cause DNA damage, which makes it a potent tool in the treatment of several forms of cancer. Cisplatin is often used as an initial chemotherapy treatment for advanced colon cancer. However, its therapeutic advantages are restricted due to the occurrence of adverse effects and the development of drug resistance (162,163). Despite its effectiveness, cisplatin may provide several options for treatment in colon cancer, as well as other forms of cancer. A prominent indication is the substantial extension of processes and advancements of medication resistance, which might restrict their long-term advantages. Colon cancer may develop resistance to cisplatin via many mechanisms, such as modifications in DNA maintenance pathways, abnormalities in gene expression, and manipulation of signaling pathways related to cell survival and growth (163, 164). Furthermore, the administration of cisplatin may be correlated with some adverse consequences. These negative consequences may need modifications or patient care interventions to ensure the medication may be properly and efficiently administered in various living situations that may arise. Recently, several metal therapy techniques, including gold, have been explored as potential anti-cancer medications, serving as an alternative to cisplatin (165). Palladium(II) humectants has antiviral and cytotoxic effects. In recent years, these compounds have been produced and used separately on a regular basis, mostly because of their anti-tumor properties and lower likelihood of causing feelings of isolation compared to cisplatin (166).

Multiple studies have consistently shown the potent anti-cancer properties of Pd (II) compounds across all forms of cancer, including stomach cancer. These compounds have been found to trigger

apoptotic cell death and may lead to DNA damage in cells via mechanisms involving H2AX, autophagy, and the generation of reactive oxygen species (ROS) (167).

A separate investigation examined the cytotoxic properties of palladium compounds in comparison to cisplatin. While palladium complexes are typically less potent, they have shown substantial cytotoxicity against some cell lines, notably L929, HeLa, and K562. He highlighted the potential features of palladium complexes as anti-cancer drugs and their impact on certain cancer cell lines (168).

A research was conducted to describe the synthesis of the first palladium metallic compounds as medicines for treating cancer. The study asserts that palladium complexes effectively impede the proliferation of highly malignant ovarian cancer tumors and function as potent anticancer agents (169).

This thesis research studied the anti-cancer effects of Pd (II) compounds [[Pd(bpma)(barb)]Cl.H2O] that produced by the Inorganic Chemistry Department on human colon cancer. The study's primary focus is in the enhanced cytotoxic and anti-cancer properties shown by the Pd (II) molecule when tested on the HCT-15 colon cancer cell line.

The MTT viability test findings showed that the administration of Pd (II) for 24, 48, and 72 hours in HCT-15 cells resulted in a reduction in cell viability compared to the control. This decrease was found at dosages of 3.125, 6.25, 12.5, 25, 50, and 100 μM, and the results were statistically significant ($p < 0.05$). Similarly for the HCT-116 and HT-29 cell lines, the administration of Pd (II) for 24, 48, and 72 hours resulted in a substantial increase in cell viability; compared to the control group at dosages of 3.125, 6.25, 12.5, 25, 50, and 100 μM. Decreases in cell viability were found ($p<0.05$).

Prior investigations have shown the notable lethal effects of the Pd(II) molecule, indicating its potential as an anticancer treatment across several cancer cell lines (170).

In a separate investigation, the biological properties of the NHC-Pd(II) complex, which is composed of N-heterocyclic carbene (NHC) ligands, were examined. The results demonstrated that all compounds had significant efficacy against various cancer cells, with an IC50 value below 1.5 μg. This work emphasizes the strong cytotoxic activity of palladium complexes, showcasing their potential as very efficient anticancer medicines against a wide range of cancer cell types (171).

In a different investigation conducted by Ulukaya et al., the IC50 value was determined using the MTT assay after 48 hours of treatment with the Pd(II) compound. The IC50 value was reported to be 2.1 μM in the A-549 lung cancer cell line and 1.8 μM in the H-1299 cell line. The concentration of 1.8 μM was also seen in PC-3, a cell line used for studying prostate cancer. Recent findings indicate that the Pd (II) bis(2-pyridylmethyl) molecule, characterized by its unique chemical structure

including an amine group, has cytotoxic properties. The IC50 values of this compound have been obtained in several cell lines (109,110).

The Pd(II) compound had an IC50 value of 86 μM in HeLa cells, while cisplatin, carboplatin, and oxaliplatin exhibited IC50 values of 94.3 μM, 104.3 μM, and 71.3 μM, respectively (172).

Based on the literature analysis and scientific results, it is believed that the variation in IC50 values is due to both the chemical composition of the Pd (II) molecule and the specific cancer cell lines used.

In this thesis research, we assessed the IC50 dosage of the Pd (II) compound, formed as [Pd(bpma)(barb)]Cl·H2O], in three distinct colon cancer cell lines, based on the IC50 data obtained using the MTT cell viability assay. The measured IC50 concentrations were determined to be 77,6 μM for HCT-15 cells, 22.5 μM for HCT-116 cells, and 51.9 μM for HT-29 cells.

The HCT-15 cell line had the lowest IC50 value among the data we obtained. Consequently, further investigations were only conducted using the HCT-15 cell line.

To ascertain the mechanism by which the Pd (II) compound induces cell death, a double labeling experiment was conducted utilizing apoptotic markers and seen under a fluorescence microscope.

Initially, the process of Annexin-V-FITC staining, which is a method used to identify apoptosis, was carried out and assessed using fluorescence microscopy. The double staining approach may be used to identify early apoptotic cells. Annexin-V (FITC) binding initiates during the nuclear condensation phase prior to cell membrane disruption (173, 174).

When cells start to experience a decline in the integrity of their cell membrane, Annexin-V (FITC) produces a beneficial outcome by attaching itself to intracellular phosphotidylserine. Therefore, it is used in conjunction with propidium iodide (PI) dye to distinguish cells with compromised membranes (175).

Following 24 and 48 hours of treatment of HCT-15 cells with a Pd (II) compound, the use of PI resulted in good outcomes in double stained cells. Consequently, after the administration of the Pd (II) compound, cells that were stained positive for Hoechst and cells that were labeled positive for PI were both seen in the same region. Furthermore, it was noted that only Hoechst positive stained cells were present in the same area. This suggests that cells undergo original necrosis or secondary necrosis as a result of membrane impairment. To enhance the differentiation, Hoechst dye was introduced to the cells and their nuclear morphology was then analyzed. The nuclei of the treated cells were shown to undergo a reduction in size and exhibit pyknosis, in contrast to the control group cells. Primary necrosis is distinguished by an enlargement in cell size without fragmented or pyknotic nuclei, while secondary necrosis is characterized by pyknotic or fragmented nuclei and represents the latter phase of apoptosis (109, 110). Based on the fluorescent microscope pictures, it was inferred that the cells in

question had membrane damage and subsequently perished via secondary necrosis, indicating that they were in the advanced stage of apoptosis.

The subsequent phase of the research included assessing the apoptotic impact of the Pd (II) compound on HCT-15 cells using flow cytometry and the Annexin-V (FITC) test.

The Annexin-V (FITC) test is a commonly used technique for identifying apoptosis in different biological situations. Annexin-V is a protein that attaches to phosphatidylserine (PS), a phospholipid that is exposed on the outer layer of the plasma membrane during apoptosis. This binding is reliant on the presence of calcium. Researchers may differentiate between early and late phases of apoptosis by using Annexin-V in conjunction with additional markers such propidium iodide (PI) or fluorescent dyes (175, 176).

The Annexin-V (FITC) test has been used in several investigations to validate the initiation of apoptosis and assess the processes of cell death. The Annexin-V test has shown to be efficacious in assessing the impact of different drugs on apoptosis in cancer research. An example of apoptosis activation in breast cancer cell lines was verified using Annexin-V (FITC) (177).

Furthermore, the impact of karanjin, a flavonoid compound and insecticide, on the halting of cell division and programmed cell death in several cancer cell types including A549, HepG2, and HL-60, was assessed using the Annexin-V-FITC/PI apoptosis method (178).

Moreover, the assessment of the harmful effects of essential oils on cervical cancer cells demonstrated that cell death occurs by apoptosis, as shown by the use of Annexin-V (179).

Our investigation found that the proportion of viable cells decreased and the percentage of apoptotic cells increased in both the control group after 12 and 24 hours of Pd (II) treatments. These findings also corroborate the pictures acquired by the Hoechst 33342, Annexin-V, Propidium iodide dual staining technique in the HCT-15 cell line.

The impact of the Pd (II) compound on HCT-15 cells' DNA damage was assessed using flow cytometry and the H2A.X Activation assay.

The conducted research have shown that Pd (II) compounds exhibit significant genotoxicity, leading to DNA damage and triggering apoptosis in various cancer cells, including those found in the lungs and breasts (110).

The activation of histone H2AX is essential in the process of apoptosis, since it becomes phosphorylated in response to several stimuli that cause DNA damage. Research has shown that the process of H2AX phosphorylation is linked to the initiation of apoptosis in many situations. For instance, it has been discovered that the p53-dependent apoptotic pathway inhibits DNA damage caused by γ-H2AX activation (180).

In addition, some mRNA species and the chemical curcumin blocked the ROS and H2AX pathways in lung and breast cancer cells, leading to death (181,182).

In many malignancies, there have been reported alterations in H2AX phosphorylation within the DNA damage response and apoptosis pathway.

Research has shown that the phosphorylation of H2AX is a significant marker for double-strand breaks and is involved in certain gene activations that occur during apoptosis. Imatinib is a novel medication used in the management of chronic myeloid leukemia. It works by inhibiting a particular tyrosine kinase kinase called PDGF-R, which is responsible for causing DNA damage. Imatinib has been shown to promote H2AX phosphorylation, which then triggers apoptosis by caspase-3 activation. After treating gastrointestinal stromal tumor cells with imatinib, researchers discovered that the H2AX pathway plays a role in triggering apoptosis (183,184).

Generally, phosphorylation of H2AX is a crucial occurrence in the process of apoptosis. Activation of H2AX is linked to the initiation of cell death by triggering a DNA damage response in different forms of cancer. Phosphorylation of H2AX is used as an indicator for DNA damage and plays a significant role in controlling apoptotic pathways in many biological situations.

This thesis investigation found that DNA damage occurred at rates of 76% and 67% in HCT-15 cells after 12 and 24 hours of treatment with the Pd (II) compound. As a result, H2AX activation increased. It was hypothesized that the reduction seen in the 24th hour may have triggered the cellular repair process in reaction to harm.

The impact of the Pd (II) compound on HCT-15 cells' DNA damage was assessed using an oxidative stress test and flow cytometry.

Reactive oxygen species (ROS) are powerful triggers of apoptosis and have a significant impact on apoptosis via the initiation of oxidative damage. Oxidative stress is recognized as a source of DNA damage, including single and double strand breaks, as well as DNA-protein cross-linking. These damages occur via several processes. Research has shown that reactive oxygen species (ROS) may stimulate intracellular signal transduction pathways that control processes such as inflammation, cell cycle, migration, and invasion in cancer cells. Furthermore, an excess of ROS may trigger apoptosis by activating genes that are reliant on NF-kB and causing DNA damage (185, 186).

The study shows that ionizing irradiation (IR) leads to the phosphorylation of signal transducer and activator of transcription 3 (STAT3) and the production of reactive oxygen species (ROS) in both wild-type and radiation-resistant MDA-MB-231 and MDA-MB-468 triple negative breast cancer (TNBC) cell lines. Niclosamide, a very effective inhibitor of STAT3, successfully overcomes radioresistance in triple-negative breast cancer (TNBC) cells by inhibiting both STAT3 and Bcl-2, while also inducing the production of reactive oxygen species (ROS). Niclosamide therapy, when

combined with radiation, resulted in a significant augmentation of reactive oxygen species (ROS) generation and the initiation of programmed cell death (apoptosis) in both regular and radiation-resistant triple-negative breast cancer (TNBC) cells under laboratory conditions. The results indicate that the activation of STAT3 and Bcl-2, as well as the decrease in ROS levels, play a role in the formation of radioresistance in TNBC. Additionally, niclosamide is shown to be an effective radiosensitizer in TNBC cells by inhibiting STAT3 and Bcl-2 and promoting the creation of ROS (187, 188).

In addition, the activation of AKT by ROS may trigger apoptosis in prostate cancer cells by means of von Hippel-Lindau protein (pVHL) (189). Reactive oxygen species (ROS) have a dual function in apoptosis. On one hand, they act as signaling molecules that participate in cellular activities including proliferation and migration. On the other hand, they also trigger apoptosis by causing oxidative damage and regulating certain cellular functions.

Flow cytometry was utilized in this investigation to quantify the level of reactive oxygen species (ROS) in order to investigate if the observed DNA damage in the HCT-15 cell was a result of oxidative stress. Significant increase in reactive oxygen species (ROS) was detected in the HCT-15 cell's Pd (II) complex, as compared to the control. The Pd(II) compound induced a rise in reactive oxygen species (ROS) inside these cells. The validity of this assay was further confirmed using MTT viability testing, in which NAC was used as a scavenger of reactive oxygen species (ROS). The MTT viability test findings indicated that the application of the ROS scavenger NAC reduced the cytotoxic impact of the Pd (II) compound on the HCT-15 cell. Thus, it is believed that ROS influences the apoptotic process initiated by the Pd (II) molecule. The excessive presence of ROS triggers apoptosis, whereas a minimal level of ROS functions as a signaling molecule, promoting cell growth and survival.

According to the findings of this thesis study, it can be inferred that the Pd (II) compound has a significant apoptotic impact on colon cancer cell lines (HCT-15, HCT-116, HT-29). Additionally, it has been observed to affect various molecular cells involved in cell survival and death processes at the molecular level. All studies (MTT Assay, Double Staining, Flow cytometry, qPCR) described in the materials, methods, and results sections of our research were conducted to investigate the anti-apoptotic and anti-cancer properties of the Pd (II) compound. The investigations revealed that the substance effectively eliminated cells by targeting the H2AX cell damage, oxidative stress, and apoptosis pathways.

In order to validate these findings, the expression levels of genes associated with these pathways were analyzed. In this thesis study we used Real Time PCR technology to analyze the gene expression of

82 target genes. These genes are known to be involved in crucial cellular pathways, including pro-survival, apoptosis, autophagy, cell damage, oxidative stress, and biological pathways related to cancer formation. Also this pathways that could be in a drug response in cancer cells after compound or drug treatment. In order to sure our CT results it is important point using more than one house keeping genes. Because we used normalization method the target genes CT values based on this house keeping genes. And we select best house keeping gene result.

We conducted two time periods to ascertain the effects of the substance we used on cell survival and apoptosis, specifically to identify whether it had pro-survival or pro-apoptotic properties. Upon application of the drug to the HCT-15 colon cancer cell, the cells were then examined under a microscope at hourly intervals. After 6 hours, the cells exhibited partial viability and did not undergo programmed cell death (apoptosis). Nevertheless, they experienced a loss of cellular condensation and a reduction in the size of their nuclei as part of the process of undergoing apoptosis. RNA isolation, cDNA synthesis, and qPCR analyses of the cells were conducted at the 6th hour based on their reaction to the chemical. Subsequently, RNA extraction, cDNA synthesis, and qPCR analysis were conducted on the cells, which were determined to be fully deceased after 24 hours, at the 6th hour, respectively. The genes that exhibited an increase in gene expression levels at both the 6th and 24th hours are as follows:

The following genes are included in the list: BAG3, BNIP1, CASP6, CASP7, BID, BNIP3L, BIRC2, BIM, BCL10, CASP3, BAG1, CASP4, LIG4, SOD1, PUMA, DR4, RAD52, and NOXA. The cellular and metabolic pathways associated with these genes are intricate and have a vital function in several biological functions. We gave information about the characteristics of some of the most changing genes according to the pathways they play a role in below.

BAG3:

Proteins that have the Bcl-2-associated athanogene (BAG) domain act as co-chaperones and interact with various partners, including heat shock proteins (Hsp), steroid hormone receptors, Bcl-2, Raf-1, and others. These interactions are involved in regulating protein folding and several cellular processes, such as proliferation and apoptosis (190, 191). One member of the BAG family is BAG3, which is also referred to as CAIR-1 or Bis. BAG3 interacts with Hsp70,1,2,4,6, a protein that may regulate apoptosis by affecting the release of cytochrome c, the assembly of apoptosome, and other processes involved in the process of cell death. Furthermore, the BAG3 polypeptide has the ability to interact with either phospholipase C-g (PLC-g) 4 or Bcl-2 protein. BAG3 may engage in the control of apoptosis due to its interaction with many apoptosis-modulating factors (192). Indeed the excessive

expression of this gene may reduce programmed cell death caused by Bax or Fas in the human epithelial cell line HeLa3 or by IL-3 deficiency in the murine hematopoietic cell line. Moreover, it has been shown that reducing the expression of BAG3 increases the sensitivity of human primary B chronic lymphocytic leukemia cells to chemotherapy-induced cell death (193). BAG3 is a protein that works as a co-chaperone and anti-apoptotic agent for HSP70. It interacts with the ATPase domain of HSP70 via its BAG domain located at the C-terminal end. BAG3 plays a crucial role in regulating cellular death. The HSP70/BAG3 complex controls the abundance of several specific client proteins by managing their degradation via the two primary routes of protein breakdown, including autophagy (194).

BNIP1:

BNip proteins, formerly known as Nip proteins, are a subset of the Bcl-2 family that includes homologues from several organisms. These proteins are classified under this family due to the presence of the Bcl-2 homology domain 3 and the carboxyl-terminal transmembrane domain. BNip proteins were first identified due to their interaction with the adenovirus E1B 19 kDa/Bcl-2 family protein. Subsequent to that, there is an ongoing investigation to determine if BNip proteins trigger apoptosis and/or necrosis. BNIP1 has significant expression levels in cardiac tissues, particularly in the heart, and is linked to pro-apoptotic characteristics. Cervical cancer tissues and cells exhibit a reversed scenario. It is downregulated and has a negative correlation with lymphatic metastasis. The BNIP protein has a dual function. Increased expression of BNIP1 inhibited the growth, movement, and infiltration and stimulated programmed cell death of cervical cancer cells. Suppression of BNIP1 with siRNAs enhanced the growth, movement, and infiltration abilities, while suppressing the programmed cell death of cervical cancer cells. In addition, our findings indicate that BNIP1 acts as an inhibitor of the mTOR pathway. Moreover, BNIP1 exerts its influence on the proliferation, apoptosis, migration, and invasion capabilities of cervical cancer cells via modulating the expression of mTOR. This discovery implies that BNIP1 may serve as a diagnostic indicator in the management of cervical cancer (195, 196).

CASP6:

CASP6 has a role in neurodegenerative disorders including Alzheimer's disease and is engaged in pathways associated with programmed cell death in brain cells. These interactions play a vital role in controlling processes such as autophagy, apoptosis, and cellular stress responses. In summary, the connections between these proteins create an intricate network that controls several cellular processes, such as cell growth, programmed cell death, removal of damaged mitochondria, and maintenance of

protein integrity. Comprehending the intricate interplay of these proteins is essential for deciphering their functions in both well-being and illness. The primary role of glandular cells that grow inside healthy ovarium tissue can generate mucus, and it remains uncertain if they are malignant. Prostate cancer cells exhibited significantly elevated expression of BNIP3 and CASP6 in comparison to these cells (197).

CASP7:

Apoptosis is a kind of planned cell death that is controlled by the Bcl-2 family and caspase proteins. The process of cell death that occurs after the release of cytochrome c is explained by the caspase cascade. Nevertheless, the precise functions of caspase-9, caspase-3, and caspase-7 in this particular pathway remain incompletely characterized (198). The CASP7 gene, responsible for encoding caspase 7, has a significant function in the apoptosis process. Caspase 7 plays a role in the terminal phases of apoptosis, a regulated cell death mechanism that is crucial for preserving tissue and cellular balance and removing impaired or unnecessary cells (199,200). Research has shown that caspase 7 plays a significant role in several pathways, including the formation and progression of cancer. For instance, studies have shown that CASP7 is implicated in the susceptibility to gastric adenocarcinoma and plays a crucial role in the development of cancer (201). The activation of caspase 7 plays a crucial role in the process of apoptosis, resulting in the fragmentation of particular cellular proteins and eventually leading to cell death (199). A further research has shown that microRNA-224 specifically targets caspase-7 in cases of lung cancer, emphasizing the significance of CASP7 in the development of lung cancer (202). CASP7 has been recognized as one of the three downstream effectors in the apoptosis pathway in human cells. This emphasizes its involvement in the execution phase of cellular apoptosis (200). CASP7 has been linked to resistance to apoptosis in chronic lymphocytic leukemia. In this case, CASP7 and other pro-apoptotic genes are progressively upregulated as the illness progresses, leading to resistance to cell death. CASP7 expression has been linked to the susceptibility of developing esophageal adenocarcinoma. Furthermore, certain genetic variants in CASP7 are correlated with an elevated risk of the illness. To summarize, CASP7 functions as an executioner caspase in apoptosis and has significant impacts on many cellular processes, disease conditions, and treatment outcomes (203, 204).

BID:

The BID gene, belonging to the Bcl-2 protein family, has a significant function in apoptosis, which is the programmed cell death process. Research has shown that BID may be split by caspases, resulting in its activation and movement to mitochondria, which then causes the release of cytochrome

c. This release of cytochrome c is a crucial step in the process of apoptosis (205, 206). It serves as a connection between death receptors located on the cell surface and mitochondria, which enables the release of cytochrome c and other substances that induce apoptosis from the mitochondria (208). According to other research has shown that BID is necessary for apoptosis triggered by DNA-damaging substances and in response to genotoxic stress. Furthermore, there is intercommunication between many apoptotic mechanisms, including BID, ER stress, and TRAIL-induced apoptosis. In addition, BID is involved in several cellular processes other than apoptosis, such as controlling cell growth and division, maintaining cell cycle checkpoints, and influencing immunological responses (209). BID is further linked to mitochondrial activity and metabolism, and it aids in the preservation of cellular homeostasis (210). The involvement of BID in apoptosis might differ based on its function inside the cell and the signaling pathways. While some research have emphasized the significance of BID in particular forms of apoptosis, such as apoptosis caused by death receptors, other studies have shown that BID may not be necessary for apoptosis generated by DNA damage in certain cell types (211, 212). The BID gene has a wide range of functions in programmed cell death and serves as a central controller of cell death pathways and the functioning of mitochondria. The investigations have shown the involvement of this substance in several cellular and metabolic processes, its significance in maintaining cellular homeostasis, and its role in the cell's response to various stress process.

BNIP3L:

The BNIP3L gene, belonging to the Bcl-2 protein family, has a significant function in apoptosis, which is the programmed cell death process. BNIP3L facilitates apoptosis in conjunction with mitochondrial activities. BNIP3L has been shown to trigger apoptosis by controlling the permeability of the mitochondrial membrane, a critical step in initiating the apoptotic cascade (213,214). Moreover, BNIP3L has shown its involvement in facilitating programmed cell death in several biological scenarios, including traumatic brain damage and podocyte apoptosis. Furthermore, BNIP3L has been linked to the inhibition of tumor growth, since it has the ability to decrease the formation of tumors and facilitate programmed cell death regulated by the p53 protein under low oxygen circumstances (215). Moreover, BNIP3L is involved in the development of some neuropsychiatric disorders such as schizophrenia (216). BNIP3L expression is increased in response to pressure overload-induced heart failure, and it plays a critical role in promoting death of cardiomyocytes (217). BNIP3L plays a crucial role in regulating apoptosis by influencing mitochondrial dynamics, autophagy, and apoptotic signaling pathways. BNIP3L, a gene with several activities in numerous cellular pathways, has been shown to play a crucial role in maintaining cellular

homeostasis and reacting to diverse stress conditions. Furthermore, it has been implicated in the pathogenesis of various disorders.

BIRC2:

The BIRC2 gene, commonly referred to as cIAP1 (cellular inhibitor of apoptosis protein 1), plays a crucial role in controlling programmed cell death (apoptosis) and the survival of cells.

BIRC2 functions as an apoptosis inhibitor. Furthermore, it has a crucial function in modulating and controlling the pathways that lead to programmed cell death, often known as apoptotic pathways (218). Research has shown that BIRC2 is necessary for the activation of the innate immune system via cell receptors and for the production of a cellular response that leads to programmed cell death in response to different stimuli (220). Research has shown that BIRC2 functions by impeding caspase-mediated apoptosis and necroptosis, hence enhancing cell survival (221). Furthermore, it has been linked to a multitude of illnesses and ailments, including cancer. The amplification or overexpression of BIRC2 may result in the suppression of caspase-mediated apoptosis, which enhances cell survival and makes cells more resistant to signals that induce cell death. BIRC2 has been identified as a promising therapeutic target in cancer treatment due to its downregulation being associated with heightened susceptibility to chemotherapy and radiation therapy in certain types of cancer (222). Furthermore, research has shown that it has a role in the advancement of rheumatoid arthritis by controlling TRADD. Additionally, it has proven efficacy in predicting and promoting the development of inflammatory and autoimmune disorders (223).

LIG4:

The LIG4 gene encodes an enzyme that is crucial for the non-homologous end joining (NHEJ) repair pathway. And is necessary for Repairing double-stranded DNA breaks (DSBs). LIG4 has also been linked to inadequate caspase activation in cancer cells (224). Research has shown that a absence of LIG4 results in the initiation of programmed cell death in brain cells, lymphocytes, and cancer cells. The absence of LIG4 in mice leads to the death of embryos, extensive neuronal cell death, and abnormalities in the development of lymphocytes (225). A severe diabetic phenotype may occur when there is a lack of p53-dependent apoptosis in individuals with LIG4 loss and mutations in p53 (226). Furthermore, the absence of Chk2 protein or mutations in p53 that hinder the process of programmed cell death explain the occurrence of apoptosis in individuals with LIG4 deficiency (227). In addition, the loss of LIG4 has been linked to heightened resistance to ionizing radiation when Ku70 is not present. This finding elucidates the interconnectedness of cellular pathways involved in DNA repair processes and apoptosis.

SOD1:

Zhang et al. (2019) found that the SOD1 gene, which encodes for a superoxide dismutase, influences cellular processes by interacting with several proteins and transcription factors, and participating in intricate pathways (229). A different research demonstrated that the SOD1 gene controls the activation of genes responsible for oxidative resistance and DNA damage repair via attaching to promoters (230). In addition, SOD1 modulates the expression of crucial genes implicated in neurodegenerative disorders like ALS via modulating gene expression in response to intracellular hydrogen peroxide (231). The interplay between DCR2-PRDX1 facilitates the process of senescence in renal tubular epithelial cells (232).

These interactions together influence the control of oxidative stress, the expression of genes, the pathways leading to cell death, and the course of diseases. To comprehend the intricate network of interactions among these genes and proteins is essential in order to decipher their functions in maintaining cellular balance and causing disease development.

The SOD1 gene, responsible for encoding the superoxide dismutase 1 enzyme, has a vital function in controlling apoptosis. Research has shown that genetic abnormalities in the SOD1 gene are linked to neurodegenerative disorders including amyotrophic lateral sclerosis (ALS) and may initiate the process of nerve cell degeneration via many mechanisms, including apoptosis (233). Mutations in the SOD1 gene are linked to mitochondrial malfunction and the initiation of apoptosis, which have a role in the development of familial ALS (234). In addition, research have shown that SOD1 is involved in the process of oxidative stress-induced apoptosis. These studies have revealed that when SOD1 activity is disrupted, it leads to inhibition of cell development and an increase in lipid buildup in cancer cells (235). Moreover, it has been shown that SOD1 interacts with other molecules in order to regulate apoptosis. For instance, SOD1 has the ability to attach to mRNA and cause instability in the mRNA molecule, which disrupts cellular balance and intensifies cellular harm in conditions like ALS (236). Moreover, it has been shown that SOD1 interacts with amyloid beta and hinders its enzymatic function, suggesting a connection between SOD1, oxidative stress, and neurodegenerative disorders including ALS and Alzheimer's (237). Furthermore, SOD1 has a function in controlling apoptosis that goes beyond neurological disorders. Research indicates that SOD1 may influence the process of determining cell fate and facilitate cell death in myeloid leukemia cells. Additionally, it has a significant part in the mechanism of apoptosis via many cellular pathways (238). Furthermore, SOD1 has been linked to apoptosis caused by oxidative stress in several kinds of cells, emphasizing its function as an antioxidant enzyme that may impact cell survival and death mechanisms (239).

PUMA:

The PUMA gene, responsible for encoding the protein p53 up-regulated modulator of apoptosis, plays a crucial role in regulating apoptosis via many pathways. PUMA functions as a pro-apoptotic gene, facilitating cell death by triggering cellular reactions to various stimuli such as DNA damage, oxidative stress, and chemotherapeutic drugs (240). Research has shown that PUMA plays a crucial role in regulating both p53-dependent and p53-independent pathways that lead to cell death. This emphasizes the significance of PUMA in controlling cell death processes (241). A research reported that PUMA participated in apoptosis triggered by green tea polyphenols and hydrogen peroxide in colorectal cancer cells, hence contributing to cell death caused by cellular stress (242). Moreover, the induction of programmed cell death by PUMA in glioblastoma cells has been linked to the anticancer properties of Hsp90 inhibitors. This implies that PUMA might serve as a promising target for cancer therapy (243). Furthermore, PUMA has been linked to ischemia-reperfusion damage in the small intestine and cerebral ischemia, indicating its involvement in the apoptotic pathways activated by both circumstances (244). PUMA has been discovered as a gene that regulates endoplasmic reticulum stress-induced apoptosis in portal hypertensive gastropathy. This indicates that this gene has varied functions in different kinds of cells and under different situations of stress (245).

DR4:

The DR4 gene, sometimes referred to as TNFRSF10A, has a vital function in controlling apoptosis by participating in the transmission of death signals. DR4 has been recognized as a crucial mediator of programmed cell death in several forms of cancer and pathological states. Research has shown that DR4 is crucial for the transmission of death signals in human B chronic lymphocytic leukemia and also has an impact on the development and prognosis of acute myeloid leukemia (246). DR4 has been identified as a crucial receptor in facilitating TRAIL-induced apoptosis, indicating its significance in cellular death mechanisms (247). Research has shown that the regulation of DR4 is influenced by transcription factors including p53 and AP-1. This indicates that DR4 plays a role in intricate regulatory processes that govern gene expression and function in apoptosis (248). The presence of DR4 has been linked to the resistance of gliomas and ovarian cancer to TRAIL, indicating its involvement in regulating how cells respond to signals that induce programmed cell death. In addition, alterations in the epigenetic regulation of the DR4 gene have been linked to resistance to TRAIL in children B cell precursor acute lymphoblastic leukemia. This highlights the significance of epigenetic mechanisms in controlling the expression of DR4 and its role in apoptotic responses (249). DR4 has shown the ability to enhance the susceptibility of cancer cells to TRAIL-induced apoptosis and augment the efficacy of anticancer treatments in different cancer types. Additionally, DR4 has

been shown to contribute to the susceptibility of prostate cancer and the efficacy of melanoma therapy, thereby emphasizing its unique functions in various cancer types. The control of DR4 expression and its influence on cellular viability and programmed cell death pathways distinguish it as a therapeutic intervention strategy targeting the induction of apoptosis in cancer cells (250).

RAD52:

The RAD52 gene plays a crucial role in homologous recombination (HR), DNA repair processes, and DNA recombination in many species, including humans. It is a vital component necessary for preserving the integrity and stability of the genome (251). Research indicates that RAD52 has a function in safeguarding Rad51 filaments from being broken down by DNA translocases and serves a crucial role in preserving the stability of essential components involved in the DNA repair process (252). In addition, RAD52 plays a role in the repair of DNA double-strand breaks by assisting in the exchange of DNA strands and the synthesis of new DNA strands during homologous recombination (253). In addition, RAD52 has been linked in facilitating DNA synthesis after replication stress, a process that is essential for tumor growth and cell survival. The role of RAD52 in the restoration of collapsed DNA replication forks has been seen in some cancer types, suggesting its involvement in the preservation of chromosomal integrity and genomic stability (254). RAD52 has also been linked in facilitating DNA synthesis after replication stress, a process that is vital for tumor growth and cell viability. The RAD52 gene plays a crucial role in safeguarding the genome by facilitating the repair of sister chromatids (255). Remarkably, RAD52 has exceptional resistance to changes in temperature, which is potentially beneficial because of its involvement in DNA repair mechanisms under elevated temperatures or other challenging circumstances. This characteristic is believed to have a function in DNA repair and recombination processes. Consequently, it is shown that it participates in several cellular processes such as homologous recombination (HR) and DNA repair, and serves to safeguard cells against programmed cell death triggered by DNA damage.

NOXA:

The NOXA gene, belonging to the BH3-only Bcl-2 protein family, plays a crucial role in controlling programmed cell death (apoptosis) in different biological situations. NOXA triggers apoptosis by interacting with anti-apoptotic members of the Bcl-2 family. Initially, it facilitates the initiation of caspase-9 activation, subsequently leading to cellular demise (256). Research has shown that NOXA-induced cell death may be activated by several external factors, including viral infections, oxidative stress, and chemotherapeutic drugs (257). The recognition of NOXA as a significant agent in triggering cell death in response to various stressors highlights its function in removing impaired or

undesired cells. Studies have shown that the elimination of NOXA enhances the ability of the host to defend against influenza virus infection, suggesting that NOXA plays a crucial role in regulating viral infections. Furthermore, the absence of NOXA has been linked to the regulation of autophagic flux and the ability to fight influenza virus infection, highlighting its significance in antiviral defenses (258). NOXA has been linked to the development of resistance to chemotherapy in chronic lymphocytic leukemia, indicating its involvement in the regulation of programmed cell death in cancer cells (259). NOXA is transcriptionally controlled by ATF3, ATF4, and p53 in response to distinct cellular stressors (260). The increase of NOXA is essential for initiating apoptosis in fibroblasts, decreasing epidural fibrosis, and overcoming chemoresistance in cancer cells (261). Furthermore, NOXA is involved in the regulation of cell growth, programmed cell death, and the process of self-degradation in human adenoid cystic carcinoma (262). Therefore, NOXA plays a crucial role in controlling apoptosis, by reacting to various stimuli and stressors to trigger programmed cell death.

BMI1:

Recently researchs have shown that suppressing the BMI1 gene may initiate programmed cell death, decrease the ability of cells to invade and migrate, and enhance the responsiveness of some cancer types to chemotherapy. BMI1 enhances cellular proliferation and viability by modulating many intracellular pathways and influencing susceptibility to programmed cell death. It has the ability to prevent cell death by regulating the process of programmed cell death that is reliant on the p53 protein or by inhibiting the activity of proteins that promote cell death, such as BIM. This contributes to the proliferation and survival of cancer cells (263). Furthermore, it has been shown that the regulation of apoptosis-related genes, such as BMI1, Bcl-2, Bax, and caspase 3, leads to the induction of apoptosis. Research has shown that BMI1 activates NF-κB, which in turn prevents apoptosis triggered by several stimuli in glioblastoma cells (264). BMI1 has been shown to control the antioxidant defense in neurons by inhibiting the activation of the p53 gene, therefore guaranteeing the survival of cells. The protein has the ability to control the growth, programmed cell death, aging, and movement of cells, emphasizing its cancer-causing properties. BMI1 has also been linked to male infertility. In this case, a lack of the gene resulted in heightened apoptosis and reduced cell proliferation in cancer cells (265).

PRDX1

In this thesis, we investigated of the gene expressions of PRDX1 and SOD1 genes, as well as their interaction with DCR2-PRDX, using the Real Time PCR method.

Our literature research has shown that a significant impact in a wide range of cellular and metabolic processes. PRDX1 known as peroxiredoxin, which influences the regulation of genes and pathways related to cell death. It does this by interacting with several proteins and transcription factors, including p53, c-Myc, NF-κB, and AR. PRDX1 functions as a nuclear transcription factor that specifically attaches to promoters and controls the expression of genes involved in oxidative resistance and repair (266). PRDX1 interacts with the LINC00460 gene, which is a Long Intergenic Non-Protein Coding RNA 460. This interaction helps the molecule enter the cell nucleus and initiates the transcription of EMT-related genes (267). Furthermore, PRDX1 engages in interactions with the APE1 gene, impeding its function and influencing the production of interleukin-8. These effects have implications for cancer invasion and metastasis (268).

GSTP1 Gene:

The GSTP1 gene, responsible for encoding the enzyme glutathione S-transferase, has a multifaceted function in cancer biology, including its involvement in apoptosis. GSTP1 has been shown to participate in several cellular functions including detoxification, antioxidative defense, and the control of cell proliferation and death pathways (269). Research has shown that GSTP1 functions as a direct suppressor of the C-Jun N-terminal kinase and is released from JNK in response to oxidative stress. This release then triggers the activation of genes related to programmed cell death (apoptosis) and cellular defense (cytoprotection). The c-Jun N-terminal kinase (JNK) pathway is a prominent component of the mitogen-activated protein kinase (MAPK) signaling system. Moreover, GSTP1 has been linked to the control of cell growth and programmed cell death, suggesting that it might be a promising target for cancer treatments. GSTP1 has been linked to medication resistance in several types of cancer, such as breast, colon, lung, and prostate malignancies. Its increased expression promotes tumor advancement and hinders response to therapy. The presence of GSTP1 in lung cancer cells has been shown to shield tumor cells from apoptosis, hence emphasizing its significance in cellular survival processes (270). Furthermore, research has shown that the reduction of GSTP1 may trigger programmed cell death in human lung fibroblasts. This indicates that GSTP1 may have a significant impact on cellular survival and the regulation of cell death. It has been linked to oxidative stress responses and the control of MAP kinase signaling in lung cells, suggesting its role in apoptotic pathways (271).

APAF1 Gene:

The APAF1 gene, responsible for encoding apoptotic protease activating factor 1, plays a crucial role in controlling apoptosis and several other cellular processes. APAF1 has been extensively studied for

its role in apoptosis and its impact on several biological systems. Studies have shown the significance of APAF1 in several molecular cancer investigations.

APAF1 plays a crucial role in initiating the caspase cascade in the programmed cell death pathway, highlighting its significance in apoptosis. APAF1 was discovered as a direct target of miR-221. Overexpression of APAF1 was shown to suppress ovarian cancer cell growth and induce apoptosis (272). It has been linked to the pathways of mitochondrial apoptosis (intrinsic pathway) and brain development, indicating its significance in the appropriate development and survival of cells. APAF1, a gene, is linked to the control of neuronal cell death. Specifically, it is an important transcriptional target for p53 in the occurrence of apoptosis caused by neuronal injury. APAF1 has been shown to be involved in several illnesses and disorders. APAF1 variants have been associated with significant depression, suggesting that APAF1 may have a role in maintaining apoptosome function and impacting depressive disorders (273).

Moreover, research has shown that APAF1 has a function in promoting increased resistance to apoptosis in monocytes derived from individuals with rheumatoid arthritis. This suggests that APAF1 may have a significant impact on the development of inflammatory and autoimmune illnesses (274). The APAF1 gene governs the processes of apoptosis, cell survival, and the development of diseases. Gaining a comprehensive understanding of the actions and mechanisms of APAF1 is crucial in order to assess its influence on cellular processes and to devise customized therapeutic approaches for a range of diseases.

Upon thorough examination of the data from this thesis study, it is evident that the Pd(II) molecule has been extensively shown to have an anti-cancer impact, with detailed insights into many metabolic pathways.

We are now advancing our research by conducting studies to validate these findings. These findings represent the first investigation of colon cancer in existing literature. They will serve as a comprehensive reference for future research on the development of anti-cancer drugs and hold promise for potential therapeutic applications in cancer therapy.

BIBLIOGRAPHY

1. Safarinejad, M. R., Shafiei, N., & Safarinejad, S. (2011). Relationship of insulin-like growth factor (IGF) binding protein-3 (IGFBP-3) gene polymorphism with the susceptibility to development of prostate cancer and influence on serum levels of IGF-I, and IGFBP-3. *Growth Hormone & IGF Research*, *21*(3), 146-154.

2. Choi, W., Porten, S., Kim, S., Willis, D., Plimack, E. R., Hoffman-Censits, J., ... & McConkey, D. J. (2014). Identification of distinct basal and luminal subtypes of muscle-invasive bladder cancer with different sensitivities to frontline chemotherapy. *Cancer cell*, *25*(2), 152-165.

3. Meyerson, M., Gabriel, S., & Getz, G. (2010). Advances in understanding cancer genomes through second-generation sequencing. *Nature Reviews Genetics*, *11*(10), 685-696.

4. Kuper, H., Adami, H. O., & Trichopoulos, D. (2001). Infections as a major preventable cause of human cancer. *Journal of internal medicine*, *249*(S741), 61-74.

5. Watson, I. R., Wu, C. J., Zou, L., Gershenwald, J. E., Chin, L., & Melanoma Analysis Working Group and The Cancer Genome Analysis Research Network. (2015). Genomic classification of cutaneous melanoma. *Cancer Research*, *75*(15_Supplement), 2972-2972.

6. Neoptolemos, J. P., Palmer, D. H., Ghaneh, P., Psarelli, E. E., Valle, J. W., Halloran, C. M., ... & Büchler, M. W. (2017). Comparison of adjuvant gemcitabine and capecitabine with gemcitabine monotherapy in patients with resected pancreatic cancer (ESPAC-4): a multicentre, open-label, randomised, phase 3 trial. *The Lancet*, *389*(10073), 1011-1024.

7. Wiesweg, M., Ting, S., Reis, H., Worm, K., Kasper, S., Tewes, M., ... & Schuler, M. (2013). Feasibility of preemptive biomarker profiling for personalised early clinical drug development at a Comprehensive Cancer Center. *European Journal of Cancer*, *49*(15), 3076-3082.

8. Hanahan, D., & Weinberg, R. A. (2011). Hallmarks of cancer: the next generation. *cell*, *144*(5), 646-674.

9. Weinberg, R. A., & Weinberg, R. A. (2006). *The biology of cancer*. WW Norton & Company.

10. Hanahan, D., & Weinberg, R. A. (2000). The hallmarks of cancer. *cell*, *100*(1), 57-70.

11. Das, C. K., Banerjee, I., & Mandal, M. (2020, November). Pro-survival autophagy: An emerging candidate of tumor progression through maintaining hallmarks of cancer. In *Seminars in Cancer Biology* (Vol. 66, pp. 59-74). Academic Press.

12. Ravi, S., Alencar Jr, A. M., Arakelyan, J., Xu, W., Stauber, R., Wang, C. C. I., ... & Wang, C. C. (2022). An update to hallmarks of cancer. *Cureus*, *14*(5).

13. Hanahan, D., & Weinberg, R. A. (2000). The hallmarks of cancer. *cell*, *100*(1), 57-70.

14. Bertram, J. S. (2000). The molecular biology of cancer. *Molecular aspects of medicine*, *21*(6), 167-223.

15. Ichim, G., Lopez, J., Ahmed, S. U., Muthalagu, N., Giampazolias, E., Delgado, M. E., ... & Tait, S. W. (2015). Limited mitochondrial permeabilization causes DNA damage and genomic instability in the absence of cell death. *Molecular cell*, *57*(5), 860-872.

16. Colotta, F., Allavena, P., Sica, A., Garlanda, C., & Mantovani, A. (2009). Cancer-related inflammation, the seventh hallmark of cancer: links to genetic instability. *Carcinogenesis*, *30*(7), 1073-1081.

17. Chiarugi, A., Dölle, C., Felici, R., & Ziegler, M. (2012). The NAD metabolome—a key determinant of cancer cell biology. *Nature Reviews Cancer*, *12*(11), 741-752.

18. Ward, P. S., & Thompson, C. B. (2012). Metabolic reprogramming: a cancer hallmark even warburg did not anticipate. *Cancer cell*, *21*(3), 297-308.

19. Günesdogan, U., Jäckle, H., & Herzig, A. (2014). Histone supply regulates S phase timing and cell cycle progression. *Elife*, *3*, e02443.

20. Vermeulen, K., Van Bockstaele, D. R., & Berneman, Z. N. (2003). The cell cycle: a review of regulation, deregulation and therapeutic targets in cancer. *Cell proliferation*, *36*(3), 131-149.

21. Hyka-Nouspikel, N., Desmarais, J., Gokhale, P. J., Jones, M., Meuth, M., Andrews, P. W., & Nouspikel, T. (2012). Deficient DNA damage response and cell cycle checkpoints lead to accumulation of point mutations in human embryonic stem cells. *Stem Cells*, *30*(9), 1901-1910.

22. Tian, R. Q., Wang, X. H., Hou, L. J., Jia, W. H., Yang, Q., Li, Y. X., ... & Tang, H. (2011). MicroRNA-372 is down-regulated and targets cyclin-dependent kinase 2 (CDK2) and cyclin A1 in human cervical cancer, which may contribute to tumorigenesis. *Journal of Biological Chemistry*, *286*(29), 25556-25563.

23. Strowig, T., Henao-Mejia, J., Elinav, E. & Flavell, R. Inflammasomes in health and disease. *Nature* **481**, 278–286 (2012)

24. Clos-Garcia, M., Garcia, K., Alonso, C., Iruarrizaga-Lejarreta, M., D'Amato, M., Crespo, A., ... & Falcón-Pérez, J. M. (2020). Integrative analysis of fecal metagenomics and metabolomics in colorectal cancer. *Cancers*, *12*(5), 1142.

25. Nie, H., Ju, H., Fan, J., Shi, X., Cheng, Y., Cang, X., ... & Yi, W. (2020). O-GlcNAcylation of PGK1 coordinates glycolysis and TCA cycle to promote tumor growth. *Nature communications*, *11*(1), 36.

26. Cairns, R. A., Harris, I. S., & Mak, T. W. (2011). Regulation of cancer cell metabolism. *Nature Reviews Cancer*, *11*(2), 85-95.

27. Yuan, Y., Li, H., Pu, W., Chen, L., Guo, D., Jiang, H., ... & Zhao, S. M. (2022). Cancer metabolism and tumor microenvironment: fostering each other?. *Science China Life Sciences*, 1-44.

28. Zhang, Y., Wang, Y., Zhao, G., Orsulic, S., & Matei, D. (2023). Metabolic dependencies and targets in ovarian cancer. *Pharmacology & Therapeutics*, 108413.

29. Hosios, A. M., Hecht, V. C., Danai, L. V., Johnson, M. O., Rathmell, J. C., Steinhauser, M. L., ... & Vander Heiden, M. G. (2016). Amino acids rather than glucose account for the majority of cell mass in proliferating mammalian cells. *Developmental cell*, *36*(5), 540-549.

30. Navarro, C., Ortega, Á., Santeliz, R., Garrido, B., Chacín, M., Galban, N., ... & Bermúdez, V. (2022). Metabolic reprogramming in cancer cells: emerging molecular mechanisms and novel therapeutic approaches. *Pharmaceutics*, *14*(6), 1303.

31. Weinberg, F., Hamanaka, R., Wheaton, W. W., Weinberg, S., Joseph, J., Lopez, M., ... & Chandel, N. S. (2010). Mitochondrial metabolism and ROS generation are essential for Kras-mediated tumorigenicity. *Proceedings of the National Academy of Sciences*, *107*(19), 8788-8793.

32. Pavlova, N. N., & Thompson, C. B. (2016). The emerging hallmarks of cancer metabolism. *Cell metabolism*, *23*(1), 27-47.

33. Romero-Garcia, S., Lopez-Gonzalez, J. S., B´ez-Viveros, J. L., Aguilar-Cazares, D., & Prado-Garcia, H. (2011). Tumor cell metabolism: an integral view. *Cancer biology & therapy*, *12*(11), 939-948.

34. Nong, S., Han, X., Xiang, Y., Qian, Y., Wei, Y., Zhang, T., ... & Ma, X. (2023). Metabolic reprogramming in cancer: Mechanisms and therapeutics. *MedComm*, *4*(2), e218.

35. Xia L, Oyang L, Lin J, et al. The cancer metabolic reprogramming and immune response. *Mol Cancer*. 2021; **20**(1): 28

36. Lue HW, Podolak J, Kolahi K, et al. Metabolic reprogramming ensures cancer cell survival despite oncogenic signaling blockade. *Genes Dev*. 2017; **31**(20): 2067-2084.

37. Allen, E., Miéville, P., Warren, C. M., Saghafinia, S., Li, L., Peng, M. W., & Hanahan, D. (2016). Metabolic symbiosis enables adaptive resistance to anti-angiogenic therapy that is dependent on mTOR signaling. *Cell Reports*, *15*(6), 1144-1160.

38. Center, M. M., Jemal, A., Smith, R. A., & Ward, E. (2009). Worldwide variations in colorectal cancer. *CA: a cancer journal for clinicians*, *59*(6), 366-378.

39. Granados-Romero, J. J., Valderrama-Treviño, A. I., Contreras-Flores, E. H., Barrera-Mera, B., Herrera Enríquez, M., Uriarte-Ruíz, K., ... & Arauz-Peña, G. (2017). Colorectal cancer: a review. *Int J Res Med Sci*, *5*(11), 4667.

40. Kim, N. K., Kim, Y. W., Han, Y. D., Cho, M. S., Hur, H., Min, B. S., & Lee, K. Y. (2016). Complete mesocolic excision and central vascular ligation for colon cancer: principle, anatomy, surgical technique, and outcomes. *Surgical Oncology*, *25*(3), 252-262.

41. He, X. K., Wu, W., Ding, Y. E., Li, Y., Sun, L. M., & Si, J. (2018). Different anatomical subsites of colon cancer and mortality: a population-based study. *Gastroenterology Research and Practice*, *2018*.

42. Gurcan, M.N.; Boucheron, L.E.; Can, A.; Madabhushi, A.; Rajpoot, N.M.; Yener, B. Histopathological image analysis: A review. *IEEE Rev. Biomed. Eng.* **2009**, *2*, 147–171.

43. Rathore, S.; Hussain, M.; Ali, A.; Khan, A. A recent survey on colon cancer detection techniques. *IEEE/ACM Trans. Comput. Biol. Bioinform.* **2013**, *10*, 545–563.

44. Sreekumar, A., Nyati, M. K., Varambally, S., Barrette, T. R., Ghosh, D., Lawrence, T. S., & Chinnaiyan, A. M. (2001). Profiling of cancer cells using protein microarrays: discovery of novel radiation-regulated proteins. *Cancer research*, *61*(20), 7585-7593.

45. Jie, D., Zhongmin, Z., Guoqing, L., Sheng, L., Yi, Z., Jing, W., & Liang, Z. (2013). Positive expression of LSD1 and negative expression of E-cadherin correlate with metastasis and poor prognosis of colon cancer. *Digestive diseases and sciences*, *58*, 1581-1589.

46. Inadomi, J. M. (2017). Screening for colorectal neoplasia. *New England Journal of Medicine*, *376*(2), 149-156.

47. Eadie, L. H., Reid, C. B., Fitzgerald, A. J., & Wallace, V. P. (2013). Optimizing multi-dimensional terahertz imaging analysis for colon cancer diagnosis. *Expert Systems with Applications*, *40*(6), 2043-2050.

48. Luoma, A. M., Suo, S., Williams, H. L., Sharova, T., Sullivan, K., Manos, M., ... & Wucherpfennig, K. W. (2020). Molecular pathways of colon inflammation induced by cancer immunotherapy. *Cell*, *182*(3), 655-671.

49. Shirai, F., Mizutani, A., Yashiroda, Y., Tsumura, T., Kano, Y., Muramatsu, Y., ... & Koyama, H. (2020). Design and discovery of an orally efficacious spiroindolinone-based tankyrase inhibitor for the treatment of colon cancer. *Journal of Medicinal Chemistry*, *63*(8), 4183-4204.

50. World Health Organization; Global Cancer Observatory (Globocan). Available online: **https://gco.iarc.fr/** (accessed on 1 March 2022).

51. Wong, M.C.S.; Huang, J.; Huang, J.L.W.; Pang, T.W.Y.; Choi, P.; Wang, J.; Chiang, J.I.; Jiang, J.Y. Global Prevalence of Colorectal Neoplasia: A Systematic Review and Meta-Analysis. *Clin. Gastroenterol. Hepatol.* **2020**, *18*, 553–561.e510

52. Arnold, M.; Sierra, M.S.; Laversanne, M.; Soerjomataram, I.; Jemal, A.; Bray, F. Global patterns and trends in colorectal cancer incidence and mortality. *Gut* **2017**, *66*, 683–691.

53. Nogueira, L.M.; Yabroff, K.R.; Bernstein, A. Climate change and cancer. *CA Cancer J. Clin.* **2020**, *70*, 239–244

54. Shen, L., Toyota, M., Kondo, Y., Lin, E., Zhang, L., Guo, Y., ... & Issa, J. P. J. (2007). Integrated genetic and epigenetic analysis identifies three different subclasses of colon cancer. *Proceedings of the National Academy of Sciences*, *104*(47), 18654-18659.

55. Xue, W., Qiu, K., Dong, B., Guo, D., Fu, J., Zhu, C., & Niu, Z. (2023). Disulfidptosis-associated long non-coding RNA signature predicts the prognosis, tumor microenvironment, and immunotherapy and chemotherapy options in colon adenocarcinoma. *Cancer Cell International*, *23*(1), 218.

56. Kanth, P., & Inadomi, J. M. (2021). Screening and prevention of colorectal cancer. *Bmj*, *374*.

57. Sun, R., Yang, Y., Lü, W., Yang, Y., Li, Y., Liu, Z., ... & Huang, C. (2023). Single-cell transcriptomic analysis of normal and pathological tissues from the same patient uncovers colon cancer progression. *Cell & Bioscience*, *13*(1), 62.

58. Zhu, G., Pei, L., Xia, H., Tang, Q., & Bi, F. (2021). Role of oncogenic KRAS in the prognosis, diagnosis and treatment of colorectal cancer. *Molecular cancer*, *20*(1), 143.

59. Ulanja, M. B., Rishi, M., Beutler, B. D., Sharma, M., Patterson, D. R., Gullapalli, N., & Ambika, S. (2019). Colon cancer sidedness, presentation, and survival at different stages. *Journal of oncology*, *2019*.

60. Gupta, P., Chiang, S. F., Sahoo, P. K., Mohapatra, S. K., You, J. F., Onthoni, D. D., ... & Tsai, W. S. (2019). Prediction of colon cancer stages and survival period with machine learning approach. *Cancers*, *11*(12), 2007.

61. Greene, F. L., Stewart, A. K., & Norton, H. J. (2002). A new TNM staging strategy for node-positive (stage III) colon cancer: an analysis of 50,042 patients. *Annals of surgery*, *236*(4), 416-421.

62. Dienstmann, R., Mason, M. J., Sinicrope, F. A., Phipps, A. I., Tejpar, S., Nesbakken, A., ... & Guinney, J. (2017). Prediction of overall survival in stage II and III colon cancer beyond TNM system: a retrospective, pooled biomarker study. *Annals of Oncology*, *28*(5), 1023-1031.

63. Ceelen, W., Van Nieuwenhove, Y., & Pattyn, P. (2010). Prognostic value of the lymph node ratio in stage III colorectal cancer: a systematic review. *Annals of surgical oncology*, *17*, 2847-2855.

64. Chang, G. J., Rodriguez-Bigas, M. A., Skibber, J. M., & Moyer, V. A. (2007). Lymph node evaluation and survival after curative resection of colon cancer: systematic review. *Journal of the National Cancer Institute*, *99*(6), 433-441.

65. Lee, J. J., & Chu, E. (2017). Adjuvant chemotherapy for stage II colon cancer: the debate goes on. *Journal of oncology practice*, *13*(4), 245.

66. Archambault, A. N., Jeon, J., Lin, Y., Thomas, M., Harrison, T. A., Bishop, D. T., ... & Hayes, R. B. (2022). Risk stratification for early-onset colorectal cancer using a combination of genetic and environmental risk scores: an international multi-center study. *JNCI: Journal of the National Cancer Institute*, *114*(4), 528-539.

67. Aglago, E. K., Cross, A. J., Riboli, E., Fedirko, V., Hughes, D. J., Fournier, A., ... & Jenab, M. (2023). Dietary intake of total, heme and non-heme iron and the risk of colorectal cancer in a European prospective cohort study. *British journal of cancer*, *128*(8), 1529-1540.

68. Slattery, M. L., West, D. W., Robison, L. M., French, T. K., Ford, M. H., Schuman, K. L., & Sorenson, A. W. (1990). Tobacco, alcohol, coffee, and caffeine as risk factors for colon cancer in a low-risk population. *Epidemiology*, *1*(2), 141-145.

69. Babcock, B. D., Aljehani, M. A., Jabo, B., Choi, A. H., Morgan, J. W., Selleck, M. J., ... & Senthil, M. (2018). High-risk stage II colon cancer: not all risks are created equal. *Annals of surgical oncology*, *25*, 1980-1985.

70. Ahmed, M. (2020). Colon cancer: a clinician's perspective in 2019. *Gastroenterology research*, *13*(1), 1.

71. Washington, M. K., Berlin, J., Branton, P., Burgart, L. J., Carter, D. K., Fitzgibbons, P. L., ... & Compton, C. C. (2009). Protocol for the examination of specimens from patients with primary carcinoma of the colon and rectum. *Archives of pathology & laboratory medicine*, *133*(10), 1539-1551.

72. Markowitz, S. D., Dawson, D. M., Willis, J., & Willson, J. K. (2002). Focus on colon cancer. *Cancer cell*, *1*(3), 233-236.

73. Armaghany, T., Wilson, J. D., Chu, Q., & Mills, G. (2012). Genetic alterations in colorectal cancer. *Gastrointestinal cancer research: GCR*, *5*(1), 19.

74. Nawa, T., Kato, J., Kawamoto, H., Okada, H., Yamamoto, H., Kohno, H., ... & Shiratori, Y. (2008). Differences between right-and left-sided colon cancer in patient characteristics, cancer morphology and histology. *Journal of gastroenterology and hepatology*, *23*(3), 418-423.

75. Sirinukunwattana, K., Raza, S. E. A., Tsang, Y. W., Snead, D. R., Cree, I. A., & Rajpoot, N. M. (2016). Locality sensitive deep learning for detection and classification of nuclei in routine colon cancer histology images. *IEEE transactions on medical imaging*, *35*(5), 1196-1206.

76. Koehler, A., Bataille, F., Schmid, C., Ruemmele, P., Waldeck, A., Blaszyk, H., ... & Dietmaier, W. (2004). Gene expression profiling of colorectal cancer and metastases divides tumours according to their clinicopathological stage. *The Journal of Pathology: A Journal of the Pathological Society of Great Britain and Ireland*, *204*(1), 65-74.

77. Labianca, R., Beretta, G. D., Kildani, B., Milesi, L., Merlin, F., Mosconi, S., ... & Wils, J. (2010). Colon cancer. *Critical reviews in oncology/hematology*, *74*(2), 106-133.

78. Jass, J. R. (2007). Classification of colorectal cancer based on correlation of clinical, morphological and molecular features. *Histopathology*, *50*(1), 113-130.

79. Ogino, S., & Goel, A. (2008). Molecular classification and correlates in colorectal cancer. *The Journal of Molecular Diagnostics*, *10*(1), 13-27.

80. SAIguSA, S., Toiyama, Y., Tanaka, K., YOkOE, T., Okugawa, Y., Fujikawa, H., ... & Kusunoki, M. (2011). Cancer-associated fibroblasts correlate with poor prognosis in rectal cancer after chemoradiotherapy. *International journal of oncology*, *38*(3), 655-663.

81. Xue, C., Xu, Y., Ye, W., Xie, Q., Gao, H., Xu, B., ... & Jiang, J. (2020). Expression of PD-L1 in ovarian cancer and its synergistic antitumor effect with PARP inhibitor. *Gynecologic oncology*, *157*(1), 222-233.

82. Mitchison, D. A. (1979). Basic mechanisms of chemotherapy. *Chest*, *76*(6), 771-780.

83. Lombardi, L., Morelli, F., Cinieri, S., Santini, D., Silvestris, N., Fazio, N., ... & Maiello, E. (2010). Adjuvant colon cancer chemotherapy: where we are and where we'll go. *Cancer treatment reviews*, *36*, S34-S41.

84. Alkema, N. G., Wisman, G. B. A., van der Zee, A. G., van Vugt, M. A., & de Jong, S. (2016). Studying platinum sensitivity and resistance in high-grade serous ovarian cancer: different models for different questions. *Drug Resistance Updates*, *24*, 55-69.

85. Allen, J. D., Brinkhuis, R. F., Deemter, L. V., Wijnholds, J., & Schinkel, A. H. (2000). Extensive contribution of the multidrug transporters P-glycoprotein and Mrp1 to basal drug resistance. *Cancer research*, *60*(20), 5761-5766.

86. Housman, G., Byler, S., Heerboth, S., Lapinska, K., Longacre, M., Snyder, N., & Sarkar, S. (2014). Drug resistance in cancer: an overview. *Cancers*, *6*(3), 1769-1792.

87. Ricci-Vitiani, L., Fabrizi, E., Palio, E., & De Maria, R. (2009). Colon cancer stem cells. *Journal of Molecular Medicine*, *87*, 1097-1104.

88. Todaro, M., Francipane, M. G., Medema, J. P., & Stassi, G. (2010). Colon cancer stem cells: promise of targeted therapy. *Gastroenterology*, *138*(6), 2151-2162.

89. Dhillon, K. K., Swisher, E. M., & Taniguchi, T. (2011). Secondary mutations of BRCA1/2 and drug resistance. *Cancer science*, *102*(4), 663-669.

90. Liu, K., Gao, L., Ma, X., Huang, J. J., Chen, J., Zeng, L., ... & Chen, Z. S. (2020). Long non-coding RNAs regulate drug resistance in cancer. *Molecular cancer*, *19*, 1-13.

91. Bukowski, K., Kciuk, M., & Kontek, R. (2020). Mechanisms of multidrug resistance in cancer chemotherapy. *International journal of molecular sciences*, *21*(9), 3233.

92. Gillet, J. P., & Gottesman, M. M. (2010). Mechanisms of multidrug resistance in cancer. *Multi-drug resistance in cancer*, 47-76.

93. Fletcher, J. I., Williams, R. T., Henderson, M. J., Norris, M. D., & Haber, M. (2016). ABC transporters as mediators of drug resistance and contributors to cancer cell biology. *Drug Resistance Updates*, *26*, 1-9.

94. Kapoor, K., Sim, H. M., & Ambudkar, S. V. (2013). Multidrug resistance in cancer: a tale of ABC drug transporters. *Molecular mechanisms of tumor cell resistance to chemotherapy: Targeted therapies to reverse resistance*, 1-34.

95. Izquierdo, M. A., Neefjes, J. J., Mathari, A. E. L., Flens, M. J., Scheffer, G. L., & Scheper, R. J. (1996). Overexpression of the ABC transporter TAP in multidrug-resistant human cancer cell lines. *British journal of cancer*, *74*(12), 1961-1967.

96. Liu, R., Chen, Y., Liu, G., Li, C., Song, Y., Cao, Z., ... & Liu, Y. (2020). PI3K/AKT pathway as a key link modulates the multidrug resistance of cancers. *Cell death & disease*, *11*(9), 797.

97. Vara, J. Á. F., Casado, E., de Castro, J., Cejas, P., Belda-Iniesta, C., & González-Barón, M. (2004). PI3K/Akt signalling pathway and cancer. *Cancer treatment reviews*, *30*(2), 193-204.

98. Huang, D., Savage, S. R., Calinawan, A. P., Lin, C., Zhang, B., Wang, P., ... & Paulovich, A. G. (2021). A highly annotated database of genes associated with platinum resistance in cancer. *Oncogene*, *40*(46), 6395-6405.

99. Lord, C. J., & Ashworth, A. (2013). Mechanisms of resistance to therapies targeting BRCA-mutant cancers. *Nature medicine*, *19*(11), 1381-1388.

100. Rottenberg, S., Disler, C., & Perego, P. (2021). The rediscovery of platinum-based cancer therapy. *Nature Reviews Cancer*, *21*(1), 37-50.

101. Abed, A., Derakhshan, M., Karimi, M., Shirazinia, M., Mahjoubin-Tehran, M., Homayonfal, M., ... & Mirzaei, H. (2022). Platinum nanoparticles in biomedicine: Preparation, anti-cancer activity, and drug delivery vehicles. *Frontiers in Pharmacology*, *13*, 797804.

102. Mironava, T., Simon, M., Rafailovich, M. H., & Rigas, B. (2013). Platinum folate nanoparticles toxicity: cancer vs. normal cells. *Toxicology in Vitro*, *27*(2), 882-889.

103. Kasinski, A. L., & Slack, F. J. (2011). MicroRNAs en route to the clinic: progress in validating and targeting microRNAs for cancer therapy. *Nature Reviews Cancer*, *11*(12), 849-864.

104. Wang, S., Li, M. Y., Liu, Y., Vlantis, A. C., Chan, J. Y., Xue, L., ... & Chen, G. G. (2020). The role of microRNA in cisplatin resistance or sensitivity. *Expert Opinion on Therapeutic Targets*, *24*(9), 885-897.

105. Morais, T. S., Fernandes, A. R., Baptista, P. V., & Gambino, D. (2022). Rational drug design of metal complexes for cancer therapy. *Frontiers in Chemistry*, *10*, 1035274.

106. Pranczk, J., Jacewicz, D., Wyrzykowski, D., & Chmurzynski, L. (2014). Platinum (II) and palladium (II) complex compounds as anti-cancer drugs. Methods of cytotoxicity determination. *Current Pharmaceutical Analysis*, *10*(1), 2-9.

107. Jahromi, E. Z., Divsalar, A., Saboury, A. A., Khaleghizadeh, S., Mansouri-Torshizi, H., & Kostova, I. (2016). Palladium complexes: new candidates for anti-cancer drugs. *Journal of the Iranian Chemical Society*, *13*, 967-989.

108. Bortolamiol, E., Novaselich, S., Tupini, C., Fagnani, S., Gambari, R., Demitri, N., ... & Scattolin, T. (2024). Palladium (II)-Imidoyl Complexes: A New Piece in the Puzzle of Organopalladium Anticancer Agents. *European Journal of Inorganic Chemistry*, *27*(8), e202300673.

109. Ulukaya, E., Ari, F., Dimas, K., Ikitimur, E. I., Guney, E., & Yilmaz, V. T. (2011). Anti-cancer activity of a novel palladium (II) complex on human breast cancer cells in vitro and in vivo. *European journal of medicinal chemistry*, *46*(10), 4957-4963.

110. Ulukaya, E., Ari, F., Dimas, K., Sarimahmut, M., Guney, E., Sakellaridis, N., & Yilmaz, V. T. (2011). Cell death-inducing effect of novel palladium (II) and platinum (II) complexes on non-small cell lung cancer cells in vitro. *Journal of cancer research and clinical oncology*, *137*, 1425-1434.

111. Chu, C., Su, M., Zhu, J., Li, D., Cheng, H., Chen, X., & Liu, G. (2019). Metal-organic framework nanoparticle-based biomineralization: a new strategy toward cancer treatment. *Theranostics*, *9*(11), 3134.

112. Jahromi, E. Z., Divsalar, A., Saboury, A. A., Khaleghizadeh, S., Mansouri-Torshizi, H., & Kostova, I. (2016). Palladium complexes: new candidates for anti-cancer drugs. *Journal of the Iranian Chemical Society*, *13*, 967-989.

113. Miklášová, N., Fischer-Fodor, E., Lönnecke, P., Tomuleasa, C. I., Virag, P., Schrepler, M. P., ... & Hey-Hawkins, E. (2012). Antiproliferative effect of novel platinum (II) and palladium (II) complexes on hepatic tumor stem cells in vitro. *European journal of medicinal chemistry*, *49*, 41-47.

114. Akdi, K., Vilaplana, R. A., Kamah, S., Navarro, J. A., Salas, J. M., & González-Vílchez, F. (2002). Study of the biological effects and DNA damage exerted by a new dipalladium-Hmtpo complex on human cancer cells. *Journal of inorganic biochemistry*, *90*(1-2), 51-60.

115. Simić, D., Zarić, M., Nikolić, I., Živković-Zarić, R., Čanović, P., Kočović, A., ... & Jevtić, V. (2022). Newly synthesized palladium (II) complexes with aminothiazole derivatives: in vitro study of antimicrobial activity and antitumor activity on the human prostate cancer cell line. *Dalton Transactions*, *51*(3), 1191-1205.

116. Moghadam, M. E., Sadeghi, M., Mansouri-Torshizi, H., & Saidifar, M. (2023). High cancer selectivity and improving drug release from mesoporous silica nanoparticles in the presence of human serum albumin in cisplatin, carboplatin, oxaliplatin, and oxalipalladium treatment. *European Journal of Pharmaceutical Sciences*, *187*, 106477.

117. Tanida, S., Mizoshita, T., Ozeki, K., Tsukamoto, H., Kamiya, T., Kataoka, H., ... & Joh, T. (2012). Mechanisms of cisplatin-induced apoptosis and of cisplatin sensitivity: potential of BIN1 to act as a potent predictor of cisplatin sensitivity in gastric cancer treatment. *International journal of surgical oncology*, *2012*.

118. Dasari, S., & Tchounwou, P. B. (2014). Cisplatin in cancer therapy: molecular mechanisms of action. *European journal of pharmacology*, *740*, 364-378.

119. Gelasco, A., & Lippard, S. J. (1999). Anticancer activity of cisplatin and related complexes. *Metallopharmaceuticals I: DNA Interactions*, 1-43.

120. Florea, A. M., & Büsselberg, D. (2011). Cisplatin as an anti-tumor drug: cellular mechanisms of activity, drug resistance and induced side effects. *Cancers*, *3*(1), 1351-1371.

121. Sacchi, A., Gasparri, A., Gallo-Stampino, C., Toma, S., Curnis, F., & Corti, A. (2006). Synergistic antitumor activity of cisplatin, paclitaxel, and gemcitabine with tumor vasculature-targeted tumor necrosis factor-α. *Clinical Cancer Research*, *12*(1), 175-182.

122. Dhorajiya, B. D., Ibrahim, A. S., Badria, F. A., & Dholakiya, B. Z. (2014). Design and synthesis of novel nucleobase-based barbiturate derivatives as potential anticancer agents. *Medicinal Chemistry Research*, *23*, 839-847.

123. Lee, S. Y., Slagle-Webb, B., Sharma, A. K., & Connor, J. R. (2020). Characterization of a novel barbituric acid and two thiobarbituric acid compounds for lung cancer treatment. *Anticancer research*, *40*(11), 6039-6049.

124. Ouyang, L., Shi, Z., Zhao, S., Wang, F. T., Zhou, T. T., Liu, B., & Bao, J. K. (2012). Programmed cell death pathways in cancer: a review of apoptosis, autophagy and programmed necrosis. *Cell proliferation*, *45*(6), 487-498.

125. Jin, Z., & El-Deiry, W. S. (2005). Overview of cell death signaling pathways. *Cancer biology & therapy*, *4*(2), 147-171.

126. Ameisen, J. C. (2002). On the origin, evolution, and nature of programmed cell death: a timeline of four billion years. *Cell Death & Differentiation*, *9*(4), 367-393.

127. Reed, J. C. (2000). Mechanisms of apoptosis. *The American journal of pathology*, *157*(5), 1415-1430.

128. Diamantis, A., Magiorkinis, E., Sakorafas, G. H., & Androutsos, G. (2008). A brief history of apoptosis: from ancient to modern times. *Oncology Research and Treatment*, *31*(12), 702-706.

129. Favaloro, B., Allocati, N., Graziano, V., Di Ilio, C., & De Laurenzi, V. (2012). Role of apoptosis in disease. *Aging (Albany NY)*, *4*(5), 330.

130. Pilati, C., Taieb, J., Balogoun, R., Marisa, L., De Reyniès, A., & Laurent-Puig, P. (2017). CDX2 prognostic value in stage II/III resected colon cancer is related to CMS classification. *Annals of Oncology*, *28*(5), 1032-1035.

131. Dienstmann, R., Vermeulen, L., Guinney, J., Kopetz, S., Tejpar, S., & Tabernero, J. (2017). Consensus molecular subtypes and the evolution of precision medicine in colorectal cancer. *Nature reviews cancer*, *17*(2), 79-92.

132. Zhang, L., & Yu, J. (2013). Role of apoptosis in colon cancer biology, therapy, and prevention. *Current colorectal cancer reports*, *9*, 331-340.

133. Giuliano, M., Pellerito, C., Celesia, A., Fiore, T., & Emanuele, S. (2021). Tributyltin (IV) butyrate: A novel epigenetic modifier with ER stress-and apoptosis-inducing properties in colon cancer cells. *Molecules*, *26*(16), 5010.

134. Yi, T., & Wagner, G. (2022). Cytocapsular tube network-tumor system is an integrated physical target for the highly effective and efficient pharmacotherapy of solid cancers. *BioRxiv*, 2022-01.

135. Pan, B., Zheng, B., Xing, C., & Liu, J. (2022). Non-canonical programmed cell death in colon cancer. *Cancers*, *14*(14), 3309.

136. Matthews, G. M., Howarth, G. S., & Butler, R. N. (2012). Short-chain fatty acids induce apoptosis in colon cancer cells associated with changes to intracellular redox state and glucose metabolism. *Chemotherapy*, *58*(2), 102-109.

137. Kashyap, D., Garg, V. K., & Goel, N. (2021). Intrinsic and extrinsic pathways of apoptosis: Role in cancer development and prognosis. *Advances in protein chemistry and structural biology*, *125*, 73-120.

138. Kashyap, D., Garg, V. K., & Goel, N. (2021). Intrinsic and extrinsic pathways of apoptosis: Role in cancer development and prognosis. *Advances in protein chemistry and structural biology*, *125*, 73-120.

139. Ulukaya, E., Kurt, A., & Wood, E. J. (2001). 4-(N-hydroxyphenyl) retinamide can selectively induce apoptosis in human epidermoid carcinoma cells but not in normal dermal fibroblasts. *Cancer investigation*, *19*(2), 145-154.

140. Hongmei, Z. (2012). Extrinsic and intrinsic apoptosis signal pathway review. In *Apoptosis and medicine*. InTechOpen.

141. Lossi, L. (2022). The concept of intrinsic versus extrinsic apoptosis. *Biochemical Journal*, *479*(3), 357-384.

142. Ashkenazi, A. (2008). Targeting the extrinsic apoptosis pathway in cancer. *Cytokine & growth factor reviews*, *19*(3-4), 325-331.

143. Bray, F., Carstensen, B., Møller, H., Zappa, M., Zˇakelj, M. P., Lawrence, G., ... & Weiderpass, E. (2005). Incidence trends of adenocarcinoma of the cervix in 13 European countries. *Cancer Epidemiology Biomarkers & Prevention*, *14*(9), 2191-2199.

144. Siegel, R., DeSantis, C., & Jemal, A. (2014). Colorectal cancer statistics, 2014. *CA: a cancer journal for clinicians*, *64*(2), 104-117.

145. Khoury, M. J., Lam, T. K., Ioannidis, J. P., Hartge, P., Spitz, M. R., Buring, J. E., ... & Schully, S. D. (2013). Transforming epidemiology for 21st century medicine and public health. *Cancer epidemiology, biomarkers & prevention*, *22*(4), 508-516.

146. Arnold, M., Sierra, M. S., Laversanne, M., Soerjomataram, I., Jemal, A., & Bray, F. (2017). Global patterns and trends in colorectal cancer incidence and mortality. *Gut*, *66*(4), 683-691.

147. Labianca, R., Beretta, G. D., Kildani, B., Milesi, L., Merlin, F., Mosconi, S., ... & Wils, J. (2010). Colon cancer. *Critical reviews in oncology/hematology*, *74*(2), 106-133.

148. Holtedahl, K., Borgquist, L., Donker, G. A., Buntinx, F., Weller, D., Campbell, C., ... & Parajuli, R. (2021). Symptoms and signs of colorectal cancer, with differences between proximal and distal colon cancer: a prospective cohort study of diagnostic accuracy in primary care. *BMC family practice*, *22*, 1-13.

149. Wu, C. (2018). Systemic therapy for colon cancer. *Surgical Oncology Clinics*, *27*(2), 235-242.

150. Showalter, S. L., Showalter, T. N., Witkiewicz, A., Havens, R., Kennedy, E. P., Hucl, T., ... & Brody, J. R. (2008). Evaluating the drug-target relationship between thymidylate synthase expression and tumor response to 5-fluorouracil: Is it time to move forward?. *Cancer biology & therapy*, *7*(7), 986-994.

151. Salonga, D., Danenberg, K. D., Johnson, M., Metzger, R., Groshen, S., Tsao-Wei, D. D., ... & Danenberg, P. V. (2000). Colorectal tumors responding to 5-fluorouracil have low gene expression levels of dihydropyrimidine dehydrogenase, thymidylate synthase, and thymidine phosphorylase. *Clinical Cancer Research*, *6*(4), 1322-1327.

153. Douillard, J., Cunningham, D., Roth, A. D., Navarro, M., James, R. D., Karasek, P., ... & Rougier, P. (2000). Irinotecan combined with fluorouracil compared with fluorouracil alone as first-line treatment for metastatic colorectal cancer: a multicentre randomised trial. *The Lancet*, *355*(9209), 1041-1047.

154. Liu, J., & Guo, B. (2020). RNA-based therapeutics for colorectal cancer: Updates and future directions. *Pharmacological research*, *152*, 104550.

155. Van der Jeught, K., Xu, H. C., Li, Y. J., Lu, X. B., & Ji, G. (2018). Drug resistance and new therapies in colorectal cancer. *World journal of gastroenterology*, *24*(34), 3834.

156. Pavlidis, E. T., & Pavlidis, T. E. (2013). Role of bevacizumab in colorectal cancer growth and its adverse effects: a review. *World journal of gastroenterology: WJG*, *19*(31), 5051.

157. Abtahi, S., Davani, F., Mojtahedi, Z., Hosseini, S. V., Bananzadeh, A., & Ghaderi, A. (2017). Dual association of serum interleukin-10 levels with colorectal cancer. *Journal of cancer research and therapeutics*, *13*(2), 252-256.

158. Lin, Z., Li, Q., Zhao, Y., Lin, Z., Cheng, N., Zhang, D., ... & Lin, D. (2021). Combination of auranofin and ICG-001 suppress the proliferation and metastasis of colon cancer. *Frontiers in Oncology*, *11*, 738085.

159. Mesas, C., Garcés, V., Martinez, R., Ortiz, R., Doello, K., Dominguez-Vera, J. M., ... & Prados, J. (2022). Colon cancer therapy with calcium phosphate nanoparticles loading bioactive compounds from Euphorbia lathyris: in vitro and in vivo assay. *Biomedicine & Pharmacotherapy*, *155*, 113723.

160. Zou, H., Li, L., Garcia Carcedo, I., Xu, Z. P., Monteiro, M., & Gu, W. (2016). Synergistic inhibition of colon cancer cell growth with nanoemulsion-loaded paclitaxel and PI3K/mTOR dual inhibitor BEZ235 through apoptosis. *International journal of nanomedicine*, 1947-1958.

161. Yu, Z., Li, X., Duan, J., & Yang, X. D. (2020). Targeted treatment of colon cancer with aptamer-guided albumin nanoparticles loaded with docetaxel. *International Journal of Nanomedicine*, 6737-6748.

162. Lin, X., Ramamurthi, K., Mishima, M., Kondo, A., Christen, R. D., & Howell, S. B. (2001). P53 modulates the effect of loss of DNA mismatch repair on the sensitivity of human colon cancer cells to the cytotoxic and mutagenic effects of cisplatin. *Cancer research*, *61*(4), 1508-1516.

163. Lacour, S., Hammann, A., Grazide, S., Lagadic-Gossmann, D., Athias, A., Sergent, O., ... & Dimanche-Boitrel, M. T. (2004). Cisplatin-induced CD95 redistribution into membrane lipid rafts of HT29 human colon cancer cells. *Cancer research*, *64*(10), 3593-3598.

164. Ding, Z. Y., Liu, G. H., Olsson, B., & Sun, X. F. (2013). Upregulation of the antiapoptotic factor Livin contributes to cisplatin resistance in colon cancer cells. *Tumor Biology*, *34*, 683-693.

165. Mármol, I., Quero, J., Rodríguez-Yoldi, M. J., & Cerrada, E. (2019). Gold as a possible alternative to platinum-based chemotherapy for colon cancer treatment. *Cancers*, *11*(6), 780.

166. Schurich, A., Pallett, L. J., Lubowiecki, M., Singh, H. D., Gill, U. S., Kennedy, P. T., ... & Maini, M. K. (2013). The third signal cytokine IL-12 rescues the anti-viral function of exhausted HBV-specific CD8 T cells. *PLoS pathogens*, *9*(3), e1003208.

167. Tanaka, M., Kataoka, H., Yano, S., Ohi, H., Kawamoto, K., Shibahara, T., ... & Joh, T. (2013). Anti-cancer effects of newly developed chemotherapeutic agent, glycoconjugated palladium (II) complex, against cisplatin-resistant gastric cancer cells. *BMC cancer*, *13*, 1-9.

168. Kapdi, A. R., & Fairlamb, I. J. (2014). Anti-cancer palladium complexes: a focus on PdX 2 L 2, palladacycles and related complexes. *Chemical Society Reviews*, *43*(13), 4751-4777.

169. Scattolin, T., Bortolamiol, E., Visentin, F., Palazzolo, S., Caligiuri, I., Perin, T., ... & Togni, A. (2020). Palladium (II)-η3-Allyl Complexes Bearing N-Trifluoromethyl N-Heterocyclic Carbenes: A New Generation of Anticancer Agents that Restrain the Growth of High-Grade Serous Ovarian Cancer Tumoroids. *Chemistry–A European Journal*, *26*(51), 11868-11876.

170. Büyükekşi, S. I., Erkısa Genel, M., Şengül, A., Ulukaya, E., & Oral, A. Y. (2018). Structural studies and cytotoxic activity of a new dinuclear coordination compound of palladium (II)-2, 2: 6, 2-terpyridine with rigid dianionic 1, 2, 4-triazole-3-sulfonate linker.

171. Al Nasr, I., Touj, N., Koko, W., Khan, T., Özdemir, I., Yaşar, S., & Hamdi, N. (2020). Biological activities of nhc–pd (Ii) complexes based on benzimidazolylidene n-heterocyclic carbene (nhc) ligands bearing aryl substituents. *Catalysts*, *10*(10), 1190.

172. Abu-Surrah, A. S., Al-Sa'doni, H. H., & Abdalla, M. Y. (2008). Palladium-based chemotherapeutic agents: Routes toward complexes with good antitumor activity. *Cancer Ther*, *6*(1), 1-10.

173. Bellosta, P., Zhang, Q., Goff, S. P., & Basilico, C. (1997). Signaling through the ARK tyrosine kinase receptor protects from apoptosis in the absence of growth stimulation. *Oncogene*, *15*(20), 2387-2397.

174. Reutelingsperger, C. P. M., & Van Heerde, W. L. (1997). Annexin V, the regulator of phosphatidylserine-catalyzed inflammation and coagulation during apoptosis. *Cellular and Molecular Life Sciences CMLS*, *53*, 527-532.

175. Aubry, J. P., Blaecke, A., Lecoanet-Henchoz, S., Jeannin, P., Herbault, N., Caron, G., ... & Bonnefoy, J. Y. (1999). Annexin V used for measuring apoptosis in the early events of cellular cytotoxicity. *Cytometry: The Journal of the International Society for Analytical Cytology*, *37*(3), 197-204.

176. Baskić, D., Popović, S., Ristić, P., & Arsenijević, N. N. (2006). Analysis of cycloheximide-induced apoptosis in human leukocytes: Fluorescence microscopy using annexin V/propidium iodide versus acridin orange/ethidium bromide. *Cell biology international*, *30*(11), 924-932.

177. Ramadani, R. D., Utomo, R. Y., Hermawan, A., & Meiyanto, E. (2021). Pentagamaboronon-0-Sorbitol Induces Apoptosis through Elevation of Reactive Oxygen Species in Triple Negative Breast Cancer Cells. *Indonesian Journal of Cancer Chemoprevention*, *12*(1), 46-56.

178. Guo, J. R., Chen, Q. Q., Lam, C. W. K., & Zhang, W. (2015). Effects of karanjin on cell cycle arrest and apoptosis in human A549, HepG2 and HL-60 cancer cells. *Biological research*, *48*, 1-7.

179. Souza, B. S., Sampaio, G. L., Pereira, C. S., Campos, G. S., Sardi, S. I., Freitas, L. A., ... & Soares, M. B. (2016). Zika virus infection induces mitosis abnormalities and apoptotic cell death of human neural progenitor cells. *Scientific reports*, *6*(1), 39775.

180. Moon, S. H., Lin, L., Zhang, X., Nguyen, T. A., Darlington, Y., Waldman, A. S., ... & Donehower, L. A. (2010). Wild-type p53-induced phosphatase 1 dephosphorylates histone variant γ-H2AX and suppresses DNA double strand break repair. *Journal of biological chemistry*, *285*(17), 12935-12947.

181. Xu, X. M., Zhang, M. L., Zhang, Y., & Zhao, L. (2016). Osthole induces lung cancer cell apoptosis through inhibition of inhibitor of apoptosis family proteins. *Oncology Letters*, *12*(5), 3779-3784.

182. Dong, Y., Yin, S., Song, X., Huo, Y., Fan, L., Ye, M., & Hu, H. (2016). Involvement of ROS-p38-H2AX axis in novel curcumin analogues-induced apoptosis in breast cancer cells. *Molecular carcinogenesis*, *55*(4), 323-334.

183. Druker, B. J., Guilhot, F., O'Brien, S. G., Gathmann, I., Kantarjian, H., Gattermann, N., ... & Larson, R. A. (2006). Five-year follow-up of patients receiving imatinib for chronic myeloid leukemia. *New England Journal of Medicine*, *355*(23), 2408-2417.

184. Czechowska, A., Poplawski, T., Drzewoski, J., & Blasiak, J. (2005). Imatinib (STI571) induces DNA damage in BCR/ABL-expressing leukemic cells but not in normal lymphocytes. *Chemico-biological interactions*, *152*(2-3), 139-150.

185. Huang, Q., Zhan, L., Cao, H., Li, J., Lyu, Y., Guo, X., ... & Xing, J. (2016). Increased mitochondrial fission promotes autophagy and hepatocellular carcinoma cell survival through the ROS-modulated coordinated regulation of the NFKB and TP53 pathways. *Autophagy*, *12*(6), 999-1014.

186. Srinivas, U. S., Tan, B. W., Vellayappan, B. A., & Jeyasekharan, A. D. (2019). ROS and the DNA damage response in cancer. *Redox biology*, *25*, 101084.

187. Lu, L., Dong, J., Wang, L., Xia, Q., Zhang, D., Kim, H., ... & Shen, Q. (2018). Activation of STAT3 and Bcl-2 and reduction of reactive oxygen species (ROS) promote radioresistance in breast cancer and overcome of radioresistance with niclosamide. *Oncogene*, *37*(39), 5292-5304.

188. Ye, T., Xiong, Y., Yan, Y., Xia, Y., Song, X., Liu, L., ... & Yu, L. (2014). The anthelmintic drug niclosamide induces apoptosis, impairs metastasis and reduces immunosuppressive cells in breast cancer model. *PloS one*, *9*(1), e85887.

189. Chetram, M. A., Bethea, D. A., Odero-Marah, V. A., Don-Salu-Hewage, A. S., Jones, K. J., & Hinton, C. V. (2013). ROS-mediated activation of AKT induces apoptosis via pVHL in prostate cancer cells. *Molecular and cellular biochemistry*, *376*, 63-71.

190. Takayama, S., Xie, Z., & Reed, J. C. (1999). An evolutionarily conserved family of Hsp70/Hsc70 molecular chaperone regulators. *Journal of Biological Chemistry*, *274*(2), 781-786.

191. Takayama, S., & Reed, J. C. (2001). Molecular chaperone targeting and regulation by BAG family proteins. *Nature cell biology*, *3*(10), E237-E241.

192. Doong, H., Vrailas, A., & Kohn, E. C. (2002). What's in the 'BAG'?–a functional domain analysis of the BAG-family proteins. *Cancer letters*, *188*(1-2), 25-32.

193. Doong, H., Price, J., Kim, Y. S., Gasbarre, C., Probst, J., Liotta, L. A., ... & Kohn, E. (2000). CAIR-1/BAG-3 forms an EGF-regulated ternary complex with phospholipase C-γ and Hsp70/Hsc70. *Oncogene*, *19*(38), 4385-4395.

194. Kögel, D., Linder, B., Brunschweiger, A., Chines, S., & Behl, C. (2020). At the crossroads of apoptosis and autophagy: multiple roles of the co-chaperone BAG3 in stress and therapy resistance of cancer. *Cells*, *9*(3), 574.

195. Li, F. H., Xiang, L., Ran, L., Zhou, S., Huang, Z., Chen, M., & Yu, W. F. (2019). BNIP1 inhibits cell proliferation, migration and invasion, and promotes apoptosis by mTOR in cervical cancer cells. *European Review for Medical & Pharmacological Sciences*, *23*(4).

196. Zhang, H. M., Cheung, P., Yanagawa, B., McManus, B. M., & Yang, D. C. (2003). BNips: a group of pro-apoptotic proteins in the Bcl-2 family. *Apoptosis*, *8*, 229-236.

197. Guo, K., Zhao, J., Jin, Q., Yan, H., Shi, Y., & Zhao, Z. (2022). CASP6 predicts poor prognosis in glioma and correlates with tumor immune microenvironment. *Frontiers in Oncology*, *12*, 818283.

198. Brentnall, M., Rodriguez-Menocal, L., De Guevara, R. L., Cepero, E., & Boise, L. H. (2013). Caspase-9, caspase-3 and caspase-7 have distinct roles during intrinsic apoptosis. *BMC cell biology*, *14*, 1-9.

199. Kello, M., & Goga, M. (2023). Lichen, Pseudevernia furfuracea (L.) Zopf: Analytical Compositional Features, Biological Activity and Use in Cancer Studies. In *Ancient and Traditional Foods, Plants, Herbs and Spices used in Cancer* (pp. 281-296). CRC Press.

200. Shi, T. Y., He, J., Wang, M. Y., Zhu, M. L., Yu, K. D., Shao, Z. M., ... & Wei, Q. (2015). CASP7 variants modify susceptibility to cervical cancer in Chinesewomen. *Scientific reports*, *5*(1), 9225.

201. Yan, S., Li, Y. Z., Zhu, X. W., Liu, C. L., Wang, P., & Liu, Y. L. (2013). HuGE systematic review and meta-analysis demonstrate association of CASP-3 and CASP-7 genetic polymorphisms with cancer risk. *Genet Mol Res*, *12*(2), 1561-1573.

202. Cui, R., Kim, T., Fassan, M., Meng, W., Sun, H. L., Jeon, Y. J., ... & Croce, C. M. (2015). MicroRNA-224 is implicated in lung cancer pathogenesis through targeting caspase-3 and caspase-7. *Oncotarget*, *6*(26), 21802.

203. Albano, F., Chiurazzi, F., Mimmi, S., Vecchio, E., Pastore, A., Cimmino, C., ... & Quinto, I. (2018). The expression of inhibitor of bruton's tyrosine kinase gene is progressively up regulated in the clinical course of chronic lymphocytic leukaemia conferring resistance to apoptosis. *Cell Death & Disease*, *9*(1), 13.

204. Izarzugaza, J. M., Grana, O., Tress, M. L., Valencia, A., & Clarke, N. D. (2007). Assessment of intramolecular contact predictions for CASP7. *Proteins: Structure, Function, and Bioinformatics*, *69*(S8), 152-158.

205. Wang, C., & Youle, R. J. (2009). The role of mitochondria in apoptosis. *Annual review of genetics*, *43*, 95-118.

206. Huang, K., Zhang, J., O'Neill, K. L., Gurumurthy, C. B., Quadros, R. M., Tu, Y., & Luo, X. (2016). Cleavage by caspase 8 and mitochondrial membrane association activate the BH3-only protein Bid during TRAIL-induced apoptosis. *Journal of Biological Chemistry*, *291*(22), 11843-11851.

207. Gonzalvez, F., Schug, Z. T., Houtkooper, R. H., MacKenzie, E. D., Brooks, D. G., Wanders, R. J., ... & Gottlieb, E. (2008). Cardiolipin provides an essential activating platform for caspase-8 on mitochondria. *The Journal of cell biology*, *183*(4), 681-696.

208. Köhler, B., Anguissola, S., Concannon, C. G., Rehm, M., Kögel, D., & Prehn, J. H. (2008). Bid participates in genotoxic drug-induced apoptosis of HeLa cells and is essential for death receptor ligands' apoptotic and synergistic effects. *PLoS One*, *3*(7), e2844.

209. Loftus, L. V., Amend, S. R., & Pienta, K. J. (2022). Interplay between cell death and cell proliferation reveals new strategies for cancer therapy. *International journal of molecular sciences*, *23*(9), 4723.

210. Rasmussen, M. L., & Gama, V. (2020). A connection in life and death: The BCL-2 family coordinates mitochondrial network dynamics and stem cell fate. *International review of cell and molecular biology*, *353*, 255-284.

211. McKenzie, M. D., Carrington, E. M., Kaufmann, T., Strasser, A., Huang, D. C., Kay, T. W., ... & Thomas, H. E. (2008). Proapoptotic BH3-only protein Bid is essential for death receptor–induced apoptosis of pancreatic β-cells. *Diabetes*, *57*(5), 1284-1292.

212. Wikström, K., Juhas, M., & Sjölander, A. (2003). The anti-apoptotic effect of leukotriene D4 involves the prevention of caspase 8 activation and Bid cleavage. *Biochemical Journal*, *371*(1), 115-124.

213. Li, Y., Zheng, W., Lu, Y., Zheng, Y., Pan, L., Wu, X., ... & Zhang, X. (2021). BNIP3L/NIX-mediated mitophagy: molecular mechanisms and implications for human disease. *Cell Death & Disease*, *13*(1), 14.

214. Burton, T. R., & Gibson, S. B. (2009). The role of Bcl-2 family member BNIP3 in cell death and disease: NIPping at the heels of cell death. *Cell Death & Differentiation*, *16*(4), 515-523.

215. Ma, J., Ni, H., Rui, Q., Liu, H., Jiang, F., Gao, R., ... & Chen, G. (2019). Potential roles of NIX/BNIP3L pathway in rat traumatic brain injury. *Cell transplantation*, *28*(5), 585-595.

216. Zhou, J., Ma, C., Wang, K., Li, X., Jian, X., Zhang, H., ... & Shi, Y. (2020). Identification of rare and common variants in BNIP3L: a schizophrenia susceptibility gene. *Human Genomics*, *14*, 1-11.

217. Nguyen, B. Y., Ruiz-Velasco, A., Bui, T., Collins, L., Wang, X., & Liu, W. (2019). Mitochondrial function in the heart: the insight into mechanisms and therapeutic potentials. *British journal of pharmacology*, *176*(22), 4302-4318.

218. Cartier, J., Berthelet, J., Marivin, A., Gemble, S., Edmond, V., Plenchette, S., ... & Dubrez, L. (2011). Cellular inhibitor of apoptosis protein-1 (cIAP1) can regulate E2F1 transcription factor-mediated control of cyclin transcription. *Journal of Biological Chemistry*, *286*(30), 26406-26417.

219. Lalaoui, N., & Vaux, D. L. (2018). Recent advances in understanding inhibitor of apoptosis proteins. *F1000Research*, *7*.

220. Cetraro, P., Plaza-Diaz, J., MacKenzie, A., & Abadía-Molina, F. (2022). A review of the current impact of inhibitors of apoptosis proteins and their repression in cancer. *Cancers*, *14*(7), 1671.

221. Finlay, D., Teriete, P., Vamos, M., Cosford, N. D., & Vuori, K. (2017). Inducing death in tumor cells: roles of the inhibitor of apoptosis proteins. *F1000Research*, *6*.

222. Lin, C. Y., Wang, C. C., Wu, R. C., Yang, L. Y., Chang, C. B., Pan, Y. B., ... & Lai, C. H. (2021). Inhibition of BIRC2 sensitizes α7-HPV-related cervical squamous cell carcinoma to chemotherapy. *International journal of molecular sciences*, *22*(20), 11020.

223. Rao, Y., Xu, S., Lu, T., Wang, Y., Liu, M., & Zhang, W. (2023). Downregulation of BIRC2 hinders the progression of rheumatoid arthritis through regulating TRADD. *Immunity, Inflammation and Disease*, *11*(10), e978.

224. Kurosawa, A., Saito, S., So, S., Hashimoto, M., Iwabuchi, K., Watabe, H., & Adachi, N. (2013). DNA ligase IV and artemis act cooperatively to suppress homologous recombination in human cells: implications for DNA double-strand break repair. *PloS one*, *8*(8), e72253.

225. Frank, K. M., Sharpless, N. E., Gao, Y., Sekiguchi, J. M., Ferguson, D. O., Zhu, C., ... & Alt, F. W. (2000). DNA ligase IV deficiency in mice leads to defective neurogenesis and embryonic lethality via the p53 pathway. *Molecular cell*, *5*(6), 993-1002.

226. Tavana, O., Puebla-Osorio, N., Sang, M., & Zhu, C. (2010). Absence of p53-dependent apoptosis combined with nonhomologous end-joining deficiency leads to a severe diabetic phenotype in mice. *Diabetes*, *59*(1), 135-142.

227. Hirao, A., Kong, Y. Y., Matsuoka, S., Wakeham, A., Ruland, J., Yoshida, H., ... & Mak, T. W. (2000). DNA damage-induced activation of p53 by the checkpoint kinase Chk2. *Science*, *287*(5459), 1824-1827.

228. Adachi, N., Ishino, T., Ishii, Y., Takeda, S., & Koyama, H. (2001). DNA ligase IV-deficient cells are more resistant to ionizing radiation in the absence of Ku70: Implications for DNA double-strand break repair. *Proceedings of the National Academy of Sciences*, *98*(21), 12109-12113.

229. Zhang, W., Xiao, D., Mao, Q., & Xia, H. (2023). Role of neuroinflammation in neurodegeneration development. *Signal Transduction and Targeted Therapy*, *8*(1), 267.

230. Xu, J., Su, X., Burley, S. K., & Zheng, X. S. (2022). Nuclear SOD1 in growth control, oxidative stress response, amyotrophic lateral sclerosis, and cancer. *Antioxidants*, *11*(2), 427.

231. Li, X., Qiu, S., Shi, J., Wang, S., Wang, M., Xu, Y., ... & Liu, C. (2019). A new function of copper zinc superoxide dismutase: as a regulatory DNA-binding protein in gene expression in response to intracellular hydrogen peroxide. *Nucleic acids research*, *47*(10), 5074-5085.

232. Jia, C., Ke-Hong, C., Fei, X., Huan-Zi, D., Jie, Y., Li-Ming, W., ... & Ya-Ni, H. (2020). Decoy receptor 2 mediation of the senescent phenotype of tubular cells by interacting with peroxiredoxin 1 presents a novel mechanism of renal fibrosis in diabetic nephropathy. *Kidney international*, *98*(3), 645-662.

233. Peggion, C., Scalcon, V., Massimino, M. L., Nies, K., Lopreiato, R., Rigobello, M. P., & Bertoli, A. (2022). SOD1 in ALS: taking stock in pathogenic mechanisms and the role of glial and muscle cells. *Antioxidants*, *11*(4), 614.

234. Magrané, J., Hervias, I., Henning, M. S., Damiano, M., Kawamata, H., & Manfredi, G. (2009). Mutant SOD1 in neuronal mitochondria causes toxicity and mitochondrial dynamics abnormalities. *Human molecular genetics*, *18*(23), 4552-4564.

235. Li, S., Fu, L., Tian, T., Deng, L., Li, H., Xia, W., & Gong, Q. (2018). Disrupting SOD1 activity inhibits cell growth and enhances lipid accumulation in nasopharyngeal carcinoma. *Cell Communication and Signaling*, *16*, 1-13.

236. Le Gall, L., Anakor, E., Connolly, O., Vijayakumar, U. G., Duddy, W. J., & Duguez, S. (2020). Molecular and cellular mechanisms affected in ALS. *Journal of personalized medicine*, *10*(3), 101.

237. Yoon, E. J., Park, H. J., Kim, G. Y., Cho, H., Choi, J. H., Park, H. Y., ... & Kang, S. (2009). Intracellular amyloid beta interacts with SOD1 and impairs the enzymatic activity of SOD1: implications for the pathogenesis of amyotrophic lateral sclerosis. *Experimental & molecular medicine*, *41*(9), 611-617.

238. Chen, Y. L., & Kan, W. M. (2015). Down-regulation of superoxide dismutase 1 by PMA is involved in cell fate determination and mediated via protein kinase D2 in myeloid leukemia cells. *Biochimica et Biophysica Acta (BBA)-Molecular Cell Research*, *1853*(10), 2662-2675.

239. Xu, J., Su, X., Burley, S. K., & Zheng, X. S. (2022). Nuclear SOD1 in growth control, oxidative stress response, amyotrophic lateral sclerosis, and cancer. *Antioxidants*, *11*(2), 427.

240. Li, M. (2021). The role of P53 up-regulated modulator of apoptosis (PUMA) in ovarian development, cardiovascular and neurodegenerative diseases. *Apoptosis*, *26*(5), 235-247.

241. Jeffers, J. R., Parganas, E., Lee, Y., Yang, C., Wang, J., Brennan, J., ... & Zambetti, G. P. (2003). Puma is an essential mediator of p53-dependent and-independent apoptotic pathways. *Cancer cell*, *4*(4), 321-328.

242. Wang, X., Wang, J., Lin, S., Geng, Y., Wang, J., & Jiang, B. (2008). Sp1 is involved in H 2 O 2-induced PUMA gene expression and apoptosis in colorectal cancer cells. *Journal of Experimental & Clinical Cancer Research*, *27*, 1-10.

243. Li, Z. N., & Luo, Y. (2023). HSP90 inhibitors and cancer: Prospects for use in targeted therapies. *Oncology Reports*, *49*(1), 1-13.

244. Wu, B., Qiu, W., Wang, P., Yu, H., Cheng, T., Zambetti, G. P., ... & Yu, J. (2007). p53 independent induction of PUMA mediates intestinal apoptosis in response to ischaemia–reperfusion. *Gut*, *56*(5), 645-654.

245. Tan, S., Wei, X., Song, M., Tao, J., Yang, Y., Khatoon, S., ... & Wu, B. (2014). PUMA mediates ER stress-induced apoptosis in portal hypertensive gastropathy. *Cell death & disease*, *5*(3), e1128-e1128.

246. Naghinezhad, J., Alenabi, A., Ayatollahi, H., Sheikhi, M., Sadeghian, M. H., Khoshnegah, Z., & Boroumand-Noughabi, S. (2023). Expression of DR4, DR5, FAS, Caspase-8 and, DDIAS Genes in AML Patients. *Medical Journal of the Islamic Republic of Iran*, *37*.

247. Yao, W., Oh, Y. T., Deng, J., Yue, P., Deng, L., Huang, H., ... & Sun, S. Y. (2016). Expression of death receptor 4 is positively regulated by MEK/ERK/AP-1 signaling and suppressed upon MEK inhibition. *Journal of Biological Chemistry*, *291*(41), 21694-21702.

248. Zhang, S., Chen, Z., Shi, P., Fan, S., He, Y., Wang, Q., ... & Sun, S. Y. (2021). Downregulation of death receptor 4 is tightly associated with positive response of EGFR mutant lung cancer to EGFR-targeted therapy and improved prognosis. *Theranostics*, *11*(8), 3964.

249. Horak, P., Pils, D., Haller, G., Pribill, I., Roessler, M., Tomek, S., ... & Krainer, M. (2005). Contribution of epigenetic silencing of tumor necrosis factor–related apoptosis inducing ligand receptor 1 (DR4) to TRAIL resistance and ovarian cancer. *Molecular cancer research*, *3*(6), 335-343.

250. Kurbanov, B. M., Geilen, C. C., Fecker, L. F., Orfanos, C. E., & Eberle, J. (2005). Efficient TRAIL-R1/DR4-mediated apoptosis in melanoma cells by tumor necrosis factor-related apoptosis-inducing ligand (TRAIL). *Journal of investigative dermatology*, *125*(5), 1010-1019.

251. Nogueira, A., Fernandes, M., Catarino, R., & Medeiros, R. (2019). RAD52 functions in homologous recombination and its importance on genomic integrity maintenance and cancer therapy. *Cancers*, *11*(11), 1622.

252. Ma, E., Dupaigne, P., Maloisel, L., Guerois, R., Le Cam, E., & Coïc, E. (2018). Rad52-Rad51 association is essential to protect Rad51 filaments against Srs2, but facultative for filament formation. *Elife*, *7*, e32744.

253. Liu, S., Wang, Z., Shah, S. B., Chang, C. Y., Ai, M., Nguyen, T., ... & Wu, X. (2023). DNA repair protein RAD52 is required for protecting G-quadruplexes in mammalian cells. *Journal of Biological Chemistry*, *299*(1).

254. Jalan, M., Olsen, K. S., & Powell, S. N. (2019). Emerging roles of RAD52 in genome maintenance. *Cancers*, *11*(7), 1038.

255. Gottifredi, V., & Wiesmüller, L. (2020). Current understanding of RAD52 functions: fundamental and therapeutic insights. *Cancers*, *12*(3), 705.

256. Oda, E., Ohki, R., Murasawa, H., Nemoto, J., Shibue, T., Yamashita, T., ... & Tanaka, N. (2000). Noxa, a BH3-only member of the Bcl-2 family and candidate mediator of p53-induced apoptosis. *Science*, *288*(5468), 1053-1058.

257. Rosebeck, S., Sudini, K., Chen, T., & Leaman, D. W. (2011). Involvement of Noxa in mediating cellular ER stress responses to lytic virus infection. *Virology*, *417*(2), 293-303.

258. Zhou, A., Zhang, W., Wang, B., Dong, X., Zhang, J., & Chen, H. (2023). Knockout of Noxa with CRISPR/Cas9 Increases Host Resistance to Influenza Virus Infection. *Cellular Microbiology*, *2023*.

259. Tonino, S. H., van Laar, J., van Oers, M. H., Wang, J. Y., Eldering, E., & Kater, A. P. (2011). ROS-mediated upregulation of Noxa overcomes chemoresistance in chronic lymphocytic leukemia. *Oncogene*, *30*(6), 701-713.

260. Núñez-Vázquez, S., Sánchez-Vera, I., Saura-Esteller, J., Cosialls, A. M., Noisier, A. F., Albericio, F., ... & Gil, J. (2021). NOXA upregulation by the prohibitin-binding compound fluorizoline is transcriptionally regulated by integrated stress response-induced ATF3 and ATF4. *The FEBS journal*, *288*(4), 1271-1285.

261. Dai, J., Sun, Y., Yan, L., Wang, J., Li, X., & He, J. (2017). Upregulation of NOXA by 10-Hydroxycamptothecin plays a key role in inducing fibroblasts apoptosis and reducing epidural fibrosis. *PeerJ*, *5*, e2858.

262. Liang, L., Weng, J., You, Y., He, Q., Fan, Y., & Liao, G. (2019). Role of Noxa in proliferation, apoptosis, and autophagy in human adenoid cystic carcinoma. *Journal of Oral Pathology & Medicine*, *48*(1), 52-59.

263. Wang, R., Fan, H., Sun, M., Lv, Z., & Yi, W. (2022). Roles of BMI1 in the initiation, progression, and treatment of hepatocellular carcinoma. *Technology in Cancer Research & Treatment*, *21*, 15330338211070689.

264. Jiang, L., Song, L., Wu, J., Yang, Y., Zhu, X., Hu, B., ... & Li, M. (2013). Bmi-1 promotes glioma angiogenesis by activating NF-κB signaling. *PloS one*, *8*(1), e55527.

265. Dai, X., Zhang, Q., Yu, Z., Sun, W., Wang, R., & Miao, D. (2018). Bmi1 deficient mice exhibit male infertility. *International Journal of Biological Sciences*, *14*(3), 358.

266. Ding, C., Fan, X., & Wu, G. (2017). Peroxiredoxin 1–an antioxidant enzyme in cancer. *Journal of cellular and molecular medicine*, *21*(1), 193-202.

267. Sharma, A., Kansara, S., Mahajan, M., Yadav, B., Garg, M., & Pandey, A. K. (2021). Long non-coding RNAs orchestrate various molecular and cellular processes by modulating epithelial-mesenchymal transition in head and neck squamous cell carcinoma. *Biochimica et Biophysica Acta (BBA)-Molecular Basis of Disease*, *1867*(11), 166240.

268. Nassour, H., Wang, Z., Saad, A., Papaluca, A., Brosseau, N., Affar, E. B., ... & Ramotar, D. (2016). Peroxiredoxin 1 interacts with and blocks the redox factor APE1 from activating interleukin-8 expression. *Scientific reports*, *6*(1), 29389.

269. Chatterjee, A., & Gupta, S. (2018). The multifaceted role of glutathione S-transferases in cancer. *Cancer letters*, *433*, 33-42.

270. Mohammad, J., Singh, R. R., Riggle, C., Haugrud, B., Abdalla, M. Y., & Reindl, K. M. (2019). JNK inhibition blocks piperlongumine-induced cell death and transcriptional activation of heme oxygenase-1 in pancreatic cancer cells. *Apoptosis*, *24*, 730-744.

271. Tan, X., Huang, X., Niu, B., Guo, X., Lei, X., & Qu, B. (2022). Targeting GSTP1-dependent ferroptosis in lung cancer radiotherapy: Existing evidence and future directions. *Frontiers in Molecular Biosciences*, *9*, 1102158.

272. Li, J., Li, Q., Huang, H., Li, Y., Li, L., Hou, W., & You, Z. (2017). Overexpression of miRNA-221 promotes cell proliferation by targeting the apoptotic protease activating factor-1 and indicates a poor prognosis in ovarian cancer. *International Journal of Oncology*, *50*(4), 1087-1096.

273. Harlan, J., Chen, Y., Gubbins, E., Mueller, R., Roch, J. M., Walter, K., ... & Katz, D. A. (2006). Variants in Apaf-1 segregating with major depression promote apoptosome function. *Molecular psychiatry*, *11*(1), 76-85.

274. Zhao, J., Jiang, P., Guo, S., Schrodi, S. J., & He, D. (2021). Apoptosis, autophagy, NETosis, necroptosis, and pyroptosis mediated programmed cell death as targets for innovative therapy in rheumatoid arthritis. *Frontiers in immunology*, *12*, 809806.